# SPECIFIC HEATS
# AT LOW TEMPERATURES

# THE INTERNATIONAL CRYOGENICS MONOGRAPH SERIES

*General Editors*

Dr. K. Mendelssohn, F. R. S.
*The Clarendon Laboratory*
*Oxford, England*

Dr. K. D. Timmerhaus
*University of Colorado*
*Boulder, Colorado*

H. J. Goldsmid
G. T. Meaden
E. S. R. Gopal

*Thermoelectric Refrigeration, 1964*
*Electrical Resistance of Metals, 1965*
*Specific Heats at Low Temperatures, 1*

*Volumes in preparation*

D. H. Parkinson and B. Mulhall
J. L. Olsen and S. Gygax
A. J. Croft and P. V. E. McClintock
G. K. Gaulé

M. G. Zabetakis
F. B. Canfield
W. E. Keller
S. Ramaseshan
P. Glaser and A. Wechsler

*Very High Magnetic Fields*
*Superconductivity for Engineers*
*Cryogenic Laboratory Equipment*
*Superconductivity in Elements,*
    *Alloys, and Compounds*
*Cryogenic Safety*
*Low-Temperature Phase Equilibria*
*Helium-3 and Helium-4*
*Low-Temperature Crystallography*
*Cryogenic Insulation Systems*

# SPECIFIC HEATS
# AT LOW TEMPERATURES

### E. S. R. Gopal
*Department of Physics, Indian Institute of Science*
*Bangalore, India*

# Preface

This work was begun quite some time ago at the University of Oxford during the tenure of an Overseas Scholarship of the Royal Commission for the Exhibition of 1851 and was completed at Bangalore when the author was being supported by a maintenance allowance from the CSIR Pool for unemployed scientists. It is hoped that significant developments taking place as late as the beginning of 1965 have been incorporated.

The initial impetus and inspiration for the work came from Dr. K. Mendelssohn. To him and to Drs. R. W. Hill and N. E. Phillips, who went through the whole of the text, the author is obliged in more ways than one. For permission to use figures and other materials, grateful thanks are tendered to the concerned workers and institutions.

The author is not so sanguine as to imagine that all technical and literary flaws have been weeded out. If others come across them, they may be charitably brought to the author's notice as proof that physics has become too vast to be comprehended by a single onlooker.

E. S. RAJA GOPAL

Department of Physics
Indian Institute of Science
Bangalore 12, India
November 1965

# Contents

# Introduction

Investigations at temperatures below room temperature have advanced our knowledge in many ways. Toward the beginning of the present century, physical chemists evolved their reference state for chemical equilibria and thermodynamic properties on the basis of such studies. Later, physicists realized that a clear manifestation of quantum effects was possible at low temperatures. In recent times, superconductors, rocket fuels, cryopumping and a multitude of other developments have lifted low-temperature studies out of academic cloisters and into the realm of technology.

In any practical attempt to study low-temperature phenomena, the question of specific heats crops up immediately, in connection with the refrigeration needed to take care of the thermal capacity of the apparatus. Apart from its significance in this perennial problem of cooling equipments to desired low temperatures, knowledge of specific heats forms a powerful tool in many other areas, such as lattice vibrations, electronic distributions, energy levels in magnetic materials, and order-disorder phenomena in molecules. No better evidence for the usefulness of specific-heat studies is needed than the presence of the Debyė characteristic temperature $\theta$ in so many branches of solid state studies. This monograph is basically a descriptive introduction to the different aspects of specific-heat studies.

Historically, the need for measuring specific heats at low temperatures arose in conjunction with the formulation of the third law of thermodynamics. Nernst realized that the specific heat of all substances should vanish as the absolute zero of temperature is approached. Einstein demonstrated the quantum effects that come into play in specific heats at low temperatures. This opened up the prospect of checking the energy states of all substances with the help of calorimetric measurements. Whatever theory of solid, liquid, and gaseous states is developed, it leads in the first place to a set of energy levels which the particles can occupy. By using suitable statistical methods, it is possible to compute the mean energy of the system and from it the specific heat. Any such calculation requires a minimum of extra theoretical assumptions. This is both a strength

and a weakness of specific-heat studies. The heat capacity provides a direct and immediate test of the theoretical model of the system, but because it is a measure of a mean quantity it cannot shed light on the finer details of the model. It is wise not to lose sight of this limitation—which, incidentally, holds true to some extent for the study of any phenomenological property of substances.

The reduction of specific heats at low temperatures is of tremendous significance in the practice of cryogenic techniques. For the ordinary materials used in the construction of apparatus, the specific heat is about 6 cal/gram-atom·degK at room temperature (300°K), approximately 4 units at liquid-air temperature (80°K), and only $10^{-2}$ units at liquid-helium temperature (4°K). The rapid fall in specific heats in the liquid hydrogen–helium temperature range makes itself felt in several ways. Once a large apparatus has been cooled to liquid-air temperature, relatively small amounts of refrigeration (measured in terms of, say, the latent heat of the liquid helium that is boiled away) are sufficient to cool it to about 4°K. It is, in fact, a standard practice to conserve liquid helium by precooling the cryostats with liquid air, and if possible liquid hydrogen, so that little helium is boiled away in reducing the temperature to the vicinity of 4°K. Secondly, if a part of the cold apparatus is thermally insulated from the main heat sink, its temperature may rise considerably because of small amounts of heat influx. Such situations commonly arise in the measurement of specific heats. For the same reason, when very low temperatures (<1°K) are achieved by adiabatic demagnetization, it is of utmost importance to cut out as much stray heat input as possible. Thirdly, because of the small heat capacity at low temperatures, thermal equilibrium among the various parts of an apparatus is established very quickly. Typically, a system which takes about an hour to come to internal equilibrium at room temperature will do so in about a minute at 4°K.

It was mentioned above that the energy levels of the particles specify the mean energy of the system, which in turn determines the specific heat of the system. These energy levels may be in the form of translational, rotational, or vibrational motions of molecules in gases, vibrations of atoms about their lattice sites in solids, the wandering of electrons free to move in metals, and so on. The enumeration of the possible modes of energy can be continued further, and it is obvious that a discussion of the specific heats of substances must inevitably cover a very wide field, since any temperature-dependent phenomenon can contribute to specific heats. In a monograph such as this, it is both unnecessary and impossible to be comprehensive in the description of all phenomena which bear some slight relationship to specific heats. The solution attempted here is to provide a reasonably

comprehensive description of the various aspects of specific-heat studies at low temperatures, leaving the discussion of allied phenomena to various other texts.[1] It has been a difficult task to steer between the Scylla of encyclopedic completeness and the Charybdis of shallow banality.

This compromise has been chosen to serve two purposes. For the interested neophyte, the monograph should be a simple survey and a stepping-stone to an understanding of the problems of specific heats. Thus, in discussing the basic principles, no attempt at rigor is made. In citing references, preference is given, if possible, to elementary texts rather than to advanced treatises. If in this process several authors feel themselves overlooked, it is because the choice is not meant to be a judgment of the scientific value of such works, but is only a didactic device for elucidating the basic questions. Further, the normal behavior of solids, liquids, and gases is treated first before taking up, in Chapter 7, abnormalities in the specific heat of some substances. No doubt, the reader will find that some instances of specific-heat anomalies are introduced surreptitiously in Chapters 3 to 6, but the present arrangement has the added advantage that by Chapter 7 enough anomalies have been mentioned to focus attention on classification of such behavior. For those actively engaged with cryogenic problems, a description of the many facets of specific-heat studies, with adequate references to the sources of more detailed analyses of any single aspect, should make the book useful.

The task of listing all the references, especially to the early literature on the subject, has been rendered superfluous by the monumental work of Partington.[2] Therefore, references to early papers are seldom given, and anyone interested can trace such papers from either the above treatise[2] or the recent reviews and books cited at the end of each chapter. Moreover, the description of cryogenic techniques has been limited to a minimum because of the availability of excellent books on the subject.[3]

## REFERENCES

1. C. F. Squire, *Low Temperature Physics*, McGraw-Hill, New York, 1953. K. Mendelssohn, *Cryophysics*, Interscience, New York, 1960. L. C. Jackson, *Low Temperature Physics*, Methuen, London, 1962. R. W. Vance and W. M. Duke, *Applied Cryogenic Engineering*, Wiley, New York, 1962. H. M. Rosenberg, *Low Temperature Solid State Physics*, Clarendon, Oxford, 1963. M. McClintock, *Cryogenics*, Reinhold, New York, 1964.
2. J. R. Partington, *Advanced Treatise on Physical Chemistry*, Longmans-Green, London; *Vol. I, Properties of Gases* (1949); *Vol. II, Properties of Liquids* (1951); *Vol. III, Properties of Solids* (1952).

3. G. K. White, *Experimental Techniques in Low Temperature Physics,* Clarendon, Oxford, 1959. R. B. Scott, *Cryogenic Engineering,* Van Nostrand, New York, 1959. F. Din and A. H. Cockett, *Low Temperature Techniques,* Newnes, London, 1960. F. E. Hoare, L. C. Jackson, and N. Kurti, *Experimental Cryophysics,* Butterworth, London, 1961. A. C. Rose-Innes, *Low Temperature Techniques,* English University Press, London, 1964.

*Chapter 1*

# Elementary Concepts of Specific Heats

## 1.1. DEFINITIONS

The specific heat of a substance is defined as the quantity of heat required to raise the temperature of a unit mass of the substance by a unit degree of temperature. To some extent, the specific heat depends upon the temperature at which it is measured and upon the changes that are allowed to take place during the rise of temperature. If the properties $x$, $y$, ..., are held constant when a heat input $dQ$ raises the temperature of unit mass of the substance by $dT$, then

$$c_{x,y,...} = \lim_{dT \to 0} \left( \frac{dQ}{dT} \right)_{x,y,...} \tag{1.1}$$

The specific heat, sometimes called the *heat capacity*, is in general a positive quantity. In the absence of any rigid convention, it seems best to use the term *specific heat* when referring to 1 g of the material and the term *heat capacity* when a more general amount of the material, i.e., a gram-atom or a gram-molecule, is involved.

In expressing the numerical values of specific heats, the MKS system, based on kilogram units of the substance, is not yet widely used in current literature, and so cgs units will be used throughout the book. By convention, $c_{x,y,...}$ refers to the specific heat per gram and $C_{x,y...}$ to the heat capacity per gram-molecule of the substance. The $c_{x...}$ value is usually expressed in cal/g·degK or in J/g·deg, the present conversion factor being 1 thermochemical calorie = 4.1840 J. In engineering literature, it is still not uncommon to find specific heats in BTU/lb·degF, which luckily has almost the same value in cal/g·degK.

5

## 1.2. THERMODYNAMICS OF SIMPLE SYSTEMS

All processes in which quantities of heat and work come into play are governed by the fundamental laws of thermodynamics. Some properties of specific heats follow immediately from these laws, and it is therefore appropriate to consider them first. A discussion of the principles of thermodynamics is given in several well-known texts.[1] If a quantity of heat $dQ$ is supplied to a substance, a part of it goes to increase the internal energy $E$ of the system and a part is utilized in performing external work $W$. In accordance with the first law,

$$dQ = dE + dW \qquad (1.2)$$

If the heat exchange is reversible, the second law of thermodynamics permits calculation of the entropy $S$ of the system from the relation

$$dQ = T \, dS \qquad (1.3)$$

Apart from the special conditions to be discussed in Section 8.5, $E$ and $S$ are proportional to the mass of the substance; that is, they are extensive variables.

It is instructive to start with a simple substance, namely, the ideal fluid. In gases and liquids, the pressure $P$ at a point is the same in all directions, and any work done by the system $dW$ is an expansion against the pressure. Then $dW$ must be of the form

$$dW = P \, dV \qquad (1.4)$$

Moreover, fluids obey an equation of state

$$f(P, V, T) = 0 \qquad (1.5)$$

This means that any one of $P$, $V$, $T$ can be expressed in terms of the other two and that only two of the three quantities can be arbitrarily varied at the same time. Hence, during the change of temperature, either $P$ or $V$ can be kept constant, and correspondingly there are two principal heat capacities:

$$C_p = \left(\frac{dQ}{dT}\right)_p = T\left(\frac{\partial S}{\partial T}\right)_p$$
$$C_v = \left(\frac{dQ}{dT}\right)_v = T\left(\frac{\partial S}{\partial T}\right)_v \qquad (1.6)$$

The case for solids is somewhat more complicated. Unlike ordinary fluids, which require forces only for changing their volume, solids require forces both to change their linear dimensions and to alter their shape. It is shown in the texts on elasticity[2] that $dW$ is of

the form

$$dW = \sum_i t_i \, de_i \qquad (i = 1, 2, ..., 6)$$

where $t_i$ are the stresses and $e_i$ are the strains. Obviously, it is possible in principle to define a large number of specific heats, allowing only one stress or strain component to change during the heating. In practice, however, such experiments are hardly feasible, and only $C_p$, $C_v$ are of importance. It can be shown[3] that they obey the same thermodynamic relations as the $C_p$, $C_v$ of liquids and gases, so there is no significant loss of generality in restricting the discussion to the simple case of fluids.

Combining (1.2) and (1.3), one can write the change in internal energy as

$$dE = T \, dS - P \, dV \qquad (1.7)$$

Often it is convenient to handle the other principal thermodynamic functions of the system, namely, enthalpy $H$, Helmholtz function $A$ and Gibbs' function $G$, whose variations are

$$dH = d(E + PV) = T \, dS + V \, dP \qquad (1.8)$$

$$dA = d(E - TS) = -S \, dT - P \, dV \qquad (1.9)$$

$$dG = d(E - TS + PV) = -S \, dT + V \, dP \qquad (1.10)$$

These four functions are nothing but measures of the energy content of the substance under various conditions, and the changes in these must depend only upon the initial and final states. Mathematically equivalent is the statement that the differentials (1.7) to (1.10) are perfect differentials; this condition leads to the four Maxwell's relations

$$\left(\frac{\partial T}{\partial V}\right)_S = -\left(\frac{\partial P}{\partial S}\right)_v \qquad \left(\frac{\partial T}{\partial P}\right)_S = \left(\frac{\partial V}{\partial S}\right)_p$$

$$\left(\frac{\partial S}{\partial V}\right)_T = \left(\frac{\partial P}{\partial T}\right)_v \qquad \left(\frac{\partial S}{\partial P}\right)_T = -\left(\frac{\partial V}{\partial T}\right)_p \qquad (1.11)$$

The four relations are useful in expressing thermodynamic formulas in terms of quantities which are experimentally measured.

## 1.3. DIFFERENCE BETWEEN $C_p$ and $C_v$

As an illustration of the use of equation (1.11), the important expressions for $C_p - C_v$ may be calculated. Take $T$ and $V$ as the independent variables in describing the entropy of a mole of substance

and write

$$dS = \left(\frac{\partial S}{\partial T}\right)_v dT + \left(\frac{\partial S}{\partial V}\right)_T dV$$

or

$$\left(\frac{\partial S}{\partial T}\right)_p = \left(\frac{\partial S}{\partial T}\right)_v + \left(\frac{\partial S}{\partial V}\right)_T \left(\frac{\partial V}{\partial T}\right)_p$$

Replacing $(\partial S/\partial V)_T$ by $(\partial P/\partial T)_v$ and using equations (1.6) yields

$$C_p - C_v = T\left(\frac{\partial S}{\partial T}\right)_p - T\left(\frac{\partial S}{\partial T}\right)_v = T\left(\frac{\partial P}{\partial T}\right)_v \left(\frac{\partial V}{\partial T}\right)_p \qquad (1.12)$$

This relation is convenient if the equation of state is known explicitly. For example, a mole of a gas obeys the relation $PV = RT$ under ideal conditions, and so equation (1.12) gives the difference between the molar heat capacities:

$$C_p - C_v = R \qquad (1.13)$$

The gas constant $R$ has a value 8·314 J/mole·deg, or 1.987 cal/mole·deg. For liquids and solids, $(\partial P/\partial T)_v$ is not easy to measure and is best eliminated from the equations. To do this, consider $P$ as a function of $T$ and $V$:

$$dP = \left(\frac{\partial P}{\partial V}\right)_T dV + \left(\frac{\partial P}{\partial T}\right)_v dT$$

At constant pressure, $dP = 0$, and

$$\left(\frac{\partial P}{\partial T}\right)_v = -\left(\frac{\partial P}{\partial V}\right)_T \left(\frac{\partial V}{\partial T}\right)_p$$

Now the coefficient of cubical expansion $\beta = V^{-1}(\partial V/\partial T)_p$ and the isothermal compressibility $k_T = -V^{-1}(\partial V/\partial P)_T$ are amenable to experimental measurements. In terms of $\beta$, $k_T$, and the molar volume $V$,

$$C_p - C_v = \frac{TV\beta^2}{k_T} \qquad (1.14)$$

The mechanical stability of a substance requires $k_T > 0$. Therefore, $C_p$ is always greater than $C_v$. They are equal when $\beta = 0$, as in the case of water near 4°C, liquid $^4$He near 1.1°K, and liquid $^3$He near 0.6°K. The reason for $C_p \geqslant C_v$ is easy to see. Heating the substance at constant pressure causes an increase in the internal energy

and also forces the substance to do external work in expanding against the pressure of the system. On the other hand, in heating at constant volume there is no work done against the pressure and all the heat goes to raise the internal energy. Hence, in the latter case the temperature rise is larger for a given $dQ$. In other words, $C_v$ is less than $C_p$.

The difference between $C_p$ and $C_v$ is about 5% in most solids at room temperature. It decreases rapidly as the temperature is lowered. Table 1.I gives the values for copper, and the behavior of other solids is very similar. However, to calculate $C_p - C_v$ exactly, a tremendous amount of data is needed. The complete temperature dependence of molar volume, volume expansion, and isothermal compressibility, besides $C_p$, should be known, and this knowledge is not always available. Under such conditions, approximate relations are used. The most successful one is the Nernst–Lindemann relation based on Grüneisen's equation of state:

$$C_p - C_v = \frac{V\beta^2}{k_T C_p^2} C_p^2 T = A C_p^2 T \qquad (1.15)$$

The parameter $A$ is nearly constant over a wide range of temperature. For example, in copper $A = 1.54 \times 10^{-5}$ mole/cal at 1000°K and $1.53 \times 10^{-5}$ at 100°K, if the mechanical equivalent of heat is taken as $4.184 \times 10^7$ ergs/cal. If $A$ is calculated at any one temperature from the values of $V$, $\beta$, and $k_T$, it may be used to calculate $C_p - C_v$ over a wide range of $T$ without serious error.

In gases at low pressures, $C_p - C_v$ is equal to $R$ [equation (1.13)], but at high pressures small corrections for nonideality are needed.[1] The values of $C_p$ or $C_v$ are not dramatically changed at low temperatures. The behavior of nitrogen is typical: $C_p$ is about 6.95 cal/mole·deg at 300°K and about 6.96 at 100°K.

The ratio of specific heats $C_p/C_v$ is nearly unity for solids and liquids, but not for gases. The value $C_p \sim \frac{7}{2}R$ for nitrogen shows that $C_v \sim \frac{5}{2}R$, and so $C_p/C_v \sim 1.4$. It is 1.67 for monatomic gases such as helium or argon, and becomes approximately 1.3 for polyatomic

**Table 1.I. $C_p$ and $C_v$ for Copper**

| $T$ | $C_p$ | $V$ | $\beta$ | $k_T$ | $C_p - C_v$ | $C_v$ | $C_p/C_v$ |
|---|---|---|---|---|---|---|---|
| 1000 | 7.04 | 7.35 | 65.2 | 0.976 | 0.778 | 6.27 | 1.12 |
| 300 | 5.87 | 7.06 | 49.2 | 0.776 | 0.157 | 5.71 | 1.03 |
| 100 | 3.88 | 7.01 | 31.5 | 0.721 | 0.023 | 3.86 | 1.00 |
| 4 | 0.0015 | 7.00 | 0.0 | 0.710 | 0.0 | 0.0015 | 1.00 |

$T$ in degK; $C_p$, $C_v$ in cal/mole·deg; $V$ in cm$^3$/mole; $\beta$ in $10^{-6}$/deg; $k_T$ in $10^{-12}$ cm$^2$/dyne.

gases. In general, the ratio $C_p/C_v$ depends upon the state of the substance and is useful in converting adiabatic elastic data to isothermal data. For example, it is a simple exercise to show that

$$\frac{k_T}{k_S} = \frac{C_p}{C_v} \tag{1.16}$$

where $k_T$ is the isothermal compressibility and $k_S$ is the adiabatic value. The ratio has greater significance for gases, where, besides being involved in the adiabatic equation $PV^{C_p/C_v} = \text{constant}$, it also gives information about the number of degrees of freedom of the molecules constituting the gas.

### 1.4. VARIATION OF SPECIFIC HEATS WITH TEMPERATURE AND PRESSURE

It was mentioned in Section 1.1 that the specific heats depend to some extent upon the state of the substance, and Table 1.I shows how $C_p$, $C_v$ in a solid are affected by temperature. The full details of such temperature dependences are very complicated, and their elucidation is the major task of the whole book. Here, only some simple consequences of general thermodynamic considerations are pointed out.

The use of Maxwell's relations (1.11) shows that

$$\left(\frac{\partial C_v}{\partial V}\right)_T = T\left(\frac{\partial^2 P}{\partial T^2}\right)_v$$

$$\left(\frac{\partial C_p}{\partial P}\right)_T = -T\left(\frac{\partial^2 V}{\partial T^2}\right)_p \tag{1.17}$$

The prime use of these relations is in reducing the measured specific heats of gases to the ideal values at zero pressure with the help of the equation of state. For a perfect gas, $C_p$ and $C_v$ are independent of pressure.

The third law of thermodynamics specifies the behavior of specific heats at very low temperature. According to it, the entropy of any system in thermodynamic equilibrium tends to zero at the absolute zero. Since $S = 0$ at $T = 0$ and $S$ is finite at higher temperatures, the difference in entropy at constant volume between $T = 0$ and $T = T_0$ may be obtained from equation (1.6) as

$$S(T_0) = \int_0^{T_0} \left(\frac{C_v}{T}\right) dT$$

For the integral to converge, i.e., remain finite definite, at the lower limit $T = 0$, $C_v/T$ must be a finite number (including zero) as $T \to 0$. In other words, when absolute zero is approached, the specific heat must tend to zero at least as the first power of $T$.

The vanishing of specific heats at $T = 0$ is of great importance because it permits the use of $0°K$ as a reference for all thermodynamic calculations. For instance, the entropy at any temperature $T$ may be uniquely expressed as

$$S(T) = \int_0^T C_v \, T^{-1} \, dT \qquad (1.18)$$

without any undetermined additive constants. Since $C_v$ is known to vanish at $0°K$, it is enough to measure it to a sufficiently low temperature from where it may be safely extrapolated to zero. Unfortunately, the laws of thermodynamics do not give any indication of how low this temperature should be. For many solids, measurements down to liquid-helium temperature are adequate, whereas for some paramagnetic salts measurements well below $1°K$ are needed before a safe extrapolation is possible.

Figure 1.1 shows the specific heats of some materials near absolute zero. Dielectric solids (Figure 1.1a) have a low-temperature specific heat proportional to $T^3$, while metals (Fig. 1.1b) obey a relation $c = A_1 T^3 + A_2 T$. These variations are simple enough to permit a ready extrapolation of the observations to $0°K$. However, if the material contains paramagnetic ions—and such materials are important in adiabatic demagnetization techniques—the behavior is often quite anomalous. The specific heat of chromium methylamine alum,[6] shown in Fig. 1.2, is not falling off to zero even at $0.1°K$. Instead it appears to be increasing as the temperature is lowered! No doubt the specific heat will eventually tend to zero as $T \to 0$, but it is quite impossible to guess its behaviour from, say, $0.5°K$. It is also noteworthy that because of the low temperatures the entropy associated with these anomalous variations is often large (of the order of $R$ per mole).

## 1.5. STATISTICAL CALCULATION OF SPECIFIC HEATS

The examples of Fig. 1.1 and 1.2 serve to illustrate the fact that while thermodynamics is powerful in specifying the general laws governing a phenomenon it does not give any clue about the detailed behavior. This belongs to the realm of statistical mechanics, and in the following chapters it will become abundantly clear that a variety of effects observed in the behavior of specific heats may indeed be satisfactorily explained. In statistical thermodynamics, the general
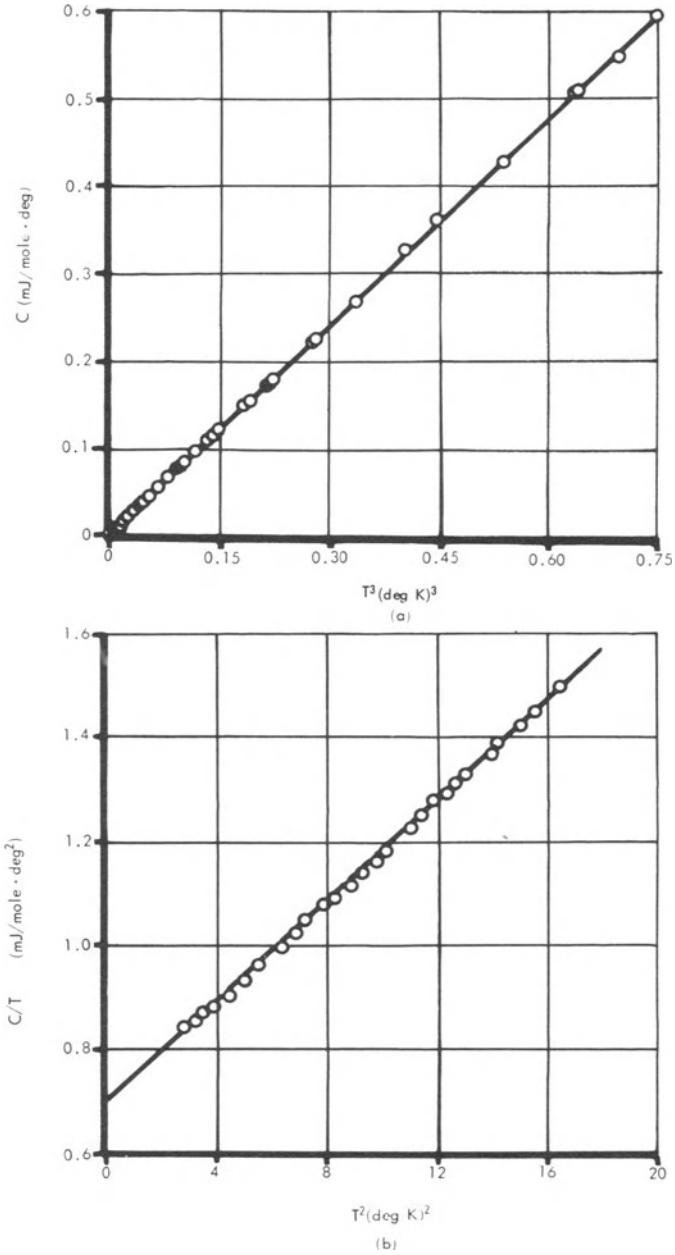
Fig. 1.1.  Well-behaved  heat  capacities  near  0°K : (a) potassium
bromide,[4] (b) copper.[5]
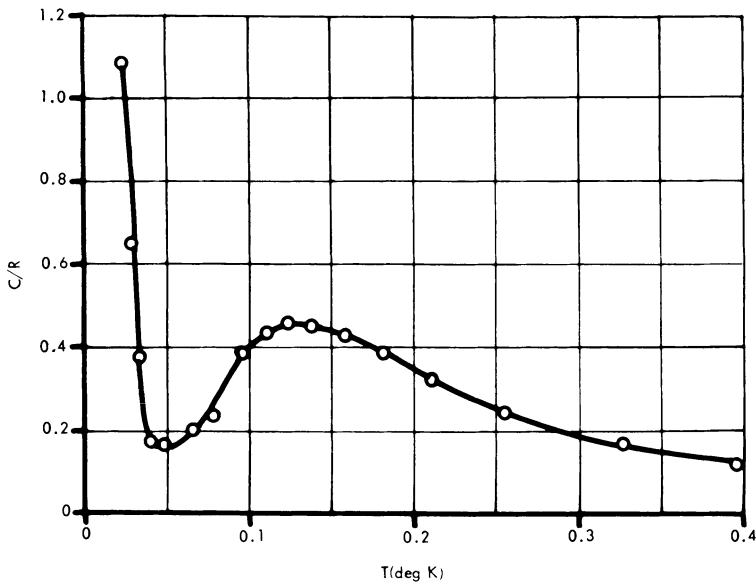
Fig. 1.2. Anomalous variation of heat capacity in chromium methylamine alum.[6]

scheme for deducing the thermal properties is quite simple, although its derivation should be left to the texts on statistical mechanics.[7]

The systems that are of interest in practical problems consist of a very large number of basic constituents, for convenience called *particles* even if they are identified as atoms, molecules, or quanta of energy. The interaction among the particles can be analyzed on the basis of theoretical models to yield the energies $E_i$ of the various possible levels of, say, a mole of the system. Once this is done—and it is in this process that the complex physical systems have to be judiciously represented by simple mathematical models—the thermo-dynamic quantities are contained in the partition function of the system

$$Z = \sum_i \exp\left(\frac{-E_i}{kT}\right) \qquad \sum_i \text{ over all levels of the system} \quad (1.19)$$

which is related to the Helmholtz free energy per mole by the relation

$$A = -kT \ln Z \qquad (1.20)$$

Here, $k$ is Boltzmann's constant, equal to $1.3805 \times 10^{-16}$ erg/degK.

It is now a simple matter to get from $A$

$$S = -\left(\frac{\partial A}{\partial T}\right)_v \qquad E = kT^2\left(\frac{\partial \ln Z}{\partial T}\right)_v \qquad C_v = T\left(\frac{\partial^2(kT\ln Z)}{\partial T^2}\right)_v \quad (1.21)$$

These are the thermodynamic quantities of interest, and they are easily calculated if the partition function is set up in a convenient form.

Clearly, the specific heat at constant volume is the quantity that arises naturally in the theoretical analysis. The experimental measurement of $C_v$ is possible in gases under favorable conditions because the pressures encountered, of the order of atmospheres, can be balanced by the walls of the container. For liquids and solids, on the other hand, the pressures needed to keep the volume constant run into thousands of atmospheres, and normally balancing such pressures is not practicable. Therefore, measurements are ordinarily done at constant pressure and $C_v$ is calculated from equation (1.14). The difference $C_p - C_v$ is usually less than a few percent at low temperatures, unless the substance is near a phase transition.

## 1.6. DIFFERENT MODES OF THERMAL ENERGY

The above discussion underlines the fact that the heat capacity of a substance is governed by the manner in which the internal energy is distributed among its constituents. The molecules in a gas can have translational, rotational, vibrational, and electronic energy levels, and each type of thermal motion contributes its share to the specific heat of a gas. The atoms in a solid are usually held fixed at their lattice sites and can at most vibrate about their mean positions. This motion is called the *lattice mode of thermal excitation*. If the lattice consists of molecules, there are motions of atoms within the molecules besides the vibrations involving molecules as units. These internal vibrations may be described as *molecular modes*. There may be free electrons wandering through the lattice, as in metals, and the *electronic contribution* to $C_v$ arises from the thermal excitation of these electrons. In some cases, the energy levels of bound electrons may be split into discrete levels. The transitions among the levels are known as *excitation modes*. Yet another complication is that in some cases the probability of exciting some mode of thermal agitation depends strongly upon the number of particles already excited. Excitations of the particles therefore increase extremely rapidly, as though by positive feedback, once the first of such modes are excited; these snow-balling processes are called *cooperative phenomena*.

The contributions from all these modes have to be added together to get the total heat capacity. This may be easily seen, since to a

first approximation the energy of a system is the sum of the energies due to the various modes of motion. An inspection of equation (1.19) shows that the partition function is the product of factors associated with each mode. For example, the partition function $Z$ of a gas is the product

$$Z = Z_t Z_r Z_v Z_e \qquad (1.22)$$

of the translational, rotational, vibrational, and electronic functions. $A$ involves $\ln Z$, which is the sum of $\ln Z_t$, $\ln Z_r$, etc., and it is clear that the thermodynamic quantities are the sums of the contributions from the various modes.

While all these possible types of thermal agitation give their share to the heat capacity of the substance, the observed specific heat depends also upon their variation with temperature. Some of the modes are excited over the entire temperature range and so contribute observable specific heat at all temperatures. The atoms in a lattice can vibrate at all temperatures, and the lattice contribution to heat capacity is significant at all temperatures. It falls off as $T^3$ when 0°K is approached, as shown in Fig. 1.1a. The free electrons in a metal have very high heat content, but this varies so little with temperature that its contribution to specific heats is overshadowed by the lattice term at room temperature. However, the electronic specific heat, varying as the first power of $T$, becomes important at liquid-helium temperature, as was seen in Fig. 1.1b.

In contrast to these types of thermal excitation, there are some modes which are excited over a restricted range of temperatures and so contribute an appreciable specific heat over that small range only. Typical is the excitation of energy in a system with two levels approximately $kT_0$ apart. At temperatures much below $T_0$, the thermal energy is insufficient to cause many excitations, as $T \sim T_0$ transitions can occur freely, while at much higher temperature the levels are equally populated and little change in energy is possible. Hence, the specific heat is significant only in the region $T \sim T_0$ and is usually detected as a sharp bump superimposed on the other specific-heat contributions. Such behavior is called a *specific-heat anomaly*; Fig. 1.2 shows a good example. The hump at about 0.1°K is due to the transitions among the energy levels of the paramagnetic ions. The substance chrome methylamine alum, $Cr(NH_3CH_3)(SO_4)_2 \cdot 12H_2O$, is peculiar in showing another nearby anomaly. The sharp peak at 0.02°K is caused by a cooperative transition from a paramagnetic state to an ordered antiferromagnetic state.

Any theory of solids, liquids, or gases must take into account the different types of thermal agitation, and so must lead in the first place to the energy levels of the system. The calculation of heat

capacities involves no further assumptions. It is thus a special feature of the specific-heat studies that they provide a first ready test of the theory. However, the specific heat is only an averaged quantity; consequently, the full details of the energy levels are not usually elucidated unless the measurements are supplemented by the investigations of other properties of the substance. This interplay among the different properties of the systems will become evident in the later chapters, where the heat capacity due to the various modes of thermal agitation will be analyzed with the help of suitable simple models. Before proceeding to this, it is convenient to indicate how the specific heats are experimentally determined. Only an outline of the experimental methods will be given here, since the matter is taken up comprehensively in a forthcoming monograph in this series.

## 1.7. CALORIMETRY

At the turn of the present century, the vacuum calorimeter was introduced by Nernst for the determination of specific heats at low temperatures; subject to minor modifications, it is still the method widely used. In its simple form, Fig. 1.3a, it consists of the block B, over which an insulated coil W of platinum wire is wound. The block B may be either a piece of the solid to be studied or merely a container for some solid, liquid, or gas. B is suspended by the leads LL in a vacuum-tight container C, which is cooled in a dewar D containing liquid air, hydrogen, or helium, as the case may be. Initially, C is filled with helium gas at a low pressure of about 1 mm of mercury, and the block B is cooled to the temperature of the bath by the heat transfer through the gas. After B has been cooled, the gas is pumped away. Thereafter, B is thermally isolated. Known quantities of heat are applied to the coil W by passing known currents for definite intervals of time, and the resulting rise of temperature is measured by the change in resistance of the platinum wire. It is now common to have separate heaters and sensitive thermometers. It is sometimes advantageous to supply heat continuously and to derive the specific heats from a continuous record of the temperatures.

The vacuum space C avoids any heat transfer by gas conduction or convection. At temperatures above 20°K, heat transfer by radiation, varying as $T^4$, becomes significant. This difficulty is avoided in adiabatic calorimetry, introduced at low temperatures by Lange, Southard, and Andrews,[8] although at room temperature it has been brought to a high degree of refinement by Richards and many other earlier workers. The adiabatic shield S (Fig. 1.3b) contains a separate heater, and is made to follow the temperature of B accurately. This can be done either manually or by suitable electronic devices making
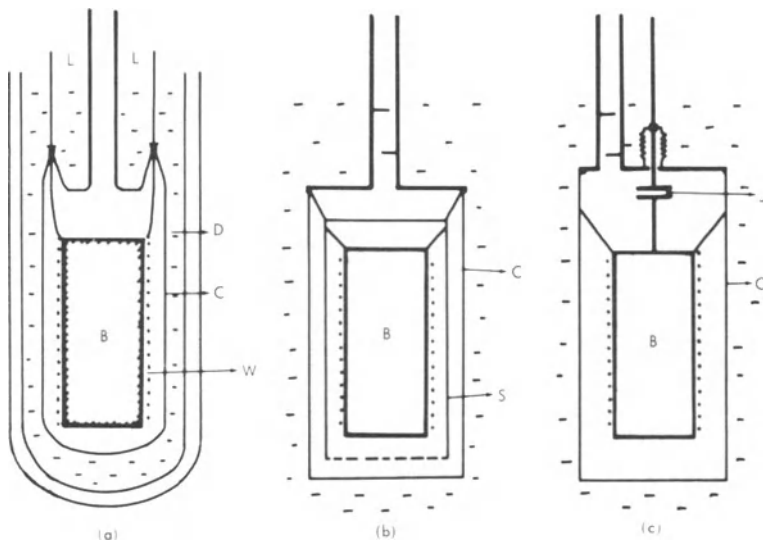
Fig. 1.3. Vacuum calorimeter and its modifications.

use of differential thermocouples between B and C to observe any temperature difference between them. In the liquid-helium range, a different problem arises because the helium gas used for precooling B is strongly absorbed on the surfaces of B and C. The vacuum is thereby spoiled, and even with fast pumps it may take a few hours to dislodge all the helium gas. So it is preferable to avoid the helium exchange gas altogether, though this necessitates alternative provisions for cooling the block B to low temperatures. In a simple form, a polished metal plate J (Fig. 1.3c), which can be operated from outside the cryostat and which is in good thermal contact with C, is made to press firmly against a similar polished metal disk attached to B. C remains evacuated throughout the operation. The drawback in this technique is that when the difference in temperature between B and C is small, especially at low temperatures, heat transfer across the mechanical contact becomes very inefficient. Several cryostats, ingeniously designed to minimize these and other difficulties, are described by White[9] and Hill.[10] These and other books[11,12] contain a full account of the general cryogenic techniques.

The above method is useful for measuring the specific heat above about 1°K. Below this temperature, one has to use the $^3$He isotope as a coolant (up to about 0.3°K), or use adiabatic demagnetization to attain low temperatures. The details of these refrigeration techniques are described in several texts.[9,10,12] Mention need be made

here only of some special methods of finding specific heats in particular cases. Below 1°K, the heat capacity of the demagnetization pill used to cool the specimen becomes large compared to the heat capacity of the specimens. One way of avoiding this interference is to pass a periodic heat-wave through the specimen and to derive $C_p$ as in the Ångstrom method of finding diffusivity at room temperatures.[13] For magnetic materials, specific heats may be obtained from studies of paramagnetic relaxation or demagnetization from various magnetic fields (Chapter 4).

In the case of gases, measurements made by having the gas in a closed container, as originally done by Eucken and others for hydrogen, yield $C_v$ directly, because the volume change under such conditions is very small. The specific heat at constant pressure can be determined by continuous-flow methods as at room temperatures. Information about $C_v$ in gases may be obtained from the heat conduction when the mean free path becomes comparable to the dimensions of the measuring apparatus. Moreover, the ratio of specific heats $C_p/C_v$ may be determined from the velocity of sound in gases (Section 8.3). A good survey of the measurement of specific heat in gases is given by Rowlinson.[14]

There are many problems associated with thermometry and heat leakages, the details of which are discussed in several reviews.[15,16,17] A point often overlooked is the need for pure specimens. Parkinson[16] has listed a number of anomalous results originally reported in such common materials as sodium, mercury, beryllium, germanium, etc., which had been puzzling and which have now proved to be not characteristic of the pure materials. When it is realized that at 0.1°K chrome methylamine alum has a molar heat capacity nearly 40,000 times that of copper, it is obvious that even traces of impurities may sometimes vitiate calorimetric measurements.

## REFERENCES

1. M. W. Zemansky, *Heat and Thermodynamics*, McGraw-Hill, New York, 1957. J. K. Roberts and A. R. Miller, *Heat and Thermodynamics*, Blackie, London, 1960.
2. H. B. Huntington, *Solid State Phys.* **7**, 213 (1958). R. F. S. Hearmon, *Introduction to Applied Anisotropic Elasticity*, Oxford University Press, Oxford, 1961.
3. R. Viswanathan and E. S. Raja Gopal, *Physica* **27**, 1226 (1961).
4. H. R. O'Neal, Ph.D. thesis (unpublished), University of California, 1963.
5. J. A. Rayne, *Austral. J. Phys.* **9**, 189 (1956). K. G. Ramanathan and T. M. Srinivasan, *J. Sci. Industr. Res.* **16B**, 277 (1957).
6. W. E. Gardner and N. Kurti, *Proc. Roy. Soc. (London), Ser. A* **223**, 542 (1954).
7. C. Kittel, *Elementary Statistical Physics*, Wiley, New York, 1958. D. K. C. MacDonald, *Introductory Statistical Mechanics for Physicists*, Wiley, New York, 1963.
8. F. Lange, *Z. Phys. Chem.* **110**, 343 (1924). J. C. Southard and D. H. Andrews, *J. Franklin Inst.* **209**, 349 (1930).

9. G. K. White, *Experimental Techniques in Low Temperature Physics*, Clarendon, Oxford, 1959.
10. F. E. Hoare, L. C. Jackson, and N. Kurti, *Experimental Cryophysics*, Butterworth, London, 1961.
11. F. Din and A. H. Cockett, *Low Temperature Techniques*, Newnes, London, 1960.
12. A. C. Rose-Innes, *Low Temperature Techniques*, English University Press, London, 1964.
13. D. H. Howling, E. Mendoza, and J. E. Zimmerman, *Proc. Roy. Soc. (London)*, *Ser. A* **229**, 86 (1955). N. V. Zavaritsky, *Progr. Cryogenics* **1**, 207 (1959).
14. J. S. Rowlinson, *The Perfect Gas*, Pergamon, Oxford, 1963, chapter 2.
15. P. H. Keesom and N. Pearlman, *Handbuch der Physik*, *XIV (I)*, 282 (1956).
16. D. H. Parkinson, *Rept. Progr. Phys.* **21**, 226 (1958).
17. R. W. Hill, *Progr. Cryogenics* **1**, 179 (1959). W. P. White, *The Modern Calorimeter*, Chem. Pub. Co., New York, 1928. J. M. Sturtevant, in: A. Weissberger (ed.), *Physical Methods of Organic Chemistry*, Part I, Interscience, New York, 1959, chapter 10.

*Chapter 2*

# Lattice Heat Capacity

## 2.1. DULONG AND PETIT'S LAW

One of the earliest empirical generalizations concerning the specific heat of solids was enunciated by Dulong and Petit in 1819. Its theoretical justification was advanced by Boltzmann in 1871, and in 1907 Einstein showed why it failed at low temperatures. These dates are among the principal landmarks in the study of specific heats. To appreciate the significance of these developments, consider the specific heats of several common elements at room temperatures, as collected in Table 2.I. The specific heat per gram of the element varies considerably, being small for the elements of high atomic weight and large for those of low atomic weight. However, the heat capacity per gram-atom of all of them is nearly equal to 6.2 cal/mole·deg,

**Table 2.I. Specific Heat of Solid Elements at Room Temperature**[1]

| | Element | | | | | | |
|---|---|---|---|---|---|---|---|
| | Bi | Pb | Au | Pt | Sn | Ag | Zn |
| $c_p$ | 0.0299 | 0.0310 | 0.0309 | 0.0318 | 0.0556 | 0.0559 | 0.0939 |
| Atomic weight | 209.0 | 207.2 | 197.0 | 195.1 | 118.7 | 107.9 | 65.4 |
| $C_p$ | 6.22 | 6.43 | 6.10 | 6.21 | 6.60 | 6.03 | 6.14 |
| | Cu | Fe | Al | Si | B | C(gr) | C(di) |
| $c_p$ | 0.0930 | 0.110 | 0.218 | 0.177 | 0.26 | 0.216 | 0.12 |
| Atomic weight | 63.6 | 55.9 | 27.0 | 28.1 | 10.8 | 12.0 | 12.0 |
| $C_p$ | 5.92 | 6.14 | 5.83 | 5.00 | 2.84 | 2.60 | 1.44 |

$C_p$ in cal/mole·deg, Sn = grey tin, C(gr) = graphite, C(di) = diamond.

**Table 2.II. Molar Heat Capacity of Compounds[1]**
**(in cal/mole·deg)**

| | Compound | | | | | | | | |
| --- | --- | --- | --- | --- | --- | --- | --- | --- | --- |
| | NaCl | KBr | AgCl | PbS | CuS | $Ag_2S$ | $PbCl_2$ | $CaF_2$ | $Fe_2O_3$ |
| $C_p$ | 11.93 | 12.25 | 12.15 | 12.01 | 12.33 | 17.83 | 18.05 | 16.56 | 27.2 |

which is the rule found by Dulong and Petit in 1819. A closer inspection shows that for "light and hard" elements (silicon, boron, and carbon) the atomic heat capacity falls much below the Dulong–Petit value.

Subsequent experiments by several workers during the period 1840 to 1860 revealed an important extension of the Dulong–Petit rule. The molar heat capacity of a compound is equal to the sum of the atomic heat capacities of the constituent elements. Table 2.II illustrates this rule, which is sometimes called the *law of Neumann and Kopp*. Diatomic solids have a molar specific heat of approximately 12cal/mole·deg, while triatomic solids have $C_p \sim 18$ units. As in Table 2.I, there are many substances that deviate greatly from this simple behavior, but on the whole there is enough evidence for taking the atomic specific heat to be about 6 cal, irrespective of the chemical structure of the substance. Since the gas constant $R = Nk$ has a value of approximately 2 cal/mole·deg, this statement implies that each atom in a solid contributes about $3k$ to the specific heat.

## 2.2. EQUIPARTITION LAW

The empirical results of the previous section can be readily interpreted on the basis of the theorem of equipartition of energy developed by Boltzmann. A derivation of this theorem may be found in the texts on statistical mechanics or in other places.[2,3] In classical mechanics, a system executing small oscillations may be described in terms of normal coordinates; its energy is then expressed as the sum of several squared terms. For example, the energy of a linear harmonic oscillator is made up of kinetic and potential energies $(2m)^{-1}p^2 + \frac{1}{2}m\omega^2q^2$, where $p$ is the momentum and $q$ the coordinate. For a three-dimensional oscillator there are three $p_x^2, p_y^2, p_z^2$ terms and three $q_x^2, q_y^2, q_z^2$ terms. Each such square term in the energy expression is said to arise from a degree of freedom of the system, which is nothing more than an enumeration of the independent variables needed to describe the system. The equipartition law states

that in thermal equilibrium each degree of freedom contributes $\frac{1}{2}kT$ to the energy of the particle. Thus, a three-dimensional oscillator has an internal energy $3kT$ when a system of such oscillators is in thermal equilibrium.

The atoms in a solid are arranged in a regular lattice and held in their lattice sites by interatomic forces acting on them. A simple model of a lattice would be a set of mass points connected to one another by elastic springs. The atoms can vibrate about their mean positions under the influence of the forces acting on them, and if the amplitude of oscillation is small, the atoms may be considered as harmonic oscillators. Each (three-dimensional) oscillator has six degrees of freedom, and by the equipartition theorem has an internal energy $3kT$. In a gram-atom of the element there are $N$ atoms and the internal energy is $3NkT$. Therefore, the heat capacity is $C_v = \partial E/\partial T = 3R \approx 5.96$ cal/mole·deg. For a compound with $r$ atoms per molecule, the molar heat capacity is $3rR$.

Classical statistical mechanics is thus able to justify the empirical observation of Dulong and Petit and others. The successful theoretical explanation of the heat capacity of solids (and of gases, which will be discussed in Chapter 6) was, at that time, partly instrumental in the acceptance of molecular mechanisms not only for mechanical properties but also for thermal properties of matter, a fact which is taken for granted nowadays.

A perusal of Table 2.I shows, however, that for some substances the heat capacity is much less than the equipartition value. Experiments performed above room temperature revealed that at high temperatures the heat capacity of even these substances increases to 3R. For example, diamond, which had $C_p \sim 1.4$ cal/mole·deg at 300°K, had $C_p \sim 5.5$ units at 1200°K. On the other hand, when cryogenic experiments were performed, it was found that the specific heat of all materials decreased at low temperatures. Illustrative is the behavior of copper with $C_p \sim 5.9$ cal/deg at 300°K and $\sim 3.9$ units at 100°K. At 4°K, its value is only 1/4000 of the equipartition value! Classical statistical mechanics could offer no cogent explanation whatsoever for such large temperature variations of specific heats. The clarification had to await the development of quantum theory.

## 2.3. QUANTUM THEORY OF SPECIFIC HEATS

In 1901, Planck was forced to conclude from his studies on the spectral distribution of blackbody radiation that the energy of an oscillator of frequency $v$ must change in discrete steps of $hv$, and not continuously, as had been assumed in classical mechanics. The constant $h$, called *Planck's constant*, has a value of $6.626 \times 10^{-27}$ erg-sec.

Einstein soon realized that electromagnetic radiation travels in packets of energy $hv$ and momentum $h/\lambda$; these wave packets have come to be called *photons*. Finally, in 1907, Einstein took the bold step of applying quantum theory outside the field of electromagnetic radiation to the thermal vibrations of atoms in solids. The floodgates had been opened for quantum concepts to pervade the whole of our physical knowledge.

Before going into the details of the theory, it is best to grasp the simple implications of the quantization of energy. It was known even in 1907 that the atomic vibrations in a solid have frequencies of the order of $10^{13}$ cps. The energy $hv$ needed to excite such a vibration is approximately $6.6 \times 10^{-14}$ erg. In a naïve way, if this is equated to the classical energy of an oscillator $3kT_0$, then $T_0$ comes out to be 150°K. At high temperatures, the atomic vibrations will be excited fully, but below about 150°K the vibrations cannot be excited because the minimum energy needed for this process is not available. Hence, the specific heat should drop from its classical equipartition value to zero below about 150°K. In practice, the reduction will not be so abrupt as in this naïve picture, because at any temperature above 0°K there is a statistical probability of exciting some vibrations, given by the Boltzmann factor $\exp(-hv/kT)$. The effect of lowering the temperature is to reduce the number of excitations, and in this manner the quantization of energy levels brings about a reduction of specific heats at low temperatures.

The formal way of handling the problem, as outlined in Section 1.5, is to calculate the partition function $Z$ and the Helmholtz free energy $A$:

$$A = -kT \ln Z \qquad Z = \sum_i \exp\left(\frac{-E_i}{kT}\right) \qquad (2.1)$$

An atom in a lattice vibrates under the influence of the forces exerted on it by all the other atoms of the system. If the amplitude of the vibrations is small, classical mechanics shows that the vibrations can be resolved into normal modes, i.e., into a set of independent one-dimensional harmonic oscillations. In a mole of the substance, the molecules of which contain $r$ atoms, there are $3rN$ such independent modes. The total energy is the sum of their energies, and the total partition function is the product of the $3rN$ modes:

$$Z_{\text{system}} = \Pi z_{\text{mode}}$$

Detailed quantum-mechanical considerations show that the energy levels of a linear oscillator are given by $\varepsilon_n = (n + \frac{1}{2})hv$, the $\frac{1}{2}hv$ being the zero-point energy. Then, summing up the geometrical

series,

$$z = \sum_{n=0}^{\infty} \exp\left(\frac{-\varepsilon_n}{kT}\right) = \frac{\exp(-\frac{1}{2}hv/kT)}{1 - \exp(-hv/kT)} = \frac{1}{2} \operatorname{csch}\left(\frac{\frac{1}{2}hv}{kT}\right) \quad (2.2)$$

Now the number of modes in a crystal is so large, of the order of $10^{23}/\text{cm}^3$, that it is advantageous to write

NUMBER OF MODES BETWEEN FREQUENCIES $v$ AND $v + dv = 3rNg(v)\,dv$
$$\text{(2.3)}$$

Obviously, the total number of modes is $3rN$, so that

$$\int_0^\infty g(v)\,dv = 1 \quad (2.4)$$

With the distribution of frequencies $g(v)$, equation (2.1) becomes

$$A = 3rNkT \int_0^\infty \ln\left[2\sinh\left(\frac{\frac{1}{2}hv}{kT}\right)\right] g(v)\,dv$$

$$= E_0 + 3rNkT \int_0^\infty \ln\left[1 - \exp\left(\frac{-hv}{kT}\right)\right] g(v)\,dv \quad (2.5)$$

where

$$E_0 = \frac{1}{2}3rN \int_0^\infty hvg(v)\,dv$$

is the zero-point energy of the solid. The calculation of the specific heat is now straightforward, and it may be verified that

$$C_v = -T\left(\frac{\partial^2 A}{\partial T^2}\right)_v = 3rNk \int_0^\infty \left(\frac{\frac{1}{2}hv}{kT}\right)^2 \operatorname{csch}^2\left(\frac{\frac{1}{2}hv}{kT}\right) g(v)\,dv \quad (2.6)$$

This general introduction serves several purposes. For the sake of simplicity, the later calculations of specific heats will start from a discussion of the mean energy of the particles. In satisfying the didactic exigencies, it should not be forgotten that a pedestrian derivation from first principles is possible. Secondly, in some of the discussions it will not be obvious whether $P$ or $V$ is held constant, that is, whether $C_p$ or $C_v$ is calculated, mainly because there is no thermal expansion if harmonic vibrations are assumed. The above derivation makes it clear that only $C_v$ is calculated. Thirdly, the thermodynamics of crystals has been reduced to the evaluation of the distribution of frequencies $g(v)$. The determination of $g(v)$ is a dynamical problem of great complexity, and it is best to introduce the subject with the simple models proposed by Einstein (1907), Debye (1912), and Born and Von Kármán (1912).

## 2.4. EINSTEIN'S MODEL

Einstein, in his fundamental paper, considered a very simple model of lattice vibrations, in which all the atoms vibrate independently of one another with the same frequency $v_E$. In a substance such as copper, for instance, an atom has the same environment as any other atom, and it is plausible to suppose as a first approximation that all atoms vibrate with the same frequency $v_E$. If that were so, $g(v)$ would be zero for $v \neq v_E$ and nonzero for $v = v_E$. Then equation (2.6) immediately gives

$$C_v = 3rNk\left(\frac{\frac{1}{2}hv_E}{kT}\right)^2 \operatorname{csch}^2\left(\frac{\frac{1}{2}hv_E}{kT}\right) \qquad (2.7)$$

which is Einstein's well-known relation.

It is, however, instructive to derive the same relation by a different method. The atoms in a solid vibrate about their mean positions, and for such localized particles Maxwell–Boltzmann statistics is applicable. This means that the probability of exciting an energy $\varepsilon$ at an equilibrium temperature $T$ is proportional to $\exp(-\varepsilon/kT)$. According to quantum theory, the energy levels of an oscillator $v$ are given by $\varepsilon_n = (n + \frac{1}{2})hv$. In thermal equilibrium, the probability that a given oscillator will be in the energy state $\varepsilon_n$ is proportional to the Boltzmann factor $\exp(-\varepsilon_n/kT)$, and so the average energy of the oscillator is

$$\bar{\varepsilon} = \frac{\sum\limits_{n} \varepsilon_n \exp(-\varepsilon_n/kT)}{\sum \exp(-\varepsilon_n/kT)} = \frac{1}{2}hv + hv\frac{\sum ne^{-nx}}{\sum e^{-nx}}$$

where $x = hv/kT$. Now

$$\frac{\sum ne^{-nx}}{\sum e^{-nx}} = -\frac{d}{dx}\ln\sum e^{-nx} = -\frac{d}{dx}\ln\frac{1}{1 - e^{-x}} = \frac{1}{e^x - 1}$$

Therefore, at a temperature $T$, the mean energy of the oscillator is

$$\bar{\varepsilon} = \frac{1}{2}hv + \frac{hv}{\exp(hv/kT) - 1} \qquad (2.8a)$$

On differentiating this, the specific-heat contribution from the oscillator is seen to be

$$\frac{\partial \bar{\varepsilon}}{\partial T} = \frac{kx^2 e^x}{(e^x - 1)^2} \qquad \left(x = \frac{hv}{kT}\right) \qquad (2.8b)$$

In the Einstein model, all the $3rN$ independent vibrations have the same frequency $v_E$. Hence, the total internal energy is

$$E = 3rRT\left[\tfrac{1}{2}x_E + \frac{x_E}{e^{x_E} - 1}\right] \qquad \left(x_E = \frac{hv_E}{kT}\right) \qquad (2.9a)$$

and the molar heat capacity is

$$C_v = 3rR\frac{x_E^2 e^{x_E}}{(e^{x_E} - 1)^2} = 3rR(\tfrac{1}{2}x_E)^2 \operatorname{csch}^2(\tfrac{1}{2}x_E) \qquad (2.7)$$

The molar entropy is

$$S = 3rR\left[\frac{x_E}{e^{x_E} - 1} - \ln(1 - e^{-x_E})\right] \qquad (2.7a)$$

The quantity $hv_E/k$ plays the role of a scaling factor for temperature and is called the *Einstein temperature* $T_E$. The Einstein functions $E(T_E/T)$ and $C_v(T_E/T)$ are tabulated in several places[4,5] (see also the appendices at the end of Chapter 8). A consideration of the values of exponentials in equation (2.7) at very high and very low temperatures shows that

$$C_v = 3rR\left[1 - \tfrac{1}{12}\left(\frac{T_E}{T}\right)^2 + \ldots\right] \qquad \text{(high temperature, } T \gg T_E)$$
$$\qquad\qquad\qquad\qquad\qquad\qquad\qquad\qquad\qquad\qquad\qquad (2.10)$$
$$= 3rR\left(\frac{T_E}{T}\right)^2 \exp\left(-\frac{T_E}{T}\right) + \ldots \qquad \text{(low temperature, } T \ll T_E)$$

The Einstein theory leads to the Dulong–Petit value at high temperatures, and shows how at low temperatures the quantization of lattice vibrations results in a reduction of heat capacity. The theory contains one unknown parameter $T_E$, which may be approximately related to the compressibility and density of the solid. For many materials, $T_E \sim 200°K$, which accounts for the success of the Dulong–Petit law at room temperature. For diamond, with a value $T_E \sim 1326°K$, Einstein was able to explain quantitatively the variation of $C_v$ then available over a range of 200 to 1200°K (Fig. 2.1). The simplicity of the theoretical analysis and the qualitative correctness of the conclusions left no doubt that the decrease of specific heats of low temperature was indeed a quantum phenomenon.

In order to check Einstein's theory in some detail, systematic calorimetric measurements were undertaken at low temperatures by Nernst, Eucken, and others. The qualitative features of Einstein's theory were confirmed very well, but the quantitative agreement was not satisfactory. In particular, equation (2.10) shows that below $T/T_E \sim 0.1$, the specific heat should become extremely small, of the
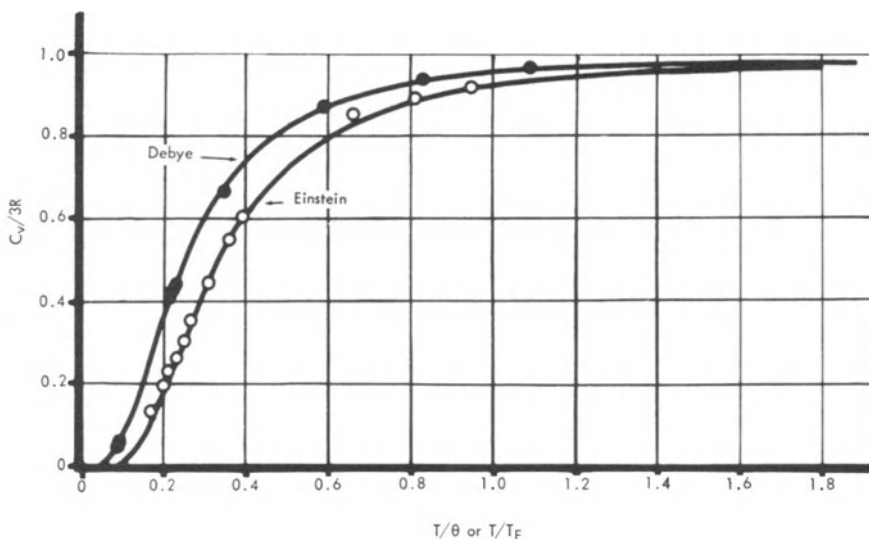
Fig. 2.1. Temperature variation of heat capacity in Einstein and Debye models. Original comparison of Einstein for diamond ($T_E = 1326°K$) and of Debye for aluminum ($\theta_D = 396°K$) are shown.

order of mJ/mole · deg, whereas experimentally the decrease was much slower (Fig. 2.1). Several workers, including Einstein himself, recognized that the model was oversimplified.[6] In a tightly coupled system, such as a lattice, the motion of one atom affects the vibrations of the others and the atoms can vibrate with several frequencies. Experimentally, Nernst and Lindemann pointed out that the observations could be fitted better if two frequencies $v_E$ and $\frac{1}{2}v_E$ were used instead of $v_E$ alone. In the simple model, there is no provision for vibrations of low frequencies, which alone can be fully excited in the region of small energies, i.e., at low temperatures. These ideas culminated in the calculations (1912) of Debye and Born and Von Kármán, who used a better description of lattice vibrational frequencies. Debye's model is the simpler and will be taken up in the following section.

Despite the cursory dismissal usually accorded to Einstein's oversimplified model, the calculation was a fundamental step in enlarging the field of application of quantum ideas. A great deal of experimental and theoretical work on the specific heats of solids and gases was inspired by it. Indeed, even today Einstein's calculation remains useful as a very simple approximation in many problems of the solid state and in discussion of molecular vibrations.

## 2.5. DEBYE'S MODEL

The quantization of vibrational energy implies that at low temperatures only the low-frequency modes of lattice vibrations will be appreciably excited. Now the usual very-low-frequency vibrations of a solid are its acoustic oscillations. They have wavelengths much larger than atomic dimensions, and so in discussing their behavior the ideas of an elastic continuum may be borrowed. Debye calculated the distribution of frequencies which result from the propagation of acoustic waves of permitted wavelengths in a continuous isotropic solid and assumed the same distribution to hold good in a crystal, also. The use of such a $g(v)$ turned out to be so extraordinarily successful in explaining the thermal behavior of solids that it merits discussion in some detail.

A plane wave propagating with velocity $c$ in an isotropic medium satisfies the equation

$$c^2 \nabla^2 \phi = \frac{\partial^2 \phi}{\partial t^2}$$

For convenience, take a rectangular parallelopiped of sides $L_1, L_2, L_3$, on the faces of which the displacement amplitude is zero. Then the wave equation has a standing-wave solution of the form

$$\phi = A \sin q_1 x \sin q_2 y \sin q_3 z \sin 2\pi v t$$

where the orders of the overtones $n_i$ are related to the wave vectors $q_i = 2\pi/\lambda_i$ by

$$q_i = \frac{n_i \pi}{L_i} \qquad (n_1, n_2, n_3 = 0, 1, 2, ...)$$

An enumeration of the values of $n_i$ which give a frequency between $v$ and $v + dv$ solves the problem of finding $g(v)dv$. In a practical case, the number of modes, approximately $10^{23}/\text{cm}^3$, is so large that the $n_i$ may well be treated as continuous variables. The number of allowed values of $n_i$ in the range $n_i$ to $n_i + dn_i$ is then equal to

$$\Delta n_1 \Delta n_2 \Delta n_3 = \frac{L_1 L_2 L_3}{\pi^3} \Delta q_1 \Delta q_2 \Delta q_3 = \frac{V}{\pi^3} \Delta q_1 \Delta q_2 \Delta q_3$$

where $V$ is the volume of the solid. Now the frequency of the wave is

$$v^2 = \frac{(q_1^2 + q_2^2 + q_3^2)c^2}{4\pi^2} = \frac{q^2 c^2}{4\pi^2}$$

Since the $n_i$ are all positive, this is nothing but the equation for the first octant of a sphere in the $q_1 q_2 q_3$-space. The volume of the shell

between $q$ and $q + dq$, equal to $\frac{1}{8}4\pi q^2\, dq$, corresponds to $(V/2\pi^2)\, q^2\, dq$ allowed values of $n_i$. In terms of frequencies, the number of allowed modes between $v$ and $v + dv$ is

$$n(v)\, dv = \frac{4\pi V}{c^3} v^2\, dv \tag{2.11}$$

In an elastic solid, three types of waves are possible.[7,8] One is the longitudinal wave with velocity $c_L$, for which $\phi_L$ may be taken as the dilatation of a volume element. The other two are transverse shear weaves, and for them $\phi_{T1}, \phi_{T2}$ are the components of the rotation of a volume element. In an isotropic solid, which is being considered at first, the transverse waves have the same velocity $c_T$. Adding the three contributions, the number of frequencies between $v$ and $v + dv$ in an elastic solid is

$$n(v)\, dv = 4\pi V(c_L^{-3} + 2c_T^{-3})v^2\, dv \tag{2.12}$$

Considerations of simplicity necessitated a derivation of equation (2.12) for a rectangular parallelepiped, but the result is not significantly altered by considering a large body with any shape. The same remark holds good for several other distributions of energy levels considered in this book (Sections 2.8 and 6.3). Mathematical proofs of this assertion have been given in various cases.[9]

Debye suggested that the collective low-frequency oscillations of the solid given by equation (2.12) should be applied even at high frequencies and that the discrete nature of the atomic lattice should be taken into account by setting a minimum to the allowed wavelengths. The corresponding upper limit $v_D$ to the frequency is to be obtained from the normalizing condition, equation (2.4), that the total number of modes is equal to $3rN$ per mole. Thus, taking the molar volume to be $V$,

$$\frac{4\pi V}{3}(c_L^{-3} + 2c_T^{-3})v_D^3 = 3rN$$

or

$$v_D = \left(\frac{9rN}{4\pi V}\right)^{1/3}(c_L^{-3} + 2c_T^{-3})^{-1/3} \tag{2.13}$$

For the cut-off procedure to be meaningful, the limiting wavelength should have atomic dimensions. In a typical solid, the minimum possible wavelength is

$$\sim \left(\frac{4\pi V}{9N}\right)^{1/3} \sim \left(\frac{4\pi \times 10}{9 \times 6 \times 10^{23}}\right)^{1/3} \approx 3\text{Å}$$

which is indeed of the same order as the lattice spacing.

The distribution of frequencies may therefore be taken as

$$g(v) = \frac{3v^2}{v_D^3} \qquad \text{for } v \leq v_D$$
$$= 0 \qquad \text{for } v > v_D \tag{2.14}$$

Each wave of frequency $v$ has an energy $hv$ and momentum $h/\lambda$. In the quantum formulation, the lattice waves are called *phonons*; equation (2.14) represents the Debye approximation to the phonon spectrum of a crystal lattice (Fig. 2.5b). The characteristic temperature

$$\frac{hv_D}{k} = \theta_D \tag{2.15}$$

is known as the *Debye temperature*.

It is now a simple matter to check that

$$E = 3rN \int_0^{v_D} \left[ \tfrac{1}{2}hv + \frac{hv}{e^{hv/kT} - 1} \right] \frac{3v^2}{v_D^3} \, dv$$

$$= \frac{9rNk\theta}{8} + \frac{9rNkT^4}{\theta^3} \int_0^{\theta/T} \frac{x^3 \, dx}{e^x - 1} \tag{2.16a}$$

$$S = \frac{9rNk\theta^3}{T^3} \int_0^{\theta/T} \left[ \frac{x}{e^x - 1} - \ln(1 - e^{-x}) \right] x^2 \, dx$$

$$= 3rNk \left[ \frac{4T^3}{\theta^3} \int_0^{\theta/T} \frac{x^3 \, dx}{e^x - 1} - \ln(1 - e^{-\theta/T}) \right] \tag{2.16b}$$

$$C_v = 3rNk \int_0^{v_D} \left( \frac{hv}{kT} \right)^2 \frac{e^{hv/kT}}{(e^{hv/kT} - 1)^2} \frac{3v^2}{v_D^3} \, dv$$

$$= \frac{9rNkT^3}{\theta^3} \int_0^{\theta/T} \frac{x^4 e^x}{(e^x - 1)^2} \, dx$$

$$= 9rNk \left[ \frac{4T^3}{\theta^3} \int_0^{\theta/T} \frac{x^3 \, dx}{e^x - 1} - \frac{\theta/T}{e^{\theta/T} - 1} \right] \tag{2.17}$$

These are the famous relations derived by Debye.

Two general remarks are appropriate here before discussing the theory in detail. According to quantum statistics[2,3], the smallest possible cell in the $p,q$-phase space (momenta $p_x, p_y, p_z$, coordinates $q_x q_y q_z$) is of volume $h^3$. In a gas of free particles contained in an enclosure of volume $V$, the number of allowed cells $n(p) \, dp$ between momenta $p$ and $p + dp$ is $h^{-3} \iiint \iiint dp_x \, dp_y \, dp_z \, dq_x \, dq_y \, dq_z$. The integration over $dq$ is equal to $V$. Next, converting the integral over

*dp* into spherical polar coordinates,

$$n(p)\, dp = \frac{4\pi V}{h^3} p^2\, dp \qquad\qquad (2.18)$$

Considering phonons as free particles with $p = h/\lambda$, this immediately gives equation (2.11). Secondly, in the preceding derivation, Maxwell–Boltzmann statistics was applied to the vibrations of localized atoms in deriving equation (2.7). Instead, one may consider a set of phonons obeying Bose–Einstein statistics and derive Debye's results. This point of view is adopted in Section 5.4 in treating a closely related problem.

## 2.6. COMPARISON OF DEBYE'S THEORY WITH EXPERIMENTS

The Debye model has been extremely successful in correlating the specific heats of solids. The temperature variation of $C_v$ given by equation (2.17) is obeyed very well by a variety of substances, a typical example being given in Fig. 2.1. At high temperatures, the integrand in equation (2.17) approaches $x^2$, so that

$$C_v = 3rR\left[1 - \tfrac{1}{20}\left(\frac{\theta}{T}\right)^2 + \ldots\right] \qquad (T \gg \theta) \qquad (2.19)$$

At very low temperatures, the upper limit of the integral may be taken as infinity, when the integral has a value $12\pi^4/45$. Thus, for $T < \theta/10$,

$$C_v = \tfrac{12}{5} rR\pi^4\left(\frac{T}{\theta}\right)^3 = 464.3\left(\frac{T}{\theta}\right)^3 \text{cal/mole} \cdot \text{deg} \qquad (2.20)$$

$$= 1944\left(\frac{T}{\theta}\right)^3 \text{J/mole} \cdot \text{deg}$$

At intermediate temperatures, the Debye function must be evaluated numerically,[10] and several tables exist.[4,11] A comprehensive numerical tabulation is reproduced at the end of Chapter 8.

The $T^3$-variation at low temperatures was one of the first predictions of the theory. The $T^4$-variation of the internal energy is the acoustic analog of the well-known Stefan–Boltzmann law that the energy density of a photon gas is proportional to $T^4$. Debye's prediction was soon verified, and the specific heat of many dielectric solids, such as rocksalt, sylvine, fluorspar, etc., show excellent agreement with the theoretical law. In Fig. 1.1a, an example was given to illustrate the $T^3$-behavior at sufficiently low temperatures. As a

matter of fact, the $T^3$-law is so universal at very low temperatures that it has found a permanent place in the theory of specific heats, although the range of validity has now been restricted to $T < \theta/50$ on account of more recent theoretical work to be described later.

Apparent deviations are found in some cases for rather obvious reasons. Graphite, boron nitride, and other layered materials, which behave like two-dimensional crystals, show a $T^2$-variation at some temperatures. Similarly, long-chain molecules such as sulfur and some organic polymers exhibit a variation linear in $T$ at some temperatures, as pointed out by Tarasov and coworkers. Even in these cases, detailed calculations show that at sufficiently low temperatures a $T^3$-law should be present, and such measurements have been carried out recently.[12]

Over wide ranges of temperature, the Debye theory has the noteworthy and attractive feature of making the specific heat depend upon a single parameter $\theta$. Therefore, with a suitable choice of the temperature scales, the heat capacities of all substances should fall on the same curve. Schrödinger[13] and later Eucken[1] reviewed the specific-heat data available prior to 1928 and found extraordinarily good agreement with Debye's theory. Figure 2.2, adapted from Schrödinger's review, makes the excellence of the agreement self-evident. Striking agreements such as this have resulted in a widespread application of Debye's theory to a variety of solid state problems, some of which will be mentioned in Section 2.11.
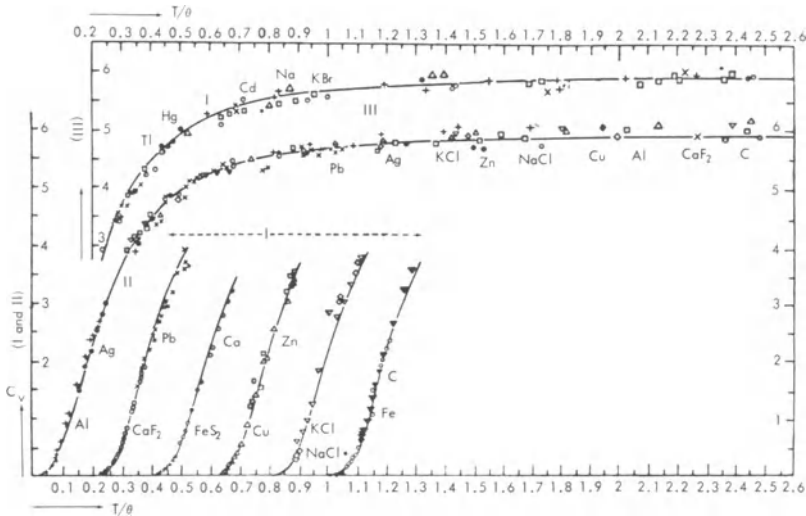


Fig. 2.2. Heat capacities of several substances (in cal/mole·deg) compared with Debye's theory. For the sake of clarity, portions I and III are shown shifted.

It will be seen later that small deviations from the theory are found and that if at each temperature the specific heat is fitted to a Debye term then the resulting values of $\theta$ vary slightly with temperature.[14] In a good many cases, the variation of $\theta$ from its mean value is less than about 10%, though a few exceptions, for instance, zinc and cadmium, show variations of more than 20%. For a preliminary calculation of specific heats, a list of Debye characteristic temperatures, as given in Table 2.III, can be used with complete confidence. The values given in Table 2.III have been taken at $T \sim \theta/2$, which gives a reasonable fit over most of the specific-heat curve.[10] In Chapter 3, $\theta$ values of some metals are given, but there $\theta$ refers to $\theta_0$, the value at very low temperatures, since the specific-heat data at very low temperatures are involved.

### Table 2.III. Debye Characteristic Temperatures of Some Representative Elements and Compounds (in deg K at $T \sim \theta/2$)

| Element | $\theta$ | Element | $\theta$ | Element | $\theta$ | Element | $\theta$ |
|---|---|---|---|---|---|---|---|
| A | 90 | Dy | 155 | Mg | 330 | Sb | 140 |
| Ac | 100 | Er | 165 | Mn | 420 | Se | 150 |
| Ag | 220 | Fe | 460 | Mo | 375 | Si | 630 |
| Al | 385 | Ga (rhom) | 240 | N | 70 | Sn (fcc) | 240 |
| As | 275 | Ga (tetra) | 125 | Na | 150 | Sn (tetra) | 140 |
| Au | 180 | Gd | 160 | Nb | 265 | Sr | 170 |
| B | 1220 | Ge | 370 | Nd | 150 | Ta | 230 |
| Be | 940 | H (para) | 115 | Ne | 60 | Tb | 175 |
| Bi | 120 | H (ortho) | 105 | Ni | 440 | Te | 130 |
| C (diamond) | 2050 | H ($n$-$D_2$) | 95 | O | 90 | Th | 140 |
| C (graphite) | 760 | He | 30 | Os | 250 | Ti | 355 |
| Ca | 230 | Hf | 195 | Pa | 150 | Tl | 90 |
| Cd (hcp) | 280 | Hg | 100 | Pb | 85 | V | 280 |
| Cd (bcc) | 170 | I | 105 | Pd | 275 | W | 315 |
| Ce | 110 | In | 140 | Pr | 120 | Y | 230 |
| Cl | 115 | Ir | 290 | Pt | 225 | Zn | 250 |
| Co | 440 | K | 100 | Rb | 60 | Zr | 240 |
| Cr | 430 | Kr | 60 | Re | 300 | | |
| Cs | 45 | La | 130 | Rh | 350 | | |
| Cu | 310 | Li | 420 | Rn | 400 | | |

| Compound | $\theta$ | Compound | $\theta$ | Compound | $\theta$ | Compound | $\theta$ |
|---|---|---|---|---|---|---|---|
| AgBr | 140 | BN | 600 | KCl | 230 | RbI | 115 |
| AgCl | 180 | $CaF_2$ | 470 | KI | 195 | $SiO_2$ (quartz) | 255 |
| Alums | 80 | $CrCl_2$ | 80 | LiF | 680 | $TiO_2$ (rutile) | 450 |
| $As_2O_3$ | 140 | $CrCl_3$ | 100 | MgO | 800 | ZnS | 260 |
| $As_2O_5$ | 240 | $Cr_2O_3$ | 360 | $MoS_2$ | 290 | | |
| $AuCu_3$ (ord) | 200 | $FeS_2$ | 630 | NaCl | 280 | | |
| $AuCu_3$ (disord) | 180 | KBr | 180 | RbBr | 130 | | |

A fundamental feature of Debye's theory is the connection between elastic and thermal properties of substances. The characteristic temperature $\theta$ may be determined from the velocities of longitudinal and transverse sound waves, using equations (2.13) and (2.15). In crystals, a complication arises because the velocity of elastic waves depends upon the direction of propagation in the anisotropic medium. In general, the three modes have different velocities and are not separable into pure longitudinal and pure shear modes.[7,8] It is then convenient to define a mean velocity

$$3(\overline{c^3})^{-1} = c_L^{-3} + 2c_T^{-3} = (4\pi)^{-1} \int \sum_{i=1,2,3} c_i^{-3} \, d\Omega$$

where $d\Omega$ is an element of solid angle in which the velocities are $c_1, c_2, c_3$. Various approximate procedures for calculating the mean velocity in terms of the elastic constants are reviewed by Blackman[10] and Hearmon.[7] Table 2.IV gives some values of $\theta$ originally calculated by Debye from the elastic constants of polycrystalline materials. A comparison with the calorimetric results at moderate temperatures reveals a surprisingly good agreement in spite of the uncertainty in the elastic constants. Equation (2.13) gives a dependence of $\theta$ upon the density of the substance; in the case of solid helium-four and solid helium-three, which are highly compressible, $\theta$ can be changed by as much as 30% with a moderate pressure of about 150 atm. Another good example is the dependence of $\theta$ upon the isotopic mass of the atom, which is easily observable in lithium isotopes of masses 6 and 7. The experimental difference[15] of $9 \pm 2\%$ is in quantitative agreement with the theoretical estimate of 8%. Such a correlation of the thermal and mechanical properties of solids must be considered a great triumph of the theory.

In view of these remarkable successes, the Debye theory has found a permanent niche in solid state physics. It is based on a simple and understandable model. $C_v$ is expressed in terms of a single parameter $\theta$ and is in reasonably good agreement with experimental values. The predicted $T^3$-behavior is verified at low tempera-

**Table 2.IV. Comparison of $\theta$-Values from Calorimetric and Elastic Data at Room Temperature**

| $\theta$-value | Substance | | | | | | | | | | |
|---|---|---|---|---|---|---|---|---|---|---|---|
| | Al | Cu | Ag | Au | Cd | Sn | Pb | Bi | Pt | Ni | Fe |
| Elastic | 399 | 329 | 212 | 166 | 168 | 185 | 72 | 111 | 226 | 435 | 467 |
| Calorimetric | 396 | 313 | 220 | 186 | 164 | 165 | 86 | 111 | 220 | 441 | 460 |

tures. Further, the theory allows a satisfactory correlation of the calorimetric measurements with elastic and other properties of the substance.

## 2.7. SHORTCOMINGS OF THE DEBYE MODEL

The great popularity of Debye's theory of specific heats should not blind us to its defects. The first hint that all was not well with the theory came from the early observations of Eucken, Grüneisen, and others that if $\theta$ was calculated from the low-temperature elastic constants, the agreement with the thermal values became worse instead of better. For instance, in aluminum, $\theta$(elastic) is 399°K at room temperature and 426° at 0°K (Tables 2.IV and 2.V), while $\theta$(thermal) is 396°. Further, $\theta$ as deduced from the $T^3$-law [equation (2.20)] did not always agree with the value needed to fit the whole of the specific-heat curve. This dilemma was resolved only after the development of the lattice theory.

When accurate values of specific heats at low temperatures became available with improved calorimetric techniques, it was found that equation (2.17) for $C_v$ did not fit the experimental results exactly. This is usually demonstrated by calculating the effective values of $\theta$ necessary to fit the experimental data with equation (2.17) at each temperature. Of course, if Debye's model is really correct, a constant value of $\theta$ should be obtained, but in practice this is not so.[14] Often, as the temperature is lowered the effective value of $\theta$ begins to decrease slightly around $\theta/2$, has a minimum, and then rises to attain a constant value below $\theta/50$. Thus, at temperatures well below $\theta/50$ and above $\theta/2$, the theory works well, with a different $\theta$-value in each range. Figure 2.3 shows a recent study of the $\theta$–$T$ dependence in sodium iodide.[16] At one time, such deviations were attributed to experimental errors, impure specimens, and other extraneous causes, but since the theoretical work of Blackman in 1937, to be discussed below, it has been known that these deviations are genuine.

The fundamental deficiency in the Debye model is the inadequate treatment of the effects arising from the discreteness of atomic arrangements in the crystal. The periodicity of the lattice causes the medium to be dispersive; that is, the velocity of propagation of the lattice wave is a function of the frequency. This phonon dispersion was correctly taken into account in the model proposed by Born and Von Kármán in the same year (1912) as Debye's work. However, the lattice model resulted in cumbersome mathematics, and Born and Von Kármán's original calculation did not give as good a fit with experiments as Debye's simpler analysis. Hence, the application of lattice dynamics (which Born continued to develop in connection
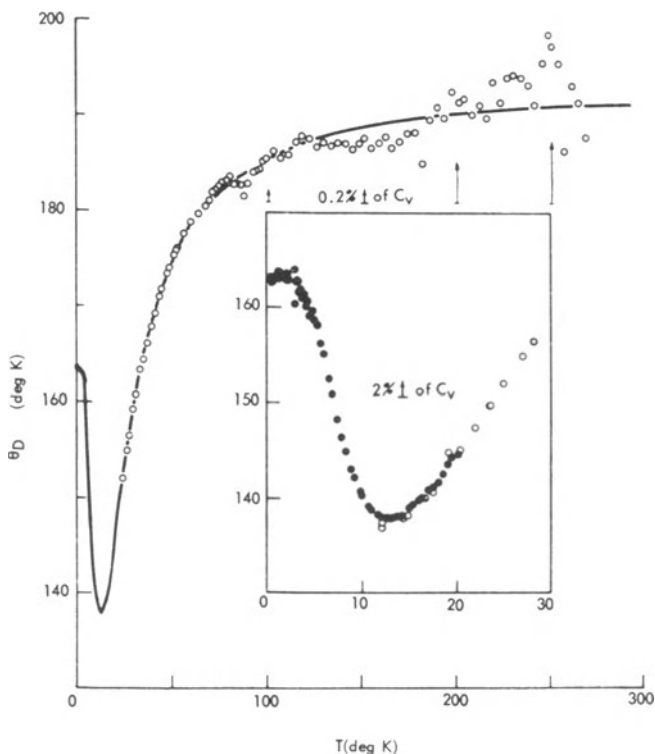
Fig. 2.3.  Variation of effective Debye temperature $\theta$ with $T$ for sodium iodide.[16]

with other problems in solid state) to the question of specific heats lay dormant until Blackman's analysis showed its fundamental significance.[17]

## 2.8. THE BORN–VON KÁRMÁN MODEL

A complete enumeration of the vibrational modes of a three-dimensional lattice involves formidable computations, as will become obvious later.  In an elementary text, it is not practicable to go into these details, and so only the simplified case of a one-dimensional lattice will be considered.  It turns out that a linear monatomic lattice does not exhibit one of the characteristic features of a three-dimensional crystal, namely, the presence of optical modes.  Therefore, the simplest illustrative case is that of a linear diatomic lattice.

To visualize the effects caused by the atomic structure of crystals, consider a one-dimensional chain with two kinds of atoms, spaced $a$ apart. Atoms of mass $m$ are placed at even lattice points ... $2na$, $(2n + 2)a, ...$, while masses $M$ are at odd sites ... $(2n - 1)a, (2n + 1)a,...$. For simplicity, assume further that each atom interacts only with its two neighbors so that a relative displacement $u_{n+1} - u_n$ causes a force $\beta(u_{n+1} - u_n)$ to act on atom $n$. Then the equations of motion for the $2n$ and $2n + 1$ particles are

$$m\ddot{u}_{2n} = \beta(u_{2n+1} - u_{2n} + u_{2n-1} - u_{2n})$$

$$M\ddot{u}_{2n+1} = \beta(u_{2n+2} + u_{2n} - 2u_{2n+1})$$

The boundary conditions do not significantly alter the distribution of frequencies,[9] and so the solutions may be taken in the simple form

$$u_{2n} = \xi \exp i(\omega t + 2nqa)$$

$$u_{2n+1} = \eta \exp i[\omega t + (2n + 1)qa] \qquad (2.21)$$

Substituting in the equations of motion,

$$-\omega^2 m\xi = \beta\eta(e^{iqa} + e^{-iqa}) - 2\beta\xi$$

$$-\omega^2 M\eta = \beta\xi(e^{iqa} + e^{-iqa}) - 2\beta\eta \qquad (2.22)$$

The condition that there are nonzero solutions $\xi,\eta$ describing a wave is that the determinant of the coefficients must vanish:

$$\begin{vmatrix} 2\beta - m\omega^2 & -2\beta\cos qa \\ -2\beta\cos qa & 2\beta - M\omega^2 \end{vmatrix} = 0 \qquad (2.23a)$$

or

$$\omega^2 = \beta(M^{-1} + m^{-1}) \pm \beta[(M^{-1} + m^{-1})^2 - 4M^{-1}m^{-1}\sin^2 qa]^{1/2}$$
$$(2.23b)$$

The two roots correspond to two different branches of the frequency–wave vector relationship, which is shown in Fig. 2.4a. For small $q$, the roots are (i) $\omega^2 = 2\beta a^2 q^2/(M + m)$ and (ii) $\omega^2 = 2\beta(M^{-1} + m^{-1})$. If the root (i) is used, equation (2.22) gives $\xi \approx \eta$; that is, the atoms move together as in ordinary sound vibrations with velocity $[2\beta a^2/(M + m)]^{1/2}$. This branch is called the *acoustical branch*. If the root (ii) is used, equation (2.22) gives $\xi \approx -(m/M)\eta$; that is, the atoms vibrate against each other. If $m$ and $M$ have opposite charges, such a motion may be excited with electric waves, as, for example, by light waves. For this reason, the branch (ii) is called the *optical branch*. The $\omega$–$q$ curve may be stopped at $q = \pi/2a$,
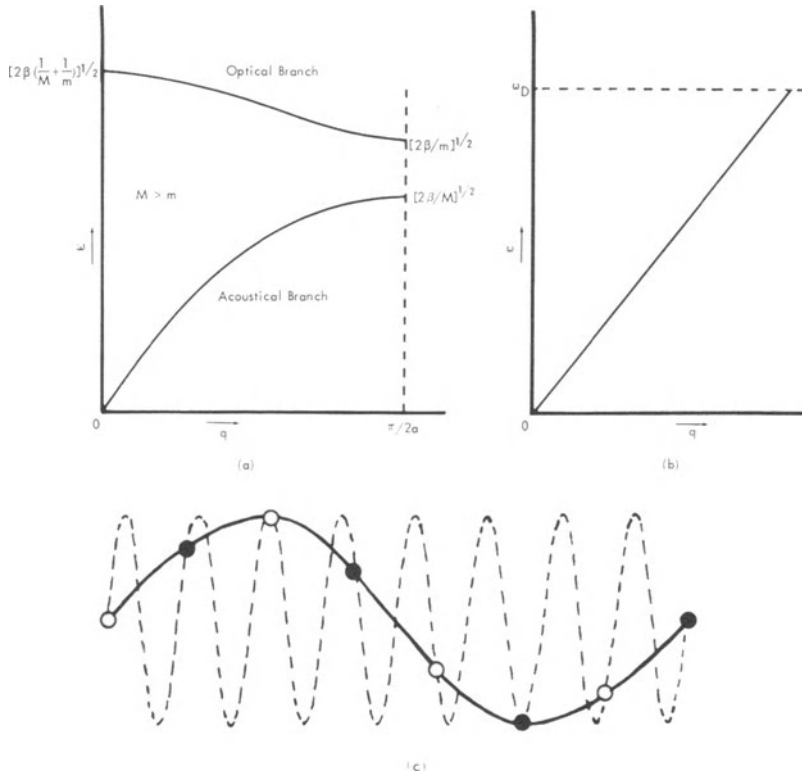
Fig. 2.4. Phonon dispersion: (a) linear diatomic lattic showing dispersion of acoustical and optical branches, (b) elastic continuum, (c) atomic displacements for a wavelength $\frac{8}{7}a$ (broken line) indistinguishable from those for a wavelength $7a$ (full line).

because a continuation beyond this gives no new frequency, and it may be shown[18] from the solutions $u_{2n}, u_{2n+1} ...$, (see also Fig. 2.4c) that the atomic displacements are indistinguishable from those corresponding to $|q| \leq \pi/2a$. In three dimensions, the lattice constant $a$ varies with direction in the crystal, and all the frequencies are included in a volume of $q$-space called the *first Brillouin zone*. Elementary discussions of wave propagation in crystals, together with several electrical and mechanical analogies, have been given by Brillouin[18] and Wannier[19].

Compared to the dispersion relation $\omega = cq$ in an elastic continuum (Fig. 2.4b), the lattice case has two special features. Firstly, the diatomic or polyatomic lattice has additional types of vibration in the form of optical modes, and secondly the phase velocity $\omega/q$ varies with $q$ even in the acoustical vibrations. In recent years,

experiments using neutrons as probes have strikingly confirmed these predictions.[20,21] It may be noted in passing that for a monatomic chain ($M = m$) the determinant (2.23a) has only the acoustical branch as a solution.

Next, it is necessary to find out which values of $q$ are allowed. For this purpose, consider first a chain of $N + 1$ atoms with the atoms 0 and $N$ fixed. Standing waves of the type $U_n = A \sin \omega t \sin nqa$ are the solutions appropriate to this case. The condition that the end atoms are fixed gives $\sin Nqa = 0$ or $q = (\pi/Na)r$, where $r = 1, 2, ..., N - 1$. The condition $r = 0$ is excluded because this gives $u_n = 0$; that is, all the particles are at rest. The number of allowed modes is the same as the number of vibrating atoms. The $\omega$–$q$ relationship consists of $N - 1$ discrete points, but when $N$ is large (of the order of $10^{23}$, as in practical cases) it may be taken as a continuous curve. While a finite chain has standing-wave solutions, it is often convenient to work with traveling waves, which are easily introduced by the Born–Von Kármán cyclic boundary condition. On account of the macroscopic homogeneity of a crystal, a segment containing a large number $N$ of atoms may be assumed to have the same microstructure as a nearby piece. In other words, it is assumed that $u_{n+N} = u_n$. This gives $\exp(iNqa) = 1$ or $q = (2\pi/Na)r$, where $r = \pm 1, \pm 2, ..., \pm N/2$. Again, $r = 0$ is omitted because there is no motion in this case. There are $N$ allowed values of $q$ describing progressive waves traveling in either direction. The number of allowed modes is equal to the number of particles in the segment. The $q$-values are uniformly distributed in the fundamental interval, and when $N$ is large the discrete distribution may be replaced by a continuous distribution. By a similar argument, it may be shown that in three dimensions the allowed values of $q$ are uniformly distributed within the first Brillouin zone and that their number is thrice the number of atoms in the crystal.

Qualitatively, it is easy to see how the dispersion of acoustical and optical phonons affects the distribution of frequencies and the specific heat of a crystal. Suppose the dispersion relations have been found for all the directions in the lattice, each involving, of course, different limiting frequencies. Now, over a solid angle $d\Omega$ (instead of over $4\pi$), equation (2.11) may be written as

$$n(v)\, dv\, d\Omega = V q^2 (dq/d\omega)\, d(2\pi v)\, d\Omega \tag{2.24}$$

so that $g(v)$ is proportional to $q^2(dq/d\omega)$. In a continuum, this term is $c^{-3}v^2$ [equation (2.11)]. In the lattice case, $n(v)$ starts as $v^2$ near zero on account of the low-frequency phonons. As the frequency is increased toward the limiting value of the acoustic mode, $dq/d\omega$ and

hence $n(v)$ become very large. With further increase of $v$, there is a gap, followed by another peak due to the limiting value of the optical modes at $q = \pi/2a$, and finally the contribution from the optical modes.

When $n(v)$ is summed over all directions, $g(v)$ has a characteristic presence of two peaks from the various limiting frequencies at $q = \pi/2a$ (Fig. 2.5c). Instead of a gap between the two peaks, there is only a smeared-out shallow minimum, because the limiting frequencies depend upon the direction of wave propagation. The frequencies of the optical modes in Fig. 2.4a do not vary very much, and since their contributions cover a narrow range of $v$, the second peak in Fig. 2.5c is very much higher than the broad acoustic peak. [In ionic crystals, the optical modes cover a wide range of frequencies, and correspondingly the optical peak is weak in comparison to the first peak (Fig. 2.6a).] Further, $g(v)$ is proportional to $v^2$ at $v \to 0$, being the result of low-frequency acoustic modes averaged over all directions. These features were pointed out first by Blackman in 1937 in the calculation of $g(v)$ for a simple cubic lattice.

The lattice heat capacity $C_g$ ($g$ from German *Gitter = lattice*) given by such a frequency distribution is easily estimated, if it is recalled that at low temperatures only the low-frequency modes with small values of $hv$ will be excited. Near $v = 0$, $g(v)$ varies in the Debye fashion, which means that at very low temperatures $\theta$ will be a constant. As the temperature is raised, more modes are excited than given by the Debye model; that is, the specific heat is greater. Therefore, the effective Debye temperature decreases. The presence of the maximum followed by a minimum ensures that the effective $\theta$ goes through a minimum and then levels off. Thus, $\theta$ varies in a manner very similar to that shown in Fig. 2.3. The lattice theory explains at one stroke why the Debye model is broadly successful and why the effective Debye temperature is slightly temperature-dependent. In Section 2.10, some examples will be given to show how the lattice calculations are successful in quantitatively explaining the observed variation of $\theta$ with $T$.

## 2.9. CALCULATION OF $g(v)$

In the elementary calculation of phonon-dispersion relations given above, drastic simplifications were made in assuming a one-dimensional lattice with nearest-neighbor interactions. In an actual case, not only is the solid a three-dimensional lattice but also the atomic interactions extend over several neighbors. Thus the computation of $g(v)$ for any lattice involves two main hurdles: knowledge of the interatomic forces and solution of the equations of motion for a

large number of wave vectors along a large number of crystal directions. Since the logical necessity of knowing $g(v)$ to calculate $C_v$ and many other properties of solids is hardly in doubt nowadays, much effort has been put into the problem of evaluating $g(v)$.[10,21,22]

Regarding the nature of interatomic forces, we know that Coulomb forces are present between charged ions, but apart from this little else can be said *ab initio*. The practice has been to assume simple models of forces, for example, bond-stretching and bond-bending forces, volume forces for electronic clouds in metals, etc., and to calculate their magnitude from the experimental values of elastic constants and optical frequencies at $q = 0$. The early calculations of $g(v)$ were made in this way with two or three force constants. More recently, inelastic neutron-scattering experiments have given the $\omega-q$ relations along several directions in many crystals. By fitting the theoretical dispersion curves with the experimental ones, numerical values of a number of force constants may be obtained. In this manner, a reasonable, though by no means completely satisfactory, amount of information about interatomic forces may be gathered.

Getting enough frequencies to have a good picture of $g(v)$ is purely a question of the labor and tedium involved in such computations. The original sampling method pioneered by Blackman was to take a set of $q$-values along different directions and calculate the corresponding $v$. Use was made of the symmetry properties of the lattice. Of late, the exploitation of electronic computers for such work has eased the formidable computational task, and the resulting $g(v)$ is limited in accuracy only by the knowledge of the force constants. A measure of the progress made in the computational problem may be inferred from the fact that in 1964 Brockhouse, Woods, and co-workers, using phonon-dispersion curves of sodium obtained from neutron-scattering experiments, determined $g(v)$ from 35 million points inside the Brillouin zone,[23] whereas in 1940 Kellerman's monumental work on sodium chloride was based on 6000 points. Actual frequencies were calculated for about one-twentieth of the total number of points, and the others were obtained by making use of the symmetry of the crystal. In the early calculations on sodium chloride and diamond lattices, symmetry considerations were not properly applied,[21,24] so that the results, quoted widely in many reviews, are somewhat doubtful.

Since the calculation of $g(v)$ is laborious, several approximate methods have been used in the past. In effect, the Einstein and Debye models may be considered very crude approximations to $g(v)$. A somewhat better approximation, first used by Houston, is to calculate $\omega-q$ relations for a few symmetric (say, [100], [111], [110]) directions in a cubic crystal and use interpolation techniques to estimate $g(v)$.

Another method, developed by Thirring, Montroll, and others, is to approximate $g(v)$ from a knowledge of its moments $\int g(v)v^{2n}\,dv$, which can be calculated from the dynamical equations of motion. Although these approximations are sometimes convenient for calculating thermodynamic quantities, they are falling into disfavor with regard to mapping $g(v)$.

Besides these numerical estimates, analytical methods have also had some success. Some one- and two-dimensional lattices are amenable to detailed discussions, and exact expressions for $g(v)$ have been obtained,[21] but so far no realistic three-dimensional lattice has yielded its secrets. However, an important advance was made by Van Hove in 1953. Using topological arguments (for which simple explanations have been attempted [19,21]), he showed that the periodicity of the lattice implies the existence of various kinds of
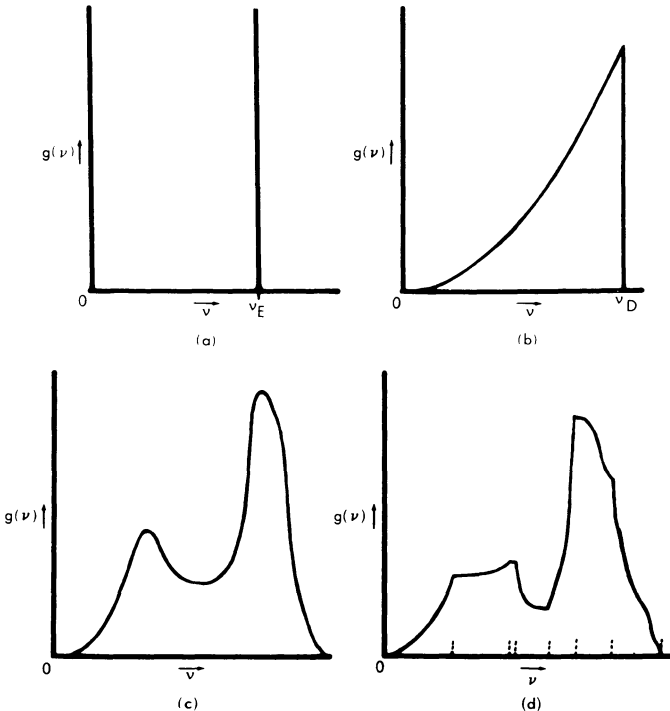
Fig. 2.5. Frequency spectra of lattice vibrations: (a) Einstein model, (b) Debye model, (c) Blackman's approximation of lattice model, (d) schematic exact spectrum with singularities.

singularities in $g(v)$. Thus, in a three-dimensional lattice, infinite discontinuities in the derivative $\partial g/\partial v$ must appear at certain critical points and the curve must have certain well-defined shapes near the singularities. In the more recent calculations of $g(v)$, a knowledge of these critical points has been fruitfully exploited; Fig. 2.5d shows a typical $g(v)$ with the location of the various singularities.

If enough information on the interatomic forces is available and if $g(v)$ is carefully delineated, the lattice theory gives a very good account of the experimental variation of $\theta$ with temperature. Often, the theoretical situation is not so fortunate, and several authors have tried somewhat *ad hoc* combinations of Einstein and Debye terms to represent specific-heat variations. Mention was already made of the Nernst–Lindemann equation using two Einstein functions with frequencies $v_E$ and $\frac{1}{2}v_E$. Simon attempted the combination of a Debye term with a Schottky term (Sections 4.9 and 7.1). Raman and coworkers have used a Debye term together with Einstein terms corresponding to optical frequencies, a practice common in representing the specific heats of organic solids. By a suitable choice of the frequencies, any type of $\theta$–$T$ curve may be obtained.[25] All these refinements of the Einstein and Debye models may yield a reasonable variation of $\theta$ with $T$, but they have neither the simplicity of Debye's theory nor the theoretical justification of lattice dynamics. Since the specific heat is the average over the entire $g(v)$, agreement with the observed $C_v$ should not be taken as a criterion for the correctness of a calculation of $g(v)$. It is also clear that any method to find $g(v)$ from the experimental values of $C_v$ is not likely to be accurate. In the past, several attempts at the inversion of specific heats to get $g(v)$ have been made, which amply demonstrated how insensitive $C_v$ is to the details of the frequency spectrum.[10,26] At present, experimental information on phonon spectra is most conveniently obtained from neutron scattering, and to a lesser extent from diffuse X-ray scattering.

## 2.10. COMPARISON OF LATTICE THEORY WITH EXPERIMENTS

The literature on the theoretical calculation of $g(v)$, both as an exercise in mathematical physics and in relation to specific heats $c_g$ of the lattice, is extensive.[10,21,22] The purpose of the present work is best satisfied by a few examples illustrating the problems involved.

The first example is sodium chloride,[27] which is a simple lattice investigated several times. The $Na^+$ and $Cl^-$ ions exert Coulomb forces on one another in addition to the short-range repulsive forces arising from the overlap of electron clouds. Dielectric studies reveal
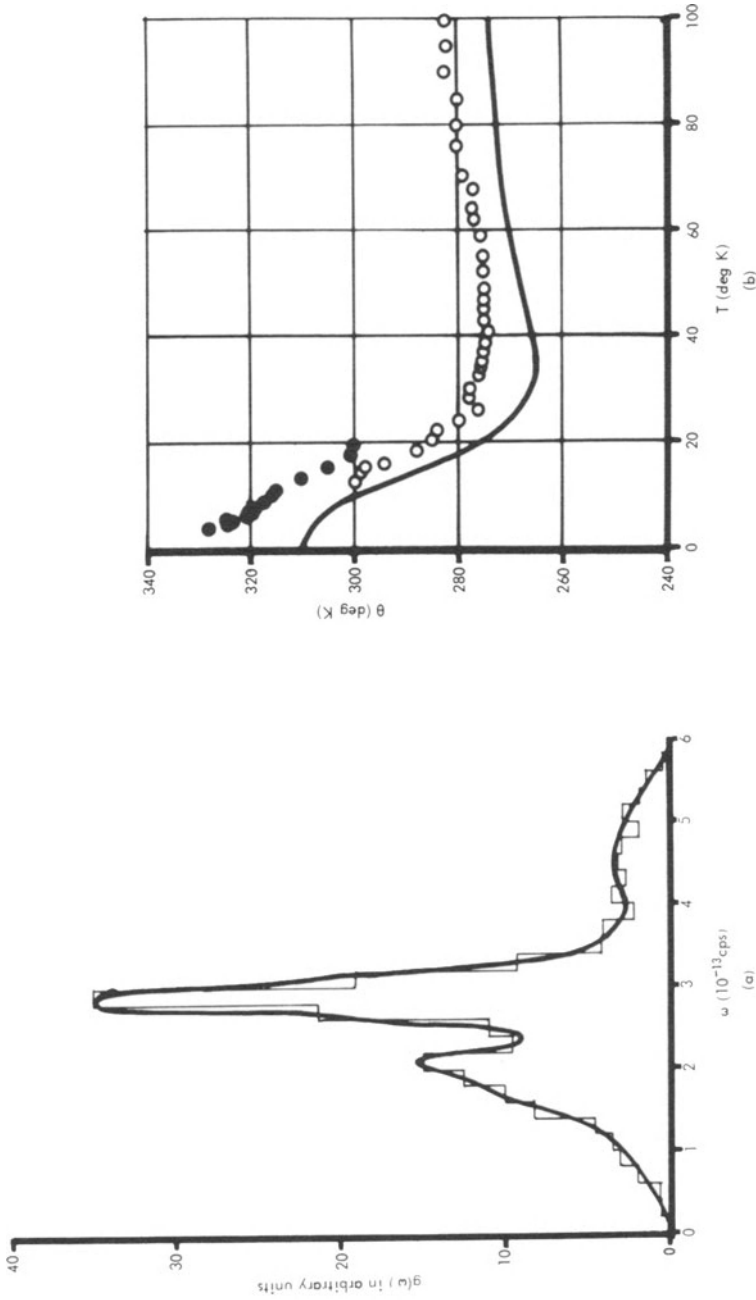
Fig. 2.6. Sodium chloride[27]: (a) frequency distribution (full line drawn through the histograms), (b) Temperature variation of effective $\theta$.

that the effective charge on the ions is about $\pm 0.8e$ rather than $\pm 1e$, on account of the partial shielding of the charges by the electronic clouds. Further, the polarizability of the ions means that small virtual dipoles will be induced during the lattice vibrations. These factors were taken into account using elastic and optical data at $q = 0$, but the distribution was calculated from only about 500 points in the Brillouin zone. A smooth line drawn through the histogram is shown in Fig. 2.6a; such $g(v)$ are typical of many early calculations. The temperature variation of $\theta$ shown in Fig. 2.6b follows the experimental results closely. Considering the uncertainties in estimating the interatomic forces and the approximate calculation of $g(v)$, we should hardly expect an exact fit with the experiments. The fact that theory and experiment follow the same trend and differ only in a normalizing factor must be considered satisfactory. It is also to be noticed that the minimum in $\theta$ is very shallow and may easily be mistaken for the true $T^3$-region reached at very much lower temperatures. For this reason, such shallow minima are called *pseudo $T^3$-regions*.

The second example to be considered is aluminum,[28] for which a model of interatomic forces was fitted to the experimental phonon dispersions along simple directions obtained from diffuse scattering of X-rays at about 300°K. The $g(v)$ was deduced from a total (including those obtained by symmetry) of 150,000 points, and is illustrated in Fig. 2.7a. The singularities were located by Phillips, and the full line shows the theoretical curve, taking into account the infinite changes in slope at, for example, $v = 4.1$, 5.9, 7.8, 8.1, 8.3, 9.0, and $9.4 \times 10^{12}$ cps. This has transformed $g(v)$ from a dull-looking affair into an interesting curve. Only after such detailed calculations can it be said that for the given force constants the curve of Fig. 2.7b is representative of $g(v)$. The calculated values of $\theta$(curve A) do not at first agree well with the experimental values for the simple reason that no account has been taken of the anharmonic effects present. (For the sake of simplicity, we have preferred to leave the complicated effects of anharmonicity in lattice dynamics to the specialized reviews[29] on the subject.) When they are approximately included (curve B of Fig. 2.7b), the agreement with the experiments is noticeably improved. At 0°K, the $\theta$-values calculated from elastic data must agree with the calorimetric values (Table 2.V); the fact that they do not in Fig. 2.7b shows that the model of force constants used in the calculations is not very accurate, as later studies have also revealed. Nevertheless, there is little doubt that if better force constants are used, the theory will accurately describe the experimental variation of $\theta$ with $T$.

Our final example is sodium,[23] subjected to one of the most detailed studies so far. Information about the interatomic forces was
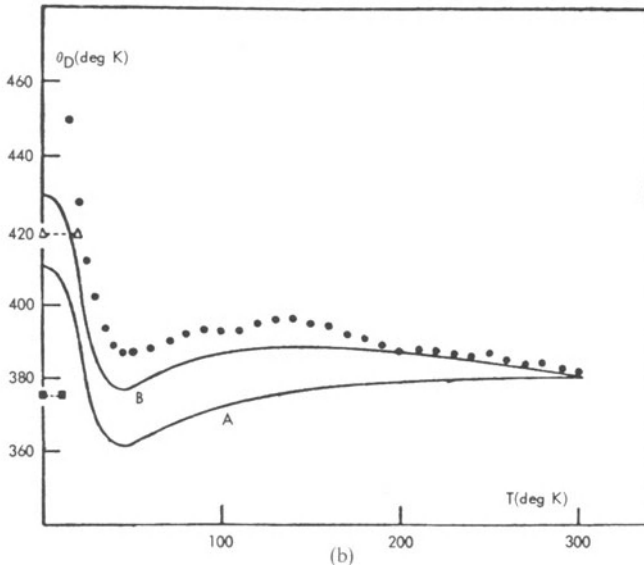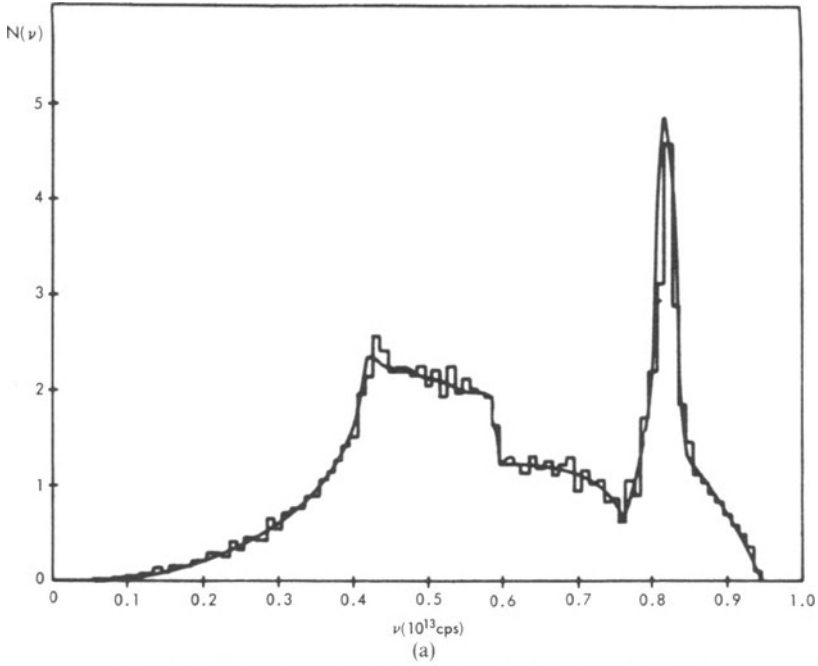
Fig. 2.7. Aluminum[28]: (a) frequency distribution (full line calculated using singularities in phonon spectra), (b) effective $\theta$-values obtained from $g(\nu)$. Curve A is with no allowance for anharmonicity, and B is with partial allowance for anharmonicity.

derived from the complete phonon-dispersion relations along several directions obtained by inelastic scattering of neutrons. The $g(v)$, given in Fig. 2.8a, was based on 35 million frequencies. Critical points are located at $v = 0.93$, 1.67, 2.56, 2.88, 3.47, 3.58, and 3.82 (units $10^{12}$ cps). The calculated specific heats are in good agreement with the experimental values. Unfortunately, a martensitic trans-formation at low temperatures makes an interpretation of the experi-ments below about 30°K very difficult, and the values given refer to a slightly different crystal structure. Nevertheless, the calculated $\theta$–$T$ curve fits reasonably well with the experimental curve. Sodium melts at 370°K, and even at about 200°K the lattice vibrations are no longer harmonic. The specific heat usually rises above the classical Dulong–Petit value of $3R$, although detailed measurements are not available in many cases. At $T \approx \theta$, anharmonic effects are appreciable, and the consequent increase in specific heats is reflected as a reduc-tion of the effective $\theta$, as in Fig. 2.8b. Theoretically, the change in $g(v)$ caused by the presence of anharmonicity has to be taken into consideration. Moreover, near the melting point, the generation of vacancies makes an additional contribution to the specific heat (Section 8.4).

There are numerous calculations of $g(v)$ and its relation to specific heats and other properties. The net impression is that the lattice theory is logically correct and esthetically satisfying. It correlates thermal, elastic, dielectric, and other properties not only with each other but also with the fundamental interactions among the atoms. In practice, it requires formidable calculations involving several para-meters. Where detailed information on the interatomic forces and facilities for computation are available, the experimental variation of $\theta$ with $T$ is explained to satisfaction, an example of the saying, "No pains, no gains." If the Debye theory is sufficient as a rule of thumb, the lattice calculation repays the labor involved in it with a significant improvement.

## 2.11. DEBYE $\theta$ IN OTHER PROPERTIES OF SOLIDS

From the above discussion, it is obvious that the Debye charac-teristic temperature $\theta$ has lost its original significance as a measure of the limiting frequency of lattice vibrations and has become an effective parameter describing the thermal behavior of the solid. Many phenomena in solids involve lattice vibrations, and their theories become far too complicated to be of practical use unless they descend to mundane levels by approximating $g(v)$ with a simple Debye function. Thus, the Debye $\theta$ is commonly encountered in solid state studies. In view of the approximations made in the theories,
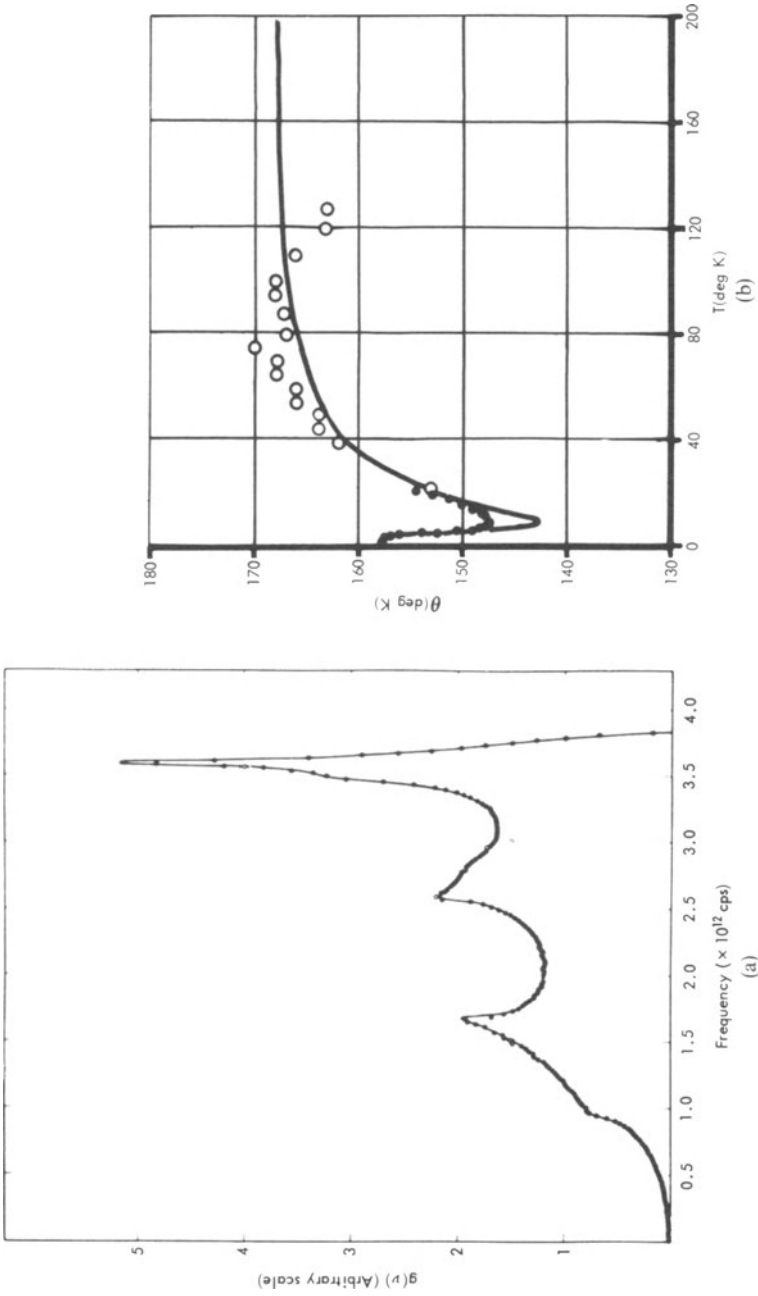
Fig. 2.8. Sodium[23]: (a) $g(\nu)$, (b) $\theta$-$T$ plot.

there is no reason to expect the numerical values of $\theta$ derived from the calorimetric measurements (denoted for clarity by $\theta_D$) to be exactly equal to those obtained from various other properties. All the same, specific heats may be roughly estimated from them if calorimetric data do not exist; conversely, a knowledge of specific heats is of use in other fields of study. In order to illustrate this inter-relationship, a brief discussion is given here, leaving the details to suitable reviews.[10,30,31]

### 2.11.1. $\theta$-Values from Elastic Properties

In Debye's theory, the correlation between thermal and elastic properties is very simple and has been mentioned earlier. In the detailed lattice calculations, $g(v) \propto v^2$ dependence holds good only near $v = 0$ and is the result of averaging low-frequency acoustic phonons over all directions. Near $0°K$, only these waves will be excited to any degree. The propagation of phonons whose wave-length is very much longer than the atomic spacings is not influenced by the details of atomic structure or interatomic forces. Thus, accord-ing to lattice theories, $\theta$-values calculated from elastic and thermal measurements should be identical as $T \to 0$. Table 2.V, taken from a careful survey by Alers and Neighbours,[32] shows how closely this relation is obeyed.

At higher temperatures, specific heats depend upon the full $g(v)$, whereas elastic constants measure $g(v)$ only at $v \to 0$. Thus, $\theta_D$ is in general different from $\theta$(elastic). This was the anomaly noted earlier in connection with Debye's theory (Section 2.7), and it is now obvious that the difference is not really "anomalous." A calculation of the difference using a quasi-harmonic theory, where the temperature variation of lattice spacings and interatomic forces are included, is obviously very involved. Even at low temperatures, small dis-crepancies between $\theta$(El.) and $\theta$(thermal) are sometimes observed in glasses, fused quartz, and other glassy materials. They are attri-buted to nonelastic low-frequency modes present in such amorphous media.[33]

Table 2.V. Comparison[32] of $\theta_D$ and $\theta$(El.) at $T \to 0$

| | Substance | | | | | |
|---|---|---|---|---|---|---|
| | Ag | Cu | Al | NaCl | KBr | LiF |
| $\theta$(El.) | 226.4 | 344.4 | 428.2 | 321.9 | 172.8 | 734.1 |
| $\theta_D$ | 226.2 | 345.1 | 426 | 320 | 174 | 737 |

### 2.11.2. $\theta$-Values from Compressibility and Melting Point

It was originally noted by Madelung and Einstein that a relation between the compressibility and the characteristic temperature can be derived using simple models of a solid. More recently, Blackman showed that for ionic crystals of NaCl or CsCl structure, the Debye temperature at high temperatures is related to the compressibility $\varkappa$ by means of the relation

$$\theta_\varkappa = \frac{\hbar}{k}\left(\frac{5r_0}{m\varkappa}\right)^{1/2} \tag{2.25}$$

where $2r_0$ is the lattice spacing and $m$ is the reduced mass of the ions. Table 2.VI compares such values of $\theta$(denoted as $\theta_\varkappa$) with the thermal values at high temperatures[10] and a reasonable correlation is found.

Another simple relation, due to Lindemann, connects the characteristic temperature with the melting point $T_m$ of the solid, assuming again a very crude model of the melting process. If $M$ is the mean atomic weight and $V$ the mean atomic volume, then

$$\theta_m = B\left(\frac{T_m}{MV^{2/3}}\right)^{1/2} \tag{2.26}$$

The quantity $B(\approx 115)$ varies slightly with the type of crystal; some values with $B = 115$ are given in Table 2.VI, where approximate agreement is evident.

**Table 2.VI. Comparison of $\theta_\varkappa$ and $\theta_m$ with High-Temperature $\theta_D$**

| | | | | Substance | | | |
|---|---|---|---|---|---|---|---|
| | LiF | NaCl | KCl | KBr | KI | RbBr | RbI |
| $\theta_\varkappa$ | 686 | 292 | 233 | 185 | 162 | 136 | 119 |
| $\theta_m$ | 1020 | 294 | 229 | 171 | 119 | 123 | 109 |
| $\theta_D$ | 607–750 | 275–300 | 218–235 | 152–183 | 115–200 | 120–135 | 100–118 |

The chief merit of these relations is that they give an estimate of the Debye temperature if calorimetric data are completely lacking. Such instances have occurred in the past.

### 2.11.3. $\theta$-Values from Thermal Expansion

The Einstein and Debye theories give a simple expression for the internal energy of a solid. Grüneisen[34] showed that if the vibrational frequency is taken to depend upon the interatomic distances, a reasonable account of the equation of state is obtained. In particular, the coefficient of thermal expansion $\beta$ is connected to the heat capacity

$C_v$ and the compressibility $\varkappa$ by

$$\beta = \frac{\gamma \varkappa C_v}{V} \tag{2.27}$$

with $\gamma = -\partial \ln v / \partial \ln V$ called *Grüneisen's constant*. Thus, a plot of $\beta$ versus $T$ should essentially be of the Debye form $D(T/\theta)$; Table 2.VII shows some values of the characteristic temperature $\theta_\beta$ obtained from such curves. The correlation with $\theta_D$ is quite good at high temperatures.

**Table 2.VII. Comparison of $\theta_\beta$ with $\theta_D$**

| | | | Substance | | | |
|---|---|---|---|---|---|---|
| | Pt | Cu | Au | Diamond | CaF$_2$ | FeS$_2$ |
| $\theta_\beta$ | 236 | 325 | 180 | 1860 | 474 | 645 |
| $\theta_D$ | 225 | 310 | 185 | 1940 | 479 | 620 |

Recent studies by Barron and others, based on lattice dynamics, have shown that the Grüneisen constant $\gamma$ does vary with temperature and that different acoustical and optical branches have different $\gamma$ values. Further, the linear expansion along some directions becomes negative for a few crystals such as Si, ZnS, AgI, and InSb at low temperatures. This can be qualitatively explained by lattice models, but cannot be understood easily from the Debye–Grüneisen equation of state.[35]

### 2.11.4. $\theta$-Values from Infrared Data

In ionic crystals, there are strong absorption bands in the infrared, associated with the "residual rays." It was one of the early suggestions to use these frequencies to calculate the characteristic temperature, and, indeed, reasonable agreement was found. The situation is somewhat complicated by the fact that the frequency of the reflection maximum is somewhat higher than that of the absorption maximum, the difference being related to the refractive index of the crystal. Thus, the Debye temperature calculated from the reflection maximum (denoted by $\theta_R$) will be larger than $\theta_A$ calculated from the absorption maximum. Table 2.VIII[10] shows that $\theta_R$ agrees well with the calorimetric $\theta_D$ values at high temperatures. The frequency of the absorption maximum is the same as that of the main maximum in the vibrational spectrum, and, since $g(v)$ extends beyond the maximum (Fig. 2.6a), it is not surprising that $\theta_A < \theta_D$. The ratio $\theta_A/\theta_R$ may be calculated from the lattice models, and fair agreement is found for some ionic crystals.

## Table 2.VIII. Debye Temperatures from Infrared Data

| | Substance | | | | | | |
|---|---|---|---|---|---|---|---|
| | LiF | NaCl | KCl | KBr | KI | RbBr | RbI |
| $\theta_R$ | 845 | 276 | 226 | 176 | 153 | 143 | 122 |
| $\theta_A$ | 440 | 235 | 203 | 162 | 141 | 126 | 122 |
| $\theta_D$ | 607–750 | 275–300 | 218–235 | 152–183 | 115–200 | 120–135 | 100–118 |

Actual infrared spectra show complicated structure, and some progress has been made in getting information about phonon-dispersion frequencies from the details of infrared and second-order Raman spectra.[36]

### 2.11.5. $\theta$-Values from Electrical Resistivity

The temperature variation of the electrical resistivity of metals has been studied extensively, and a calculation of $\theta$, denoted here as $\theta$(E.R.), on the basis of Bloch's theory of electrical conductivity was suggested by Grüneisen. He showed that the ratio of the specific resistance $\sigma$ to its value $\sigma_\infty$ at high temperatures is of the form

$$\frac{\sigma}{\sigma_\infty} = \frac{20}{x^4} \int_0^x \frac{\xi^4 \, d\xi}{e^\xi - 1} - \frac{4x}{e^x - 1} \qquad \left( x = \frac{\theta}{T} \right) \qquad (2.28)$$

However, as pointed out by Blackman,[10] $\theta$(E.R.) involves only longitudinal phonons in the theory, hence, it should differ considerably from $\theta_D$. In practice, there is a very surprising correlation between $\theta$(E.R.) and $\theta_D$ for many metals, as shown by Table 2.IX. At present, there is no satisfactory explanation of the agreement!

## Table 2.IX. Correlation of $\theta$ (E.R.) with $\theta_D$

| | Metal | | | | | | |
|---|---|---|---|---|---|---|---|
| | Li | Cu | Ag | Au | Pb | Al | W |
| $\theta$(E.R.) | 363 | 333 | 203 | 175 | 86 | 395 | 333 |
| $\theta_D$ | 340–430 | 310–330 | 212 | 168–186 | 82–88 | 385 | 305–357 |

### 2.11.6. Scattering of X-Rays, $\gamma$-Rays, and Neutrons

The vibrations of atoms in a solid affect the reflection of X-rays and other radiations of similar wavelength $\lambda$ from the crystal lattices. There are two principal effects—a reduction of the intensity of Bragg

**Table 2.X. Values of $\theta$ (X.R.), $\theta$ (El.), and $\theta_D$ at 300°K**

| | Substance | | | | | |
|---|---|---|---|---|---|---|
| | Al | Cu | Pb | Fe | Diamond | Si |
| $\theta$(X.R.) | 379 | 307 | 80 | 393 | 1491 | 593 |
| $\theta_D$ | 396 | 310 | 93 | 425 | 1850 | 640 |
| $\theta$(El.) | 406 | 331 | 91 | 464 | 2242 | 647 |

reflections (by the so-called Debye–Waller factor) and a diffuse scattering of radiation in the non-Bragg directions. The intensity of the Bragg reflection at an angle $\phi$ from a monatomic solid depends upon the temperature $T$ in the form $I = I_0 \exp(-2M)$, where $M = 8\pi^2 u^2 \sin^2 \phi / \lambda^2$. The mean square amplitude $u^2$ perpendicular to the reflecting plane may be calculated if a model of the lattice vibration is assumed. For a Debye solid at high temperatures,

$$M = \left(\frac{2kT \sin \phi}{m\lambda}\right)^2 \frac{3h^2}{k^2\theta^2}$$

and thus from the Debye–Waller factor, the characteristic temperature, denoted as $\theta$(X.R.) in Table 2.X, may be calculated. In the lattice case, the term $3h^2/k^2\theta^2$ is replaced by $\int g(v)v^{-2}\,dv/\int g(v)\,dv$, so that $\theta$(X.R.) is in general different from $\theta_D$. Some representative values[30] of $\theta$(X.R.), $\theta$(El.), and $\theta_D$ at 300°K are given in Table 2.X. In general, $\theta$(X.R.) is less than $\theta$(El.) or $\theta_D$; this is roughly what is expected from the lattice theory. Herbstein[30] has given a detailed discussion of the thermal effects in X-ray, Mössbauer, and neutron scattering, which may be referred to for further details.

The use of diffuse X-ray reflections and inelastic neutron-scattering in providing information about phonon-dispersion relations has already been mentioned.[20–22,37]

## REFERENCES

1. A. Eucken, *Handbuch der experimental Physik, VIII (I)* (1929), chapter 5.
2. A. J. Rutgers, *Physical Chemistry*, Interscience, New York, 1954, chapters 11 and 33.
3. J. C. Slater, *Introduction to Chemical Physics*, McGraw-Hill, New York, 1939, chapters 3 and 4.
4. *Landolt–Börnstein physikalish chemische Tabellen*, Springer-Verlag, Berlin, ed. 5, suppl. 1, p.702 (1927); ed. 6, Vol. 2, Part 4, p.736 (1961).
5. J. Sherman and R. B. Ewell, *J. Phys. Chem.* **46**, 641 (1942). D. R. Stull and F. D. Mayfield, *Ind. Eng. Chem.* **35**, 639 (1943). H. Zeise, *Thermodynamik*, Vol. 3, Hirzel, Leipzig, 1954. W. C. Overton and J. H. Hancock, *Tables of Einstein Functions*, U.S. Naval Res. Lab. Rept. No. 5502 (1960). J. Hilsenrath and G. G. Ziegler, *Tables of Einstein Functions*, Nat. Bur. Std. Monograph No. 49 (1962).

6. J. de Launay, *Solid State Phys.* **2**, 219 (1956).
7. R. F. S. Hearmon, *Introduction to Applied Anisotropic Elasticity*, Oxford University Press, Oxford, 1961.
8. M. J. P. Musgrave, *Rept. Progr. Phys.* **22**, 74 (1959); *Progr. Solid Mech.* **2**, 63 (1961).
9. H. Weyl, *Math. Ann.* **71**, 441 (1911). R. D. Courant, *Math. Ztschr.* **7**, 14 (1920). W. Ledermann, *Proc. Roy. Soc. (London), Ser. A.* **182**, 362 (1944). R. E. Peierls, *Proc. Nat. Inst. Sci. India* **20A**, 121 (1954).
10. M. Blackman, *Handbuch der Physik, VII (I)*, 325 (1955).
11. J. A. Beattie, *J. Math. Phys. (MIT)*, **6**, 1 (1926).
12. G. F. Newell, *J. Chem. Phys.* **23**, 2431 (1955). L. S. Kothari and V. K. Tewary, *J. Chem. Phys.* **38**, 417 (1963). B. J. C. van der Hoeven and P. H. Keesom, *Phys. Rev.* **130**, 1318 (1963).
13. E. Schrödinger, *Handbuch der Physik, X*, 275 (1926).
14. D. Bijl, *Progr. Low Temp. Phys.* **2**, 395 (1957).
15. J. D. Filby and D. L. Martin, *Proc. Roy. Soc. (London), Ser. A* **276**, 187 (1963).
16. W. T. Berg and J. A. Morrison, *Proc. Roy. Soc. (London), Ser. A* **242**, 467 (1957).
17. M. Blackman, *Rept. Progr. Phys.* **8**, 11 (1941).
18. L. Brillouin, *Wave Propagation in Periodic Structures,* Dover, New York, 1954.
19. G. H. Wannier, *Elements of Solid State Theory,* Cambridge University Press, Cambridge, 1959, chapter 3.
20. L. S. Kothari and K. Singwi, *Solid State Phys.* **8**, 109 (1959).
21. A. A. Maradudin, E. W. Montroll, and G. H. Weiss, *Theory of Lattice Dynamics in the Harmonic Approximation* (suppl. 4 to *Solid State Physics*), Academic Press, New York, 1963.
22. W. Cochran, *Rept. Progr. Phys.* **26**, 1 (1963).
23. A. E. Dixon, A. D. B. Woods, and B. N. Brockhouse, *Proc. Phys. Soc. (London)* **81**, 973 (1963). G. Gilat and G. Dolling, *Phys. Letters* **8**, 304 (1964).
24. B. Dayal and S. P. Singh, *Proc. Phys. Soc. (London)* **76**, 777 (1960). B. Dayal and B. B. Tripathi, *Proc. Phys. Soc. (London)* **77**, 303 (1961).
25. G. Leibfried, *Handbuch der Physik, VII (I)*, 104 (1955).
26. R. G. Chambers, *Proc. Phys. Soc. (London)* **78**, 941 (1961).
27. S. O. Lundqvist, V. Lundstrom, E. Tenerz, and I. Waller, *Ark. Fysik* **15**, 193 (1959).
28. C. B. Walker, *Phys. Rev.* **103**, 547 (1956).
29. G. Liebfried and W. Ludwig, *Solid State Phys.* **12**, 275 (1961). T. H. K. Barron and M. L. Klein, *Phys. Rev.* **127**, 1997 (1962). R. A. Cowley, *Advan. Phys.* **12**, 421 (1963).
30. F. H. Herbstein, *Advan. Phys.* **10**, 313 (1961).
31. J. R. Partington, *Advanced Treatise on Physical Chemistry, Vol. 3*, Longmans–Green, London, 1952, section 9N.
32. G. A. Alers and J. R. Neighbours, *Rev. Mod. Phys.* **31**, 675 (1959). J. L. Feldman, *Proc. Phys. Soc. (London)* **84**, 361 (1964).
33. O. L. Anderson, *J. Phys. Chem. Solids* **12**, 41 (1959). P. Flubacher, A. I. Leadbetter, J. A. Morrison, and B. P. Stoicheff, *J. Phys. Chem. Solids* **12**, 53 (1959). H. B. Rosenstock, *J. Phys. Chem. Solids* **23**, 659 (1962).
34. E. Grüneisen, *Handbuch der Physik X*, 1 (1926). J. K. Roberts, and A. R. Miller, *Heat and Thermodynamics,* Blackie, London, 1960, chapter 22.
35. C. Domb in *Proceedings of the Eighth International Conference on Low Temperature Physics* (London, 1962, R. O. Davies, editor), Butterworth, London, 1963, p.385. J. G. Collins and G. K. White, *Progr. Low Temp. Phys.* **4**, 450 (1964).
36. S. S. Mitra, *Solid State Phys.* **13**, 1 (1962). F. A. Johnson and R. Loudon, *Proc. Roy. Soc. (London), Ser. A* **281**, 274 (1964).
37. W. A. Wooster, *Diffuse X-Ray Reflections from Crystals,* Clarendon, Oxford, 1962.

*Chapter 3*

# Electronic Specific Heat

## 3.1. SPECIFIC HEAT OF METALS

Metals are characterized by their high electrical and thermal conductivities at ordinary temperatures. When the discrete nature of electric charges became clear, by about 1900, it was also realized that freely moving electrons were the charge carriers in metals. Drude, Lorentz, and others applied the methods used in the kinetic theory of gases to explain how these electrons were responsible for the observed high thermal and electrical conductivities.[1]

In spite of the success of the free-electron gas model, the classical theory had a fundamental inconsistency. If the electrons are considered as small particles freely moving through the crystal lattice, the equipartition law attributes to each electron an internal energy $\frac{3}{2}kT$, associated with the three translational degrees of freedom. Therefore, the electrons should contribute $\frac{3}{2}R$ per mole to the specific heat. A monovalent metal such as copper should thus have $C_v \approx 9$ cal/mole·degK, $3R$ from the lattice and $\frac{3}{2}R$ from the conduction electrons. The experimental value of 6 cal/mole·degK is entirely accounted for by the lattice contribution. The same is true for almost all metals at room temperature, as can be seen from the values given in Table 2.I. The model of an electron gas in a metal explained the transport properties reasonably well, but the caloric behavior was in complete disagreement with the equipartition theorem.

It was only in 1928, after Sommerfeld's application of quantum statistics to free electrons in a metal, that the reason for the small electronic specific heat became evident. Even as Bose–Einstein statistics applied to phonons brings about a reduction of lattice heat capacity at low temperatures, the Fermi–Dirac statistics obeyed by electrons makes the electronic specific heat comparatively small at room temperatures. It became clear that the electronic contribution could be observed only at very low temperatures, in the liquid-

helium range, and the first experiments to study electronic specific heats in detail were performed by Keesom and coworkers in the early 1930's.

## 3.2. QUANTUM STATISTICS OF AN ELECTRON GAS

It is a fundamental feature of quantum statistics, as explained in several texts,[1,2] that because of the Pauli exclusion principle and because the various electrons are indistinguishable from one another, Fermi–Dirac statistics should be applied to electronic systems. According to F–D statistics, the probable number $N_k$ of particles in energy state $\varepsilon_k$ is

$$N_k = \frac{g_k}{\exp[(\varepsilon_k - \varepsilon_F)/kT] + 1} \tag{3.1}$$

where $g_k$ is the number of levels with energy $\varepsilon_k$ and the parameter $\varepsilon_F$ (the Fermi energy) is so chosen that the total number of particles is equal to $N$. The energy levels are often so closely spaced that it is convenient to define the density of states $\mathfrak{N}(\varepsilon)\,d\varepsilon$ as the number of energy states per unit volume between $\varepsilon$ and $\varepsilon + d\varepsilon$.

For a F–D system, marked deviations from classical Maxwell–Boltzmann behavior occur when the temperatures are lower than the Fermi temperature $T_F = \varepsilon_F/k$, which in ordinary metals is of the order of $10^5\,°K$. The shape of the F–D function

$$f(\varepsilon) = \frac{1}{1 + \exp[(\varepsilon - \varepsilon_F)/kT]} \tag{3.2}$$

is shown in Fig. 3.1 for various temperatures. As $T \to 0$, $f(\varepsilon)$ equals unity for any energy less than $\varepsilon_F$ and then abruptly drops to zero for $\varepsilon > \varepsilon_F$. In other words, all the energy states below $\varepsilon_F$ are fully occupied, while all states above $\varepsilon_F$ are empty. At a finite temperature $T$, some of the particles within a distance of approximately $kT$ of $\varepsilon_F$ have enough thermal energy to become excited to higher energy states, as shown in Fig. 3.1. However, at $T/T_F \sim 0.01$, the distribution has changed little from the behavior at $T \sim 0$; it is only for $T \sim T_F$ that the familiar Boltzmann tail of the distribution makes its appearance.

The magnitude of the Fermi temperature $T_F$, which is obviously fundamental to an understanding of the behavior of an electron gas, can be easily calculated as follows. In Chapter 2, it was shown that for free particles in a volume $V$, the number of allowed energy states between momenta $p$ and $p + dp$ is

$$n(p)\,dp = \frac{4\pi V}{h^3} p^2\,dp \tag{2.18}$$
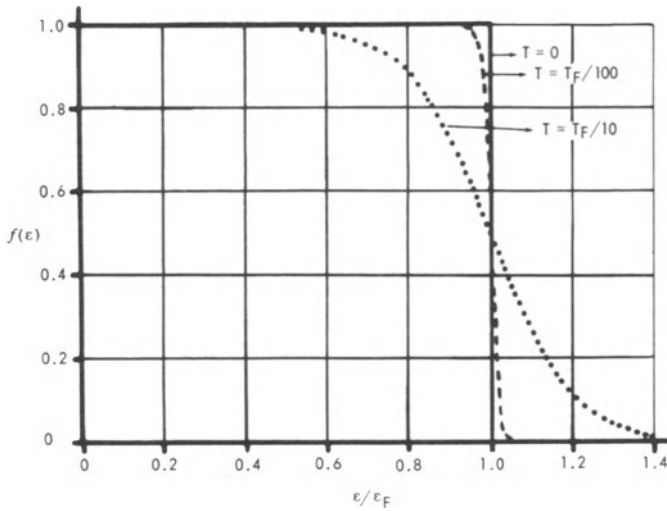
Fig. 3.1. Shape of the $F$–$D$ function [equation (3.2)] at various temperatures.

If $m$ is the mass of an electron, the number of allowed states can be written in terms of the energy $\varepsilon = p^2/2m$ as

$$V\,\mathfrak{N}(\varepsilon)\,d\varepsilon \;=\; 2\pi(2m)^{3/2}\,\frac{V}{h^3}\,\varepsilon^{1/2}\,d\varepsilon \tag{3.3}$$

At 0°K, all states below $\varepsilon_F$ are occupied, and, further, each state can be filled by two electrons of opposite spins. So the total number of states is

$$\frac{N}{2} \;=\; \tfrac{4}{3}\pi(2m)^{3/2}\,\frac{V}{h^3}\,\varepsilon_F^{3/2}$$

or

$$\varepsilon_F \;=\; \frac{1}{2m}\left(\frac{\tfrac{3}{8}Nh^3}{\pi V}\right)^{2/3} \tag{3.4}$$

This formula is valid for a gas of free electrons; nevertheless, suppose a value typical of a metal $N/V \approx 10^{23}/\text{cm}^3$ is substituted. Then

$$T_F \;=\; \frac{\varepsilon_F}{k} \;\approx\; 90{,}000°\text{K}$$

The Fermi energy $\varepsilon_F$ of a gas of electrons with metallic densities is two or three orders of magnitude greater than the thermal energy of

approximately $kT$ at room temperatures. The electron gas is said to be *highly degenerate* under such conditions.

It is very surprising that in spite of such high energy content the specific heat of the electron gas is quite small. This comes about because the internal energy changes very little at ordinary temperatures. To a first approximation, a fraction ($\sim kT/\varepsilon_F$) of the number of electrons is excited at a temperature $T$ into higher energy states (see Fig. 3.5). Each electron gains an energy of about $kT$, and so the increase in energy per mole is $\delta E \sim RT(kT/\varepsilon_F)$. The heat capacity is therefore approximately $2R(T/T_F)$ per mole. Since $T_F \approx 10^4$ to $10^5\,°K$, the electronic heat capacity is about $10^{-2}R$ at room temperature. This is only 1 % of the lattice heat capacity at ordinary temperatures. However, at very low temperatures, the lattice heat capacity, falling off as $T^3$, decreases much faster and becomes comparable to the electronic term, which decreases only linearly with $T$. These qualitative conclusions are in excellent agreement with experimental results.

## 3.3. SPECIFIC HEAT OF ELECTRONS IN METALS

The model of a free-electron gas, although forming an elementary introduction to the behavior of electronic systems, is unnecessarily crude when applied to actual metals. The electrons in the inner shells of an atom are tightly bound to the nucleus; only the electrons in the outer unfilled shells have any chance to wander through the metal. Their movement is subject to the three-dimensional periodic potential field associated with the atoms of the lattice. Under these conditions, the energy levels, instead of being a continuous function $p^2/2m$ of the momentum, become grouped into energy bands.[3] In each band, the energy is a continuous function of momentum, but the bands themselves are separated by gaps in which there are no energy levels (Fig. 3.2). Ordinarily, the first band is completely filled (valence band), while the second band is only partially filled (conduction band). Electrons in any unfilled band can move under applied electric fields and thereby transport quantities of electricity or heat. In an ordinary dielectric, the valence band is just full; in the absence of any free carriers, the material behaves as an insulator. In three momentum dimensions, the surfaces of constant energy have complicated shapes because the energy–momentum relationship depends upon the crystallographic directions. The shape of the Fermi surface, i.e., the surface in the momentum space enclosing the occupied states of electrons in a metal, can in some cases be determined from other electronic properties of the metal.[4,5]
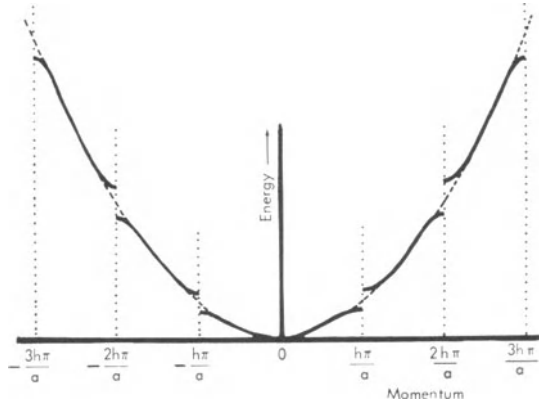
Fig. 3.2. Energy–momentum relation for an electron in a one-dimensional periodic lattice. Dotted line is the parabolic relation for free electrons.

A complete knowledge of the energy levels is luckily not required for calculation of the specific heat of electrons in a metal. The discussions of the previous section show that only electrons within approximately $kT$ of the Fermi surface are excited at room temperature; consequently, knowledge of the number of energy states in the vicinity of the Fermi surface is sufficient to evaluate the electronic specific heat $c_e$.

Quantitatively, the discussion is fairly straightforward. The energy per mole of the electronic system is

$$E = 2V \int_0^\infty \varepsilon f(\varepsilon) \mathfrak{N}(\varepsilon)\, d\varepsilon = 2V(kT)^2 \int_0^\infty \frac{\mathfrak{N}(kTx)x\, dx}{e^{x-\xi} + 1}$$

where $x = \varepsilon/kT$ and $\xi = \varepsilon_F/kT$. The integral may be split into two ranges, $(0, \xi)$ and $(\xi, \infty)$, so that

$$\frac{E}{2(kT)^2 V} = \int_0^\xi \mathfrak{N}x\, dx - \int_0^\xi \frac{\mathfrak{N}x\, dx}{1 + e^{\xi - x}} + \int_\xi^\infty \frac{\mathfrak{N}x\, dx}{e^{x-\xi} + 1}$$

where the first range has itself been decomposed into two terms. On substituting $u = x - \xi$ in the third term, it becomes the integral 0 to $\infty$ of $(u + \xi)\mathfrak{N}/(e^u + 1)$. If we set $u = \xi - x$ in the second term, it becomes the integral $\xi$ to 0 of $(\xi - u)\mathfrak{N}/(e^u + 1)$, but extending its range of integration from $\infty$ to 0 causes a negligible error of only

$e^{-\xi}$. Therefore, to the lowest-order terms,

$$E = 2V \int_0^\xi \mathfrak{N}(\varepsilon)\varepsilon \, d\varepsilon + 4V(kT)^2 \mathfrak{N}(\varepsilon_F) \int_0^\infty \frac{u \, du}{e^u + 1}$$

The first term on the right is the internal energy at 0°K, while the integral 0 to $\infty$ of $u/(e^u + 1)$ may be transformed into the series

$$\sum_1^\infty (-1)^{s+1} s^{-2}$$

which has the value $\pi^2/12$. So the energy per mole is

$$E = E_0 + \tfrac{1}{3}\pi^2 V(kT)^2 \mathfrak{N}(\varepsilon_F) \tag{3.5}$$

The molar heat capacity of the electronic system is

$$C_e = \tfrac{2}{3}\pi^2 k^2 V \mathfrak{N}(\varepsilon_F)T = \gamma T \tag{3.6}$$

The electronic specific heat is determined only by the density of states at the Fermi surface $\mathfrak{N}(\varepsilon_F)$, as was expected earlier. To make a numerical estimate of $C_e$, assume the metallic electrons to be free. From equations (3.3) and (3.4), the molar density of states is

$$V\mathfrak{N}(\varepsilon_F) = \frac{2\pi m}{h^2}\left(\frac{3NV^2}{\pi}\right)^{1/3} \tag{3.7}$$

Consequently,

$$\begin{aligned}
C_e &= \frac{4\pi^3 m k^2}{3h^2}\left(\frac{3NV^2}{\pi}\right)^{1/3} T \\
&= 3.26 \times 10^{-5} V^{2/3} n_\alpha^{1/3} T \text{ cal/mole·deg} \tag{3.8} \\
&= 1.36 \times 10^{-4} V^{2/3} n_\alpha^{1/3} T \text{ J/mole·deg}
\end{aligned}$$

where $n_\alpha$ is the number of free electrons per atom. For a typical metal, say, copper at room temperature, $V \sim 7 \text{ cm}^3/\text{mole}$, $n_\alpha = 1$, $T \sim 300°\text{K}$, and so $C_e \approx 0.04 \text{ cal/mole·deg}$. This is less than 1% of the lattice heat capacity of 6 cal/mole·deg at the same temperature. Therefore, the electronic specific heat is not normally detected in room-temperature measurements. This explanation was indeed one of the great triumphs of Sommerfeld's application of quantum statistics to the theory of metals.

The above linear variation of electronic specific heat is valid only at low temperatures ($T \ll T_F$). At higher temperatures, the calculations are involved[6]; the full variation is shown in Fig. 3.3. For $T \gg T_F$, the limiting value is $\tfrac{3}{2}R$, which is the classical equipartition value for a gas of structureless mass points (Section 6.2).
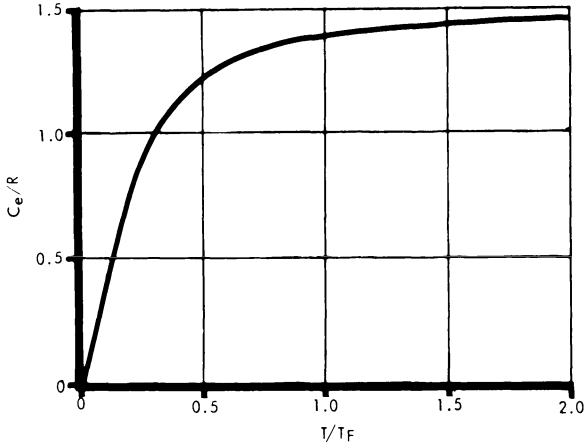
Fig. 3.3. Temperature variation of the heat capacity of an electron gas.

## 3.4. ELECTRONIC SPECIFIC HEAT AT LOW TEMPERATURES

Although at room temperature the electronic contribution to the heat capacity of a metal is insignificant compared to the lattice contribution, the situation is quite different at low temperatures. $C_e$ decreases linearly with $T$, whereas $C_g$, as seen in the previous chapter, is proportional to $T^3$ at low temperatures. Therefore, at some temperature, the two terms become equal; at still lower temperatures, $C_e$ is larger than $C_g$ (Fig. 3.4). For instance, copper at about 4°K has $C_v \sim 6 \times 10^{-3}$ J/mole·degK, which is equally shared between electronic and lattice contributions. Above about 4°K, the lattice part rapidly dominates the specific heat, while below that temperature the electronic part remains significant. In general, at liquid-helium temperature, both terms are of comparable magnitude and the observed specific heat is of the form

$$C = C_g + C_e = \beta T^3 + \gamma T \qquad (3.9)$$

A plot of $C/T$ against $T^2$ should therefore be a straight line, and, indeed, a typical example was given in Fig. 1.1b to illustrate how well the relation (3.9) is obeyed, if the $T^3$-region of the lattice specific heat has been reached. Such a plot permits determination of both $\beta$ and $\gamma$. From equation (2.20) it is evident that $\beta = 12\pi^4 R/5\theta^3$. The value of the Debye temperature at very low temperatures ($\theta_0$) and the coefficient $\gamma$ of the electronic specific heat for a number of metals are given in Table 3.I. The values refer to materials of the highest-
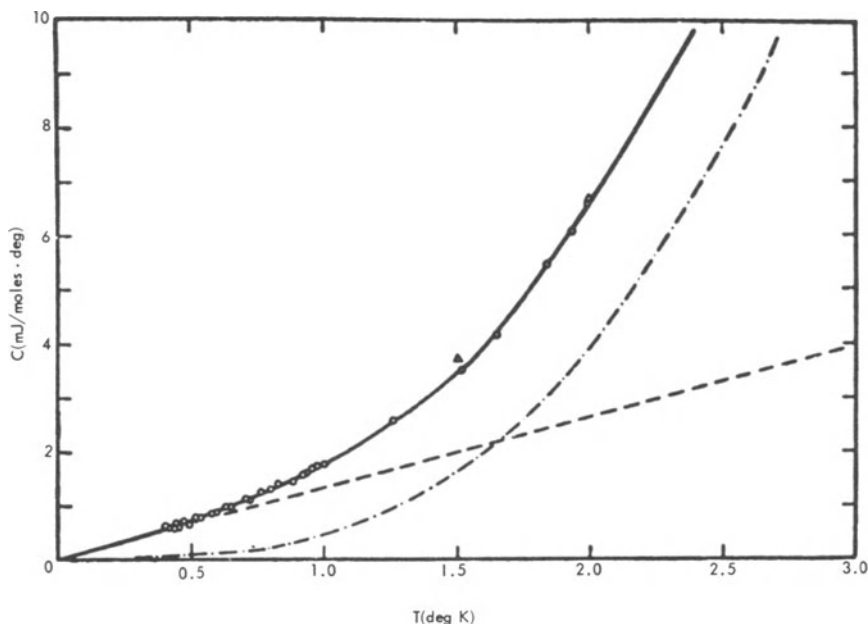
Fig. 3.4. Typical low-temperature heat capacity of a metal, sodium:[7] – ∘ – ∘ – ∘ –
observed $C_p$; – · – · – · lattice term; – – – – electronic term.

available purity. Impurities in the metal affect the specific heat
slightly, and in some cases anomalous values have been obtained.[8]
Besides the possible changes in $\mathfrak{N}(\varepsilon_F)$ due to the impurities, dilute
magnetic contaminations may in some cases give a term linear in $T$;
careful analysis is needed to unravel the various effects (Section 3.6).

The free-electron gas model is obviously oversimplified. Never-
theless, equation (3.8) gives a value of $\gamma$ of the right order of magnitude.
For example, in sodium, there is one electron in the outer unfilled
shell, which is almost free to move; according to (3.8), $\gamma$ should have a
value of $11 \times 10^{-4}$ J/mole·deg$^2$. Similarly, copper, which also has
one outer electron, should have $\gamma = 5.4$ in the same units. The
experimental values are Na = 13.7 and Cu = 7.0. A simple way of
illustrating the difference between theory and experiment is to intro-
duce an "effective mass" $m^*$ which takes into account the partial
binding, namely, the fact that the electrons are not completely free
but are only loosely bound to the metallic ions. The electron mass $m$
in equation (3.8) is now replaced by $m^*$, so that

$$\frac{\gamma_{exp}}{\gamma_{theor}} = \frac{m^*}{m} \tag{3.10}$$

**Table 3.I.  Representative Values of $\theta_0$ (in deg K) and $\gamma$**
**(in $10^{-4}$ J/mole·deg$^2$)**

| Metal | $\theta_0$ | $\gamma$ | Metal | $\theta_0$ | $\gamma$ |
|-------|-----------|----------|-------|-----------|----------|
| Ag | 225 | 6.09 | Na | 158 | 13.7 |
| Al | 426 | 13.6 | Nb | 250 | 88.2 |
| Au | 164 | 7.0 | Ni | 440 | 72.8 |
| Ba | 110 | 27.0 | Os | 500 | 23.5 |
| Be | 1160 | 2.22 | Pb | 108 | 33.6 |
| Ca | 229 | 27.3 | Pd | 299 | 99 |
| Cd | 209 | 6.9 | Pt | 221 | 66.3 |
| Co | 443 | 47.5 | Rb | 55 | 24.1 |
| Cr | 585 | 15.5 | Re | 450 | 24.5 |
| Cs | 39 | 32.0 | Rh | 478 | 48.9 |
| Cu | 348 | 7.0 | Ru | 600 | 33.5 |
| Fe | 464 | 50.2 | Sn (white) | 195 | 17.5 |
| Ga | 324 | 6.0 | Sr | 147 | 36.5 |
| Hf | 261 | 26.4 | Ta | 245 | 58.5 |
| Hg | 72 | 18.6 | Th | 170 | 46.8 |
| In | 109 | 18.4 | Ti | 430 | 35.5 |
| Ir | 420 | 31.4 | Tl | 90 | 15.2 |
| K | 91 | 20.8 | U | 200 | 109 |
| Li | 369 | 17.5 | V | 380 | 92 |
| Mg | 342 | 13.7 | W | 405 | 12.1 |
| Mn | 450 | 180 | Zn | 310 | 6.27 |
| Mo | 470 | 21.1 | Zr | 310 | 30.3 |

Thus, $m^*/m$ has a value of about 1.2 for sodium and about 1.3 for copper. For other metals, the appropriate valence of the atom is used to represent $n_\infty$ the number of electrons per atom. In this manner, $m^*/m$-values have been calculated and tabulated in several reviews.[8–10]

Although the value of $m^*/m$ suggests the degree of departure from the electron gas model, the quantity has only a limited significance. In metals, the bands usually overlap, and the details of the band structure are quite complicated.[4,5] The idea of an effective mass, which can be easily introduced in the case of a single band, is not appropriate under such conditions. Moreover, in cyclotron resonance, the de Haas–van Alphen effect, and other phenomena which reveal the properties of Fermi surfaces more directly, different "effective masses" are introduced, leading to some confusion in comparing the values of $m^*/m$ for any particular substance. The situation corresponds to the confusion concerning the indiscriminate use of the Debye $\theta$ to characterize different physical properties, as mentioned in Chapter 2. Therefore, it appears best to express the experimental results in terms of $\gamma$, as done in Table 3.I.

Electrons, because of their electric charge, exert Coulomb forces upon one another; these forces are of long range, falling off as $1/r^2$. It would appear that the use of a perfect-gas model is inconsistent with the existence of such long-range interactions. In fact, early approximate calculations showed that the specific heat would be about ten times smaller than the Sommerfeld value and would also have a different temperature dependence, thereby destroying even the qualitative agreement between equation (3.8) and experiments. More recently, the exchange and correlation effects of the Coulomb interaction have been analyzed in detail, using the mathematical techniques developed for handling many-body problems. It turns out that each electron is shielded, as it were, by the nearby polarization cloud of the electron gas. The interaction potential $V(r)$ becomes screened, $V(r) \sim e^2 r^{-1} \exp(-\lambda r)$, so that it becomes a short-range force, which is compatible with the perfect-gas model of the electrons. The collective motion of the electron clouds is then described in terms of what are called *plasma modes*, which have too high a frequency to be involved in specific-heat studies. The details of these calculations are left to suitable reviews.[11]

Another aspect of the electronic specific heats of metals, which cannot be treated here, is the interaction between electrons and phonons. In writing equation (3.9), it is implictly assumed that electronic motions are independent of lattice vibrations, so that the two terms are simply added together. It is, however, obvious that the vibrations of an atom will influence the motion of electrons in its neighborhood; conversely, the presence of the electron cloud will affect the lattice vibrations. For many metals, the effect is very small,[12] but two exceptional situations occur. In some cases, the electron–phonon interaction results in the phenomenon of superconductivity, as originally suggested by Fröhlich in 1950. The properties of super-conductors are so striking that they are discussed separately in Sections 3.8 to 3.10. In a few special cases, electron–phonon inter-actions result in small anomalies, known as *Kohn anomalies*, in the lattice $\omega$–$q$ dispersion relations.[13]

## 3.5. SPECIFIC HEAT AND BAND STRUCTURE OF METALS

A discussion of the values of $\gamma$ for all metals is clearly to be left to special reviews on the subject.[8,9,10,14] Only a few typical metals are considered here, in order to illustrate the special factors involved in a study of electronic specific heats.

The alkali metals lithium, sodium, potassium, rubidium, and cesium, have one "free" electron in the outer shells. The inner closed shells are tightly bound to the nucleus, and consequently we may

assume that there are $N$ electrons per gram-atom. The number of states in the valence band is $N$, which can be filled by $2N$ electrons. The first Brillouin zone is thus only half-filled, and the free-electron model may be expected to be useful. This model gives

$$V\mathfrak{N}(\varepsilon)\,d\varepsilon = 2\pi(2m)^{3/2}Vh^{-3}\varepsilon^{1/2}\,d\varepsilon$$

as shown in Fig. 3.5. Nevertheless, the observed values of $\gamma$ are not in good agreement with equation (3.8). Apart from sodium, mentioned earlier, $m^*/m$ has a value[15] of 1.25 (K), 1.26 (Rb), and 1.43 (Cs), showing that even in such simple cases the free-electron model is not adequate. Calculations using details of the band structure, electron–phonon and electron–electron couplings, account reasonably well for the experimental values of $m^*/m$.

The noble metals, copper, silver, and gold, are also monovalent and have their first Brillouin zones half-empty. The values of $m^*/m$, 1.36 (Cu), 1.05 (Ag), and 1.16 (Au), differ appreciably from unity, which at this stage is not surprising. The Fermi surface of copper has been investigated by several methods; its shape is shown in Fig. 3.6. In a free-electron gas model, it will be a sphere, whereas in copper it is actually pulled out and touches the zone boundaries along the $\langle 111\rangle$ directions. Detailed calculations based on such Fermi surfaces do fit in well with the experiments. The specific-heat data are not very useful for finding the shape of the Fermi surface, because the electronic term measures merely an averaged density of states at
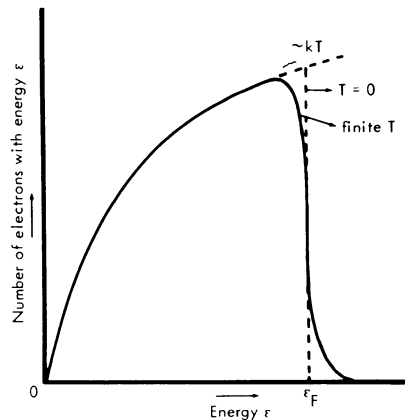


Fig. 3.5. Energy distribution in an electron gas. Full line is the number of electrons at a finite temperature, broken line is that at absolute zero.
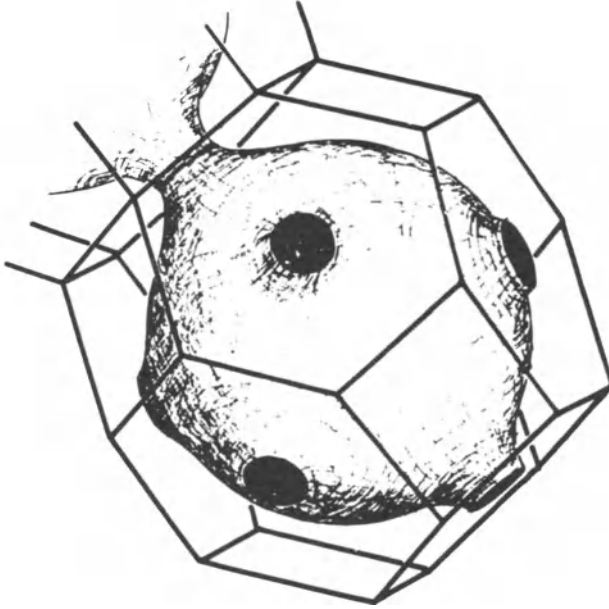
Fig. 3.6. Fermi surface of copper.

the Fermi surface. If the shape of the Fermi surface is known from other studies,[4,5] $\gamma$ can be used as a final check.

The divalent metals, beryllium, magnesium, calcium, zinc, cadmium, etc., have hexagonal crystal structure. With two "free" electrons per atom, the Brillouin zones should be exactly filled and the substances should be insulators. As a matter of fact, the first and second bands overlap to some extent, which accounts for the electrical conductivity of the metals. The Fermi surface intersects the zone boundary and has a complex shape. The theoretical calculation of $\mathfrak{N}(\varepsilon_F)$ is a matter of considerable labor. The only simple statement that can be made[16] is that $\mathfrak{N}(\varepsilon_F)$ varies rapidly when the axial ratio $c/a$ of the hexagonal lattice is small and is nearly constant when the ratio is large. Beryllium ($c/a = 1.57$, $\gamma = 2.22 \times 10^{-4}$ J/mole·deg²) and magnesium ($c/a = 1.62$, $\gamma = 13.7$) belong to the first set, while zinc ($c/a = 1.86$, $\gamma = 6.3$) and cadmium ($c/a = 1.89$, $\gamma = 6.3$) are examples of the second case.

The transition metals form another interesting example of the effect of electronic structure, as was first pointed out by Mott. An inspection of the values of $\gamma$ for the first group of metals (Table 3.II) shows that the electronic specific heats are unusually large. In

**Table 3.II. Values of $\gamma$ for the First Group of Transition Metals**

| | Metal | | | | | | |
|---|---|---|---|---|---|---|---|
| | Ti | V | Cr | Mn | Fe | Co | Ni |
| $\gamma \times 10^4$ J/mole·deg$^2$ | 35.5 | 92 | 15.5 | 180 | 50.2 | 47.5 | 72.8 |

isolated atoms of these metals, the filled 4s-subshell, containing two electrons, has as usual a lower energy than the partially filled 3d-states (chromium has only one electron in the 4s-level, and the value of $\gamma$ is also exceptional). When the atoms are brought together to form a metal, the wave functions of the states overlap, which produces a characteristic broadening of the energy levels. The wave functions for the 4s-states are more extended than those of the 3d-states. Consequently, the 4s-band is broader and covers a much wider range than does the 3d-band. This occurs to such an extent that some states in the 4s-band have higher energies in the metal than those of the 3d-band, as schematically represented in Fig. 3.7a. Moreover, the 4s-band contains only two states per atom, or 2N states per mole of the metal. It has a large energy spread, and so its density of states is low. The 3d-band contributes 10 N states to the metal; since its energy spread is small, the density of states is large. The resultant density of states as shown in Fig. 3.7b, has a sharp maximum. The Fermi levels lie in this region, and hence $C_e$ is unusually large for
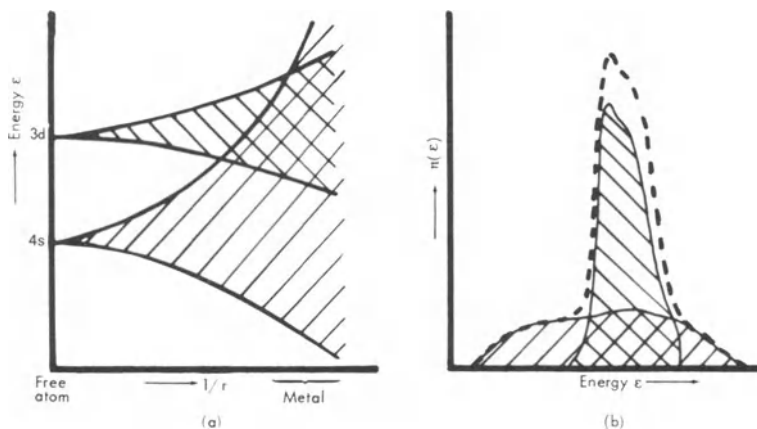


Fig. 3.7. (a) Broadening of 4s- and 3d-bands in a metal due to overlap. (b) Density of states for 4s- and 3d-bands. Dotted line is the resultant density of states.

these metals. For a quantitative analysis, the details of the band structure must be worked out.[14]

The metals of the second and third transition groups also have large values of $\gamma$, for similar reasons. Furthermore, the unfilled shells give rise to magnetic interactions among the atoms. The resulting para-, ferro-, and antiferromagnetic behavior produces interesting effects in specific heats which will be discussed in the next chapter. The ions of rare-earth metals also have unfilled shells. But the coupling among the ions is weak, and various magnetic and other transitions occur below room temperature. Rare-earth specific heats are discussed in Chapter 7, Section 6.

## 3.6. SPECIFIC HEAT OF ALLOYS

When two metals are alloyed, there is in general a change in the lattice structure. A structural change alters not only the lattice specific heat directly, as is clear from Chapter 2, but also the electronic term, through the influence of the lattice structure upon the energy-band scheme. In such general cases, no simple rule can be given. It is only in special circumstances that simple correlations exist. One such instance is that of a binary alloy, for instance, $\beta$-brass (CuZn), which exhibits an order–disorder transition, but this is more appropriately taken up in Chapter 7.

In several dilute alloys, especially of elements of near atomic number and similar atomic radii, the elements go into solid solution without any appreciable change of crystal structure. The observed variation of specific heats may then be attributed to variation in $\mathfrak{N}(\varepsilon)$, and some information may be obtained about the shape of the density-of-states curve. The simplest hypothesis, the rigid-band model, is to assume that in the process of alloying, the band structure remains unchanged and only the number of available electrons is altered. The value of $\mathfrak{N}(\varepsilon_F)$ at the new Fermi level determines the electronic specific heat of the alloy [equation (3.6)]; depending upon the slope of the $\mathfrak{N}(\varepsilon)$ curve at the band edge, the $\gamma$ of the alloy will be larger or smaller than that of the pure metal. In this manner, the electronic specific heat may be correlated with the shape of the energy-band scheme.

As an instance, palladium can be freely alloyed with its neighboring elements silver and rhodium. The $\gamma$-values of these alloys[17] are shown in Fig. 3.8a. In the rigid-band model, the addition of silver to palladium gives an extra electron per atom of silver; these extra electrons fill the band to a higher energy level. The alloying with rhodium gives one hole per Rh atom, and so the Fermi level occurs at a lower value of energy. Thus, the density-of-states curve (Fig. 3.8b)
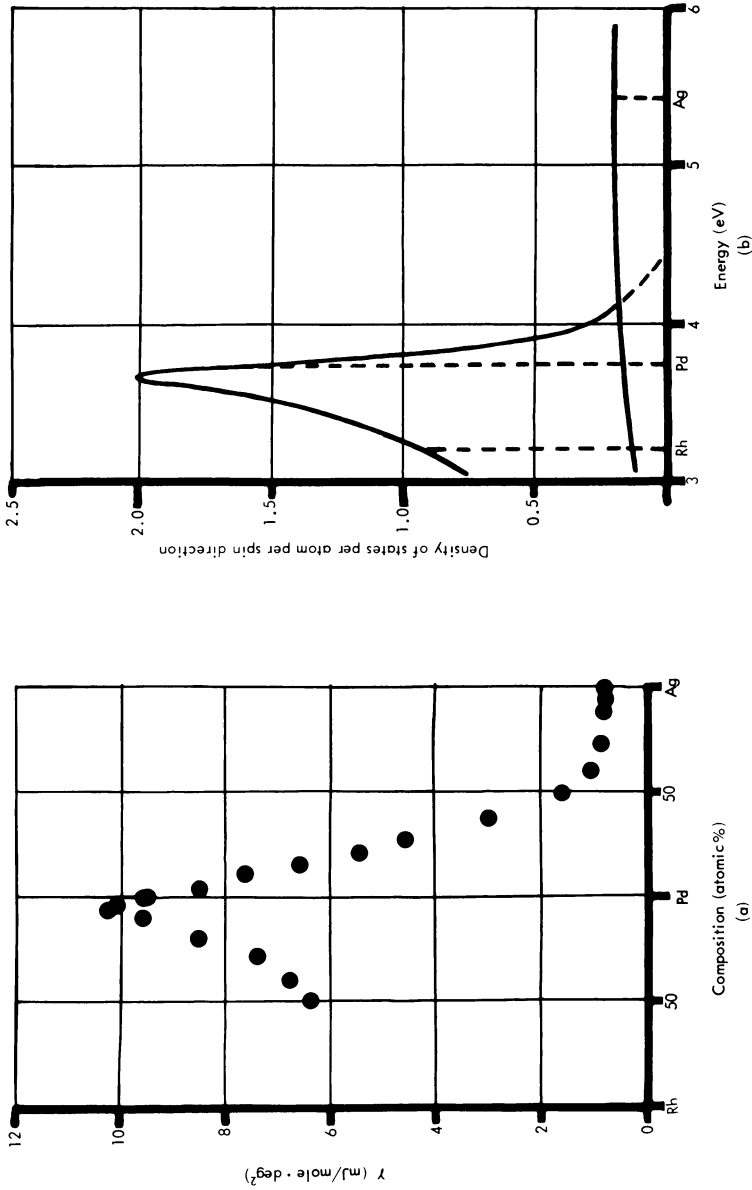
Fig. 3.8. (a) Electronic specific-heat coefficients for palladium–silver and palladium–rhodium alloys. (b) Density of states per atom, rhodium–palladium–silver, for one direction of spin.[17]

may be drawn at once. For reasons set forth in the previous section, the 4d-band in a metal of the second transition group should be sharply peaked, while the 5s-band should be comparatively flat. There is indeed a striking similarity between Figs. 3.7b and 3.8b. Theoretical calculations of the band structures are in good agreement with Fig. 3.8b, but the details of such studies[14,17] cannot be included here.

Dilute alloys of transition elements show several peculiarities which have not yet been clarified.[18] As an example, if small amounts of manganese are added to copper, the specific heat in the liquid-helium range is abnormally increased.[19] The heat capacity is linear in $T$ at very low temperatures and is roughly independent of the manganese concentration $c$. At higher temperatures, it falls rapidly to the pure-metal value. The temperature at which this decrease occurs is proportional to $c$, so that the entropy associated with the extra heat capacity $\Delta C$ is proportional to the number of manganese ions. Figure 3.9 shows how at low concentrations of manganese, the $\gamma$-values are abnormally high and independent of $c$, while at high concentrations normal behavior is approached. Similar results are obtained in dilute alloys of iron in copper, also. In some alloy systems, the specific heat shows a definite maximum before the $\Delta C \propto T$ region is reached. These deviations are accompanied by corresponding anomalies in other properties such as magnetic susceptibility and electrical conductivity.

The theoretical picture of dilute alloys of transition elements is
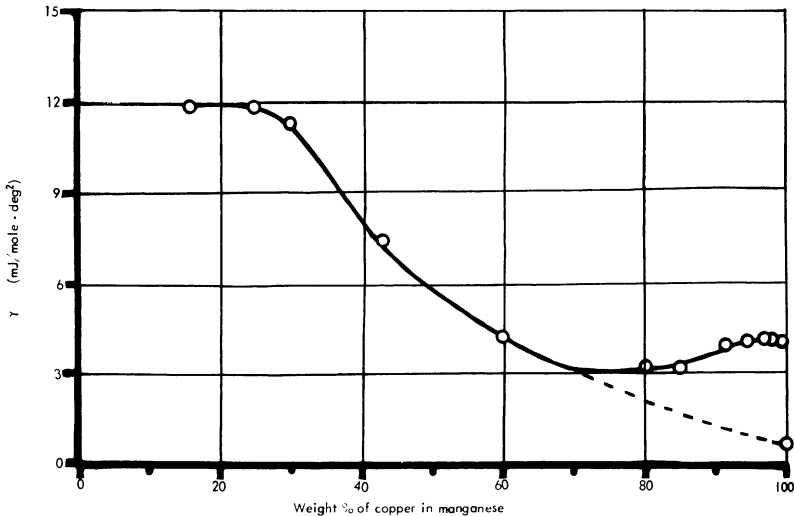


Fig. 3.9. Electronic specific-heat coefficients of copper–manganese alloys.[19] The broken line shows the expected behavior of dilute manganese in copper.

still under debate, although considerable progress has been made by Friedel and others[18] regarding the formation of localized moments. It was Overhauser[20] who suggested an explanation for the observed specific-heat behavior; subsequent developments have been due to Marshall and others.[20] They all involve some form of magnetic ordering and the extra specific heat $\Delta C$ arises when a number of spins are located in regions of near-zero magnetic field. The near-zero field regions may arise from the stationary spin–density waves, from the large separation between the magnetic ions, or from the approximate cancellation of the exchange interactions of opposite sign. Although magnetic interactions are taken up in Chapter 4 only, the effects may be calculated in a crude manner as follows. At a temperature $T$ and in a field $H$, a magnetic dipole $\mu$ has an average energy [see equation (4.15)] $-\mu H \tanh(\mu H/kT)$. In an alloy, the local magnetic field varies from site to site, and, if $f(H)$ is the probability of having a field $H$ at the site of $\mu$, the internal energy is

$$E \approx -\tfrac{1}{2}Nc \int_{-\infty}^{\infty} f(H)\mu H \tanh\left(\frac{\mu H}{kT}\right) dH$$

where $c$ is the concentration of manganese ions and $Nc$ their total number. Most of the ions will be rigidly aligned because they are in effective fields much larger than $kT/\mu$ at low temperatures. So they do not contribute to the heat capacity. Only the ions situated in near-zero fields $\mu|H| \lesssim kT$ will be able to change their orientations and hence give an excess specific heat $\Delta C$. Thus

$$\Delta C \sim \tfrac{1}{2}Ncf(0) \int_{-\infty}^{\infty} \left(\frac{\mu^2 H^2}{kT^2}\right) \text{sech}^2\left(\frac{\mu H}{kT}\right) dH$$

In a fully aligned perfect lattice, the magnetic field at an ion has a definite value, though thermal fluctuations smear out the field to some extent. In an alloy, the field is completely smeared out and has a wide range of values. Under these conditions, the probability of finding zero field at a site is proportional to $1/\langle H \rangle$, where $\langle H \rangle$ is the mean field at an ion. Since the interactions are mainly dipolar, $\langle H \rangle$ will be proportional to $R^{-3}$ ($R$ is the mean distance between Mn ions) and hence to $c$, the concentration of Mn ions. Therefore, with suitable constants $A$, $A'$,

$$\Delta C \approx AT \int_{-\infty}^{\infty} x^2 \,\text{sech}^2 x \, dx = A'T$$

At low temperatures, the specific heat is proportional to $T$ and independent of the manganese concentration; these are the two important experimental observations. Detailed calculations[20] show

that at higher temperatures $\Delta C$ falls off as $T^{-2}$; the temperature at which this occurs is proportional to $c$, which again agrees with the observations. The subject is of current interest, and the overall picture is just emerging.

## 3.7. SPECIFIC HEAT OF SEMICONDUCTORS

A pure semiconductor differs from a metal in that, at absolute zero, the first Brillouin zone is completely filled by electrons and the next zone is completely empty. There is no overlap between the bands (Fig. 3.10a). The energy gap is small, however, and at ordinary temperatures some electrons are excited from the valence band to the conduction band (Fig. 3.10b.) The material is now electrically conducting and becomes more so when the temperature is raised, unlike pure metals, which become less conducting when $T$ is increased. In practical applications, materials with controlled amounts of suitable impurities (dope) are of tremendous importance. The impurity atoms introduce extra energy levels into what was earlier the forbidden energy gap. The presence of such levels alters the electrical properties profoundly, because electrical conduction can take place without thermal activation of electrons across the energy gap. The special properties of semiconductors are far too numerous to chronicle here; for an introduction, one may refer to the elementary texts mentioned earlier.[3]

In all types of semiconductors, whether pure or slightly doped, the density of excited current carriers decreases rapidly as the temperature is reduced. Therefore, at low temperatures only the lattice specific heat is observed for most semiconductors.[21] Germanium, silicon, and indium antimonide are among the most intensely studied
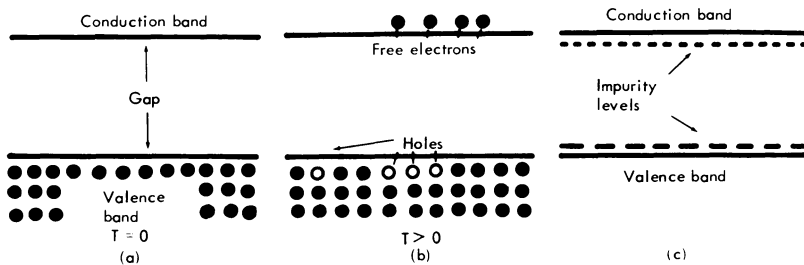


Fig. 3.10. Simplified energy-level diagram of semiconductors. (a) Pure semiconductor at 0°K. The valence band is full, the conduction band is empty, and there is no electrical conduction. (b) At $T > 0°$K, some excitation of electrons across the gap takes place, permitting electrical conduction. (c) Doped semiconductor, with impurity levels depending upon the dope.
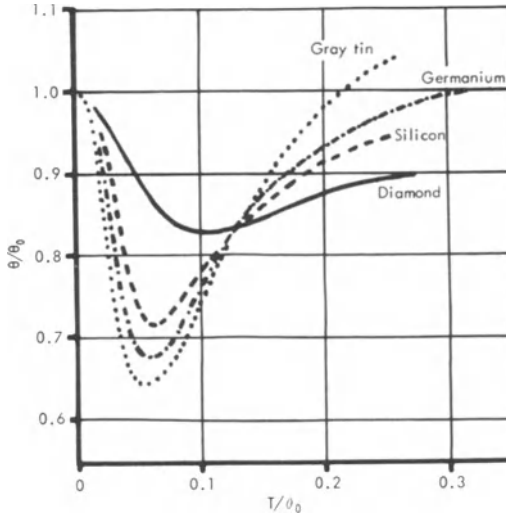
Fig. 3.11. Temperature variation of Debye $\theta$ for
several diamond-type lattices.

semiconductors. They all have the diamond-type of crystal structure,
and the lattice vibrational spectra may be expected to be of a similar
form for all of them. This is supported by the fact that the Debye $\theta$
has the same type of temperature dependence for these substances, as
shown in Fig. 3.11. The true $T^3$-region is observed below $\theta/100$. At
higher temperatures, $\theta$ drops considerably and passes through a
minimum at about $\theta/20$. The actual $\theta$-values form a regular sequence,
as shown in Table 3.III.

In heavily doped silicon and germanium (containing approxi-
mately $10^{19}$ carriers/cm$^3$), the specific heat of free carriers has been
observed.[22] In these specimens, the impurity states overlap the con-
duction or valence band, so that free carriers are present even without
thermal activation. The specific heat at low temperatures is of the
form $C = \beta T^3 + \gamma T$ [equation (3.9)], as in a metal. The value of the

## Table 3.III. Values of $\theta$ for Semiconductors with Diamond-Type Crystal Structure

|  | Material | | | | |
| --- | --- | --- | --- | --- | --- |
|  | Diamond | Si | Ge | Sn(grey) | InSb |
| $\theta$(degK) | 2200 | 636 | 360 | 212 | 200 |

effective mass $m^*$ calculated from the values of $\gamma$ agrees well with the effective mass derived from measurements of cyclotron resonance.

While on the subject of semiconductors, it is appropriate to point out that the use of semiconductors (in particular, commercial carbon radio resistors and suitably doped germanium crystals) as thermometers has greatly facilitated calorimetric measurements at low temperatures. Nowadays, almost all workers dealing with the liquid-helium range use such semiconducting thermometers for ease of operation and accuracy of thermometry.

## 3.8. PHENOMENON OF SUPERCONDUCTIVITY

In 1911, Kamerlingh Onnes discovered superconductivity in mercury. The electrical resistance of the substance, which was gradually decreasing as the temperature was lowered from room temperature (Fig. 3.12a), abruptly became immeasurably small at 4.2°K. Experiments showed that in the superconductive state below $T_c$ the resistance is for all practical purposes equal to zero. Another fundamental property of superconductors, namely, perfect diamagnetism, was discovered by Meissner and Ochsenfeld in 1933. If placed in a small magnetic field, the superconductor completely expels the magnetic flux from its inside (Fig. 3.12b). This perfect diamagnetism as well as the perfect conductivity are destroyed if the magnetic field $H$ is increased beyond a critical value $H_c$. For many common superconductors, mercury, lead, tin, vanadium, cadmium, tantalum, etc., the dependence of $H_c$ upon temperature is approximately of the form

$$H_c = H_0 \left[ 1 - \left( \frac{T}{T_c} \right)^2 \right] \tag{3.11}$$

Detailed studies show, however, that the magnetic field penetrates the surface layers to a depth of about $10^{-4}$ cm. Further, the critical field $H_c$ and the critical temperature $T_c$ depend upon the purity and perfection of the specimen. If a suitable magnetic field is applied to a spherical specimen, some layers of the specimen become normal, while some remain superconductive, resulting in what is known as the intermediate state. Superconductors exhibit other special electrodynamic and transport properties. These matters belong to the special texts on the subject.[23] For the present simple discussion of specific heats, an idealized sharp transition at $(H_c, T)$ may be assumed and demagnetization effects dependent upon the shape of the specimen may be neglected.

In the following chapter it will be shown that in many magnetic problems $H$ behaves in the same way as $P$ in ordinary thermodynamic

(a)

(b)

(c)
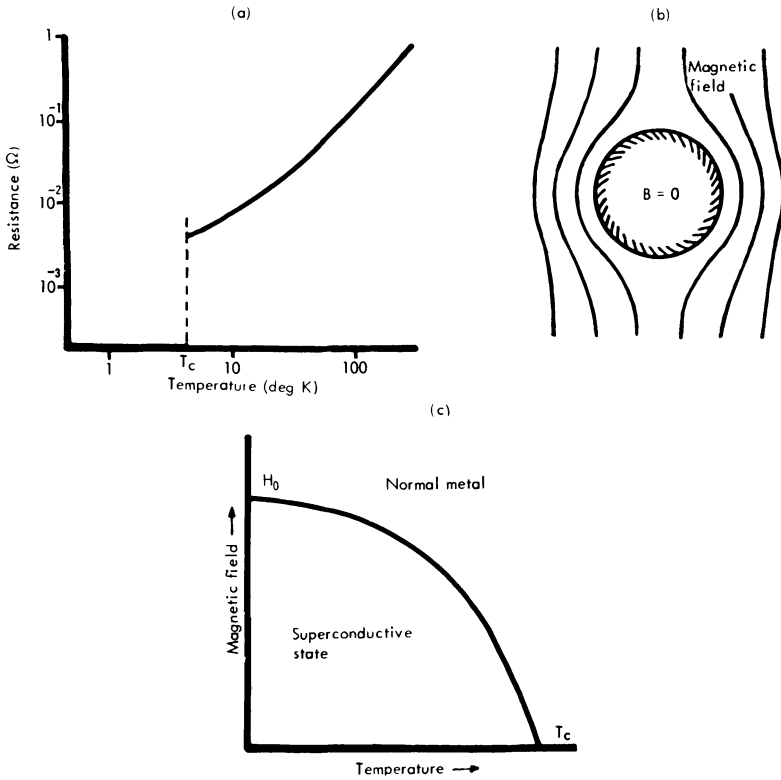
Fig. 3.12. (a) Temperature variation of resistance, showing sudden infinite conductivity at superconducting transition $T_c$. (b) Meissner effect. Magnetic flux is expelled by a superconductor. (c) $H$–$T$ phase diagram of a superconductor.

considerations. It is therefore natural to represent the equilibrium between the normal and superconductive states as a curve in the $H$–$T$ plane (Fig. 3.12c) which separates the two phases. If $G_s$ is the Gibbs' free energy of the superconductive phase at zero field, its value at a field $H$ is $G_s - \frac{1}{2}MH$ (see Chapter 4), where because of perfect diamagnetism the moment induced per unit volume is $M/V = -H/4\pi$. On the equilibrium curve, the free energies of both phases must be equal, and so

$$G_n - G_s = \frac{H_c^2}{8\pi} V \qquad (3.12)$$

Since $S = -\partial G/\partial T$, the entropy difference is

$$S_n - S_s = -\frac{H_c V}{4\pi} \frac{\partial H_c}{\partial T} \qquad (3.13)$$

The temperature variation of $H_c$, given by equation (3.11), shows that $\partial H_c/\partial T$ is always negative, and hence $S_s \leqslant S_n$; that is, the superconductive state is more ordered than the normal state. The entropy difference vanishes at $T_c$ ($H_c = 0$ at $T = T_c$) and at $0°$K ($\partial H_c/\partial T = 0$ at $T \rightarrow 0$). At an intermediate temperature, about $0.3 T_c$, $S_n - S_s$ reaches a maximum. $S = 0$ at $T \rightarrow 0$, it will be recalled, is in consonance with the third law of thermodynamics. $S = 0$ at $T = T_c$ implies that in the transition at zero field, no latent heat is involved. (This is an example of a phase change of the second order to be discussed in Section 8.1.) At intermediate temperatures, the liberated latent heat $L$ is equal to

$$L = -T \frac{H_c V}{4\pi} \frac{\partial H_c}{\partial T} \tag{3.14}$$

which agrees well with the experiments.

The entropy difference (3.13) shows that there is a difference between the heat capacities of the superconductive and normal phases:

$$C_n - C_s = T\frac{\partial}{\partial T}(S_n - S_s) = -\frac{TV}{4\pi}\left[H_c\frac{\partial^2 H_c}{\partial T^2} + \left(\frac{\partial H_c}{\partial T}\right)^2\right] \tag{3.15}$$

At the transition temperature, there is an abrupt jump in the specific heats

$$(C_n - C_s)_{T_c} = -\frac{T_c V}{4\pi}\left(\frac{\partial H_c}{\partial T}\right)^2 \tag{3.16}$$

a relation often called *Rutger's relation*. Near $T_c$, the superconductive phase has a higher specific heat than the normal state, whereas at very low temperatures the normal phase has a higher heat capacity. At a temperature where the magnitude of $\Delta S$ is maximum, $C_n$ and $C_s$ are equal.

The above formulas are strictly valid only when the magnetic field destroying the superconductivity is along the axis of a long cylindrical specimen. For other orientations and shapes, an intermediate state must be considered. It was shown by Peierls that the specific heat then exhibits two discontinuities, a sharp rise and a sharp fall, marking the beginning and the end of the intermediate state.[24] For the sake of simplicity, these calculations are not worked out here.

## 3.9. SPECIFIC HEAT OF SUPERCONDUCTORS

The measurements of specific heat made immediately after the discovery of superconductivity showed no striking difference between $C_n$ and $C_s$. With improvements in thermometry, Keesom and Van
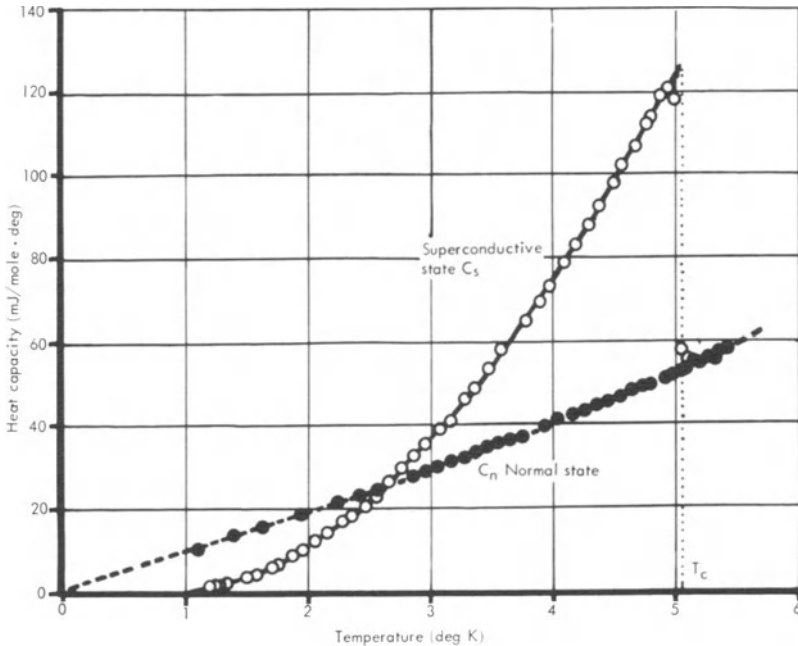
Fig. 3.13. Typical variation of heat capacities in the superconductive and normal states (vanadium[25]).

den Ende discovered the discontinuity [equation (3.16)] in the specific heat of tin at the superconducting transition. A typical variation of specific heat, shown in Fig. 3.13, brings out the characteristic features: $C_n$ is greater than $C_s$ at very low temperatures, $C_s$ overtakes $C_n$ as the transition is approached, and a sharp discontinuity occurs at $T_c$.

If the $H_c$–$T$ threshold curve is known completely, equation (3.15) enables $C_n - C_s$ to be calculated. In general, the calculation involves a double differentiation of the $H_c$–$T$ curve and is therefore not very accurate. At $T_c$, however, only the first derivative is needed, and a test of the thermodynamic relation (3.16) is possible. The measured values of $(C_s - C_n)_{T_c}$ in the carefully studied cases of indium, tin, and tantalum are In = 9.75, Sn = 10.6, Ta = 41.5 mJ/mole·deg, while the values calculated from the threshold curves are In = 9.62, Sn = 10.56, Ta = 41.6, showing excellent agreement. In some cases, especially with alloys, discrepancies arising from a different cause are found (Section 3.10). In most cases, the experimental confirmation of the thermodynamic relations is good.

Besides the simple relation given in Section 3.8, a somewhat more involved relation connecting the coefficients of thermal expansion and the compressibility of the two phases may be derived by taking the higher derivatives of equation (3.12) with respect to $p$ and $T$ (see *Ehrenfest relations* in Section 8.1). There are many experimental difficulties in confirming these relations, but, on the whole, reasonable agreement is found.[23]

Thermodynamics by itself does not give any further information on the variation of $C_s, C_n$ with $T$. In general, the observed specific heat may be separated into lattice and electronic contributions $C_n = C_{gn} + C_{en}, C_s = C_{gs} + C_{es}$. In the normal state, equation (3.9) shows that $C_{gn} = \beta T^3, C_{en} = \gamma T$ at low temperatures. Now, in the superconducting transition, no structural changes are observed in the lattice, and the elastic properties are changed only minutely. Therefore, it is reasonable to assume that the lattice part of $C_s$ and $C_n$ are equal, so that

$$C_n - C_s = C_{en} - C_{es} \qquad (3.17)$$

By such an analysis, $C_{es}$ may be calculated; in many cases, it is approximately proportional to $T^3$. This variation is indeed compatible with equations (3.11) and (3.15). From them, it follows that

$$C_n - C_s = C_{en} - C_{es} = \frac{H_0^2 V}{2\pi T_c^2} T \left[1 - 3\left(\frac{T}{T_c}\right)^2\right] \qquad (3.18)$$

and therefore

$$\gamma = \frac{H_0^2 V}{2\pi T_c^2} \qquad (3.19)$$

$$C_{es} = \left(\frac{3H_0^2 V}{2\pi T_c^4}\right) T^3 \qquad (3.20)$$

$$(C_s - C_n)_{T_c} = 2\gamma T_c \qquad (3.21)$$

These relations [equations (3.18 to 3.21)] suggest several methods of finding $\gamma$, the coefficient of electronic specific heat in the normal state, from the magnetic threshold curves. Actual computations[26] show that $\gamma$ calculated in this manner from magnetic measurements agrees well with the calorimetric determinations. Such a comparison depends upon the assumed $T^3$-variation of $C_{es}$ or the equivalent parabolic variation of $H_c$. Without invoking this, but assuming that $C_{es}$ contains no term linear in $T$, it follows from equation (3.17) that

$$\lim_{T \to 0} \frac{C_n - C_s}{T} = \gamma \qquad (3.22)$$

The advantage of this procedure in not assuming the parabolic temperature dependence of $H_c$ is to some extent countered by the need for making magnetic measurements down to very low temperatures. Where this has been done, the relation (3.22) is found to be obeyed very well.

While all these results show the internal consistency in the application of thermodynamic relations to superconductors, they do not throw much light on the microscopic mechanism of superconductivity. Very accurate measurements of $C_{es}$ made since 1954 have revealed that at low temperatures it varies as

$$C_{es} \approx ae^{-b/T} \qquad (3.23)$$

A typical result based on one of the early measurements is shown in Fig. 3.14. Departures from a $T^3$-law occur at very low temperatures, and thus probably escaped notice in the experiments made earlier. Similar small deviations of the $H_c$–$T$ curve from the parabolic law were also observed. By analogy to the studies of Einstein's model of lattice vibrations (Section 2.4), the Schottky peak in paramagnetic salts (Section 4.9), and the roton specific heat in liquid helium II (Section 5.4), it may be inferred that such an exponential variation
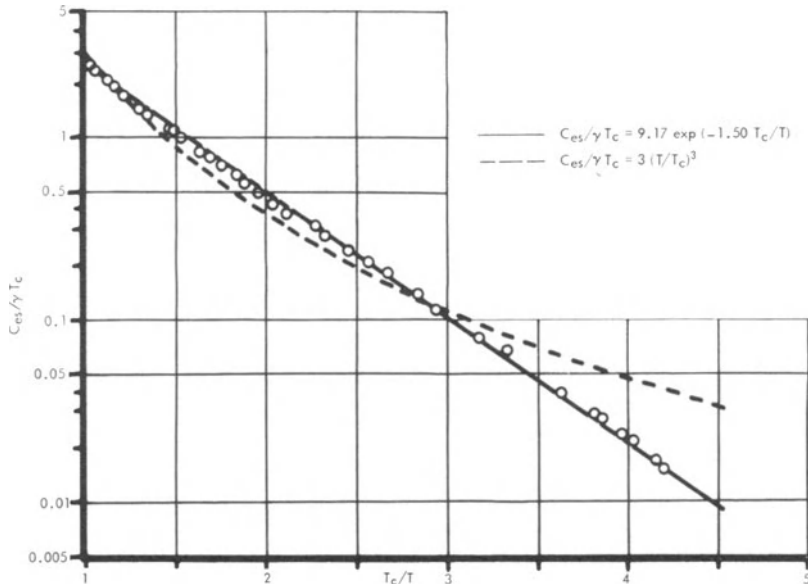


Fig. 3.14. Variation of $C_{es}$ in vanadium.[25]

of the specific heat is characteristic of the presence of an energy gap separating the normal and superconducting electrons.

In 1950, it was also found that the transition temperature $T_c$ depended on the isotopic mass $M$ of the atom, $T_c \sim \alpha M^{-1/2}$, which suggested that the interaction of the electrons with the lattice was somehow responsible for superconductivity. These ideas culminated in a satisfactory theory of simple superconductors by Bardeen, Cooper, and Schrieffer in 1957.

## 3.10. RECENT STUDIES

It is hardly possible here to do justice to the theoretical concepts underlying the Bardeen–Cooper–Schrieffer (BCS) theory, which has successfully correlated several effects discovered earlier and predicted new phenomena as well. The task is ameliorated by the existence of several texts.[27] The theory shows that owing to the presence of virtual phonons, there is a tendency for the electrons to be correlated in pairs, called *Cooper pairs*. It requires an energy of approximately $kT_c$ to break up this correlation, and the presence of such pairs allows a dissipationless flow of electric current. We shall content ourselves with a brief exposition of how the specific-heat studies fit into the theory.

The fact that an exponential variation of $C_{es}$ [equation (3.23)] indicates the presence of an energy gap is easily visualized from Section 4.9, where it is proved that if two energy levels are separated by a gap $\varepsilon$, the specific heat at low temperatures has a dominant term of the form $\exp(-\varepsilon/kT)$. The detailed calculations of the BCS theory yield

$$\frac{C_{es}}{\gamma T_c} = 8.5 \exp \frac{-1.44 T_c}{T} \qquad \text{for } 2.5 < \frac{T_c}{T} < 6 \qquad (3.24)$$

$$= 26 \exp \frac{-1.62 T_c}{T} \qquad \text{for } 7 < \frac{T_c}{T} < 12$$

where the gap $2\varepsilon_0$ is related to $T_c$ by means of the relation

$$2\varepsilon_0 = 3.52 \, kT_c \qquad (3.25)$$

The form of the specific-heat curves resemble equation (3.24) closely, and some values of $2\varepsilon_0/kT_c$ determined by fitting this equation are given in Table 3.IV. For widely different metals, the values do cluster around the idealized 3.52 of the BCS model, which incidentally assumes the metal to be isotropic.

Another simple prediction of the theory is that

$$C_{es}(T_c) = 2.43\gamma T_c \qquad (3.26)$$

**Table 3.IV. Values of $2\varepsilon_0/kT_c$ Obtained from $C_{es}-T$ Curves**

|  | Metal | | | | |
|---|---|---|---|---|---|
|  | In | Ta | Tl | Sn | V |
| $\dfrac{2\varepsilon_0}{kT_c}$ | 3.9 | 3.6 | 3.2 | 3.6 | 3.6 |

analogous to equation (3.21). A few values shown in Table 3.V show that many metals do not deviate much from this equation. Considering the simplicity of the model chosen for analysis and the wide variety of phenomena explained by it, the BCS theory must surely be considered as a significant advance toward the elucidation of a very complicated physical phenomenon.

Earlier, it was mentioned that the thermodynamic relations (3.12) to (3.16) are not very well satisfied for many alloys. Recent studies have shown that superconductors must be broadly divided into two categories. The superconductors of the first kind exhibit complete Meissner diamagnetism and seem to obey the thermodynamic relations derived for them. The BCS model explains their behavior reasonably well. Superconductors of the second kind do not exhibit the full Meissner effect. As shown in Fig. 3.15b, the magnetic field begins to penetrate the specimen at a lower critical field $H_{c1}$, but the last traces of superconductivity are destroyed only at a much higher field $H_{c2}$. Thus, type II superconductors show even in longitudinal magnetic fields the characteristics similar to the intermediate state of an ordinary type I superconductor. Following some earlier suggestions by Ginzburg and Landau, Abrikosov showed that the mixed state between $H_{c1}$ and $H_{c2}$ of a type II superconductor may be considered as a bundle of normal filaments in a superconductive medium. The filaments, or fluxoids, which are the magnetic analogs of hydrodynamic vortices, have special quantum properties and may also be pinned down by dislocations and other defects in the solid. Therefore,

**Table 3.V. Values of $C_{es}$ at $T_c$**

|  | Metal | | | | | |
|---|---|---|---|---|---|---|
|  | Hg | Sn | Al | Ta | Zn | Tl |
| $\dfrac{C_{es}(T_c)}{\gamma T_c}$ | 3.18 | 2.60 | 2.60 | 2.58 | 2.25 | 2.15 |
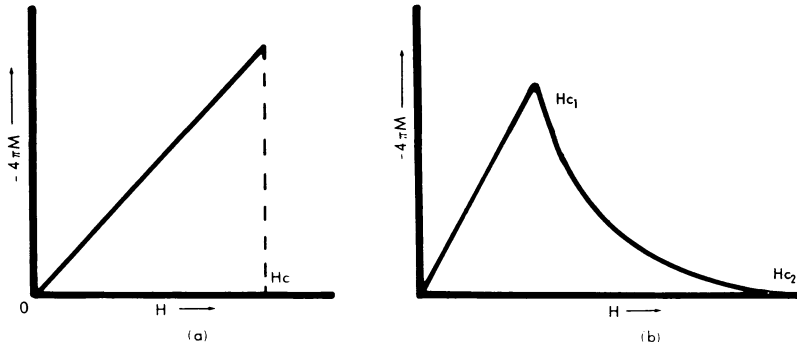
Fig. 3.15. (a) Expulsion of flux in a superconductor of the first kind up to a critical field $H_c$. (b) Incomplete Meissner effect in a superconductor of the second kind. Flux penetration begins at $H_{c1}$ and is complete at $H_{c2}$.

the model allows the irreversibility of magnetization observed in type II superconductors. Further, the magnetization measurements do not have the same simple relationship to the measurement of electrical resistivity, as in type I superconductors. Many alloys are type II superconductors, and obviously the simple relations derived in Section 3.8 have to be generalized suitably.[28] Indeed, careful measurements on ideal type II superconductors, clearly exhibiting the specific-heat singularities at the transitions, are only now available.[29] The theory of Ginzburg and Landau, developed by Abrikosov and Gor'kov, explains many features of the behavior of type II superconductors, which are gaining technical importance in the generation of high magnetic fields. These matters are taken up at length in some recent reviews of the field.[27,30]

# REFERENCES

1. J. L. Olsen, *Electron Transport in Metals*, Interscience, New York, 1962.
2. M. Born, *Atomic Physics*, Blackie, London, 1962, chapter 8. D. ter Haar, *Elements of Statistical Mechanics*, Rinehart, New York, 1954, chapter 4.
3. C. Kittel, *Solid State Physics*, Wiley, New York, 1956, chapters 11 and 13. A. J. Dekker, *Solid State Physics*, Prentice-Hall, New York, 1957, chapters 10 and 13. L. V. Azaroff and J. J. Brophy, *Electronic Processes in Materials*, McGraw-Hill, New York, 1963, chapters 7, 8, and 10.
4. J. M. Ziman, *Contemp. Phys.* 3, 241, 321, 401 (1962); 4, 1, 81 (1963).
5. W. A. Harrison and M. B. Webb (editors), *The Fermi Surface*, Wiley, New York, 1960.
6. E. C. Stoner, *Phil. Mag.* 21, 145 (1936).
7. R. E. Gaumer and C. V. Heer, *Phys. Rev.* 118, 955 (1960).
8. D. H. Parkinson, *Rept. Progr. Phys.* 21, 226 (1958).
9. J. G. Daunt, *Progr. Low Temp. Phys.* 1, 202 (1955).

10. P. H. Keesom and N. Pearlman, *Handbuch der Physik*, *XIV(I)*, 282 (1956).
11. D. Pines, *Solid State Phys.* **1**, 367 (1955). S. Raimes, *Rept. Progr. Phys.* **20**, 1 (1957).
12. G. V. Chester, *Advan. Phys.* **10**, 357 (1961).
13. P. L. Taylor, *Phys. Rev.* **131**, 1995 (1963). S. K. Koenig, *Phys. Rev.* **135**, A 1693 (1964).
14. N. F. Mott, *Rept. Progr. Phys.* **25**, 218 (1962); *Advan. Phys.* **13**, 325 (1964).
15. W. H. Lien and N. E. Phillips, *Phys. Rev.* **133**, A1370 (1964).
16. W. Hume-Rothery, *Electrons, Atoms, Metals, and Alloys*, Iliffe, London, 1955, chapter 29.
17. F. E. Hoare, in: *Electronic Structure and Alloy Chemistry of Transition Elements*, P. A. Beck (ed.), Interscience, New York, 1963, p. 29.
18. G. J. van den Berg, *Progr. Low Temp. Phys.* **4**, 194 (1964).
19. J. E. Zimmerman and F. E. Hoare, *J. Phys. Chem. Solids* **17**, 52 (1960). J. E. Zimmerman and H. Sato, *J. Phys. Chem. Solids* **21**, 71 (1961). J. P. Franck, F. D. Manchester, and D. L. Martin, *Proc. Roy. Soc. (London), Ser. A* **263**, 494 (1961).
20. A. W. Overhauser, *J. Phys. Chem. Solids* **13**, 71 (1960). W. Marshall, *Phys. Rev.* **118**, 1519 (1960). K. P. Gupta, C. H. Cheng, and P. A. Beck, *J. Phys. Chem. Solids* **25**, 73 (1963).
21. V. A. Johnson and K. Lark-Horovitz, *Progr. Low Temp. Phys.* **2**, 187 (1957).
22. P. H. Keesom and G. Seidel, *Phys. Rev.* **113**, 33 (1959).
23. D. Shoenberg, *Superconductivity*, Cambridge University Press, Cambridge, 1952. E. A. Lynton, *Superconductivity*, Methuen, London, 1962.
24. D. C. Rorer, H. Meyer, and R. C. Richardson, *Z. Naturforsch.* **18a**, 130 (1963).
25. W. S. Corak, B. B. Goodman, C. B. Satterthwaite, and A. Wexler, *Phys. Rev.* **102**, 656 (1956).
26. J. Eisenstein, *Rev. Mod. Phys.* **26**, 277 (1954). B. Serin, *Progr. Low Temp. Phys.* **1**, 138 (1955).
27. J. Bardeen and J. R. Schrieffer, *Progr. Low Temp. Phys.* **3**, 170 (1961). J. M. Blatt, *Theory of Superconductivity*, Academic, New York, 1964. G. Rikayzen, *Theory of Superconductivity*, Interscience, New York, 1965. J. R. Schrieffer, *Theory of Superconductivity*, Benjamin, New York, 1965.
28. R. R. Hake (in press).
29. T. McConville and B. Serin, *Phys. Rev. Letters* **13**, 365 (1964). B. B. Goodman, *Phys. Letters* **12**, 6 (1964).
30. Proceedings of the IBM Conference on Superconductivity, *IBM J. Res. Dev.* **6**, 1–125 (1962). Proceedings of the Colgate Conference on Superconductivity, *Rev. Mod. Phys.* **36**, 1–331 (1964).

*Chapter 4*

# Magnetic Contribution to Specific Heats

## 4.1. THERMODYNAMICS OF MAGNETIC MATERIALS

The behavior of magnetic materials at low temperatures is of widespread interest, be it in demagnetization techniques to produce very low temperatures or in the use of superconducting magnets. Therefore, it is worthwhile to consider the specific heats of magnetic materials separately. It is well known that the magnetic energy depends upon the operative magnetic field $H$, and so it is first necessary to inquire how the specific heat is defined for a system capable of magnetization.

For a simple fluid, the basic thermodynamic relation used in Chapter 1 was

$$T \, dS = dE + dW = dE + P \, dV \qquad (4.1)$$

If the fluid is magnetizable, a term $\mathbf{M} \cdot d\mathbf{H}$ must be added to $dW$ as the work done in changing the magnetic field. For simplicity, the scalar product $\mathbf{M} \cdot d\mathbf{H}$ may be replaced by $M dH$ where $M$, the magnetic moment of the substance, is interpreted as the component of $\mathbf{M}$ in the direction of $\mathbf{H}$. Then

$$T \, dS = dE + P \, dV + M \, dH = dE' + P \, dV - H \, dM$$

where $E' = E + MH$. It is somewhat arbitrary whether $E$ or $E'$ is considered as the internal energy of the substance. This depends on whether the energy $MH$ arising from the simultaneous presence of the field and the body is included in the energy content of the field or of the body. In several cases, it is advantageous and logical[1] to use $E'$ as the internal energy. Further, in the problems of interest here, the mechanical work $P \, dV$ may be neglected in comparison with the magnetic part $-H \, dM$. So the fundamental relation may be written as

$$T \, dS = dE' - H \, dM \qquad (4.2)$$

A comparison of equations (4.1) and (4.2) shows immediately that all the relations derived in Chapter 1 may be taken over to the magnetic case simply by replacing $P$ and $V$ by $H$ and $-M$, respectively. The principal magnetic heat capacities, $C_H$ at constant field and $C_M$ at constant magnetization, are

$$C_H = \left(\frac{dQ}{dT}\right)_H = T\left(\frac{\partial S}{\partial T}\right)_H \qquad C_M = \left(\frac{dQ}{dT}\right)_M = T\left(\frac{\partial S}{\partial T}\right)_M \quad (4.3)$$

The equations (1.12) and (1.14) between $C_p$ and $C_v$ are transformed into

$$C_H - C_M = -T\left(\frac{\partial H}{\partial T}\right)_M\left(\frac{\partial M}{\partial T}\right)_H = \frac{T(\partial M/\partial T)_H^2}{(\partial M/\partial H)_T} \quad (4.4)$$

while the relation (1.16) giving the ratio of isothermal to adiabatic compressibility becomes

$$\frac{(\partial M/\partial H)_T}{(\partial M/\partial H)_S} = \frac{C_H}{C_M} \quad (4.5)$$

In general, $(\partial M/\partial H)$ depends upon the shape of the body. For a long rod set parallel to $H$, the field $H_i$ inside the body is the same as the outside field $H$, whereas for other orientations and shapes, appropriate coefficients of demagnetization have to be introduced. Assuming this to be done, the differential molar susceptibility $\chi$ may be introduced by the relation

$$\frac{\partial M}{\partial H} = \chi \quad (4.6)$$

where $M$ refers to the moment per mole.

The correspondence $C_p \leftrightarrow C_H$ and $C_v \leftrightarrow C_M$ suggests that $C_M$ is the quantity of greater theoretical interest. This is true to some extent because in an "ideal" paramagnetic material, which obeys the relation $M = f(H/T)$, $C_M$ is independent of the external field. A simple way of showing this is to write the magnetic analogs of equation (1.17), namely,

$$\left(\frac{\partial C_M}{\partial M}\right)_T = -T\left(\frac{\partial^2 H}{\partial T^2}\right)_M \qquad \left(\frac{\partial C_H}{\partial H}\right)_T = T\left(\frac{\partial^2 M}{\partial T^2}\right)_H \quad (4.7)$$

For an "ideal" paramagnet, $M = f(H/T)$ or $H = Tf^{-1}(M)$. Therefore, $(\partial C_M/\partial M)_T = 0$, whereas $C_H$ depends upon $H$.

These relations concerning the magnetic contributions to the heat capacity and hence to the entropy of a substance are of importance in the process of adiabatic demagnetization. A full discussion of the question may be found in the many reviews on the subject.[2]

## 4.2. TYPES OF MAGNETIC BEHAVIOR[3]

The molecules of most materials have no permanent magnetic moments. Under such conditions, an applied field $H$ induces a magnetic moment in the electronic system of the molecules which is in a direction opposite to that of $H$; this behavior is said to be *diamagnetic*. Diamagnetism is independent of temperature, and so it is of little interest in specific-heat studies. Some molecules, oxygen, for example, have elementary magnetic moments $\mu$; at high temperatures, they are ordinarily oriented at random. On applying a magnetic field, there is a preferential orientation of the moments along $H$, resulting in a magnetization parallel to $H$ (paramagnetic behavior). At low temperatures, an ordered arrangement of the elementary magnets is possible. This ordering process was attributed phenomenologically to internal magnetic fields by Weiss in 1907, but in 1928 Heisenberg showed that it is due to the quantum-mechanical exchange interaction between neighboring electrons. An ordered state with parallel spins and therefore parallel magnetic moments (Fig. 4.1b) produces a large spontaneous magnetization even in the absence of $H$. In this ferromagnetic state, $M$ becomes a nonlinear function of $H$ and hysteresis effects are also present.

The exchange interaction is able to overcome the thermal randomization of the spins at a sufficiently low temperature. The Curie temperature $T_c$, below which the spins become ordered, is as high as 1080°K for iron and less than 1°K for some alums. However, the ordered state need not always be ferromagnetic, as was shown by Néel. In some cases, the adjacent spins may be aligned antiparallel (Fig. 4.1c). In this antiferromagnetic state there is no net spontaneous magnetization, but hysteresis is present and the susceptibility shows a sharp maximum at the transition temperature (Néel point). In a few cases, alternate magnetic moments are unequal and become arranged with adjacent spins antiparallel (Fig. 4.1d). This ferrimagnetic state is macroscopically similar to a ferromagnetic state, but the substances—ferrites and garnets find important practical
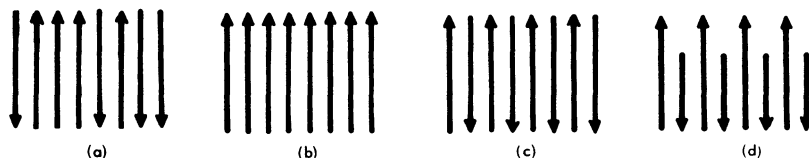
Fig. 4.1. Schematic order–disorder state in a lattice of elementary magnets: (a) paramagnetism—disordered spins; (b) ferromagnetism—parallel spins; (c) antiferromagnetism—adjacent spins antiparallel; (d) ferrimagnetism—adjacent unequal spins antiparallel.

applications—are poor conductors of electricity. Other types of ordering in which the spins are arranged along spirals are also possible (Section 7.6), and simple surveys of para-,[4] ferro-,[5] antiferro-,[6] and ferrimagnetic[7] states are available.

It is clear that, if the atoms or molecules of a substance possess permanent magnetic moments, the magnetic state depends very much upon the temperature, which means that interesting effects may be expected in the specific heats. In discussing them, it is convenient to start from the ordered state at low temperatures and then to pass on to the behavior as the temperature is raised.

## 4.3. SPIN WAVES—MAGNONS

The ideal ordered state described above exists only in the absence of thermal agitation. Taking first the case of ferromagnets, the spins at the lattice sites are aligned at $0°K$ along, say, $Z$ so that the angular momentum $\hbar s$ is along $Z$. At a finite temperature, the spins at some sites $j$ may be excited to higher energy states, i.e., point in other directions. Such distributions may be Fourier-analyzed into a set of waves. A spin wave may then be described as a sinusoidal disturbance of the spin system. The usefulness of describing a ferromagnet at finite temperatures as a superposition of spin waves was pointed out by Bloch in 1930. It permits a correlation of the various magnetic and other properties. A full description of the subject[8] is outside the scope of the present work, and only a qualitative derivation[9] of the spin wave spectrum in a ferromagnet can be given here. Unfortunately, this conceals some of the difficulties involved in the concept of spin waves, which are treated at length elsewhere.[8]

For simplicity, consider a linear ferromagnetic chain with a small field $H_0$ along $-Z$. Then the spins will all be pointing up with angular momenta $\hbar s_i$ about $Z$. Further, $s_i = \mu_i/g\beta = \mu_i/\hbar\gamma$ where $\beta = he/4\pi mc$ is the Bohr magneton, $\gamma = ge/2mc$ is the magneto-mechanical ratio, and $g$ is the Landé factor equal to approximately 2 in ferromagnets. Classically, at $0°K$ all the spins will precess in phase about $Z$ at the Larmor frequency $\omega_0 = \gamma H_0$. If now a spin wave is excited, the situation will be as shown in Fig. 4.2a. The spins are no longer in phase, and the phase angle between successive spins is equal to $qa$, where $a$ is the lattice constant and $2\pi/q$ is the wavelength.

In an effective field $H_{eff}$, each spin, because of its magnetic moment, will experience a torque $\mu_i \times H_{eff} = \gamma\hbar s_i \times H_{eff}$. This torque is equal to the time rate of change of angular momentum

$$\frac{d(\hbar s_i)}{dt} = \gamma\hbar s_i \times H_{eff}$$
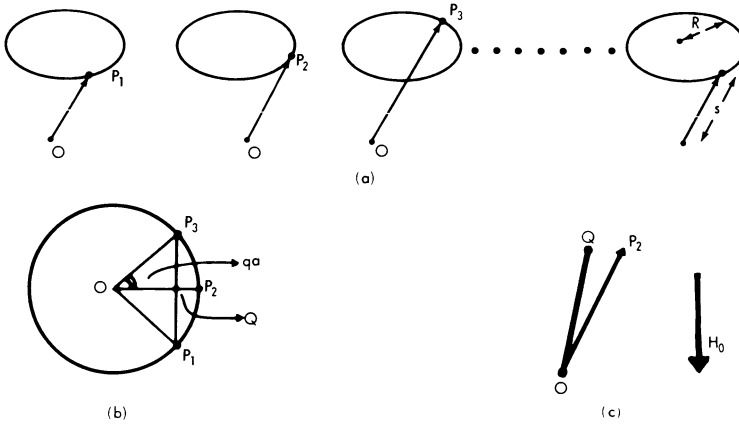
Fig. 4.2.  Classical picture of a spin wave $q$ in a linear ferromagnetic chain.

The effective field is calculated from the Hamiltonian [compare equation (4.18)]

$$\mathscr{H}_i = -g\beta \mathbf{s}_i \cdot \left( \mathbf{H}_0 + \frac{2J}{g\beta}\sum_j \mathbf{s}_j \right) = -g\beta \mathbf{s}_i \cdot \mathbf{H}_{\mathrm{eff}}$$

where the sum $\Sigma_j$ is over the two near neighbors and $J$ is the quantum-mechanical exchange constant.  Using this value of $\mathbf{H}_{\mathrm{eff}}$,

$$\frac{d(\hbar \mathbf{s}_i)}{dt} = \gamma \hbar \mathbf{s}_i \times \left( H_0 + \frac{2J}{g\beta}\sum_j \mathbf{s}_j \right) \tag{4.8}$$

If $R$ is the amplitude of precession, $\mathbf{s}_i \times \mathbf{H}_0 = sH_0 \sin(s, H_0) = RH_0$. Figures 4.2 (a and b) shows that the resultant of $OP_1$ and $OP_3$ is $2\,OQ$ where $P_2Q = \frac{1}{2}Rq^2a^2$, and from Fig. 4.2c $\phi = \angle P_2OQ = \frac{1}{2}Rq^2a^2s^{-1}$. Therefore, the right-hand side of equation (4.8) is equal to $\gamma\hbar[RH_0 + (2J/g\beta)sRq^2a^2]$. The left-hand side is $\hbar\omega'R$, where $\omega'$ is the angular velocity of precession, and so

$$\omega' = \gamma H_0 + \frac{2J}{g\beta} sq^2 a^2$$

The Larmor frequency of the spin system is $\gamma H_0$, and the frequency of the spin wave itself is

$$\omega = \frac{2J}{\hbar} sa^2 q^2 \tag{4.9}$$

In a three-dimensional crystal, the same dispersion law $\omega \propto q^2$, first found by Bloch, is obeyed, and the general ferromagnetic spin

wave frequency may be taken as

$$\omega_q = \alpha_f \frac{2Jsa^2}{\hbar} q^2 \qquad (4.10)$$

The constant $\alpha_f$ depends upon the details of the crystal structure and has been calculated in several practical cases.[8] The same $\omega \propto q^2$ is also obeyed by the spin waves in a ferrimagnet. However, in anti-ferromagnets, special considerations come into play in defining the normal modes of disturbances. It was first shown by Hulthén that the spin-wave spectrum is given as

$$\omega_q = \alpha_a \frac{2J'sa^2}{\hbar} q \qquad (4.11)$$

where $J'$ is the magnitude of the exchange constant. The antiferro-magnetic spectrum is linear in $q$, unlike the quadratic dependence in ferro- and ferrimagnets. To establish equation (4.11) would require a longer discussion than is warranted here, and so it suffices to mention the references to elementary[9] and rigorous[8] derivations.

It is interesting to compare the spin waves with the lattice waves analyzed in Chapter 2. At low frequencies, the normal modes of a lattice have a dispersion relation $\omega \propto q$, whereas the allowed modes in the spin system may be either $\omega \propto q^2$ as in ferromagnets or $\omega \propto q$ as in antiferromagnets. A set of mass points connected by elastic springs will form a model for lattice vibrations. A model for spin waves will be a set of arrows, each connected to its two neighbors by torsional springs. The angular displacement of a spin out of the line with its neighbors gives rise to a torque proportional to the excess displacement and tending to restore equilibrium. The analogy with lattice waves is actually very deep. The spin waves may be quantized into magnons, which play the same role in magnetic phenomena as phonons do in lattice dynamics. Magnons and phonons obey Bose–Einstein statistics. These similarities have been very fruitful in the study of magnetic systems.

## 4.4. SPIN WAVE SPECIFIC HEATS

The fact that magnons obey Bose statistics allows easy calculation of the low-temperature thermal properties of magnetic materials. It was seen in Chapter 2 that at a temperature $T$ the mean energy of a Bose oscillator of angular frequency $\omega$ is $\hbar\omega/[\exp(\hbar\omega/kT) - 1]$ [equation (2.8a)] and that the number of energy states between momenta $p$ and $p + dp$ is $(4\pi V/h^3)p^2\,dp$ [equation (2.18)]. Using the dispersion relations (4.10) and (4.11), the specific-heat contributions at low temperatures can be easily derived.

Taking first ferro- and ferrimagnets, where $\omega \propto q^2$,

$$E = 4\pi V \int_0^{} \frac{(2\alpha_f J s a^2 q^2) q^2 \, dq}{\exp(2\alpha_f J s a^2 q^2 / kT) - 1}$$

$$= 4\pi V (2\alpha_f J s a^2) \left(\frac{kT}{2\alpha_f J s a^2}\right)^{5/2} \int_0^{} \frac{x^4 \, dx}{e^{x^2} - 1} \tag{4.12}$$

The upper limit of integration over $q$ cannot be specified without detailed analysis, but at low temperatures the upper limit for $x$ may be taken as infinity without serious error and the integral may be evaluated suitably. The specific heat now follows as

$$C_M = \frac{dE}{dT} = c_f N k \left(\frac{kT}{2Js}\right)^{3/2} \tag{4.13}$$

where the constant $c_f$ has been calculated for several crystal structures.[8] For example, $c_f \sim 0.113$ in a simple cubic arrangement of spins. Equation (4.13) is an important result, that at low temperatures the ferromagnetic contribution to specific heats is proportional to $T^{3/2}$. A similar $T^{3/2}$-variation is obeyed by the saturation magnetization of ferromagnets, for which the $T^{3/2}$ behavior had been observed for a long time. In specific heats, the measurement of spin wave contributions has been only recently successful.

In metals (Chapter 3), the conduction electrons give a specific heat proportional to $T$, the phonons give a $T^3$-term, and, if the above magnetic term is added, the low-temperature specific heat will be of the form

$$C_v = \gamma T + \beta T^3 + \delta T^{3/2}$$

The temperature variation of the heat capacity will be dominated by the term with the lowest power of $T$, namely, the electronic term. With a few exceptions discovered recently, most ferromagnets are metallic; therefore, a clear resolution of the magnetic $T^{3/2}$-term is a matter of considerable experimental difficulty. Not surprisingly, the spin wave effects were not easily observed in the specific heats of ferromagnets, although the magnetic measurements had borne out the theoretical predictions. The situation is quite different in ferrimagnets. They are electrical insulators, and in the absence of free electrons the specific heat is of the form

$$C_v = \beta T^3 + \delta T^{3/2}$$

At low temperatures, the spin wave is dominant, and a plot of $CT^{-3/2}$ against $T^{3/2}$ should be a straight line. The first such experiments
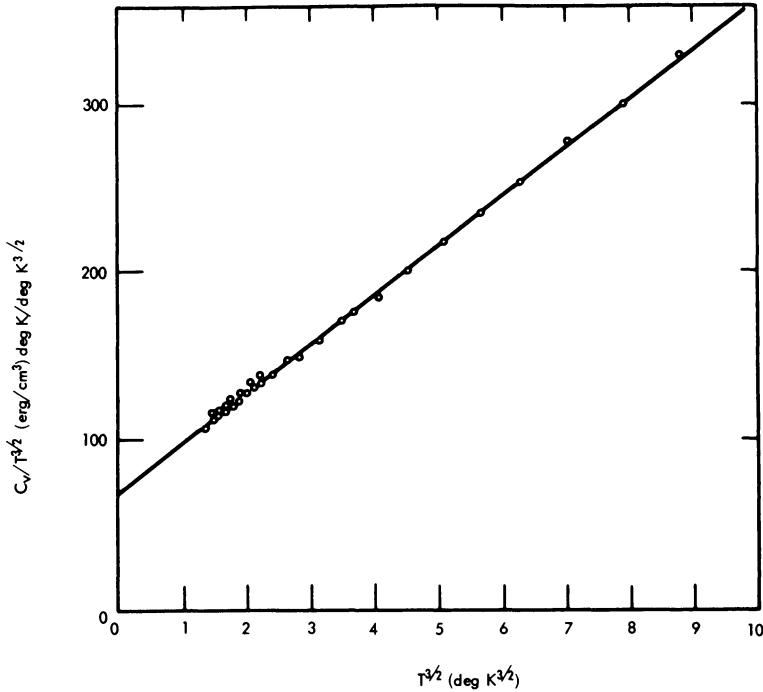
Fig. 4.3.  Low-temperature specific heat of YIG showing the spin wave $T^{3/2}$-contribution.[10]

were made on magnetite $Fe_3O_4$ by Kouvel in 1956; since then, similar measurements have been made on several garnets, ferrites, and very recently on some ferromagnetic insulators. Figure 4.3 shows a typical result for yttrium iron garnet (YIG), with clear evidence for the $T^{3/2}$-term.[10] The exchange constant $J$ may also be obtained from various other experiments, such as magnetic resonance and neutron scattering. The agreement among the values of $J$ is fair, when the large corrections for demagnetizing effects and anisotropy are taken into account.

Going now to the case of antiferromagnets, the dispersion relation $\omega = \alpha_a(2J'sa^2/\hbar)q$ means that

$$E = 4\pi V \int_0^{\cdot} \frac{2\alpha_a J' sa^2 q^3 \, dq}{\exp(2\alpha_a J' sa^2 q/kT) - 1}$$

$$= 4\pi V (2\alpha_a J' sa^2) \left(\frac{kT}{2\alpha_a J' sa^2}\right)^4 \int_0^{\cdot} \frac{x^3 \, dx}{e^x - 1}$$
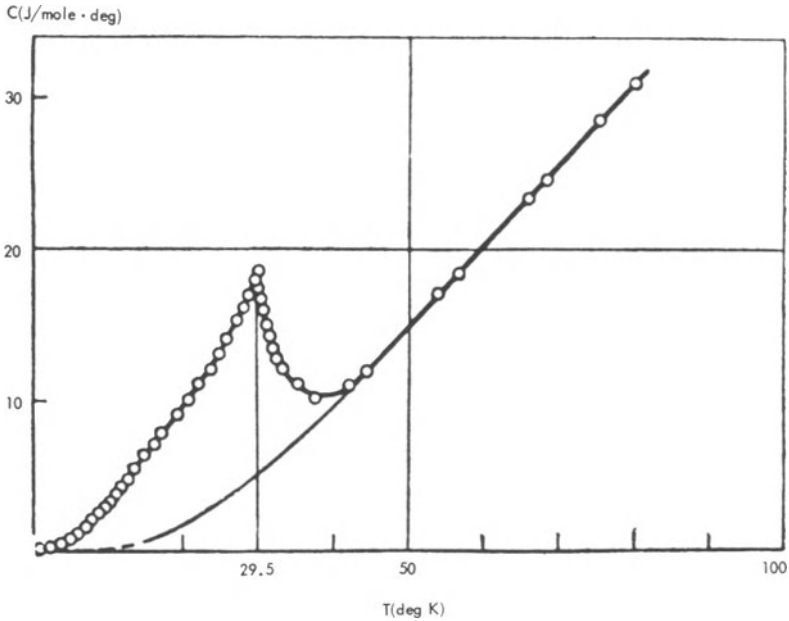
Fig. 4.4. Heat capacity of $MnCO_3$ (circles and thick lines) and $CaCO_3$ (thin lines) showing antiferromagnetic contribution.[11]

At low temperatures, the upper limit for $x$ may again be taken as infinity, and the specific heat becomes

$$C_M = c_a N k \left( \frac{kT}{2J's} \right)^3 \tag{4.14}$$

The constant $c_a$ has been calculated for several types of lattices. The $T^3$ spin wave specific heat in antiferromagnets is strikingly different from the $T^{3/2}$-dependence in ferromagnets. The temperature dependence is of the same form as the lattice contribution in the Debye $T^3$-region. This makes an experimental separation of the spin wave and lattice specific heats almost impossible in metals and very difficult in nonmetallic antiferromagnets. In the carbonates of manganese and cobalt, the antiferromagnetic $T^3$-contribution is about ten to twenty times larger than the lattice term, as may be seen in Fig. 4.4, where the specific heat of $MnCO_3$ is compared with that of $CaCO_3$, which has no magnetic contribution.[11] The experimental values agree very well with those calculated from magnetic measurements.

It must be added that the spin wave specific-heat relations (4.13) and (4.14) hold good at moderate temperatures only. At very low

temperatures, some of the approximations made above are not valid and the specific heat may decrease exponentially. At high temperatures, interactions among magnons give rise to other terms, as shown in detail by Dyson, and the simple spin wave picture is no longer very useful. For the sake of simplicity, these details[8] are left out here.

## 4.5. THE WEISS MODEL FOR MAGNETIC ORDERING

As mentioned earlier, the ordered ferro-, ferri-, or antiferromagnetic states go over into the paramagnetic state at sufficiently high temperatures. The change in the magnetic properties is accompanied by a sharp peak in the specific-heat curve at $T_c$. Figure 4.5 shows the typical example of nickel. The magnetic contribution $C_M$ is obtained by subtracting the lattice and electronic terms from the total $C_v$. The behavior near $T_c$ is typical of a general class of cooperative transitions, which will be discussed at length in Chapter 7.

Historically, it was Weiss who in 1907 gave a simple explanation of ferromagnetism. A few years earlier, Langevin had shown that the
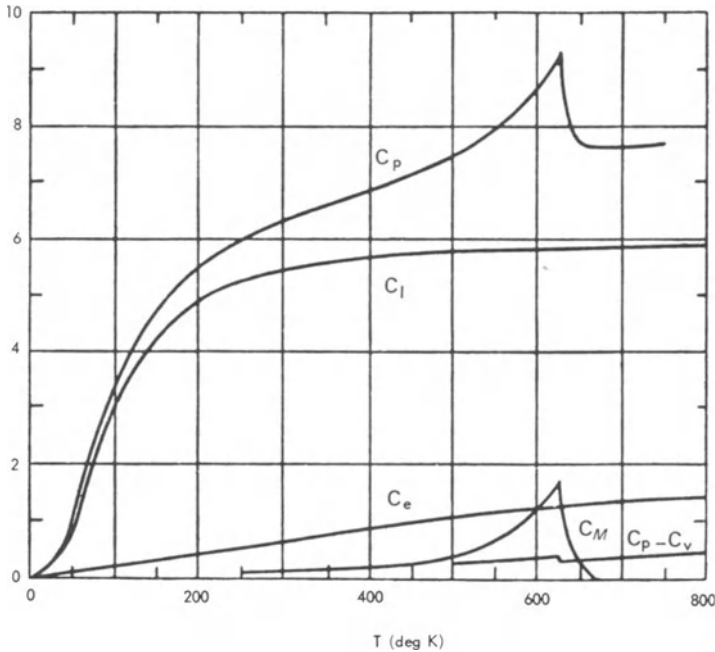


Fig. 4.5. Heat capacity of nickel (in cal/g-atom·deg) showing the magnetic contribution $C_M$ besides lattice and electronic terms.

competition between the magnetic field **H** tending to align the elementary magnets $\mu$ and the thermal agitation causing a random arrangement results in a net magnetization of the form

$$M = N\mu \tanh\left(\frac{\mu H}{kT}\right) \tag{4.15}$$

Langevin's theory explained many aspects of paramagnetic behavior—in particular, Curie's law, that the susceptibility varies as $1/T$, arises because for ordinary fields and temperatures $\mu H/kT \ll 1$. Weiss suggested that because of the magnetization of the other parts of a solid there is an internal magnetic field $\alpha M$ ($\alpha$ a constant) and that the effective field acting on the elementary dipoles is

$$H_{\text{eff}} = H_{\text{ext}} + \alpha M$$

Substitution of $H_{\text{eff}}$ in place of $H$ in equation (4.15) shows that even in the absence of an external field $H_{\text{ext}}$ there is a spontaneous magnetization given by the implicit equation

$$M_s = N\mu \tanh\left(\frac{M_s T_c}{N\mu T}\right) \tag{4.16}$$

where $T_c = \alpha N\mu^2/k$. This is the ferromagnetic state. Weiss's theory also explained hysteresis and other features of $M$–$H_{\text{ext}}$ curves. For many metals, equation (4.16) satisfactorily describes the variation of $M_s$ with $T$, except very near the transition temperature $T_c$. The moment $\mu$ comes out to be equal to the Bohr magneton $he/4\pi mc$, showing that ferromagnetism is due to the magnetic moment of electrons. [As a matter of fact, equation (4.15) is the quantum-mechanical expression for particles of spin $\frac{1}{2}\hbar$.]

The energy of magnetization in the absence of $H_{\text{ext}}$ is

$$E_M = -\int_0^M H_{\text{int}}\, dM = -\tfrac{1}{2}\alpha M^2$$

and so the magnetic contribution to specific heat is

$$C_M = -\tfrac{1}{2}\alpha\frac{dM^2}{dT} \tag{4.17}$$

The magnetic specific heat given by the Weiss model is shown in Fig. 4.6. $C_M$ steadily increases from zero at $T = 0$ to a maximum $\frac{3}{2}R$ at $T = T_c$. This maximum is followed by a discontinuous drop to $C_M = 0$ in the paramagnetic state $T > T_c$. No latent heat is liberated at $T_c$, and the transition in the Weiss model is a phase change of the second order (see Section 8.1).
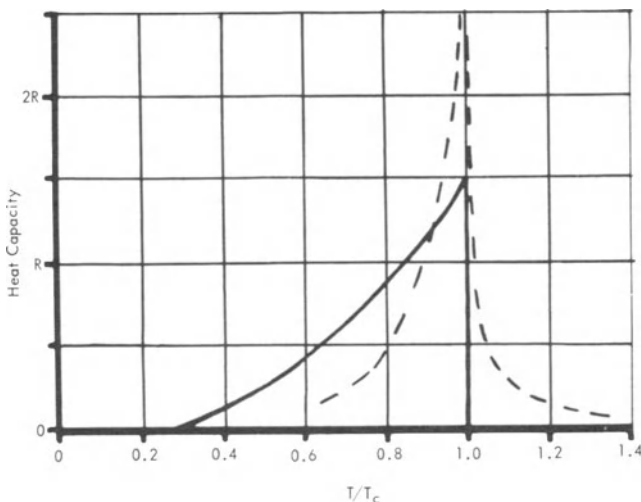
Fig. 4.6. Schematic variation of magnetic heat capacity near $T_c$ in the Weiss model (full line) and in statistical theories (broken lines).

The experimental values of $C_M$, as seen in Figs. 4.4 and 4.5, follow the general trend in being small at low temperatures and beginning to rise as $T_c$ is approached. Near $T_c$, there is not even qualitative agreement with the above theory. $C_M$ often rises to a value much higher than the predicted maximum; furthermore, the specific-heat curve has a "tail" above the transition. $C_M$ decreases sharply, no doubt, but instead of falling abruptly to zero it lingers on for a considerable range of temperatures before becoming immeasurably small.

The phenomenological theory may be suitably modified to give a small "tail" to the specific-heat curve,[12] but the agreement is not very much improved. It is generally believed that an explanation of the behavior of ferro- and antiferromagnets near $T_c$ belongs to the realm of proper statistical theories.

## 4.6. THE HEISENBERG AND ISING MODELS

Very soon after the development of quantum mechanics, Heisenberg (in 1928) gave an explanation of the origin of Weiss's internal magnetic fields, whose large magnitudes of around $10^5$ Oe remained puzzling. On account of the Pauli exclusion principle, two electrons with spins $s_1$, $s_2$ have an interaction energy of the form $-2J s_1 \cdot s_2$, where the exchange integral $J$ is a function of distance. For large separations of the electrons, $J$ is very small, but for spacings of the

order of a few Ångstroms the exchange energy becomes large enough
to be comparable to chemical binding energies. Thus, if the energy
were written in terms of the electronic magnetic moments $\mu$, it would
be of the same form and magnitude as the internal magnetic energy
in the Weiss model, even though it is basically electrostatic in origin.
If $J$ were positive, a parallel (ferromagnetic) alignment of spins would
be favored, while a negative $J$ results in antiparallel alignment.

The statistical theory of magnetic systems thus involves the
calculation of the partition function $\Sigma \exp(-E_r/kT)$ of the system.
With the general form of the exchange interaction, the calculations are
so prohibitively complicated that it is normal to make two stages of
approximations. The Heisenberg model assumes that, since $J$ falls
off rapidly with increasing distance, it is enough to take the interactions
as extending only to the nearest neighbors. Thus the energy of the
system in this model is

$$E(\text{Heisenberg}) = -2J \sum_{i,j} \mathbf{s}_i \cdot \mathbf{s}_j - \mu \mathbf{H} \cdot \sum_i \mathbf{s}_i \qquad (4.18)$$

where $\Sigma$ is over all pairs of direct neighbors. This model has been
quite successful in explaining, for example, the spin waves at low
temperatures (Section 4.3). However, even this approximation in-
volves formidable difficulties, so that in many statistical problems a
further simplification is commonly used, though the model was intro-
duced slightly earlier by Ising. In the Ising model, the scalar product
$\mathbf{s}_i \cdot \mathbf{s}_j$ is replaced by $s_{iz}s_{jz}$ on the basis that if $Z$ is the direction of
alignment, the expectation value of $\mathbf{s}$ in $X$, $Y$ directions is zero. Then

$$E(\text{Ising}) = -2J \sum_{i,j} s_{iz}s_{jz} - \mu H \sum_i s_{iz} \qquad (4.19)$$

where $\Sigma$ is again over pairs of adjacent neighbors.

The Ising model is a scalar problem in that it deprives magnetism
of its intimate connection with the angular momentum of electrons.
Further, it does not admit a spin wave picture at low temperatures.
Hence, it may be considered a poor model for magnetic studies.
However, near or above $T_c$, the statistical enumeration of the states,
which is correctly taken into account, assumes dominant importance
in the thermodynamic and other properties of the system. Therefore,
a large amount of theoretical work has been done on the behavior of
the simple Ising model near $T_c$, where its deficiencies are unimportant.
There are two reasons for the great interest in the field: In the first
place, the Ising and Heisenberg models furnish instructive theoretical
schemes not only for magnetic transitions but also for other coopera-
tive transformations, which will be discussed in Chapter 7. The Ising
model is the simplest one which appears to reproduce many of the

features observed experimentally. Secondly, the general problem for a three-dimensional solid has remained so far an unsolved challenge. The exact solution for a two-dimensional Ising model was given by Onsager in 1944, but even this is a remarkable *tour de force* to be savored only by professional theoreticians.[13]

It is now superfluous to add that the solutions of the Heisenberg and Ising models, even in their approximate form, are far too sophisticated to be reproduced here. As regards the specific heat, which is the prime concern in this text, the two-dimensional Ising lattice exhibits a logarithmic singularity:

$$\begin{aligned} C_M &\approx A \log (T - T_c) \dots & T > T_c \\ &\approx B \log (T_c - T) \dots & T < T_c \end{aligned} \qquad (4.20)$$

where the constants $A$, $B$ have been calculated for several lattices. In a three-dimensional case, such exact relations are not yet available, and various approximate calculations have been made. The nature of the singularity, whether an inverse power of $|T - T_c|$ or logarithmic in $|T - T_c|$, cannot be described with certainty, although for a diamond-type Ising lattice the approximations have been carried sufficiently far to suggest a logarithmic infinity in specific heat below the ferromagnetic transition.[14] To be fair, it must be mentioned that a logarithmic singularity at the cooperative transition had been revealed by calorimetric measurements performed somewhat earlier (Figs. 4.9 and 5.5). Above $T_c$ the experiments can be fitted to a logarithmic term in some cases and to a power law singularity in others.[14a]

It is also possible to estimate the ferromagnetic transition temperature $T_c$, as well as the magnetic part of the entropy $S$ and internal energy $E$ that are removed at the transition. For a fcc lattice, the values are

| | | |
|---|---|---|
| $2kT_c/zJ$ | 0.68 | 0.82 |
| $(S_\infty - S_c)/k$ | 0.27 | 0.10 |
| $(E_\infty - E_c)/kT_c$ | 0.44 | 0.15 |

$$(4.21)$$

Here $z$ is the number of nearest neighbors and $J$ is the exchange constant. The values are for spin $\frac{1}{2}$, and the first column refers to the Heisenberg model and the second to the Ising model. The entropy values show that the Heisenberg model has a larger tail on the high-temperature side than the Ising model. For bcc or other types of lattices, the constants in (4.21) are slightly different. Similar small variations arise for spins greater than $\frac{1}{2}$. In particular, the specific

heat on the high-temperature side rises more rapidly for larger spins. Antiferromagnetic transitions may be studied similarly, but calculations are scanty. A schematic variation of the specific heat near $T_c$ is shown in Fig. 4.6.

In contrast to these approximate values, which depend upon the model chosen for calculations, a very general result may be given for the total magnetic entropy $S_M$. It is well known that a particle with spin $s\hbar$ has $2s + 1$ quantized orientations. In a field $H$, the levels have slightly different energies, but in the absence of $H$ the energies are all equal and there is a $2s + 1$ degeneracy in the state of the system. The entropy corresponding to this is $k \ln (2s + 1)$ per particle, which is the entropy that comes into play here. The rule

$$S_M = R \ln (2s + 1) \text{ per mole} \tag{4.22}$$

has been verified in many cases.[15] Only a small part of this entropy is removed as the substance is cooled to $T_c$ from a high temperature. This percentage is slightly larger in a Heisenberg model with its larger tail above $T_c$. Most of the ordering takes place below the transition.

## 4.7. SPECIFIC HEATS NEAR THE TRANSITION TEMPERATURE

It is only recently that careful experimental studies have been made to check the various predictions of the statistical theories; on the whole, reasonable agreement is found.[16] As an example of ferromagnets, the complete magnetic and calorimetric studies[17] on copper ammonium and copper potassium chlorides, $Cu(NH_4)_2Cl_4 \cdot 2H_2O(T_c = 0.70°K)$ and $CuK_2Cl_4 \cdot 2H_2O(T_c = 0.88°K)$, may be considered. Below about $0.5T_c$, the specific heat follows the variation given by this spin wave theory (Section 4.3). For the ammonium salt, the exchange constant $J/k$ given by the spin wave variation is about $0.28°K$, compared to the values of approximately $0.30°K$ calculated from the Curie–Weiss constant and approximately $0.29°K$ derived from the behavior of the specific heat in the paramagnetic state $T > T_c$. Near $T_c$, the statistical theory suggests that the specific heat is a function of $T/T_c$ only; Fig. 4.7 shows how closely this is verified. (The lattice contribution is negligible at these low temperatures.) The entropy calculated from the full line has a value of $5.8$ J/mole·degK, whereas the theoretical value for $s = \frac{1}{2}$ of $Cu^{2+}$ ion is $R \ln 2 = 5.76$ J/mole·degK. Further, the authors obtain $2kT_c/zJ = 0.75$, $(S_\infty - S_c)/k = 0.22$, $(E_\infty - E_c)/kT_c = 0.38$. These values are in between the numbers given in (4.21), although the Heisenberg model gives a good explanation of the other properties of the substance. A part of the discrepancy may be due to the bcc structure of these salts,
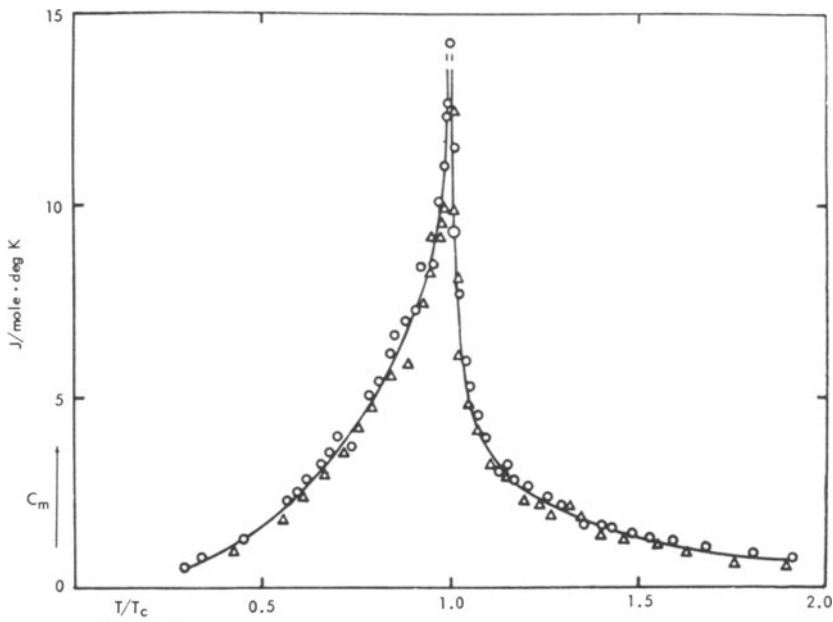
Fig. 4.7. Heat capacity of $CuK_2Cl_4 \cdot 2H_2O$ ($T_c = 0.882°K$, circles) and $Cu(NH_4)_2Cl_4 \cdot 2H_2O$ ($T_c = 0.704°K$, triangles) plotted as a function of $T/T_c$.[16]

whereas equation (4.21) refers to a fcc lattice. Support for this view is given by the fact that a Heisenberg model for a bcc lattice gives $2kT_c/zJ = 0.72$, in much better agreement with the experiments.

Antiferromagnetic transitions are exemplified by the study[18] of nickel and cobalt chlorides, $NiCl_2 \cdot 6H_2O$($T_N = 5.34°K$), $CoCl_2 \cdot 6H_2O$ ($T_N = 2.29°K$). The specific heat of the nickel salt is shown in Fig. 4.8, while that of the cobalt salt is similar except for the change in the Néel temperature. The lattice term, which is nearly the same in both salts, was found from the $T^3$-behavior of the lattice specific heat and the $T^{-2}$-variation of the paramagnetic specific heat at $T \gg T_N$ (compare Section 4.9). The magnetic specific heat is obtained by subtracting the lattice contribution from the total specific heat. Because of the influence of the crystalline electric field upon the electronic levels of the transition metal ions, one should expect $s = \frac{1}{2}$ for the cobaltous ion and $s = 1$ for the nickelous ion. The magnetic entropy was equal to 9.13 J/mole·degK for the nickel salt, which is within 1% of $R \ln 3$. That of cobaltous chloride was 5.80 J/mole·degK $\sim R \ln 2$. The exchange constant $|J|/k$ has a value of approximately 1.6°K for $CoCl_2 \cdot 6H_2O$ if calculated from the total ordering energy and about 1.5°K if calculated from the Néel temperature. Of more interest is
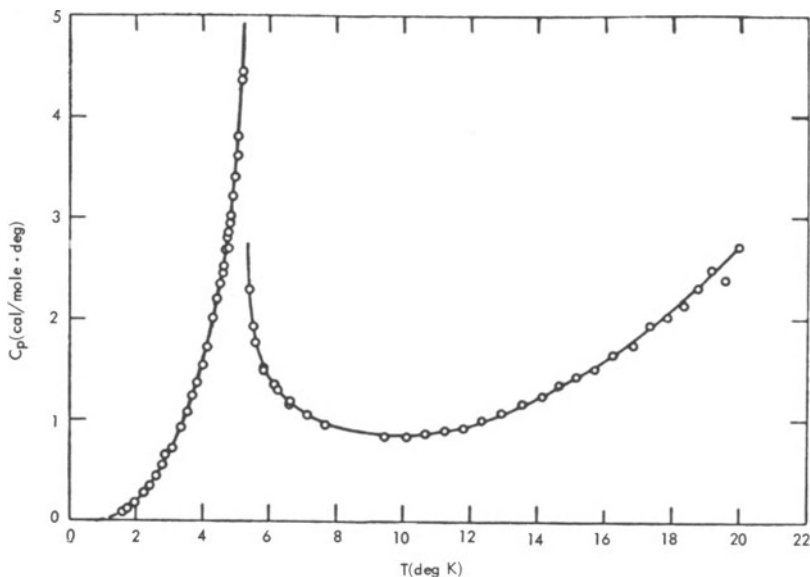
Fig. 4.8.  Heat capacity of $NiCl_2 \cdot 6H_2O$.[18]

the behavior of $C_M$ found near $T_N$ (Fig. 4.9). The data appear to suggest that the specific heat becomes logarithmically infinite at the Néel temperature. This singularity and the similar behavior found in liquid $^4He$ (Fig. 5.6) are of special interest because Onsager's solution for a two-dimensional cooperative transition shows a logarithmic infinity, while no firm predictions are as yet available for a three-dimensional case.

## 4.8. PARAMAGNETIC RELAXATION

Specific-heat studies in paramagnetic salts are important in two respects. In the first place, the attainment of temperatures much lower than 1°K by adiabatic demagnetization techniques involves a thorough knowledge of the magnetic entropy which can be extracted from the system. Secondly, paramagnetic salts furnish an interesting class of specific-heat anomalies, namely, the Schottky peak. Before these matters are taken up in detail, it is convenient to discuss a special method of measuring specific heats which is very useful when they are not easily separated from the lattice contributions.

The method is based on paramagnetic relaxation,[3,4] discovered by Gorter. If a magnetic field is applied to a paramagnetic salt, the internal energy of the system is changed. It is found that the time

taken for the transfer of the heat of magnetization from the dipoles to the crystal lattice (spin–lattice relaxation time) is much longer than the time needed for the establishment of thermal equilibrium among the dipoles themselves (spin–spin relaxation time). On suddenly changing $H$, the dipoles very quickly (in about $10^{-10}$ sec) follow the field, but the magnetic energy is given to the lattice only in a leisurely (of the order of $10^{-6}$ sec) fashion. Therefore, for any variation of $H$ over a time long compared to the spin–spin relaxation time but short compared to the spin–lattice relaxation time, the dipoles are in equilibrium among themselves but do not exchange heat with the lattice. A measurement of the variation of $M$ under such conditions gives the adiabatic susceptibility $\chi_S$. The normal DC measurement yields the isothermal susceptibility $\chi_T$. Equations (4.4) to (4.6) now show that

$$\frac{\chi_T}{\chi_S} = 1 + \frac{T(\partial M/\partial T)_H^2}{\chi_T C_M} \qquad \text{or} \qquad C_M = T\left(\frac{\partial M}{\partial T}\right)_H^2 \frac{\chi_S}{(\chi_T - \chi_S)\chi_T} \qquad (4.23)$$

As pointed out first by Casimir, du Pre, and de Haas in 1938–1939, the lattice temperature is not changed during the measurement, and so the lattice specific heat does not enter the calculation.
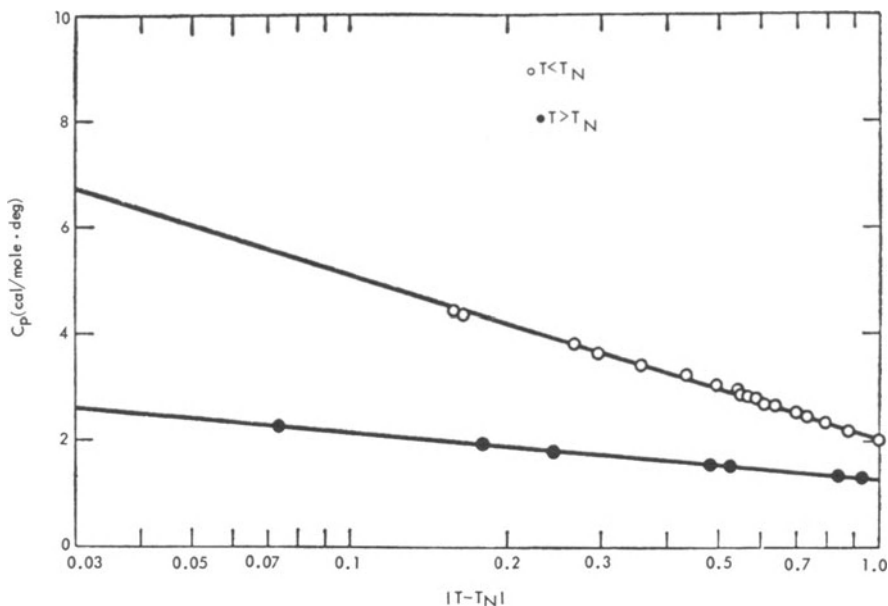


Fig. 4.9. Plot of $C_M$ versus $\log |T - T_N|$ for $NiCl_2 \cdot 6H_2O$.

By this technique it is possible to measure magnetic contributions to specific heats at liquid-nitrogen temperatures, where they may amount to only $10^{-6}$ of the total heat capacity of the salt. Since the spin–lattice relaxation time is about $10^{-6}$ sec at these temperatures, the adiabatic susceptibility must be determined at radio frequencies. At liquid-helium temperatures the spin–lattice relaxation time is usually of the order of $10^{-3}$ sec and audiofrequency measurements suffice. The details of the experimental techniques are thoroughly discussed by Benzie and Cooke.[19] At very low temperatures ($\ll 1°$K), the heating produced in AC measurements is considerable, and direct calorimetry is preferred. At these temperatures, the lattice specific heat is so small that the entire specific heat measured calorimetrically may be taken as arising from magnetic effects. At higher temperatures, the paramagnetic relaxation technique is very useful, because the lattice and magnetic terms are nearly comparable and not easily separated out.

At very low temperatures, since the spin system can exist for an appreciable time without interacting with the lattice, it is advantageous in magnetic studies to attribute a separate (spin) temperature and specific heat to the spin system. Discussions of such nonequilibrium concepts can be found in the treatises on magnetic resonance and are not appropriate here.

## 4.9. SCHOTTKY EFFECT

It is well known that a particle with spin $s\hbar$ has $2s + 1$ possible orientations of the spin; in a magnetic field, the particle has a number of discrete energy levels. This spacing of the quantized energy levels is reflected in the specific heat in an interesting way. Consider for a moment a system with two levels, $\Delta$ apart. At $T \ll \Delta/k$, the upper level will scarcely be populated, whereas at $T \gg \Delta/k$ both levels will be nearly equally populated. Only at temperatures comparable to $\Delta/k$ will transitions from one level to another take place in appreciable amounts. This rapid change in the internal energy corresponds to a large specific heat which becomes zero at both high and low temperatures. Thus there is the intriguing possibility of a hump in $C_v$, which will in general be superimposed on the lattice and other contributions.

A general problem of this kind was considered by Schottky in 1922. Suppose there is a system in which the particles can exist in a group of $m$ levels, separated from the ground state by energies $\varepsilon_1, \varepsilon_2, ..., \varepsilon_m$ and with degeneracies $g_1, g_2, ..., g_m$. Using the Boltzmann factor $\exp(-\varepsilon/kT)$, the probability of a particle occupying the $r$th

level is

$$\frac{g_r \exp(-\varepsilon_r/kT)}{\displaystyle\sum_n g_r \exp(-\varepsilon_r/kT)}$$

With $N$ independent particles in the system, the mean energy at a temperature $T$ is

$$E = \frac{N \displaystyle\sum_{r=0}^{m} \varepsilon_r g_r \exp(-\varepsilon_r/kT)}{\displaystyle\sum_{r=0}^{m} g_r \exp(-\varepsilon_r/kT)} \qquad (4.24)$$

The specific heat is obtained by calculating $dE/dT$. The simple case of two levels illustrates all the features of such calculations. For a two-level system, equation (4.24) becomes

$$E = \frac{N g_1 \varepsilon_1 \exp(-\varepsilon_1/kT)}{g_0 + g_1 \exp(-\varepsilon_1/kT)}$$

and the Schottky specific heat is

$$\begin{aligned}
C_{\text{Sch}} &= \frac{N\varepsilon_1^2}{kT^2} \frac{g_0}{g_1} \frac{\exp(\varepsilon_1/kT)}{[1 + (g_0/g_1)\exp(\varepsilon_1/kT)]^2} \\
&= R\left(\frac{\delta}{T}\right)^2 \frac{g_0}{g_1} \frac{\exp(\delta/T)}{[1 + (g_0/g_1)\exp(\delta/T)]^2}
\end{aligned} \qquad (4.25)$$

where $\delta = \varepsilon_1/k$ is the energy separation measured in degK. $C_{\text{Sch}}$ is plotted in Fig. 4.10 for a few values of $g_1/g_0$.

The qualitative remarks made earlier about the behavior at low and high temperatures may now be made quantitative. From equation (4.25) it is easy to see that

$$C_{\text{Sch}} = R\left(\frac{g_1}{g_0}\right)\left(\frac{\delta}{T}\right)^2 \exp\left(-\frac{\delta}{T}\right) \qquad T \ll \delta \qquad (4.26)$$

$$= R g_0 g_1 (g_0 + g_1)^{-2} \left(\frac{\delta}{T}\right)^2 \qquad T \gg \delta \qquad (4.27)$$

The specific heat attains a maximum value at an intermediate temperature $T_m$ given by

$$\left(\frac{g_0}{g_1}\right)\exp\left(\frac{\delta}{T_m}\right) = \frac{(\delta/T_m) + 2}{(\delta/T_m) - 2} \qquad (4.28)$$

and the maximum itself is equal to

$$C_{\text{Sch}}(\text{max}) = \frac{R}{4}\frac{T_m}{\delta}\left[\left(\frac{\delta}{T_m}\right)^2 - 4\right] \qquad (4.29)$$
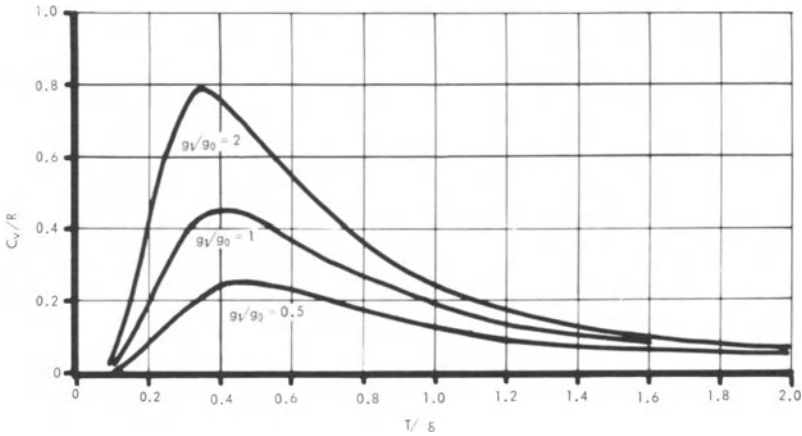
Fig. 4.10. Schottky heat capacity of a two-level system for several values of $g_1/g_0$.

Thus if $g_0/g_1 = 1$, the maximum occurs at $T_m = 0.42\delta$ and has a value $C_{Sch}(max) = 3.6$ J/mole·deg. Table 4.I gives $T_m/\delta$ and $C_{Sch}(max)$ for several values of $g_1/g_0$. When these values are compared with the typical lattice and electronic contributions of $10^{-2}$ J/mole·deg at 4°K, it is evident that a Schottky peak occurring at liquid-helium temperatures will dominate the variation of specific heat (see Fig. 4.11).

If $C_{Sch}$ is isolated from the observed total specific heat, by the methods to be discussed below, there are several ways of finding $\delta$ and $g_1/g_0$. The position and magnitude of the peak, the behavior at high temperatures ($C_{Sch} \cdot T^2 = $ constant) or at low temperatures ($\log(C_{Sch} \cdot T^2)$ linear in $1/T$) may all be used. This, of course, assumes that there are only two energy levels to be considered. If more levels are involved, the full equation (4.24) has to be used, or, alternatively,

$$C_{Sch} = T \frac{d^2(RT \ln z)}{dT^2} = RT^{-2} \frac{d^2 \ln z}{d(1/T)^2}$$

## TABLE 4.I

| $g_1/g_0$ | $C_{Sch}$ (max) J/mole· deg | $T_m/\delta$ | Total entropy |
|-----------|------------------------------|--------------|---------------|
| 0.5 | 2.00 | 0.448 | $R \ln \frac{3}{2}$ |
| 1.0 | 3.64 | 0.417 | $R \ln 2$ |
| 1.5 | 5.06 | 0.394 | $R \ln \frac{5}{2}$ |
| 2.0 | 6.31 | 0.377 | $R \ln 3$ |
| 5.0 | 12.0 | 0.320 | $R \ln 6$ |

where

$$z = \sum g_r \exp\left(-\frac{\varepsilon_r}{kT}\right)$$

Apart from the behavior $C_{\text{Sch}} \propto T^{-2}$ at high temperatures, no simple results can be given. In such cases it is necessary to start with some schemes of energy levels derived either theoretically or from susceptibility, paramagnetic resonance, and other data. The specific-heat curve then serves as a check on the correctness of the assumed model.

The entropy associated with the Schottky peak may be obtained by integrating $C_{\text{Sch}} \cdot T^{-1}$; the values for the two-level case are given in Table 4.I. These results may also be obtained by enumerating the possible configurations of the system, as was done with equation (4.21). For example, if there are $m$ levels of equal degeneracy, the extra entropy is $R \ln m$ per mole. In the two-level case, $S = R \ln [1 + (g_1/g_0)]$. Usually, a comparison of the theoretical and experimental values of the excess entropy serves to verify the correctness of separating out $C_{\text{Sch}}$ from the observed total specific heat.

The problem of getting $C_{\text{Sch}}$ from the observed specific heat by subtracting the lattice and other contributions is one of considerable difficulty. If the Schottky peak occurs at low temperatures, the lattice term may be taken as $\beta T^3$. At temperatures well above the peak, $C_{\text{Sch}} \propto T^{-2}$, and the total specific heat will be of the form $C = \beta T^3 + BT^{-2}$. Thus a plot of $CT^2$ versus $T^5$ should be a straight line, which permits the desired resolution to be carried out. The magnetic contribution in Fig. 4.9 was obtained from Fig. 4.8 in this manner. For this separation to work, the lattice term must be proportional to $T^3$ and the two terms must be of similar magnitude. If this restriction cannot be satisfied, it is usual to take for $C_{\text{lattice}}$ the specific heat of a salt of similar composition and same crystal structure, but which does not have an anomaly. The case of $MnCO_3$ and $CaCO_3$ (Fig. 4.4) is an example of this type of analysis. In some cases, the magnetic contribution may be evaluated separately from measurements of paramagnetic relaxation or adiabatic demagnetization from different magnetic fields. In general, the Schottky term, if present at liquid-helium temperatures, is so large a fraction of the observed specific heat that small errors in evaluating the lattice corrections are not serious.

## 4.10. SPECIFIC HEAT OF PARAMAGNETIC SALTS

Paramagnetic salts, in which the magnetic dipoles have energy levels with spacings of approximately 1 to 10°K, form the natural examples of simple systems exhibiting a variety of Schottky peaks. That such a close relationship should exist may be inferred in the

following way. For the magnetic moment of a paramagnet, Langevin's theory gives an expression of the form

$$M = N\mu \tanh (\mu H/kT) \qquad (4.15)$$

In a field $H$, the energy of the magnetic moment of the body is $MH$; this corresponds to a specific heat

$$C_M = (N \mu^2 H^2/kT^2) \operatorname{sech}^2 (\mu H/kT) \qquad (4.30)$$

If the energy difference between two levels $2\mu H$ of a particle is put equal to $\varepsilon_1$, this is nothing but equation (4.25) with $g_0 = g_1$. Figure 4.10 with $kT/2\mu H$ instead of $T/\delta$ and $g_1/g_0 = 1$ will represent equation 4.30 equally well. In a paramagnetic gas, the position of the specific-heat maximum may be shifted at will by applying a magnetic field. For the fields normally used, this is practicable only at low temperatures.[20] The entropy of the spin system can be increased merely by demagnetizing a magnetically saturated specimen. If the process is done adiabatically, a compensating decrease of temperature is enforced to keep the entropy constant. This forms the basis of the adiabatic demagnetization technique to reach temperatures below $1°K$ and to measure the magnetic specific heats in that region.[2]

A similar electrocaloric effect is also possible, in which excitations occur between the different levels of electric dipoles.[20a]

In a solid, the magnetic ions have energy levels about $1°K$ apart even in the absence of external fields. These closely spaced levels arise in several ways. In any solid, there are crystalline electric fields which remove the spin degeneracy of some atomic energy levels through the familiar Stark effect. There are magnetic dipole and exchange interactions among neighboring ions, which also split the energy levels, though Stark-splitting accounts for the major share in the level splitting. Besides these causes attributed to the electronic spin, nuclear effects may also arise from the energy levels of the nuclear dipoles and quadrupoles. The specific-heat studies, being integrated measurements, give no clue to the origin of the energy splittings. This must come from other theoretical and experimental studies, especially those on magnetic susceptibility and paramagnetic resonance. The resonance studies are particularly fruitful in directly giving the separation and degeneracy of the various levels. A good account of the interrelations among the various measurements is given by Rosenberg.[21]

A prerequisite for applying the simple Schottky theory is that the various ions should be independent of one another. Since the magnetic interactions do not fall off very rapidly with increasing distance, the ions will not respond independently, except as a first approximation, to the applied magnetic fields. An approximate correction for the

lack of statistical independence may be applied, but it is more usual to dilute the specimen with isomorphous diamagnetic salts so that the various ions are far removed from one another. In some salts, such as alums and Tutton salts, the water molecules in the crystal provide the necessary dilution, but where nature does not perform the decoupling well enough, artificial measures have to be employed. Even when a complete picture of the energy levels is available, small discrepancies between the calculated and theoretical specific heats are often present. They are usually attributed to the lack of statistical independence caused by coupling among the ions themselves and among the ions and the lattice phonons.[22]

An example of the good agreement between theory and experiment is the Schottky effect in $\alpha - NiSO_4 \cdot 6H_2O$.[23] The $Ni^{2+}$ ion can have in general three energy levels on account of the removal of spin degeneracy by the crystalline electric and magnetic fields, although approximate calculations suggested two levels with $g_1 = 2$ and $g_0 = 1$. The experimental curve does resemble Fig. 4.10, with
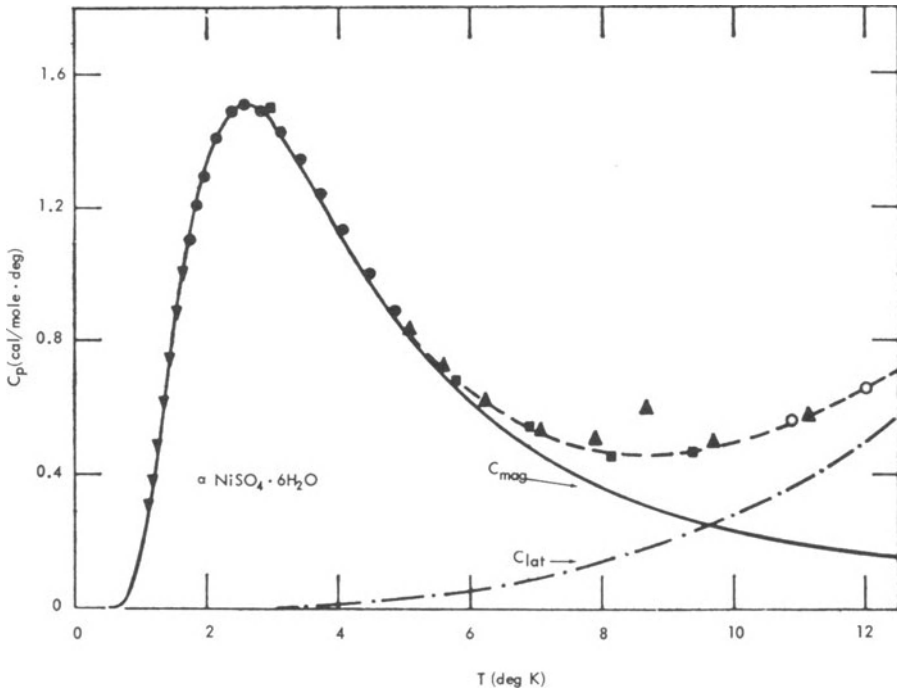


Fig. 4.11. Heat capacity of $\alpha$-NiSO$_4$·6H$_2$O.[23] Full line is the calculated magnetic term. Dot-dashed line is the lattice heat capacity.

$g_1/g_0 = 2$ as regards $C_{Sch}$ (max). Detailed comparisons showed three levels with spacings 6.44 and 7.26°K above the lowest spin state. The agreement with the experimental values, after taking into account the lattice contribution (which is about 7% of the total $C_v$ at 6°K and about 1% at 4°K), is seen to be very good. The total entropy of the magnetic system is $R \ln 3$. With this knowledge of the energy levels, other properties, such as susceptibility and magnetization, have been calculated in reasonable agreement with the observed values.

An illustration of the great utility of calorimetric data in supplementing the information from paramagnetic resonance and susceptibility measurements is furnished by the case of ferric methylammonium sulfate $Fe(NH_3CH_3)(SO_4)_2 \cdot 12H_2O$.[24] Paramagnetic resonance studies by Bleaney and coworkers showed that $Fe^{3+}$ ion has three doublet states. The middle $S_z = \pm\frac{3}{2}$ level is separated from the other two by energies of 1.05 and 0.58°K, but it was not known which of the levels $\pm\frac{1}{2}, \pm\frac{5}{2}$ was the lowest spin level. Therefore two schemes, shown in Fig. 4.12, are possible, and the corresponding $C_{Sch}$ are compared with the experimental specific heats. There is no doubt that scheme 2, with $S_z = \pm\frac{1}{2}$ as the lowest level, is the correct one. The addition of
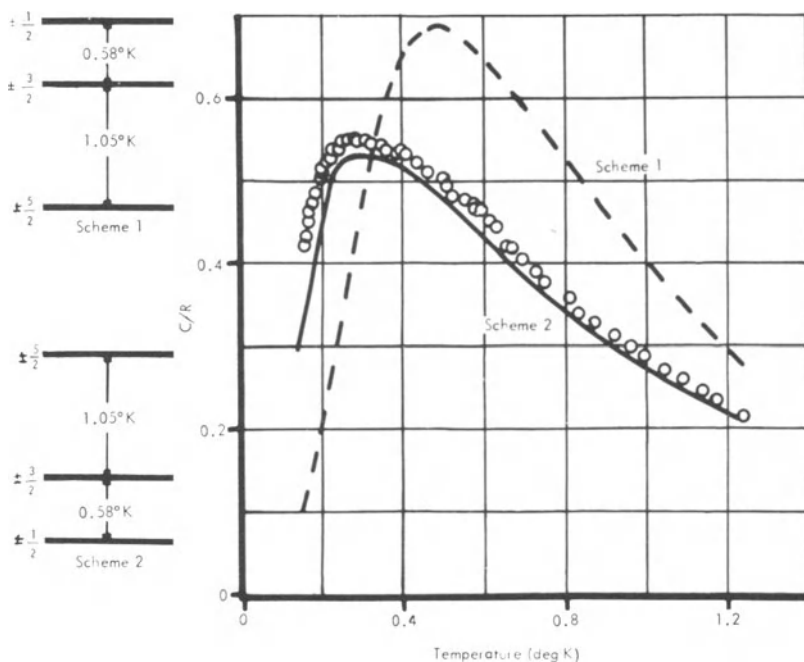


Fig. 4.12. Heat capacity of $Fe(NH_3CH_3)(SO_4)_2 \cdot 12H_2O$ compared with two possible level schemes. Obviously, scheme 2 with $\pm\frac{1}{2}$ level lowest gives a better fit.

the magnetic dipolar contribution removes the small discrepancy found in Fig. 4.12. In this salt, measurements of susceptibility could not throw much light on the energy level schemes, and the calorimetric data gave an elegant solution to the problem.

Although the spin disorder in the paramagnetic state, which gives a $T^{-2}$ specific heat at high temperatures, should eventually be removed at 0°K, it is not easy to say whether the removal will involve a Schottky peak or a cooperative singularity. In general, with dilute systems, the spin disorder is removed with a Schottky peak. If the exchange interactions are strong, a cooperative transition to the ferromagnetic, antiferromagnetic, or other states occurs before a Schottky peak can be observed.

## 4.11. NUCLEAR SCHOTTKY EFFECTS

Schottky effects are widely observed in the electron paramagnetism of crystalline salts or of some gases such as nitric oxide and oxygen. In the solid state, Schottky peaks may arise from a different source. If the atomic nucleus has a magnetic moment $\mu_N$, it may have a set of energy levels in an effective field $H_{eff}$, arising from orbital and conduction electrons. The splitting is similar to the hyperfine structure (hfs) observed in spectroscopy. Moreover, if the nucleus has a quadrupole moment, its interaction with the field gradients produced by neighboring atoms will cause small level splittings. The change in population of these levels is readily observed as a Schottky effect in the specific heats.

The hfs effect was first observed in ferromagnetic materials, where the presence of internal fields of the order of $10^5$ Oe obviously suggests that the nuclear levels will be appreciably split. Since then, such effects have been observed in antiferromagnets and more prominently in many ferromagnetic rare-earth metals. In holmium, the peak occurs at a reasonable temperature of 0.3°K, and so the complete anomaly has been mapped out.[25] The levels of a nucleus of spin $I$ may be written as

$$\varepsilon_i/k \approx ai$$

where $i = -I, -I + 1, ..., I$ and $a$ is the hfs coupling constant. For holmium, $I = \frac{7}{2}$ and there are eight levels. From paramagnetic-resonance studies, Bleaney had calculated $a \approx 0.31$°K. The specific-heat studies give $a \approx 0.32$°K, in excellent agreement with paramagnetic-resonance data. Actually, in holmium there is a small quadrupole contribution which is taken into account in the theoretical curve of Fig. 4.13. The excellent fit with the experiments needs no further description.
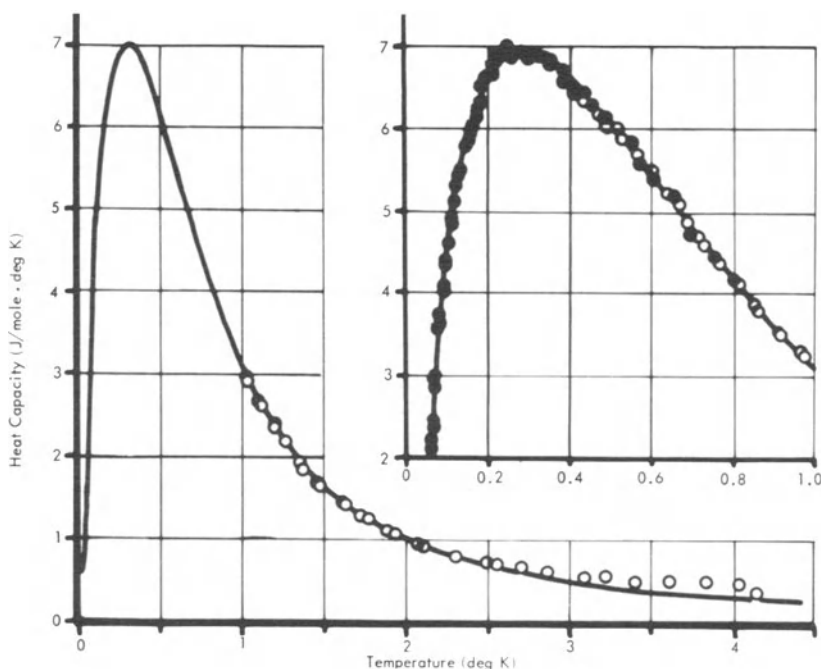
Fig. 4.13. Heat capacity of holmium metal.[25] Full line is theoretical Schottky curve.

If a nucleus with a quadrupole moment is situated in a non-spherical or noncubic electronic environment, the quadrupole interaction with the electric field gradient gives a set of energy levels

$$\varepsilon_i/k \approx P'[i^2 - \tfrac{1}{3}I(I + 1)]$$

Here $P'$ is the quadrupole coupling constant, which may be related to the quadrupole moment and the field gradient. The $T^{-2}$ high-temperature Schottky term arising from such splittings has been observed in substances such as rhenium, mercury, indium, and gallium.[26]

Because of the smallness of the nuclear moments compared to the electronic moments, the nuclear anomalies occur in the region of $10^{-2}$ K, whereas the electronic peaks are present at 1 to 10°K. On the other hand, the nuclear effects may arise even in diamagnetic materials.

## REFERENCES

1. E. A. Guggenheim, *Thermodynamics*, North Holland, Amsterdam, 1957, chapter 12.
   A. B. Pippard, *Elements of Classical Thermodynamics*, Cambridge University Press, Cambridge, 1957, pp. 23 and 63.

2. C. G. B. Garrett, *Magnetic Cooling,* Harvard University Press, Cambridge, 1954.
   D. de Klerk and M. J. Steenland, *Progr. Low Temp. Phys.* **I,** 273 (1955).
   D. de Klerk, *Handbuch der Physik,* *XV(2),* 38 (1956).
   E. Ambler and R. P. Hudson, *Rept. Progr. Phys.* **18,** 251 (1955).
   W. A. Little, *Progr. Cryogenics* **4,** 99 (1964).

3. A. J. Dekker, *Solid State Physics,* Prentice-Hall, New York, 1957, chapters 18 and 19.
   J. B. Goodenough, *Magnetism and the Chemical Bond,* Interscience, New York, 1963, chapter 2.

4. J. H. van den Handel, *Advan. Electron. Electron Phys.* **6,** 463 (1954).

5. E. C. Stoner, *Rept. Progr. Phys.* **11,** 43 (1948); **13,** 83 (1950).

6. A. B. Lidiard, *Rept. Progr. Phys.* **17,** 201 (1954). T. Nagamiya, K. Yosida and R. Kubo, *Advan. Phys.* **4,** 1 (1955).

7. W. P. Wolf, *Rept. Progr. Phys.* **24,** 212 (1961). R. K. Wangsness, *Progr. Cryogenics* **4,** 73 (1964).

8. J. van Kronendonk and J. H. van Vleck, *Rev. Mod. Phys.* **30,** 1 (1958). A. I. Akhiezer, V. G. Bar'yakhtar, and M. I. Kagano, *Soviet Phys. Uspekhi* **3,** 567, 661 (1960).

9. F. Keffer, H. Kaplan, and Y. Yafet, *Am. J. Phys.* **21,** 250 (1953).

10. D. T. Edmonds and R. G. Petersen, *Phys. Rev. Letters* **2,** 499 (1959).

11. A. S. Borovik-Romanov and I. N. Kalinkina, *Soviet Phys. JETP* **14,** 1205 (1962). I. N. Kalinkina, *Soviet Phys. JETP* **16,** 1432 (1963).

12. K. P. Belov, *Magnetic Transitions,* Consultants Bureau, New York, 1959.

13. G. H. Wannier, *Elements of Solid State Theory,* Cambridge University Press, Cambridge, 1959, chapter 4. H. Eyring, D. Henderson, B. J. Stover, and E. M. Eyring, *Statistical Mechanics and Dynamics,* Wiley, New York, 1964, chapter 10.

14. J. W. Essam and M. F. Sykes, *Physica* **29,** 378 (1963).

14a. A. R. Miedema, R. F. Wielinga, and W. J. Huiskamp, *Phys. Letters* **17,** 87 (1965). D. T. Teaney, *Phys. Rev. Letters* **14,** 898 (1965).

15. J. A. Hofmann, A. Paskin, K. J. Tauer, and R. J. Weiss, *J. Phys. Chem. Solids* **1,** 45 (1956).

16. C. Domb and A. R. Miedema, *Progr. Low Temp. Phys.* **4,** 296 (1964).

17. A. R. Miedema, H. van Kempen, and W. J. Huiskamp, *Physica* **29,** 1266 (1963).

18. W. K. Robinson and S. A. Friedberg, *Phys. Rev.* **117,** 402 (1960). J. S. Skalyo and S. A. Friedberg, *Phys. Rev. Letters* **13,** 133 (1964).

19. R. J. Benzie and A. H. Cooke, *Proc. Phys. Soc. (London), Ser. A* **63,** 213 (1950).

20. W. F. Giauque, D. N. Lyon, E. W. Hornung, and T. E. Hopkins, *J. Chem. Phys.* **37,** 1446 (1962).

20a. I. Shepherd and G. Feher, *Phys. Rev. Letters* **15,** 194 (1965).

21. H. M. Rosenberg, *Low Temperature Solid State Physics,* Oxford University Press, Oxford, 1963, chapters 1 and 9.

22. J. H. van Vleck, *J. Chem. Phys.* **5,** 320 (1937). M. H. Hebb and E. M. Purcell, *J. Chem. Phys.* **5,** 338 (1937). V. F. Sears, *Proc. Phys. Soc. (London)* **84,** 951 (1964). J. W. Tucker, *Proc. Phys. Soc. (London)* **85,** 559 (1965).

23. J. W. Stout and W. B. Hadley, *J. Chem. Phys.* **40,** 55 (1964).

24. A. H. Cooke, H. Meyer, and W. P. Wolf, *Proc. Roy. Soc. (London), Ser. A* **237,** 404 (1956).

25. O. V. Lounasmaa, *Phys. Rev.* **128,** 1136 (1962). H. van Kempen, A. R. Miedema, and W. J. Huiskamp, *Physica* **30,** 229 (1964).

26. P. H. Keesom and C. A. Bryant, *Phys. Rev. Letters* **2,** 260 (1959). H. R. O'Neal, N. M. Senozan, and N. E. Phillips, *Proceedings of the Eighth International Conference on Low Temperature Physics* (London, 1962, R. O. Davies, ed.), Butterworth, London, 1963. N. E. Phillips, M. H. Lambert, and W. R. Gardner, *Rev. Mod. Phys.* **36,** 131 (1964). J. C. Ho and N. E. Phillips, *Phys. Letters* **10,** 34 (1964).

*Chapter 5*

# Heat Capacity of Liquids

## 5.1. NATURE OF THE LIQUID STATE

Among the three states of aggregation, solids $\rightleftharpoons$ liquids $\rightleftharpoons$ gases, less is known about the liquid state than about the other two. To some extent this is not surprising, because the limiting cases of solids and gases are sufficiently clear-cut and simple to allow schematic models to represent their behavior. In gases, the molecules are far apart and have no spatial correlation. In solids, the atoms are arranged in lattice sites. Such situations can be analyzed to a first approximation on the basis of idealized models, perfect gases, or perfect lattices, and these elementary calculations may then be refined, if necessary. The difficulty in developing an adequate theory of the liquid state is that such convenient starting points are not available. Near the freezing point, liquids exhibit many of the characteristics of solids, whereas near the boiling point the behavior of liquids is to some extent similar to that of gases.[1] In liquids, the atomic arrangement in the immediate vicinity of any atom is partially ordered (short-range order), but at great distances the arrangement is completely random (long-range disorder). The absence of long-range order distinguishes a liquid from a solid, while the presence of short-range order differentiates between a liquid and a gas.

The phenomena that occur in a liquid may be described as follows. After melting, the system is no longer crystalline, but each atom still retains much the same relationship to its nearest neighbors as it did in a solid. The thermal energy of vibration of each atom is changed only slightly. In the liquid, rotational motion is possible; furthermore, the atoms can jump from one position to another. The fluidity of a liquid arises because such a jumping process can relax an applied shear stress in a very short time, of the order of $10^{-10}$ sec; as a matter of fact, at frequencies higher than about $10^{10}$ cps, liquids do behave like solids in supporting shear waves. As the liquid is

warmed, the molecules acquire more freedom of motion and the distance up to which there is short-range order is progressively reduced. This continues until the boiling point is reached, when the molecules are liberated from the liquid lattice at the expense of considerable latent heat.

## 5.2. SPECIFIC HEAT OF ORDINARY LIQUIDS AND LIQUID MIXTURES

On the basis of the above ideas, one would expect the specific heat to show a small increase on melting, and thereafter in the liquid state it should show a gradual increase until the boiling point is reached. Many liquids do behave in this way. Table 5.I shows the measured specific heat under saturated vapor pressure $C_s$ for some common cryogenic liquids. The gradual increase in $C_s$ up to the boiling point of the liquid is in conformity with the expected behavior.

The specific heat at saturated vapor pressure $C_s$ is the quantity of practical relevance in liquids, since it is more easily measured than $C_p$ or $C_v$. In Section 8.2 it will be proved that if $\beta$ is the coefficient of volume expansion, then

$$C_s = C_p - TV\beta\left(\frac{\partial P}{\partial T}\right)_{svp} \tag{5.1}$$

The term $TV\beta(\partial P/\partial T)_{sat}$ increases as the liquid is warmed so that $(C_p - C_s)/C_s$ is about $1\%$ near the melting point and about $25\%$ near the boiling point. Thus in Table 5.I the increase in $C_p$ as the liquid is warmed is somewhat larger than the rise in $C_s$. The behavior of $C_v$ is not so simple. The difference between $C_p$ and $C_v$

$$C_p - C_v = \frac{TV\beta^2}{k_T} \tag{5.2}$$

where $k_T$ is the isothermal compressibility [equation (1.14)], and the ratio $C_p/C_v$ both increase with rise in temperature. $C_p/C_v$ may become

## Table 5.I. Heat Capacity of Some Cryogenic Liquids (in cal/mole·deg)

| Substance | $T$ (degK) | $C_p$(solid) | $C_s$(liquid) | $T$ (degK) | $C_s$(liquid) | $C_p$(gas) |
|---|---|---|---|---|---|---|
| $N_2$ | 63.2 | 5.7 | 6.7 | 77.3 | 6.9 | 6.8 |
| $O_2$ | 54.4 | 5.6 | 6.4 | 90.2 | 6.5 | 6.9 |
| A | 83.8 | 4.2 | 5.0 | 87.3 | 5.1 | 5.0 |

as high as 1.5 in some cases. The specific heat at constant volume, as calculated from the measured values of $C_s$, $\beta$, and $k_T$, increases with temperature near the melting point, reaches a shallow maximum, and then decreases as the boiling point is approached.[2] In the gaseous state, there are no mean positions for the atoms to vibrate, and only free translation and rotation are possible. Under such conditions, $C_v$ becomes about $\frac{5}{2} R$ for gases such as nitrogen and oxygen and $\frac{3}{2} R$ for gases such as argon, as will be seen in the next chapter.

There are some exceptions to the above general behavior. Water, for instance, is an exception to many of the above statements. This most common of all liquids is in many ways the most exceptional one as well.

Although the behavior of liquids is understood qualitatively, there is no satisfactory theory to explain the details. Several approximate models have been proposed with varying degrees of success. Space does not permit an elaboration of these attempts to calculate the properties of liquids.[1,2] Only in the case of quantum liquids, $^4$He and $^3$He, has any reasonable theory accounted for the mass of available observations. Since these two unique liquids are almost ubiquitous in cryogenic laboratories, they are treated separately in detail.

Curiously, the special properties of liquid mixtures are somewhat better understood. When two liquids are mixed, the specific heat, density, and other properties of the mixture are slightly different from what may be expected from a mere addition of the contribution due to the parent liquids. Simple thermodynamic and statistical considerations permit correlation of the various excess quantities with one another. There is a considerable physicochemical literature on this subject, and it appears best to consult some of the introductory texts.[2,3]

## 5.3. LIQUID $^4$He AT LOW TEMPERATURES

The helium isotope of mass 4 exhibits several bizarre properties in the condensed state. The atoms obey Bose–Einstein statistics, and the liquid becomes a degenerate Bose system below 2.17°K. Helium-four exists as a liquid even at 0°K and becomes a solid only under a pressure of about 25 atm or more. Below 2.17°K, it flows through narrow channels with practically zero viscosity; it can sustain undamped temperature waves; sometimes it creeps in the form of thin films even against gravitational potential; in fact, its unusual behavior has formed a fascinating field of study in its own merit. Rather than do injustice to the subject by trying to summarize the field,[4] we must content ourselves with an account of the caloric properties.

A fundamental step toward an understanding of the behavior of liquid $^4$He was taken by Landau in 1941. The zero-point energy of the atoms is so large that the substance remains a liquid even at 0°K. In such a quantum region, one cannot identify any single particle and follow its motion. Instead, we should look at the collective behavior of the system as a whole and enumerate the quantum states. This amounts to the formulation of a theory assuming solid-like behavior rather than gas-like, on the grounds that the determining feature of the entire situation is the interaction among all the atoms.

As seen in Chapter 2, the simplest type of thermal excitation possible in a condensed system is a sound wave or a phonon. In a solid, it can be either longitudinal or transverse, but a liquid can support only longitudinal oscillations. The energy $\varepsilon = \hbar\omega$ and the momentum $p = \hbar q$ of a phonon are related by

$$\varepsilon = cp \tag{5.3a}$$

where $c$ is the velocity of sound. A molecule in a liquid is capable of much more complicated motions than mere back-and-forth oscillations. Rotational or vortex motions are simple examples of the more general motions. On the basis of some plausible arguments, Landau assumed for such motions (called *rotons*) the energy-momentum dispersion relation of the form

$$\varepsilon = \Delta + \frac{(p - p_0)^2}{2\mu} \tag{5.3b}$$

This equation has turned out to be so useful in interpreting the behavior of liquid helium that the uncertain foundations on which it was based were rather glossed over for a long time. Recent theoretical work by Feynman and several others has shown that in a Bose system the dispersion relation has the phonon form (5.3a) at low momenta and the roton form (5.3b) at high momenta, so that the complete spectrum has the form shown in Fig. 5.1. Neutron-scattering experiments carried out since 1958 have strikingly confirmed the details of Landau's energy–momentum relationship.[5]

At thermal equilibrium, the excitations in the liquid are distributed mainly in the regions of energy minima, that is, near $\varepsilon = 0$ and $\varepsilon = \varepsilon(p_0) = \Delta$. Thus it is convenient to speak of long-wave excitations (phonons, $p \sim 0$) and short-wave excitations (rotons, $p \sim p_0$) separately, even though the spectrum of Fig. 5.1 is continuous. The thermodynamic properties may then be calculated as phonon and roton contributions. In the following section, this is carried out in a simple manner.
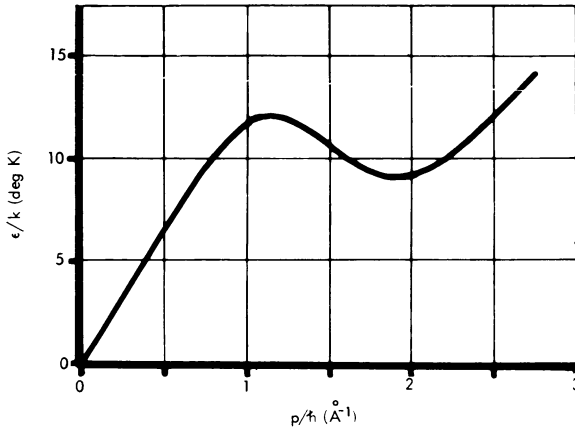
Fig. 5.1. Energy–momentum spectrum in liquid $^4$He.

The specific heat of liquid $^4$He has been measured by several investigators,[6] and is shown in Fig. 5.2. This plot immediately exhibits the interesting features of the specific-heat variation. At very low temperatures $(T < 0.6°\text{K})$,, the specific heat is given by $c_s = (0.0205 \pm 0.0004)T^3$ J/g · deg. The $T^3$-proportionality is reminiscent of the low-temperature behavior of the lattice specific heat and indeed arises from the same reasons, as will be explained in the following section. Above $0.6°\text{K}$, the specific heat rises faster, somewhat as $T^6$ or exp $(-10/T)$, culminating in a high narrow peak at the transition temperature $2.17°\text{K}$. The specific heat drops sharply above this temperature and reaches a value of about $3J/\text{g} \cdot \text{deg}$, which is typical of an ordinary liquid at low temperatures. Much above $2.17°\text{K}$, liquid $^4$He behaves like an ordinary liquid. It is the curious transition at $2.17°\text{K}$ and the exotic properties below the transition that are responsible for the great interest in the subject.

## 5.4. PHONON AND ROTON SPECIFIC HEATS

An instructive way of calculating the specific-heat contributions from phonons and rotons is to evaluate first the number of thermal excitations. The number of energy states per mole between momenta $p$ and $p + dp$ is $(4\pi V/h^3)p^2 \, dp$ [equation (2.18)] and the number of Bose excitations in this range is $(4\pi V/h^3)p^2 \, dp/[\exp(\varepsilon/kT) - 1]$. Therefore, the total number of excitations $N$ and the total energy
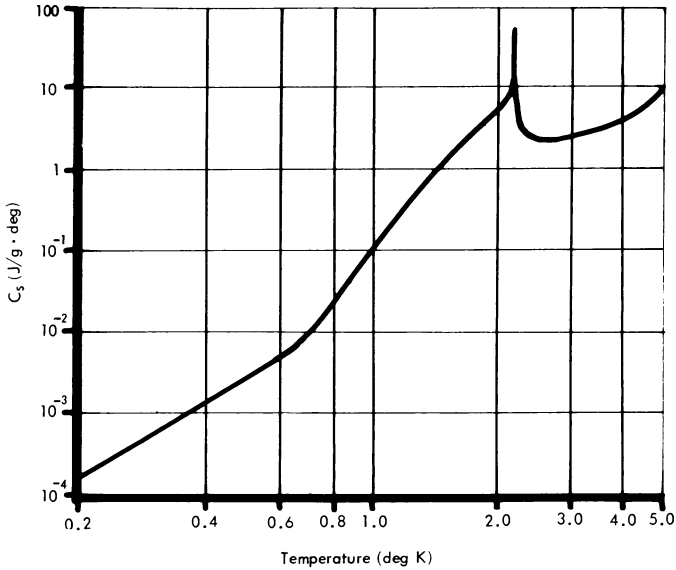
Fig. 5.2. Specific heat of liquid $^4$He under its saturated vapor pressure.[6]

$E$ per mole are

$$N = \frac{4\pi V}{h^3} \int \frac{p^2 \, dp}{\exp(\varepsilon/kT) - 1} \tag{5.4a}$$

$$E = \frac{4\pi V}{h^3} \int \frac{\varepsilon p^2 \, dp}{\exp(\varepsilon/kT) - 1} \tag{5.4b}$$

Consider first the case of phonons $\varepsilon = cp$. The situation is the same as that occurring in the Debye theory of lattice heat capacity except that only longitudinal phonons are possible in the liquid state. The Debye temperature in the helium problem, obtained as usual by terminating $g(v)$ at $v_D$, is

$$\theta = \frac{hc}{2\pi k} \left( \frac{18\pi^2 \rho}{m_{\text{He}}} \right)^{1/3} \tag{5.5}$$

and has a value of about 30°K. Therefore, regions up to 2°K may be considered as the Debye $T^3$-region. In this low-temperature region no serious error is made in extending to infinity the integration in

equation (5.4) over $p/kT$, and hence per mole

$$N_{\text{phon}} = \frac{4\pi V}{h^3}\left(\frac{kT}{c}\right)^3 \int_0^\infty \frac{x^2\, dx}{e^x - 1} = \frac{4\pi V}{h^3}\left(\frac{kT}{c}\right)^3 \times 2.404 \qquad (5.6)$$

$$E_{\text{phon}} = \frac{4\pi Vc}{h^3}\left(\frac{kT}{c}\right)^4 \int_0^\infty \frac{x^3\, dx}{e^x - 1} = \frac{4\pi Vc}{h^3}\left(\frac{kT}{c}\right)^4 \times \frac{\pi^4}{15} \qquad (5.7)$$

The corresponding specific heat per gram is

$$c_{\text{phon}} = \frac{16\pi^5 k^4}{15h^3 c^3 \rho} T^3 \qquad (5.8)$$

For rotons, $\varepsilon = \Delta + (p - p_0)^2/2\mu$. In practice, $\Delta/k$ is found to have a value of about $10°K$; therefore, nothing is lost by using the simpler Maxwell–Boltzmann statistics, so that

$$N_{\text{rot}} = \frac{4\pi V}{h^3}\int p^2\, dp \exp\left\{\frac{-[\Delta + (p - p_0)^2/2\mu]}{kT}\right\}$$

Further, the parameter $p_0$ in the helium problem is found to be much greater than $\mu kT$, so that in the integration over $dp$ the quantity $p^2$ may be replaced by $p_0^2$. Moreover, because of the rapid reduction of the exponential factor for large values of $p - p_0$, the integration may be performed over $p - p_0$ from $-\infty$ to $\infty$. Thus per mole

$$N_{\text{rot}} = \frac{4\pi V}{h^3}p_0^2\, e^{-\Delta/kT}\int_{-\infty}^\infty e^{-x^2/2\mu kT}dx = \frac{4\pi V p_0^2}{h^3}(2\pi\mu kT)^{1/2}\, e^{-\Delta/kT} \quad (5.9)$$

A similar calculation gives the specific heat per gram as

$$c_{\text{rot}} = \frac{4\pi}{\rho h^3}\left(\frac{2\pi\mu}{kT^3}\right)^{1/2} p_0^2\Delta^2\left[1 + \frac{kT}{\Delta} + \tfrac{3}{4}\left(\frac{kT}{\Delta}\right)^2\right]e^{-\Delta/kT} \qquad (5.10)$$

The temperature dependence of the roton part of the thermo-dynamic quantities is basically of the form $\exp(-\Delta/kT)$. This is a consequence of the finite energy gap $\Delta$ and the need for the Boltzmann-type excitation across the gap [compare equations (2.10) and (4.26)]. The number of phonons is proportional to $T^3$, and a numerical esti-mate shows that below $0.6°K$, practically all the excitations are of the phonon type. Around $0.7°K$, the number of rotons overtakes the number of phonons; at temperatures above about $1°K$, most of the excitations are of the roton type. Figures 5.2 and 5.3 show how the specific heat follows the gradual transition in the nature of the thermal excitations.

The phonon-type behavior at low temperatures is similar to the Debye $T^3$-region discussed in Chapter 2. As a matter of fact, if only
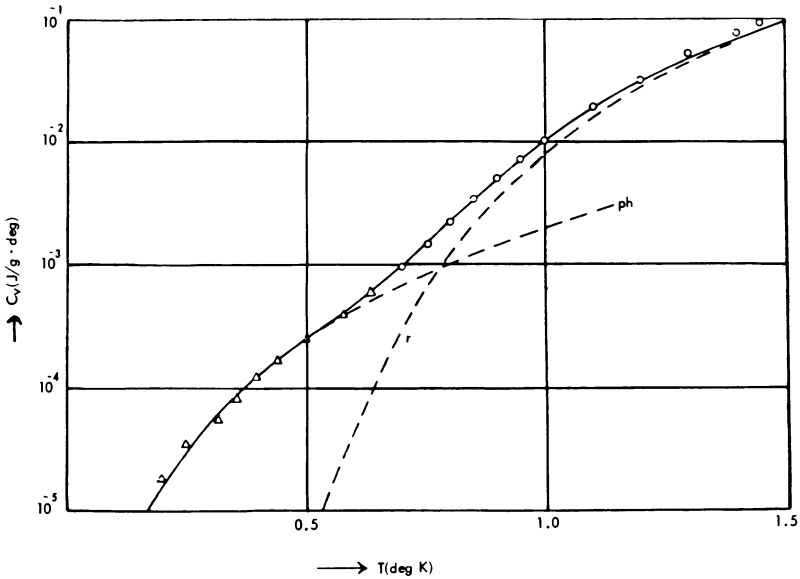
Fig. 5.3. Specific heat of liquid $^4$He showing phonon and roton contributions.[7]

longitudinal phonons are present, equations (2.13) and (2.20) become

$$\theta = \frac{hc}{k}\left(\frac{9N}{4\pi V}\right)^{1/3}$$

$$C_v = \tfrac{16}{15}\frac{\pi^5 k^4 V}{c^3 h^3}T^3$$

and they are similar to equations (5.5) and (5.8). The velocity of sound in liquid $^4$He at low temperatures is $239 \pm 2$ M/sec. Equation (5.8) now gives $c_{\text{phon}} = (0.0204 \pm 0.0005)T^3$ J/g·deg, which is to be compared with the experimental value $c_v = (0.0205 \pm 0.0004)T^3$ mentioned earlier. The excellent agreement provides strong support for the above picture of thermal excitations in liquid $^4$He at low temperatures.

Above 0.6°K, the roton contribution becomes significant; up to about 1.6°K, the specific heat can be accurately fitted by the addition of phonon and roton contributions. In 1947, Landau calculated the values of $\Delta$, $p_0$, and $\mu$ from such an analysis of specific-heat data (which at that time were not known with any great accuracy). A similar analysis was performed by Kramers and coworkers in 1956,

## Table 5.II.  Comparison of the Values of $\Delta$, $p_0$, and $\mu$

|  | $\dfrac{\Delta}{k}$ (deg K) | $\dfrac{p_0}{\hbar}$ (Å$^{-1}$) | $\dfrac{\mu}{m_{^4\mathrm{He}}}$ |
|---|---|---|---|
| Calorimetry |  |  |  |
|   Landau (1947) | 9.6 | 2.0 | 0.77 |
|   Kramers (1956) | 8.8 ± 0.1 | 1.96 ± 0.05 | 0.23 ± 0.1 |
| Neutron scattering |  |  |  |
|   1.1°K | 8.65 ± 0.04 | 1.92 ± 0.01 | 0.16 ± 0.01 |

using carefully determined values of specific heats.  In Table 5.II the numerical values of $\Delta$, $p_0$, and $\mu$ are compared with the results of neutron-scattering experiments in which the energy–momentum dispersion relation[5] was studied directly.  The close agreement between the values must be taken as a striking vindication of Landau's calculation of the properties of liquid $^4$He on the basis of the special $\varepsilon$–$p$ relation (5.3).

Above 1.6°K, the number of rotons becomes so large that it is no longer possible to neglect the interactions among the excitations. (The analogy in the case of solids is the anharmonicity of lattice vibrations.) The neutron-scattering experiments show that the parameter $\Delta$ changes slightly because of the interactions among the rotons. Taking into account the small temperature dependence of the parameters and also using the full $\varepsilon$–$p$ curve, the Los Alamos group of workers[8] has calculated the specific heats and find excellent agreement over the whole temperature range up to 2°K.

Finally, it must be added that the above picture of a gas of phonon and roton excitations accounts satisfactorily for a number of other properties of liquid $^4$He.  A full account is given in the works cited earlier.[4,5]

## 5.5. TRANSITION IN LIQUID $^4$He

It was the specific-heat measurement by Keesom and coworkers in 1932 that gave a definite indication of the special phase change in liquid helium at 2.17°K.  There is a sharp peak at 2.17°K, and the shape of the curve (Fig. 5.2) resembles the Greek letter lambda ($\lambda$). Phase transitions in which there is a similar sharp $\lambda$-peak in the specific heat are now commonly called *lambda-transitions*; they are the result of cooperative effects in the system.  A few other $\lambda$-anomalies will be discussed in Chapter 7, while the thermodynamics of such phase changes is taken up in Chapter 8.

The characteristic feature of the $\lambda$-transitions in liquids and solids is the appearance of a sharp peak in the specific heat (and hence calorimetric measurements are frequently used to detect such transitions). It is obviously of interest to know whether the peak is a sharp maximum or really an infinite singularity with $\int C\,dT$ still remaining finite. The question assumes fundamental importance in the theoretical understanding of such transitions. On the one hand, approximate statistical calculations on reasonable models of substances predict a finite maximum at the transition $T_\lambda$, the peak being rounded off in a temperature interval of about $10^{-3}$°K near $T_\lambda$ in some calculations and there being a jump in the specific heat in other theories. On the other hand, exact calculations on highly simplified models predict that the specific heat has a logarithmic or other infinity, i.e., of the form $C \approx \text{constant} \times \log|T_\lambda - T|$ near $T_\lambda$ (see Section 4.6). No reliable guidance could be obtained from experiments on solids, owing to the difficulty of keeping the temperature constant throughout the specimen to within about $10^{-6}$°K. Fairbank, Buckingham, and Kellers[9] realized that a temperature resolution of about $10^{-6}$°K was possible in liquid helium. It was also pointed out in the *Introduction* that thermal equilibrium occurs very quickly, in a few seconds at temperatures below around 4°K. These workers placed the liquid in intimate contact with copper fins and succeeded in measuring the specific heat to within a microdegree of the $\lambda$-point.

In order to exhibit the nature of the specific heat very near $T_\lambda = 2.17$°K, the results are shown on successively expanded temperature scales in Fig. 5.4. The very large amount of expansion of each successive curve is vividly demonstrated by the fact that the width of the small vertical line directly above the origin indicates the fraction of the curve which is shown enlarged in the next curve on the right. The specific-heat curve maintains the same geometrical shape on all the expanded scales, and clearly there is no indication of any rounded maximum within $10^{-4}$°K of $T_\lambda$, as suggested by some approximate theories. There was also no hysteresis between the values measured with increasing and decreasing temperatures.

The same data are plotted on a logarithmic scale in Fig. 5.5. On both sides of the $\lambda$-point the data fall in two parallel straight lines over a factor of $10^4$ in $|T - T_\lambda|$. The observations (in J/g·degK) near the $\lambda$-point are well fitted by the equation

$$c = 4.55 - 3.00 \log_{10}|T - T_\lambda| - 5.20\delta \qquad (5.11)$$

where $\delta = 0$ for $T < T_\lambda$ and $\delta = 1$ for $T > T_\lambda$. The inclusion of a logarithmic term permits a simple representation of the specific heat
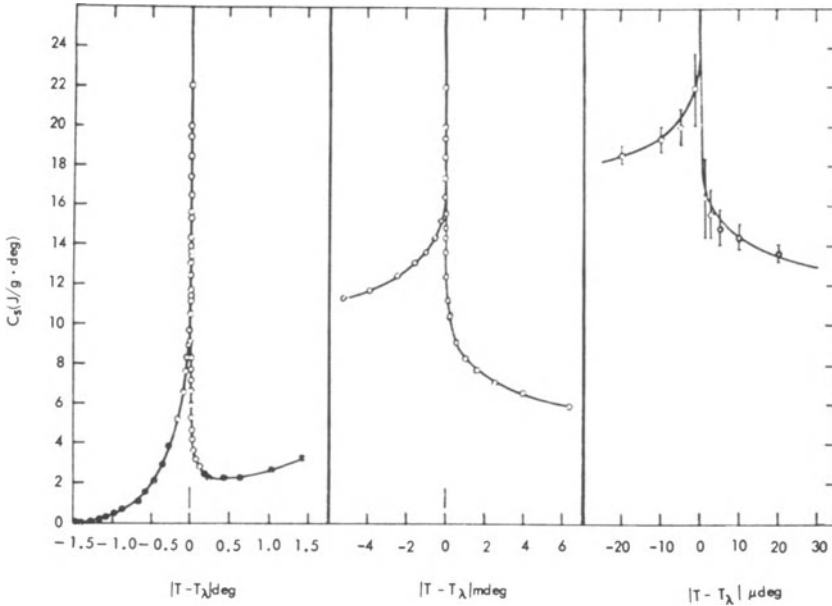
Fig. 5.4. Specific heat of liquid $^4$He near the $\lambda$-point.[9] The solid lines represent equations (5.11) and (5.12). The width of the small line above the origin indicates the fraction of the curve which is expanded in the next figure on the right.

in joules per gram of liquid helium up to about 3.5°K:

$$c = c_D(T) + [130 - 90.9 \log |T - T_\lambda|] \exp\left(\frac{-7.40}{T}\right) \qquad T < T_\lambda$$

$$= c_D(T) + [23.5 - 16.4 \log |T - T_\lambda|] \exp\left(\frac{-3.70}{T}\right) \qquad T > T_\lambda$$

$$(5.12)$$

where $c_D(T)$ represents the Debye function, evaluated at each temperature with the appropriate value of density and velocity of sound.

Besides the specific heat, the thermal expansion coefficient also shows a logarithmic infinity as the $\lambda$-point is approached, although measurements have been performed up to $|T - T_\lambda| \approx 10^{-4}$°K only. It will be seen in Section 8.1 that the behaviors of the two quantities are interconnected and that

$$\left(\frac{T_\lambda}{T}\right)C_p = T_\lambda\left(\frac{\partial S}{\partial T}\right)_\lambda - \frac{T_\lambda}{\rho_\lambda}\left(\frac{\rho_\lambda}{\rho}\right)\left(\frac{\partial P}{\partial T}\right)_\lambda \beta \qquad (5.13)$$
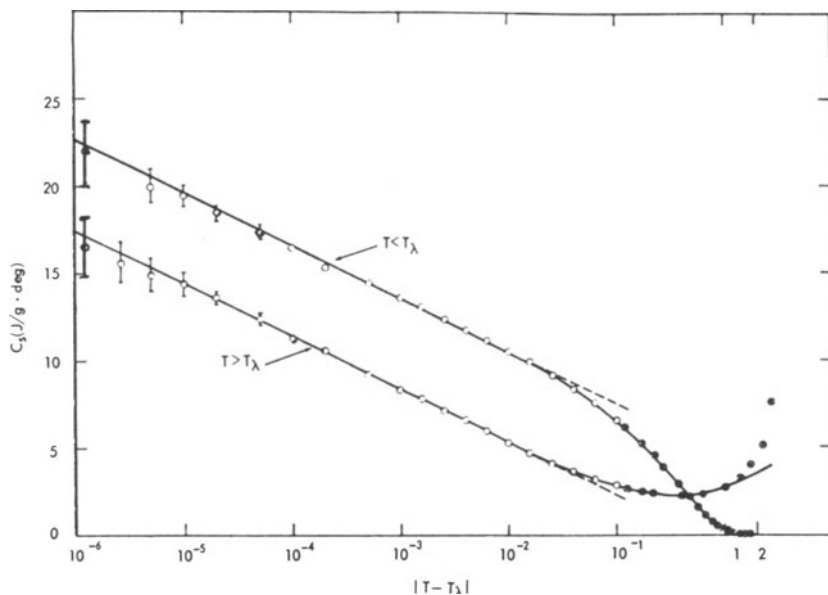
Fig. 5.5. Specific heat of liquid helium versus $\log |T - T_\lambda|$.[9] Solid lines represent equations (5.11) and (5.12).

Figure 5.6 shows a parametric plot of the specific heat and the expansion coefficient.[9] The straight line is the asymptotic value given by equation (5.13) with the experimental values of the various other quantities. The tendency of the observations to attain the limiting value is clear. Thus we must conclude that both the expansion coefficient and the specific heat are consistent with an infinite logarithmic singularity at $T_\lambda$.

At present, there is no complete theory of cooperative transitions. In special cases, as with magnetic transitions treated in Section 4.6, much progress has been made in expressing the thermodynamic quantities in powers of $|T - T_\lambda|$. The outstanding observation of a logarithmic singularity in $C_p$ and $\beta$ is an experimental property which must be explained by any proper statistical theory.

## 5.6. SPECIFIC HEAT OF LIQUID $^3$He

The ordinary liquid helium used in bulk is the isotope of mass 4. The isotope $^3$He is present to about 1 part in $10^7$ in natural helium. However, since 1948, small quantities of $^3$He, produced by nuclear
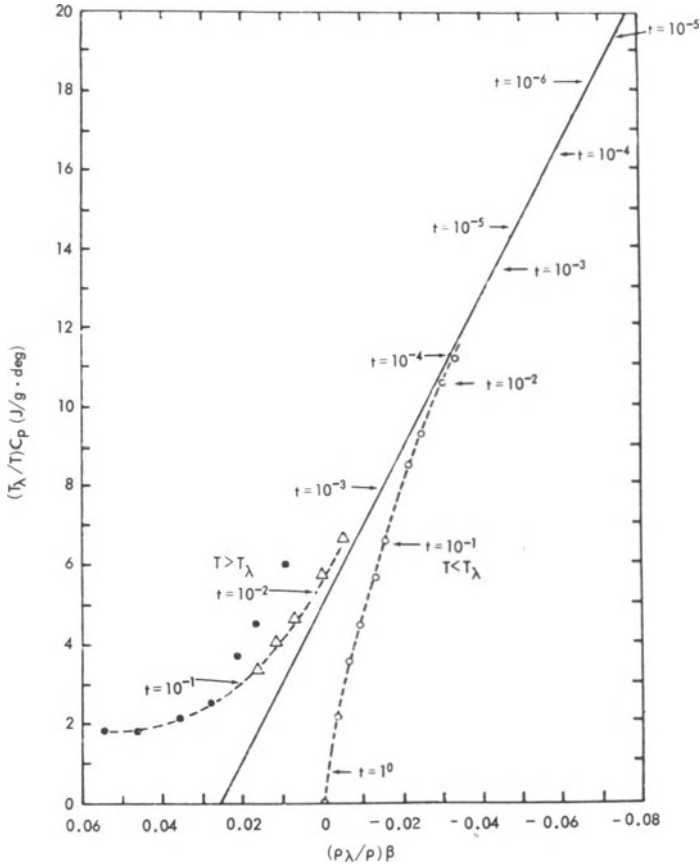
Fig. 5.6. Cylindrical approximation near $T_\lambda$.[9] Parametric plot of $(T_\lambda/T)C_p$ versus $(\rho_\lambda/\rho)\beta$. Full line is the calculated asymptotic value.

reactions, have been available for research, and its use in cooling cryostats to approximately 0.3°K was mentioned in Chapter 1. Helium-three exists as a liquid even at 0°K and becomes a solid only under a pressure of about 30 atm or more. It obeys Fermi–Dirac statistics, and the properties of liquid $^3$He are quite different from those of $^4$He. The experimental and theoretical evidence unequivocally points out that liquid $^3$He must be considered a Fermi system, whereas the superfluid properties of liquid $^4$He arise from the Bose–Einstein condensation.[5] Since $^3$He offers the possibility of studying a simple Fermi liquid, it has of late become the subject of an active field of study.[10,11]

The equations derived in Chapter 3 for an ideal Fermi–Dirac gas were initially considered as a convenient framework for describing the properties of liquid $^3$He. For a F–D gas, the degeneracy temperature is

$$T_F = \frac{1}{2mk}\left(\frac{3}{8}\frac{Nh^3}{\pi V}\right)^{2/3} \tag{5.14}$$

which for the density of liquid $^3$He has a value of about 5°K. Early measurements of nuclear susceptibility showed that $\chi T$ was constant down to about 1.5°K, and the deviations at lower temperatures could be fitted to a perfect-gas model with a degeneracy temperature of about 0.5°K, nearly ten times smaller than the expected value. In a simple-minded way, this could be explained by saying that the effective mass $m^*$ is about ten times the mass of the $^3$He atom. The measurements[12] of specific heat above 0.5°K destroyed this naïve
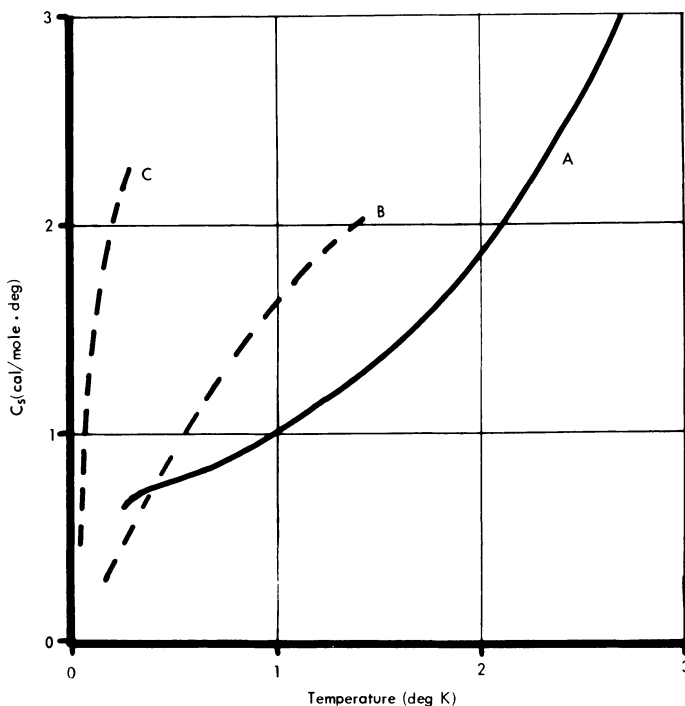


Fig. 5.7. Heat capacity of liquid $^3$He under its saturated vapor pressure (curve A).[12] Curve B is the specific heat of F–D gas with $T_F = 5.0$°K and curve C is that with $T_F = 0.5$°K.
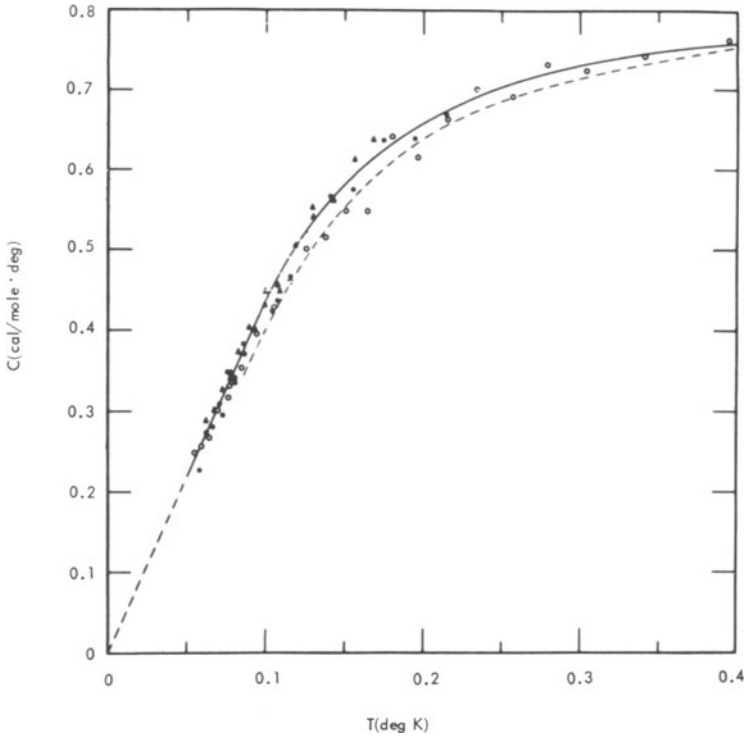
Fig. 5.8. Heat capacity of liquid $^3$He below 0.4°K.[14]

picture. The specific heat does not resemble, even qualitatively, the behavior of an ideal F–D gas with any value of $m^*$. Figure 5.7 compares the specific heats of a F–D gas having $T_F = 5.0$ or 0.5°K with the experimental results. (Strictly, $C_v$ should be compared instead of $C_{sat}$, but this does not improve matters. In fact, the deviations of $C_v$ are equally serious.[13])

Below 0.2°K, the specific heat of the liquid does vary proportionally with $T$, as may be expected from the F–D gas relationship:

$$C_v = \frac{4\pi^3 mk^2}{3h^2}\left(\frac{3NV^2}{\pi}\right)^{1/3} T \qquad (5.15)$$

Any satisfaction at such simple behavior is, however, short-lived.

The F–D theory also shows that if $\gamma_0$ is the magnetic moment per atom, the molar susceptibility $\chi$ should tend to the value

$$\frac{\chi}{V} = \frac{4\pi m \gamma_0}{h^2}\left(\frac{3N}{\pi V}\right)^{1/3} \tag{5.16}$$

This functional relationship is obeyed very well, but quantitatively the agreement is very poor. The $m^*/m_{^3\text{He}}$ calculated from the specific-data has a value of about 2, that from susceptibility is about 10, from compressibility data about 0.3, and so on. In other words, even though the F–D gas formulas give the correct temperature dependence at very low temperatures ($\ll 0.3°\text{K}$), the observations are not consistent with the quantitative interrelationships among the various formulas.

## 5.7. LIQUID $^3$He AS A FERMI LIQUID

A solution to this dilemma at very low temperatures was suggested in 1956 by Landau; since then, the microscopic foundations of such theories have been intensely studied by Brueckner and others.[5,11] According to Landau's theory of a Fermi liquid, the presence of strong interactions among the atoms renders a description of the behavior of single particles meaningless and the statistical behavior is determined by the elementary excitations of the whole system. These excitations or quasiparticles obey Fermi–Dirac statistics and may be taken as an effective description of an atom together with its polarization field caused by the correlated interactions. At low temperatures, the system may be visualized as made up of $N$ quasiparticles of effective mass $m^*$, but in calculating any physical property the fundamental quantity to be considered is the interaction function. Thus, in calculating the magnetic susceptibility, we must consider the dependence of the interaction function upon the nuclear orientations. In compressibility, the volume dependence of the interactions is involved. The specific heat is determined by the density of states at the Fermi level, and so on.

Detailed calculations show that the specific heat is given by equation (5.15) with $m^*$ instead of $m$. Therefore, from the experimental data, we can conclude that $m^*/m_{^3\text{He}} \approx 2$. The expression for susceptibility involves besides $m^*$ the constants of the spin-dependent part of the interaction function. Thus a calculation of $m^*$ using (5.16) will not give the same effective mass as that calculated from specific-heat data. In this manner, the Fermi-liquid theory gives different

interrelationships among the various properties of liquid $^3$He, although the temperature dependence is in many cases the same as that given by the F–D gas calculations. The details of the theory are unfortunately very complicated, and the mathematical techniques used in these many-body problems are not commonly known. Hence, it seems best to suggest suitable reviews[5,15] for those interested rather than give a garbled version of the theory here. On the whole, the Fermi-liquid theory of the behavior of liquid $^3$He below 0.2°K appears to be in reasonable accord with the experiments.

The situation at higher temperatures ($T > 0.5$°K) is not very satisfactory. As seen from Fig. 5.7, the curve bears no resemblance to the variation expected for a F–D gas. A heuristic approach[13] has been to assume that the alignment of the nuclear spins gives a spin contribution (similar to the Schottky term discussed in Section 4.9) with a peak around 0.3°K and that at high temperatures there are contributions from excitations not dependent upon the quantum statistics of the atoms. Such calculations have had quite some success in explaining thermal and magnetic properties. However, the concept of splitting the entropy into such contributions has been questioned by others as having no fundamental justification. Further, nothing is said about the origin of the assumed high-temperature contribution, which is independent of the statistics.[11] On account of these factors, the calculations are not here discussed in any detail.

The electrons in a metal form another example of an interacting Fermi system, which has already been considered in Chapter 3. Several authors have conjectured that a phenomenon analogous to superconductivity of the electronic system (Sections 3.8 to 3.10) should occur in liquid $^3$He, also. The transition temperature cannot be calculated precisely, but is estimated to be approximately $10^{-3}$°K, if not lower. One of the characteristics of the transition, which has been reviewed by Sessler[5,10], for example, is that the specific heat should exhibit an anomaly (Fig. 5.9) similar to the anomaly at the superconducting transition (Fig. 3.11). As mentioned earlier, phase transitions are best detected by specific-heat measurements, and so calorimetric measurements are being made to as low a temperature as possible. At the time of writing, Peshkov[16] has reported a small bump at 0.0055°K. Above $8 \times 10^{-3}$°K, the specific heat increases linearly with $T$ (Fig. 5.8), the value being given by $C_{sat} \approx 20T$ J/mole·deg. The evidence is not quite conclusive,[17] but Peshkov's observations will constitute the discovery of an eagerly sought phase transition in liquid $^3$He—of course, by specific-heat studies!

One question which cannot be answered here is why although sound waves can be propagated through liquid $^3$He as through any
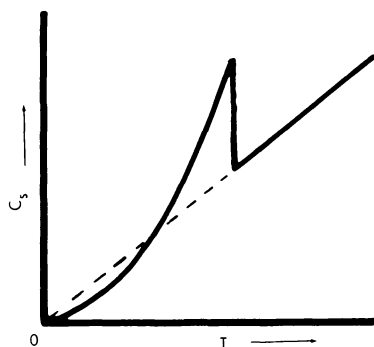
Fig. 5.9.  Predicted specific heat of the
superphase of liquid $^3$He.

other system, phonon terms are not included in the specific heat of liquid $^3$He. The answer lies deeply involved in quantum statistics.[18] Phonon-type thermal excitations obey Bose–Einstein statistics, whereas the system of $^3$He atoms obeys Fermi–Dirac statistics.

## 5.8. MIXTURES OF $^4$He AND $^3$He

Liquid $^4$He and $^3$He are completely miscible, except at low temperatures, where phase separation occurs for a range of concentrations. It has already been mentioned that the properties of mixtures are of considerable interest in chemical thermodynamics.[2,3] In the helium case, since the two pure liquids exhibit peculiar properties of their own, a study of the mixtures has special significance in quantum statistics.[19]

Although considerations of space prohibit a detailed account of the various studies,[10,20] one interesting result is worth mentioning. Taconis, Beenakker, and de Bruyn Ouboter[5] have found that for dilute mixtures of $^3$He in liquid $^4$He, the specific heat at low temperatures ($< 1°K$) is nearly constant and equal to $\frac{3}{2}Rx$ per mole of the mixture where $x$ is the mole fraction of $^3$He. This may be explained simply on the basis of an idea put forward by Pomeranchuk that in dilute solutions the $^3$He atoms do not interact with the superfluid $^4$He, and so form a gas of excitations. At low concentrations, the $^3$He atoms may be taken as nondegenerate and so will have a perfect-gas specific heat $C_v = \frac{3}{2}R$ per mole (as will be explained in Chapter 6). Therefore, the excess specific heat of the solution will be $\frac{3}{2}Rx$ per

mole of the mixture. Other properties, such as the velocity of sound, confirm this simple picture of the role of $^3$He atoms.

## 5.9. SUPERCOOLED LIQUIDS—GLASSES

When a liquid is cooled ordinarily, it solidifies into a crystalline state at its normal freezing point; however, some substances can be supercooled. A classic example is glycerine, which can be easily cooled below its normal freezing point of about 290°K. With some care in avoiding nucleation, the supercooled liquid can be taken right down to approximately 0°K without any crystallization. At about $T_g \sim 180°K$, the behavior of glycerine changes from a liquid-like fluidity above $T_g$ to a solid-like rigidity below $T_g$. The free energy of this solid is greater than that of the crystalline solid, but it represents a metastable thermodynamic state which can exist indefinitely under certain conditions. This highly supercooled liquid state is typical of most glasses; hence it is called the *glassy state*. The situation is thermodynamically the same with allotropes such as diamond, a metastable form of carbon.

The specific heat of glycerol has been measured by several workers and is summarized in the review on the glassy state by Davies and Jones.[21] The heat capacity of the crystalline state [curve (a) in Fig. 5.10] is due to the vibrations of the molecules in the lattice, as analyzed in Chapter 2. The specific heat of the supercooled liquid [curve (b)] is considerably greater because of the additional complex motions possible in the liquid state. However, over a narrow interval of temperature around $T_g \sim 180°K$, the specific heat falls rapidly to a value just above that of the crystalline solid. Only a small difference persists at lower temperatures. Similar marked decrease around $T_g$ is shown in the thermal-expansion coefficient, electrical conductivity, and other properties. It is an important characteristic of supercooled liquids that the viscosity increases by several orders of magnitude as the temperature is lowered through the transition region. In glycerine, it increases from about $10^6$ poise at 190°K to about $10^{13}$ poise at 170°K. Thus at about 170°K, the stress applied to maintain a strain relaxes to $1/e$ of its initial value in hours, compared to $10^{-3}$ sec at about 190°K, so that for practical purposes the substance behaves like a solid. Above $T_g$, the molecules have all the mobility characteristic of liquids, but below $T_g$ they cannot change their configurations in any reasonable amount of time; the only other modes of motion are the lattice vibrations about their mean positions, as in a solid. This is the reason why the specific heat decreases sharply in the transition region.
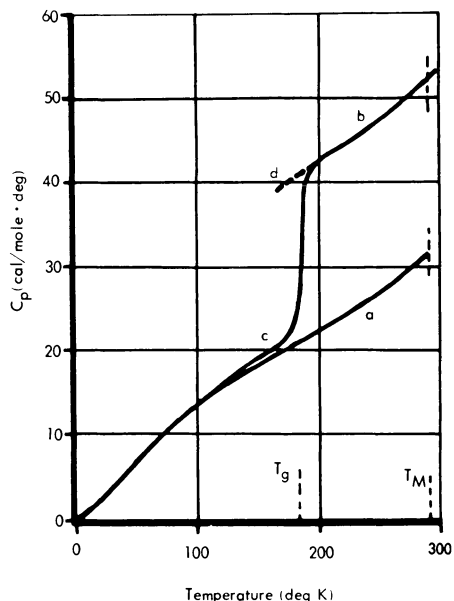
Fig. 5.10. Measured heat capacity of glycerine:
(a) crystalline solid, (b) supercooled liquid,
(c) glassy state, (d) very slowly cooled liquid.

However, the glassy state is not a crystalline state. The viscosity increases so rapidly as the substance is cooled through $T_g$ that the spatial disorder of the liquid has been abruptly "frozen-in." X-ray diffraction studies[22] confirm the molecular disorder in the glassy state. An interesting check is the calculation of the entropy difference between the supercooled glass and the crystalline state (Fig. 5.11). At the melting point, the entropy difference, obtained from the latent heat, is about 15 cal/mole·deg, but below $T_g$ a difference of about 5 units persists right down to 0°K. This is a measure of the configurational entropy of glass which is "frozen-in" at $T_g$. The persistence of such an entropy difference at 0°K is not really a contradiction of the third law of thermodynamics,[23] because the glassy state is not one of stable internal equilibrium. Suitable nucleation can precipitate a crystallization of the whole system (devitrification of glass). Figure 5.11 shows that above $T_g$ the difference in entropy between the supercooled liquid and the crystal decreases rapidly with lowering temperature. At $T_g$, however, the liquid
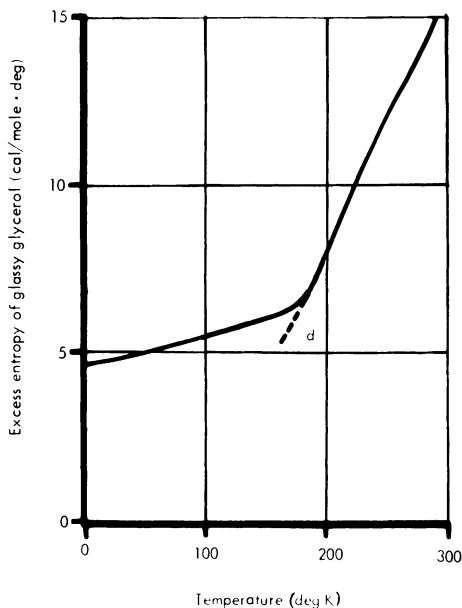
Fig. 5.11. Excess entropy of the glassy solid
over the crystalline state (full line). Curve d
shows the excess entropy if the liquid is cooled
very slowly at $T_g$.

becomes so viscous that configurational changes to lower the entropy
do not take place in short periods of time.  Oblad and Newton showed
experimentally that if glycerine is kept undisturbed for a long time
before the measurement is made at any temperature, the specific-heat
curve appears as a smooth extension of the behavior above $T_g$ [broken
curves (d) in Figs. 5.10 and 5.11].  This shows clearly that if sufficient
time (a whole week of undisturbed waiting just a few degrees below
$T_g$) is allowed, molecular rearrangements do take place.  Because of
the experimental difficulties, measurements could be made to only a
few degrees below $T_g$.  Nevertheless, an inspection of Fig. 5.11 shows
that the entropy difference will undoubtedly extrapolate to zero at
0°K.  If a liquid can exist in internal equilibrium, such as liquid $^4$He
and $^3$He, its entropy will vanish at absolute zero.

     The entropy difference between crystalline and glassy states is
similar to the problem of entropy differences between the various

allotropes of some solids. Materials such as sulfur, tin, and carbon exist in different crystalline states with different specific heats. An investigation of the entropy differences among them was originally used by Nernst and coworkers to check the validity of the third law of thermodynamics. With crystalline solids, it is, of course, possible to calculate the vibrational specific heats from suitable theoretical models.[24]

Numerical values of the specific heat of glasses are of importance in practice, and Stevels[22] has collected the data for a variety of glasses. Some cases of cryogenic interest are mentioned in Table 8.I.

# REFERENCES

1. J. Frenkel, *Kinetic Theory of Liquids,* Dover, New York, 1954.
2. J. S. Rowlinson, *Liquids and Liquid Mixtures,* Butterworth, London, 1959.
3. E. A. Guggenheim, *Mixtures,* Clarendon, Oxford, 1952.
4. K. Mendelssohn, *Handbuch der Physik, XV* (2), 370 (1956). J. Wilks, *Rept. Progr. Phys.* **20**, 38 (1957). K. R. Atkins, *Liquid Helium,* Cambridge University Press, Cambridge, 1957.
5. *Liquid Helium, Proceedings of the International Summer School "Enrico Fermi,"* (Varenna, 1961, G. Careri, ed.), Academic, New York, 1963. J. Wilks, *Liquid Helium,* Clarendon, Oxford, 1966.
6. H. C. Kramers, J. Wasscher, and C. J. Gorter, *Physica* **18**, 329 (1952). R. W. Hill and O. V. Lounasmaa, *Phil. Mag.* **2**, 143 (1957). J. Wiebes, C. G. Niels-Hakkenberg, and H. C. Kramers, *Physica* **23**, 625 (1957).
7. H. C. Kramers, *Progr. Low Temp. Phys.* **2**, 59 (1957).
8. P. J. Bendt, R. D. Cowan, and J. L. Yarnell, *Phys. Rev.* **113**, 1386 (1959).
9. M. J. Buckingham and W. M. Fairbank, *Progr. Low Temp. Phys.* **3**, 80 (1961).
10. J. C. Daunt (ed.), *Helium Three,* Ohio State University Press, Columbus, 1960.
11. E. R. Grilly and E. F. Hammel, *Progr. Low Temp. Phys.* **3**, 113 (1961). N. Bernades and D. F. Brewer, *Rev. Mod. Phys.* **34**, 190 (1962). D. F. Brewer, *Progr. Cryogenics* **4**, 25 (1964).
12. G. de Vries and J. G. Daunt, *Phys. Rev.* **92**, 1572 (1953); **93**, 631 (1954). T. R. Roberts and S. G. Sydoriak, *Phys. Rev.* **93**, 1418 (1954). D. W. Osborne, B. M. Abraham, and B. Weinstock, *Phys. Rev.* **94**, 202 (1954).
13. L. Goldstein, *Phys. Rev.* **112**, 1465 (1958).
14. D. F. Brewer, J. G. Daunt, and A. K. Sreedhar, *Phys. Rev.* **115**, 836 (1959). M. Strongin, G. O. Zimmerman, and H. A. Fairbank, *Phys. Rev. Letters,* **6**, 404 (1961). A. C. Anderson, G. F. Salinger, W. A. Steyert, and J. C. Wheatley, *Phys. Rev. Letters* **7**, 295 (1961).
15. A. A. Abrikosov and I. M. Khalatnikov, *Rept. Progr. Phys.* **22**, 329 (1959).
16. V. P. Peshkov, *Soviet Phys. JETP* **19**, 1023 (1964).
17. E. S. R. Gopal, *J. Sci. Indus. Res.* **23**, 496 (1964). W. R. Abel, A. C. Anderson, W. C. Black, and J. C. Wheatley, *Phys. Rev. Letters* **14**, 129 (1965).
18. K. Huang, *Statistical Mechanics,* Wiley, New York, 1963, pp.262, 384.
19. I. Prigogine, A. Bellemans, and V. Mathot, *Molecular Theory of Solutions,* North Holland, Amsterdam, 1957, chapters 18 and 19.
20. J. J. M. Beenakker and K. W. Taconis, *Progr. Low Temp. Phys.* **1**, 108 (1955). K. W. Taconis and R. de Bruyn Ouboter, *Progr. Low Temp. Phys.* **4**, 38 (1964).

21. R. O. Davies and G. O. Jones, *Advan. Phys.* **2**, 370 (1953).
22. J. M. Stevels, *Handbuch der Physik, XIII*, 510 (1962).
23. J. Wilks, *Third Law of Thermodynamics*, Oxford University Press, Oxford, 1961, chapter 5.
24. F. Seitz, *Modern Theory of Solids*, McGraw-Hill, New York, 1940, chapter 14.

*Chapter 6*

# Specific Heats of Gases

## 6.1. $C_p$ AND $C_v$ OF A GAS

The heat capacity of a gas depends strongly upon the conditions under which heating is done, whether at constant pressure or at constant volume. Indeed, it was pointed out in Chapter 1 that the ratio $C_p/C_v$ is as high as 1.67 for a monatomic gas. It is possible to measure directly both $C_p$ and $C_v$ in gases and vapors, and a representative list[1] of the values at 300°K is given in Table 6.I. The specific heats refer to the "ideal" state of a gas at zero pressure and are calculated from the values at higher pressures by using a knowledge of the equation of state [see equation (1.17)]. Typically, at a pressure of 1 atm, $C_p$ and $C_v$ are higher than the "ideal" values by less than 1% in the so-called permanent gases and by about 1 to 2% in organic vapors.

The specific heat per gram is different for different gases. For heavy gases, the value of $C_v$ is small, and for light gases, $C_v$ is large.

**Table 6.I. Molar Heat Capacities (in cal/mole·deg) at 300°K and $P = 0$ atm**

| | Gas | | | | | | | | |
| --- | --- | --- | --- | --- | --- | --- | --- | --- | --- |
| | He | A | $H_2$ | $N_2$ | $O_2$ | CO | NO | HCl | $Cl_2$ |
| $C_p$ | 4.97 | 4.97 | 6.85 | 6.94 | 7.02 | 6.96 | 7.08 | 6.97 | 8.02 |
| $C_v$ | 2.98 | 2.98 | 4.86 | 4.96 | 5.03 | 4.97 | 5.10 | 4.98 | 6.02 |
| $C_p - C_v$ | 1.99 | 1.99 | 1.99 | 1.98 | 1.99 | 1.99 | 1.98 | 1.99 | 2.00 |
| | $CO_2$ | $N_2O$ | $SO_2$ | $H_2S$ | $NH_3$ | $CH_4$ | $C_2H_2$ | $C_2H_4$ | $C_2H_6$ |
| $C_p$ | 8.77 | 9.25 | 9.20 | 8.15 | 8.49 | 8.48 | 10.35 | 10.15 | 12.25 |
| $C_v$ | 6.78 | 7.27 | 7.20 | 6.15 | 6.50 | 6.49 | 8.35 | 8.15 | 10.25 |
| $C_p - C_v$ | 1.99 | 1.98 | 2.00 | 2.00 | 1.99 | 1.99 | 2.00 | 2.00 | 2.00 |

The consideration of molar heat capacities provides a great simplification: $C_v$ turns out to be about 3 cal/mole·deg for monatomic gases (such as helium and argon) and about 5 cal/mole·deg for diatomic gases (such as $H_2$, $N_2$, $O_2$, CO, NO, HCl). $C_p - C_v$ is approximately equal in all cases to 2 cal/mole·deg. When it is recalled that the gas constant $R$ has a value 1.987 in the same units, the difference between $C_p$ and $C_v$ is nothing other than equation (1.13):

$$C_p - C_v = R$$

a relation first used by Mayer in 1842. Since the natural unit for the molar heat capacity is $R$, the striking feature of Table 6.I, demanding an immediate explanation, is that $C_v \sim \frac{3}{2}R$ for monatomic gases and $C_v \sim \frac{5}{2}R$ for diatomic gases.

## 6.2. CLASSICAL THEORY OF $C_v$ OF GASES

Boltzmann's equipartition theorem is able to provide an explanation for the simple coefficients $\frac{3}{2}$ and $\frac{5}{2}$. This theorem, as explained in Section 2.2, connects the internal energy of a system with its number of degrees of freedom (that is, the number of squared terms in the Hamiltonian function, which is the same as the number of independent coordinates required to describe the motion of the system). Each degree of freedom contributes $\frac{1}{2}RT$ to the internal energy of a mole of the substance at thermal equilibrium. A mass point is a good model of the atoms in a monatomic gas. It has three translational degrees of freedom (Hamiltonian $(p_x^2 + p_y^2 + p_z^2)/2m$ where the $p$ are the momenta of the molecules). Therefore, the internal energy is $E = 3 \times \frac{1}{2}RT$ and $C_v = \partial E/\partial T = \frac{3}{2}R$, as is found to be the case. The molecules of a diatomic gas may be represented by a pair of masses rigidly connected together, i.e., a rigid dumbell. Then, besides having the three translatory motions, the molecules can rotate about any pair of directions perpendicular to its axis. There are altogether five degrees of freedom; consequently, $E = \frac{5}{2}RT$ and $C_v = \frac{5}{2}R$. Thus the specific heats of permanent gases are readily understood in classical statistics.

A closer study of Table 6.I reveals, however, that this agreement between the equipartition law and the observed values is only limited. A linear triatomic molecule, such as $CO_2$ or $N_2O$, should behave like a diatomic molecule, because it can rotate only about the directions perpendicular to its axis. Therefore, $C_v$ should be $\frac{5}{2}R$, whereas the actual values for $CO_2$ and $N_2O$ exceed $\frac{5}{2}R$ quite significantly. A general polyatomic molecule which can rotate about all three principal axes should have $C_v = \frac{6}{2}R$, which is also not the case. Even

a diatomic molecule such as chlorine exceeds its equipartition value of $C_v = \frac{5}{2}R$.

The discrepancy is partly due to the fact that the molecules can have internal vibrations. Each mode of vibration has two square terms in the Hamiltonian, one for kinetic and one for potential energy, and so counts as two degrees of freedom. A diatomic molecule has one vibrational frequency, and a general polyatomic molecule has $3n - 6$ vibrational modes. If the vibrational contributions are added, $C_v = \frac{7}{2}R \sim 7$ cal/mole·deg for diatomic gases and $C_v = 3(n - 1)R$ for polyatomic gases. (If the molecules of a polyatomic gas are linear, there are only $3n - 5$ vibrations, and $C_v$ is correspondingly less.) The specific heats in Table 6.I are all less than this value. The vibrational heat capacity of polyatomic gases (and of chlorine) falls short of this equipartition value. Experiments made at higher temperatures (Table 6.II) revealed that at 2000°C $H_2O$, $CO_2$, and $SO_2$ attain their equipartition value of $3(n - 1)R \sim 12$ cal/mole·deg, while $N_2$, $O_2$, HCl, CO, and $H_2$ are obviously moving toward their value of approximately 7 cal/mole·deg. (Chlorine exceeds the equipartition value because of anharmonicity and dissociation[1,2], both of which are not considered in this elementary account.)

Measurements at low temperatures revealed another short-coming of the classical theory. Eucken, as early as 1905, noticed that the heat capacity of hydrogen at liquid-nitrogen temperatures was significantly lower than the room-temperature value. Table 6.III shows that $C_v$ has become equal to about $\frac{3}{2}R$ below about 60°K. $C_p$ decreases by the same amount (recall $C_p - C_v = R$), and the ratio $C_p/C_v$ goes from 1.40 at room temperature to 1.67 at 50°K. The values below 60°K are typical of a monatomic gas, for which only translational degrees of freedom are possible.

The equipartition law provides no reasonable explanation for the observation that at low temperatures the vibrational and rotational degrees of freedom remain "frozen in" and begin to "thaw out" as the temperature is raised. The clarification came from the application

**Table 6.II. $C_v$ at High Temperatures (in cal/mole·deg)**

| Temperature (deg C) | Gas | | | | | |
|---|---|---|---|---|---|---|
| | A | $N_2$, $O_2$, HCl, CO | $H_2$ | $Cl_2$ | $H_2O$ | $CO_2$, $SO_2$ |
| 0 | 2.98 | 4.98 | 4.90 | 5.90 | 5.93 | 6.90 |
| 500 | 2.98 | 5.35 | 5.29 | 6.30 | 6.95 | 9.43 |
| 2000 | 2.99 | 6.22 | 6.10 | 7.4 | 11.9 | 11.5 |

### Table 6.III. Heat Capacities of Hydrogen (in cal/mole·deg)

|  | Temperature (deg K) | | | | | |
|---|---|---|---|---|---|---|
|  | 300 | 200 | 100 | 80 | 60 | 40 |
| $C_v$ | 4.86 | 4.49 | 3.42 | 3.18 | 3.05 | 3.00 |
| $C_p/C_v$ | 1.41 | 1.45 | 1.56 | 1.62 | 1.66 | 1.67 |

of quantum concepts to the problem. Inspired by Einstein's funda-
mental resolution of the temperature variation of vibrational specific
heat in 1907, Nernst suggested in 1911 the quantization of rotational
and vibrational levels in gases. Hydrogen remained somewhat
anomalous until Dennison suggested an explanation in 1927, following
the earlier calculation of Hund. The advances made in quantum
mechanics and spectroscopy after 1925 brought the theoretical
calculation of thermodynamic properties of simple gases over wide
ranges of temperatures to such a high degree of precision that it
surpassed the accuracy of the experimental measurements.

### 6.3. QUANTUM THEORY OF $C_v$ OF GASES

It is qualitatively easy to see why the rotational and vibrational
degrees of freedom are not fully excited at low temperatures. For
the common molecules, the vibrational frequencies are in the range
of about $10^{14}$/sec, and the associated energy levels have a spacing
equivalent to $h\nu/k \sim 1000°K$. So, at room temperature ($\sim 300°K$),
only a few molecules have enough energy to excite the vibrational
modes. The rotational frequencies are about 100 times smaller, so that
at any temperature above $10°K$ the rotational modes are fully
excited. The rotational energy levels in hydrogen are rather high
because of the low moment of inertia of the molecule; therefore,
hydrogen begins to contribute the rotational specific heat only above
$60°K$. The translation of these ideas into quantitative results is, of
course, a standard problem in statistical mechanics.[3,4] The present
discussion is limited to some simple cases, which are nevertheless
sufficient to illustrate the principles involved.

The simplest case to consider is a monatomic gas, schematically
taken as a set of mass points with no interatomic forces. Let a large
number of such atoms, each of mass $m$, be enclosed in a vessel of
sides $L_1$, $L_2$, $L_3$ in which they obey the Schrödinger equation

$$\nabla^2 \psi + \frac{8\pi^2 mE}{h^2} \psi = 0$$

for free particles of energy $E$. The wave functions should vanish at the walls, but because the number of particles $N$ is very large in any physical system, the boundary conditions do not affect the final result (see also Section 2.5). It is therefore mathematically convenient to impose a periodic boundary condition, as in lattice dynamics,

$$\psi(x,y,z) = \psi(x \pm L_1,y,z) = \dots = \psi(x,y,z \pm L_3)$$

so that the solutions can be taken as progressive waves instead of standing waves. The wave functions satisfying these conditions are

$$\psi = A \exp[2\pi i(p_1 x + p_2 y + p_3 z)]$$

where $p_i = hn_i/L_i$ and $n_i$ are positive or negative integers. The energy of a molecule is $\varepsilon = (p_1^2 + p_2^2 + p_3^2)/2m$. The energy of the system is the sum of the energies of the particles, and so the final partition function of the system will involve the product of $N$ terms each equal to

$$z = \sum_{n_i = -\infty}^{\infty} \exp\left[\frac{-(p_1^2 + p_2^2 + p_3^2)}{2mkT}\right] \tag{6.1}$$

A simple calculation shows that the energy levels are approximately $h^2/2mkL^2 \approx 10^{-15}{}^\circ\mathrm{K}$ apart, so that the summation over $n_i$ may be replaced by an integration over $p_i$:

$$z = \frac{V}{h^3}\int\int\int \exp\left[\frac{-(p_1^2 + p_2^2 + p_3^2)}{2mkT}\right] dp_1\, dp_2\, dp_3$$

Here $V = L_1 L_2 L_3$ is the volume of the system. The integral from $-\infty$ to $\infty$ of $e^{-x^2}$ is well known to be $\pi^{1/2}$, and so

$$z = V\left(\frac{2\pi mkT}{h^2}\right)^{3/2} \tag{6.2}$$

The partition function of the system $Z$ would have been just the product of $N$ such terms but for the fact that all the particles are indistinguishable. This means that

$$Z = \frac{1}{N!}(z)^N \tag{6.3}$$

because the $N!$ ways of permuting the particles are indistinguishable from one another and must hence be counted as only one way. Therefore,

$$A = -kT\ln Z = -NkT\ln\left[V\left(\frac{2\pi mkT}{h^2}\right)^{3/2}\right] + NkT\ln N - NkT \tag{6.4}$$

where Stirling's approximation $\ln N! \approx N \ln N - N$ is used. It is now a simple matter to calculate

$$E = -kT^2\left(\frac{\partial \ln Z}{\partial T}\right)_v = \tfrac{3}{2}RT \qquad C_v = \tfrac{3}{2}R \qquad (6.5)$$

The specific heat at constant volume is approximately 3 cal/mole·deg, as was borne out in Table 6.I. This value was also explained by the equipartition law, but the present calculations give the absolute value of the entropy at a pressure $P = NkT/V$ as

$$S = -\left(\frac{\partial A}{\partial T}\right)_v = R\left\{\tfrac{5}{2} + \ln\left[\frac{(kT)^{5/2}}{P}g\left(\frac{2\pi m}{h^2}\right)^{3/2}\right]\right\} \qquad (6.6)$$

(Here a weight factor $g$, equal to 1 for structureless particles and equal to 2 for vapors of sodium, potassium, and thallium, which have doubly degenerate ground state, has been added for completeness.) This equation, first derived in a different manner by Sackur and Tetrode in 1912, is in excellent agreement with the experimental values of entropy determined calorimetrically (see Table 6.VII). As a matter of historic interest, Tetrode, from the calorimetric entropy of mercury vapor, obtained Planck's constant $h$ to within 5% of the accepted value.

## 6.4. ROTATIONAL PARTITION FUNCTION

The power of statistical thermodynamics becomes obvious when the rotational degrees of freedom are considered. The simplest case is a heteronuclear molecule of moment of inertia $I$ perpendicular to its axis. With spherical polar coordinates, the expression for the kinetic energy is $\mathscr{T} = \tfrac{1}{2}I(\dot\theta^2 + \sin^2\theta\dot\varphi^2)$. The generalized momenta are $p_\theta = \partial\mathscr{T}/\partial\dot\theta = I\dot\theta$, $p_\phi = \partial\mathscr{T}/\partial\dot\varphi = I\sin^2\theta\dot\varphi$, and so the classical Hamiltonian is $\mathscr{H} = (p_\theta^2 + \sin^{-2}\theta p_\phi^2)/2I$. The transcription into quantum mechanical operators leads to the Schrödinger equation

$$\frac{\partial^2\psi}{\partial\theta^2} + \frac{1}{\sin^2\theta}\frac{\partial^2\psi}{\partial\phi^2} + \frac{8\pi^2 IE}{h^2}\psi = 0 \qquad (6.7)$$

The eigenfunctions of this equation are $\psi = P_j^{|m|}(\cos\theta)e^{im\phi}$, with $m = -j, -j+1, ..., j-1, j$, where $P_j^{|m|}(\cos\theta)$ are the associated Legendre functions. The energy levels are $\varepsilon_j = j(j+1)h^2/8\pi^2 I$, where $j = 0, 1, ...$. Each energy level $j$ possesses $2j+1$ independent wave functions and so must be assigned a weight $2j+1$. Proceeding as before, the partition function is

$$Z = \frac{1}{N}(z)^N$$
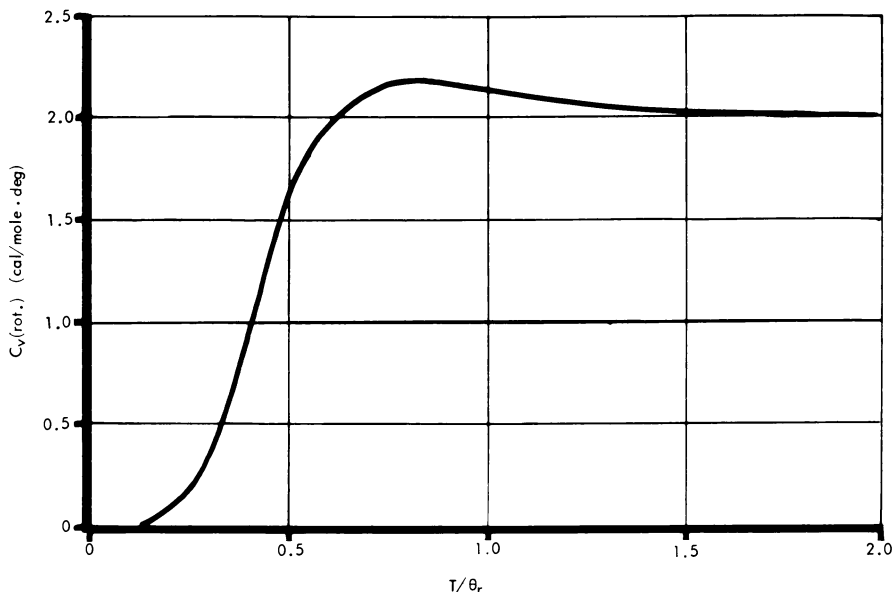
Fig. 6.1. Rotational heat capacity of a gas of heteronuclear diatomic molecules.

where the partition function $z$ for a single molecule is

$$z = \sum_{j=0}^{\infty} (2j + 1) \exp\left[ -\frac{j(j + 1)\theta_r}{T} \right]$$ (6.8)

where $\theta_r = h^2/8\pi^2 Ik$. Over the entire range of temperatures, the summation has to be carried out by numerical methods[3,4], and the rotational specific heat has the values shown in Fig. 6.1. $C_v(\text{rot.})$ has a simple form at high or low temperatures:

$$C_v(\text{rot.}) = R\left[ 1 + \tfrac{1}{45}\left(\frac{\theta_r}{T}\right)^2 + \dots \right] \qquad \text{for } T \gg \theta_r$$ (6.9)

$$= 12R\frac{\theta_r}{T}\exp\left( -\frac{\theta_r}{T} \right) + \dots \qquad \text{for } T \ll \theta_r$$ (6.10)

The rotational heat capacity of diatomic molecules has the equipartition value $R \sim 2$ cal/mole·deg at high temperatures. As the temperature is lowered, $C_v(\text{rot.})$ attains a shallow maximum of about $1.1R$ at $T/\theta_r \sim 0.8$ and then drops down steeply. Below about $T/\theta_r \sim 0.2$, the rotational specific heat becomes too small to be resolved experimentally.

**Table 6.IV. Rotational Characteristic Temperatures $\theta_r$ of Gases (in deg K)**

| | Gas | | | | | | | | | |
|---|------|------|------|------|------|------|------|------|------|------|------|
| | $H_2$ | HD | HT | $D_2$ | DT | $T_2$ | HCl | $N_2$ | $O_2$ | CO | $NH_3$ |
| $\theta_r$ | 85.4 | 65.7 | 58.4 | 43.0 | 36.5 | 29.1 | 15.2 | 2.86 | 2.07 | 2.77 | 12.3 |

Clearly, $\theta_r$ is the characteristic temperature governing the behavior of $C_v(\text{rot.})$. Now a study of the band spectra enables the moment of inertia of the molecules to be determined,[5] and some values of $\theta_r$ calculated from such spectroscopic observations are given in Table 6.IV. For most gases, $\theta_r$ is in the region where the substances would have become liquids or solids, and so in the gaseous state they have the limiting value of $R$, thus accounting for the success of the equipartition law. Only in the case of the light hydrogeneous molecules is there any possibility of observing the "freezing" of the rotational degrees of motion. Hydrogen and deuterium are specially treated below because of the additional interesting effects arising from nuclear symmetry in the molecules. The rotational heat capacity of hydrogen deuteride (HD), obtained by subtracting the translational contribution $\frac{3}{2}R$ from the observed heat capacity, is in good agreement with the theoretical curve of Fig. 6.1 if $\theta_r$ is taken as 65.7°K. However, the observations are incomplete.

The treatment of polyatomic molecules is along similar lines, taking into account the possibility of rotation about all three axes and the molecular symmetry. For all polyatomic molecules, the equipartition value is reached in the gaseous state. The interest in the polyatomic gases is in calculating the entropy from the statistical partition function. The relevant formulas are analogous to the Sackur–Tetrode equation (6.6) and may be found in several treatises.[3,4,6] A comparison of the statistical entropy with the experimental value often gives information about the ordered state of the solid. This will be taken up in Section 6.7.

## 6.5. HOMONUCLEAR MOLECULES—ISOTOPES OF HYDROGEN

The heat capacity of homonuclear molecules, of which $H_2$ and $D_2$ are of great interest,[7] involves a consideration of the symmetry of the wave functions of the nuclei. Quantum mechanics shows that if the nuclei have an even mass number (for example, the deuteron), the wave function describing their motion must be symmetrical in

nuclear coordinates, while if the nuclei have an odd mass number (for example, the proton) the wave functions must be antisymmetrical. Since the total wave function contains the product of the rotational and the nuclear spin functions, it is convenient to consider the two separately.

Interchanging the two nuclei of a diatomic molecule is equivalent to replacing $\theta$ by $\pi - \theta$ and $\phi$ by $\pi + \phi$ in the rotational eigenfunction $P_j^{|m|}(\cos \theta)e^{im\phi}$, that is, replacing the function by $(-1)^m P_j^{|m|}(-\cos \theta)e^{im\phi}$, which is equal to $(-1)^j P_j^{|m|}(\cos \theta)e^{im\phi}$ because $P_j^{|m|}(\cos \theta)$ is even or odd according to whether $j + |m|$ is even or odd. Hence the molecular rotational function is symmetric in the nuclear coordinates for even values of $j$ and antisymmetrical for odd $j$. It is convenient to write

$$z_e = \sum_{j=0,2,4,\ldots} (2j + 1) \exp\left[-j(j + 1)\frac{\theta_r}{T}\right] \tag{6.11}$$

$$z_0 = \sum_{j=1,3,5,\ldots} (2j + 1) \exp\left[-j(j + 1)\frac{\theta_r}{T}\right] \tag{6.12}$$

If the nucleus has a spin $I$ (in units of $\hbar$), there will be orientational quantization in an external magnetic field, with an eigenfunction for each of the $\rho = 2I + 1$ states. In the absence of a magnetic field, the orientated states become indistinguishable, but their number remains unaltered. Thus there are $\rho$ spin wave functions $\psi_r(a)$, $\psi_s(b)$, where $r, s = 1, 2, \ldots, \rho$, for each nucleus $a, b$ of a homonuclear diatomic molecule. From them, there are $\frac{1}{2}\rho(\rho - 1)$ combinations of the type $\psi_r(a)\psi_s(b) - \psi_r(b)\psi_s(a)$ (where $r \neq s$), which are antisymmetric in the nuclear coordinates, and there are $\frac{1}{2}\rho(\rho - 1)$ combinations of the type $\psi_r(a)\psi_s(b) + \psi_r(b)\psi_s(a)$ (where $r \neq s$), symmetric in the nuclei, as well as $\rho$ products $\psi_r(a)\psi_r(b)$ also symmetric in the nuclei. In all, there are $\frac{1}{2}\rho(\rho - 1)$ antisymmetric and $\frac{1}{2}\rho(\rho + 1)$ symmetric spin wave functions of the molecule. These are the spin weight factors.

After these preliminaries, the rotational specific heat of hydrogen may be taken up. The hydrogen nucleus (proton spin $I = \frac{1}{2}$, $\rho = 2$) has an odd mass, and so the total wave function must be antisymmetric. This means that the symmetric rotational functions $z_e$ must be combined with the antisymmetric spin functions, while the antisymmetric rotational functions $z_0$ are to be associated with the symmetric spin functions of degeneracy $\frac{1}{2}\rho(\rho + 1)$. If these weight factors $\frac{1}{2}\rho(\rho - 1) = 1$, $\frac{1}{2}\rho(\rho + 1) = 3$ are taken into account, the partition function for the equilibrium state of hydrogen becomes

$$z = z_e + 3z_0$$

and the specific heat will be

$$C_v(\text{rot.}) = \frac{d}{dT}\left[RT^2\frac{d}{dT}\ln(z_e + 3z_0)\right]\tag{6.13}$$

This formula, derived by Hund,[8] did not agree with the measured specific heats of hydrogen if the spectroscopic value of the moment of inertia, $4.67 \times 10^{-40}$ g-cm$^2$, was used.

The reason was very soon pointed out by Dennison.[9] The transitions between the states of different nuclear spins are due to the very small interaction of the nuclear magnetic moment with the magnetic field produced by the rotation. The normal hazards of molecular collision do not affect the nuclear spins, and so the transitions between the two states are extremely rare. Therefore, hydrogen normally behaves as if it were a metastable mixture of two entirely separate species of molecules—parahydrogen and orthohydrogen. In parahydrogen, the nuclear spins are antiparallel (resultant spin and magnetic moment of the molecule are zero), and so this antisymmetric spin state is associated with even rotational states. Orthohydrogen has the spins of the nuclei parallel and corresponds to odd rotational states. In normal hydrogen, the relative abundance of the two types of molecules will be determined by the equilibrium conditions at room temperature. Since at high temperatures, $z_0$ is approximately equal to $z_e$, the relative abundance of para and ortho molecules will be in the ratio $p\text{-H}_2 : o\text{-H}_2 = 1:3$. The specific heat of normal hydrogen must be calculated by adding the contributions from the two species in this ratio, because during the course of an ordinary calorimetric measurement the ratio does not change appreciably. Thus

$$C_v(\text{rot.}) = \tfrac{1}{4}\frac{d}{dT}\left(RT^2\frac{d}{dT}\ln z_e\right) + \tfrac{3}{4}\frac{d}{dT}\left(RT^2\frac{d}{dT}\ln z_0\right)\tag{6.14}$$

This formula is in excellent agreement with the observations on ordinary hydrogen (for which the usual abbreviation is $n\text{-H}_2$).

Although the transitions between the ortho and para forms of hydrogen are so infrequent that the mixture retains its room-temperature composition of $o\text{-H}_2 : p\text{-H}_2 = 3:1$ during normal measurements of the specific heat, it is possible to catalyze the transitions by bringing the gas into contact with activated charcoal or paramagnetic salts. Substances such as ferric hydroxide are commonly used as catalysts. The lowest energy state of the ortho molecule is the $j = 1$ state, unlike the para molecule with a zero-energy $j = 0$ state. So, at low temperatures the equilibrium gas contains mostly para molecules. Typically, equilibrium hydrogen contains 25% $p\text{-H}_2$ at 300°K and over 99% $p\text{-H}_2$ at 20°K. This almost pure parahydrogen, or any
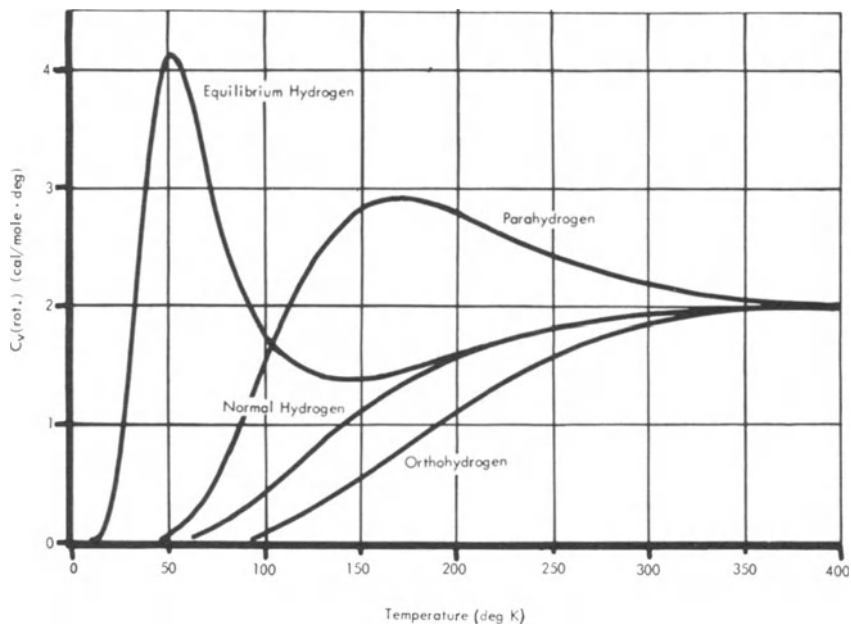
Fig. 6.2. Rotational heat capacity of ortho, para, normal, and equilibrium hydrogen ($\theta_r = 85.4°K$).

other mixture, will remain in metastable equilibrium if the temperature is changed in the absence of catalysts. Therefore, the specific heats of various ortho–para mixtures have been studied; the results are in excellent agreement with the theoretical calculations if $\theta_r$ is taken as 85.4°K. By selective adsorption of the ortho molecules on alumina, 99% pure orthohydrogen has been prepared recently[10] and its properties studied.

The rotational specific heat of the various forms (ortho, para, normal, and equilibrium states) of hydrogen are shown in Fig. 6.2.

For deuterium, the nuclear spin $I$ is 1, and so $\rho = 3$. Since the deuteron contains two particles (proton and neutron), the total wave function must be symmetrical. The even rotational functions $z_e$ are to be coupled to even nuclear spin functions of weight $\frac{1}{2}\rho(\rho + 1) = 6$, while the antisymmetrical rotational functions $z_0$ are to be associated with the antisymmetrical spin functions of weight $\frac{1}{2}\rho(\rho - 1) = 3$. So for a metastable mixture of deuterium ($n$-$D_2$),

$$C_v(\text{rot.}) = \tfrac{6}{9}\frac{d}{dT}\left(RT^2\frac{d}{dT}\ln z_e\right) + \tfrac{3}{9}\frac{d}{dT}\left(RT^2\frac{d}{dT}\ln z_0\right) \qquad (6.15)$$

The measurements on ordinary deuterium are in good agreement with this relation.

The para molecules have antiparallel nuclear spins. Therefore, paradeuterium is associated with odd rotational states, unlike parahydrogen, which is associated with even $j$-states because of the difference in nuclear mass and hence symmetry. The temperature variation of $C_v$(rot.) for paradeuterium is thus similar to that of orthohydrogen. The specific heat of orthodeuterium resembles the behavior of parahydrogen in having a maximum in $C_v$(rot.), but because of the increased moment of inertia, the peak occurs at about 85°K in orthodeuterium as compared to about 170°K in parahydrogen. Further, because of the higher percentage of even rotational states, normal deuterium shows a weak maximum in the specific heat at about 100°K. The theoretical variation of $C_v$(rot.) shown in Fig. 6.3 is in good agreement with experiments if $\theta_r$ is taken as 43.0°K. At low temperatures, orthodeuterium is the more favored
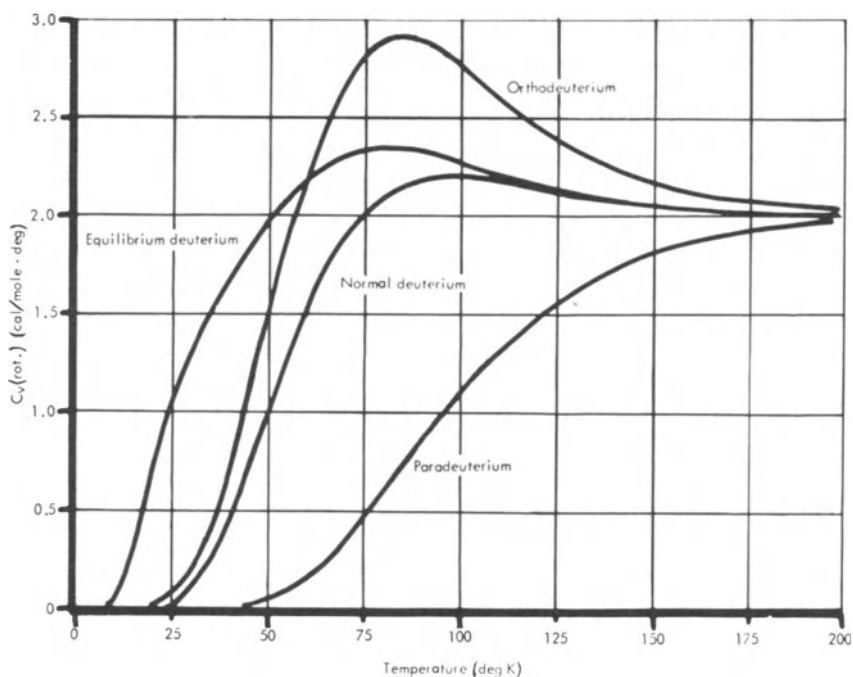


Fig. 6.3. Rotational heat capacity of para, ortho, normal, and equilibrium deuterium ($\theta_r = 43.0°K$).

state, and so almost pure metastable orthodeuterium can be prepared for experimental studies. Enrichment of paradeuterium requires a special process.[10]

Similar considerations apply to other cases such as that of $CH_4$, where the four hydrogen atoms are indistinguishable. However, these substances are no longer in the gaseous state when the deviations from the equipartition value are expected to arise. The study of tritium and its hydrides is barely possible.[11]

## 6.6. VIBRATIONAL AND ELECTRONIC SPECIFIC HEATS

The vibrational levels of molecules are 100 to 1000 times higher than the rotational levels; consequently, for many "permanent" gases the vibrational contribution becomes appreciable only at high temperatures. There are some substances, especially the organic vapors, which have rather low vibrational frequencies; for them, the vibrations are excited at room temperatures, as shown in Table 6.I.

The vibrational specific heat has been already calculated, in a different context. In Chapter 2, it was pointed out that a harmonic vibrator of frequency $v$ has energy levels $\varepsilon_n = (n + \frac{1}{2})hv$, and so

$$z = \sum_{n=0}^{\infty} \exp\left[-\frac{(n + \frac{1}{2})hv}{kT}\right] = \frac{\exp(\frac{1}{2}hv/kT)}{1 - \exp(hv/kT)}$$

Thus

$$C_v(\text{vib.}) = R\left(\frac{\theta_v}{T}\right)^2 \frac{\exp(\theta_v/T)}{[\exp(\theta_v/T) - 1]^2} \tag{6.16}$$

where $\theta_v = hv/k$. This is the well-known Einstein function [equation (2.9)], and the temperature variation of $C_v$ was represented in Fig. 2.1. (There is a small difference in that three-dimensional oscillators were considered in Chapter 2, whereas the present $C_v(\text{vib.})$ for the one-dimensional case is one-third the $C_v$ considered in Section 2.4.) From spectroscopic studies of the vibrational frequencies, the values of $\theta_v$ may be calculated, some of which are given in Table 6.V. For simple molecules, the vibrational specific heat is barely excited at

**Table 6.V. Vibrational Characteristic Temperatures $\theta_v$ (in $10^3\,°K$)**

| | $H_2$ | HD | $D_2$ | HCl | HBr | CO | $N_2$ | $O_2$ | $Cl_2$ | $Br_2$ |
|---|---|---|---|---|---|---|---|---|---|---|
| | | | | | | Gas | | | | |
| $\theta_v$ | 6.0 | 5.3 | 4.3 | 4.1 | 3.7 | 3.1 | 3.4 | 2.2 | 0.80 | 0.46 |

**Table 6.VI.  Vibrational Heat Capacity of Chlorine (in cal/mole·deg)**

| | Temperature (deg K) | | | | |
|---|---|---|---|---|---|
| | 243 | 270 | 319 | 391 | 452 |
| Calculated | 0.848 | 0.985 | 1.188 | 1.407 | 1.530 |
| Experimental | 0.840 | 0.977 | 1.148 | 1.459 | 1.557 |

300°K, i.e., at about one-tenth $\theta_v$. Chlorine is an exception; the values, calculated from a band-spectrum value of $v = 16.95 \times 10^{12}$/sec, are compared with the experimental results[1] in Table 6.VI. There is indeed good agreement.

In polyatomic molecules, there are several vibrational frequencies, and the corresponding Einstein terms must be summed up. In many cases, to get full agreement with experiments, corrections have to be applied for the coupling between vibrational and rotational levels of the molecule and for the anharmonicity of the vibrations at higher temperatures. These problems are treated in several texts.[3,4]

Electronic energy levels, being of the order of $10^{4}$°K apart, are not excited at room temperatures. In nitric oxide (NO) and a few free radicals, there are exceptionally low-lying levels with spacings of about 100°K. The excitations between such levels give rise to the Schottky type of specific heat (Section 4.9). Measurements in the gaseous state, which exists only at temperatures well above the specific-heat peak, are in reasonable accord with the calculations.[4]

## 6.7.  CALORIMETRIC AND STATISTICAL ENTROPIES— DISORDER IN SOLID STATE

The study of the entropy of gases offers some interesting information about possible disorder in the solid state, which is of fundamental interest in connection with the third law of thermodynamics.[12] Statistical thermodynamics allows calculation of the absolute entropy of gases,[6] as was outlined for the case of translational degrees of freedom. The expressions involve, besides the fundamental constants $h, k, m$, etc., the frequencies of rotational and vibrational modes and the possible degeneracy of the states of the gas. These quantities can be determined from spectroscopic observations, and the entropy can be calculated.[5] On the other hand, from the measured specific heats of the solid and liquid phases as well as the latent heats of the phase changes, it is easy to calculate the entropy of the gas at, say, the normal boiling point. The calorimetrically determined values must agree with the statistically calculated values, if the conceptions

### Table 6.VII. Statistical and Calorimetric Entropies (in cal/mole·deg)

| | Gas and boiling point (deg K) | | | | | | | | | |
|---|---|---|---|---|---|---|---|---|---|---|
| | A<br>87.3 | Kr<br>120.2 | $N_2$<br>77.4 | $Cl_2$<br>238.6 | HCl<br>188.2 | HI<br>237.5 | $CH_4$<br>111.5 | $C_2H_4$<br>169.3 | $CO_2$<br>194.7 | $NH_3$<br>239.7 |
| Statistical | 30.87 | 34.65 | 36.42 | 51.55 | 41.45 | 47.8 | 36.61 | 47.35 | 47.55 | 44.10 |
| Calorimetric | 30.85 | 34.63 | 36.53 | 51.56 | 41.3 | 47.8 | 36.53 | 47.26 | 47.59 | 44.13 |

of the third law and the statistical mechanics of the substances are correct. Table 6.VII, giving the relevant data at the boiling point of several simple substances, shows that the agreement is very good in most cases. This is indeed gratifying.

In some cases, calorimetric and statistical entropies do not agree so well as in Table 6.VII. Among the possible reasons for the discrepancy are (i) errors of calorimetry in the form of impure specimens, etc.; (ii) anomalous variations of specific heat below the temperatures up to which measurements have been made, resulting in an incorrect extrapolation to 0°K (compare Section 1.4); and (iii) inadequate knowledge of the molecular parameters or the equation of state. Even when these reasons are ruled out, differences between the statistical and calorimetric values persist in some cases.[13] Table 6.VIII shows that they are significantly greater than the limits of experimental error, which is of the order of $\pm 0.1$ cal/mole·deg in the unfavorable cases involving specific-heat anomalies in the solid state. Although at one time there was considerable discussion about these discrepancies, it is now settled that in these substances the solid phases are not in internal equilibrium. As in the case of glassy materials discussed in Section 5.9, the solid state contains "frozen-in" configurational disorder not revealed in the calorimetric measurements of specific heats and hence in the evaluation of the entropy. Whereas the statistical calculations give the entropy difference between the gas at its boiling point and a perfectly ordered state at 0°K, calorimetry gives the entropy difference between the gas at its boiling point and a slightly disordered state at 0°K. Therefore, the calorimetric values must be *smaller* than the statistically calculated results, which is in fact one of the salient features of Table 6.VIII.

Carbon monoxide is a molecule with quite similar atoms; in an ideal solid state, the atoms should be arranged in the perfect order ... CO CO CO CO .... A disordered state ... CO CO OC CO ... will have a slightly higher energy $\Delta$, dependent upon the difference between C and O atoms. If the temperature $T$ is much larger than $\Delta/k$, fluctuations in thermal energy of the order of $\Delta/k$ are possible,

### Table 6.VIII. Discrepancies Between Statistical and Calorimetric Entropies[13]

| | Gas and boiling point (deg K) | | | | | | | |
|---|---|---|---|---|---|---|---|---|
| | CO<br>83 | N$_2$O<br>184.6 | CH$_3$D<br>99.7 | FClO$_3$<br>226.5 | SO$_2$F$_2$<br>217.8 | NO<br>121.4 | H$_2$O<br>298* | D$_2$O<br>298* |
| Statistical | 38.32 | 48.50 | 39.49 | 62.59 | 64.14 | 43.75 | 45.10 | 46.66 |
| Calorimetric | 37.2 | 47.36 | 36.72 | 60.17 | 62.66 | 43.03 | 44.28 | 45.89 |
| Statistical −<br>Calorimetric | 1.1 | 1.1 | 2.8 | 2.4 | 1.5 | 0.7 | 0.8 | 0.8 |

\* H$_2$O and D$_2$O at room temperature.

and the molecule rotates freely from the CO to OC configuration and back. At very low temperatures ($T \ll \Delta/k$), the solid will become completely ordered if allowed to do so. However, in any solid there are always intermolecular potential barriers $\delta$ opposing the molecular motions. If these barriers are small compared to $\Delta$, an ordered state sets in at $T \sim \Delta/k$. If, however, the potential barriers are much larger than $\Delta$, then the high-temperature disordered state becomes frozen at $T \sim \delta/k$. The ordering at lower temperatures is not possible, because the mismatch energy $\Delta$ is not sufficient to overcome the potential barrier $\delta$. If a molecule can take up one of two possible sites, the entropy of the frozen disorder is $R \ln 2$ per mole. The discrepancy in Table 6.VIII is 1.1 cal/mole·deg, which is slightly smaller than $R \ln 2 \sim 1.38$ units, suggesting that a part of the disorder had been removed before the potential barriers in the solid prevented any trend toward a perfect arrangement. Similar arguments apply to nitrous oxide. This is a linear molecule with the atoms nearly alike, so that its orientation in the solid state may be either NNO or ONN. The discrepancy, 1.1 units, is again a little smaller than $R \ln 2$. The same end-for-end disorder occurs in the long-chain 1-olefins with more than eleven carbon atoms,[14] while 1-decene and smaller molecules are fully ordered in the solid state.

The magnitude of the difference in CH$_3$D is about 2.7 cal/mole·deg, which immediately gives a clue to the nature of the disorder. In a completely ordered state, the CH$_3$D molecules may be expected to take up a position with the deuterium atoms in one particular site among the four tetrahedral carbon–hydrogen bonds. If the rotational motion has been frozen at relatively high temperatures, there will be a residual entropy of $R \ln 4 \sim 2.75$ units, which is very close to the experimental value. The same is the situation with the perchloryl fluoride FClO$_3$, where the crystal fails to distinguish

between the oxygen and the fluorine atoms in orienting the molecule in the solid state. There are four possible positions for the fluorine atoms, giving a disorder entropy $R \ln 4 \sim 2.75$ units, which is close to the observed value of 2.42 units. In sulfuryl fluoride ($SO_2F_2$), the slightly asymmetric top molecules have two possible orientations in the solid state, resulting in an entropy difference of about 1.5 units.

The statistical entropy of nitric oxide is only 0.7 units higher than the calorimetric values. X-ray studies[15] show that nitric oxide is present as a dimer

$$\begin{array}{cc} N & .. & O \\ O & .. & N \end{array}$$

with nitrogen–oxygen bonds of 1.1 and 2.4 Å, respectively. The X-ray diffraction patterns suggest that the dimer is distributed in the crystal without distinguishing between the corners occupied by the N atoms and those occupied by the O atoms. This randomness gives an entropy of $R \ln 2$ per mole of the dimer and so accounts for the observed difference $\frac{1}{2} R \ln 2 \sim 0.69$ units per mole of the monomer NO.

Ice provides a celebrated example of a more complicated type of disorder which was first elucidated by Pauling.[16] In gaseous $H_2O$, the HOH angle is about 105°, and the two H atoms are at a distance of 0.95 Å from the oxygen atom. In ice, the various molecules are bound together into a loose open structure by hydrogen bonds, and each O atom is surrounded by four other O, tetrahedrally situated at a distance of 2.76 Å. The water molecules retain their individuality to a large extent, but there is space only for one H atom along each tetrahedral O–O direction at a distance of 0.95 Å from either oxygen. In a mole of ice there are $2N$ H atoms, and if there are two possible positions along each O–O bond, the possible number of configurations is $2^{2N}$. Of these, only a few are acceptable. Consider any O atom and the available sites along the four tetrahedral directions. There is one way of putting four hydrogens close to the O atom, giving $(OH_4)^{2+}$ ionic arrangement; there are four ways of getting $(OH_3)^+$, six ways of getting $(OH_2)$, and four ways of getting $(OH)^-$; and there is one way of getting $(O)^{2-}$ ionic arrangement. Of these sixteen possibilities, only six yield the desired $H_2O$ molecule; that is, only three-eighths of all possible configurations are acceptable to that O atom. Thus the total number of possible arrangements of a mole of the solid is $(2)^{2N} \cdot (\frac{3}{8})^N = (\frac{3}{2})^N$. Therefore, the entropy associated with this is $R \ln\frac{3}{2} = 0.81$ cal/mole·deg. This agrees very well with the difference of 0.8 units observed for both $H_2O$ and $D_2O$. There is considerable evidence from neutron- and electron-diffraction studies for the essential correctness of the statistical disorder in ice, and the matter has been recently reviewed by Chidambaram.[17]

The hydrated sodium sulfate $Na_2SO_4 \cdot 10H_2O$ shows a residual entropy of about 1.5 units, which has been explained on the basis of X-ray structural work.[18] A four-member hydrogen-bonded ring exists in the structure, with the protons unsymmetrically located in the hydrogen bonds. Therefore, two arrangements,

```
H                        H         H                              H
 \                      /           \                            /
  O—H————————O          O————————H—O
  |          |          |             |
  |          H          H             |
  |   other  |   and    |   other     |
  |   atoms  |          |   atoms     |
  H          |          |             H
  |          |          |             |
  O————————H—O          O—H————————O
 /            \        /                \
H              H      H                  H
```
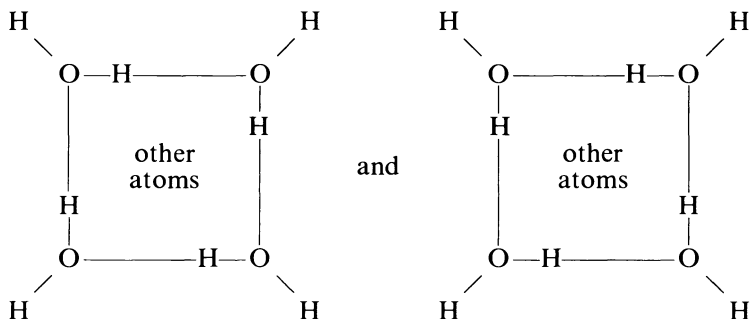
are possible, and a random population of the two schemes gives a disorder entropy of $R \ln 2$. Isomorphous $Na_2 CrO_4 \cdot 10H_2O$ has the same structure and presumably would have the same residual entropy.

It was mentioned earlier that if the mismatch energy $\Delta$ is much larger than the intermolecular potential barriers, an ordered state is achieved at a temperature $T \sim \Delta/k$. Consider, for example, HI instead of CO. The atoms are so different that the energy difference $\Delta$ between HI and IH configurations is very large. Even at relatively high temperatures, there is insufficient thermal energy to permit such a disorder. As a matter of fact, such substances display the ordering process in spectacular specific-heat singularities, the typical example[19] of HI and DI being given in Fig. 6.4. These cooperative anomalies were first found in ammonium chloride by Simon in 1922 and have since been found in a large number of substances. They are discussed fully in the following chapter. The configurational entropy in these materials is removed at relatively high temperatures. Hence there should be no discrepancy between statistical and calorimetric entropies. The examples given in Table 6.VII confirm this.

## 6.8. HINDERED ROTATION

A molecule does not always rotate as a rigid body, as was implied in the calculations of Section 6.4. In many organic molecules, groups of atoms can rotate freely or partially about the bond directions. A classic example is the difference between ethane $H_3C–CH_3$ and dimethylacetylene $H_3C–C{\equiv}C–CH_3$. In ethane, the influence of the hydrogen atoms of one methyl group can be felt by the other $CH_3$
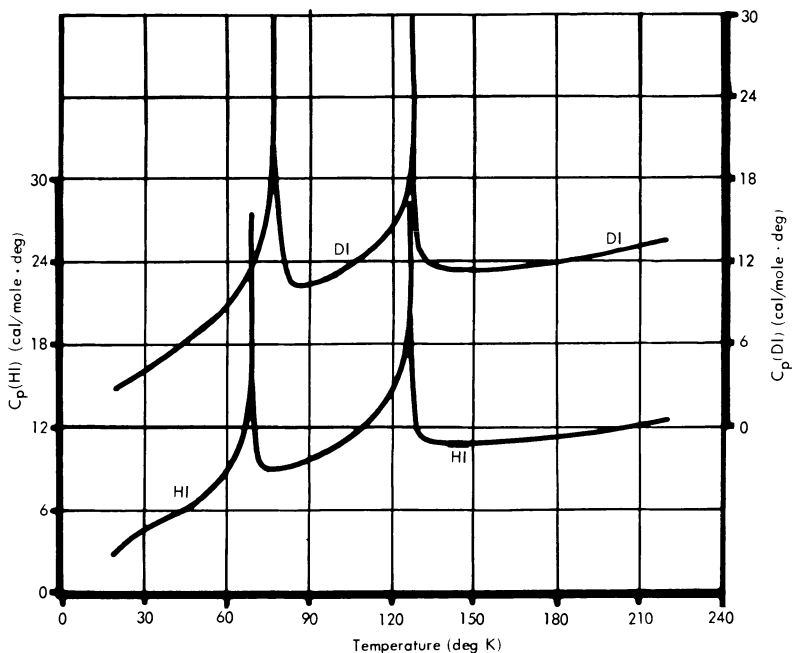
Fig. 6.4. Heat capacities of HI and DI.[19]

group, and so a rotation of one group about the C–C axis may be expected to have a potential of the form $V = V_0 (1 - \cos 3\phi)$. In dimethylacetylene, the $CH_3$ groups are far away, and so the methyl groups experience little, if any, potential barrier for rotation about the C≡C bond. In fact, the entropy calculated by assuming a free rotation of the methyl group agrees well with the calorimetric value in the case of this substance. On the other hand, the measured entropy of ethane falls between the entropies calculated by assuming free or no rotation about the C–C bond. It is clear that from such entropy differences a knowledge of the potential barriers may be obtained.

The hindered rotation of the radicals in a molecule can also be studied from infrared and microwave spectra of the substance. Wilson[20] has recently reviewed the various methods of determining $V_0$. The thermodynamic method, though used first to obtain this information (mainly by Pitzer and his coworkers), is rather inaccurate because it depends upon the small difference between two large quantities, namely, the calorimetric entropy and the statistical contribution from translational, vibrational, and other modes. The

spectroscopic determination is more accurate; $V_0$ thus determined can be used to interpret the calorimetric data. Methyl chloroform is one of the early substances for which spectroscopic data made possible the satisfactory interpretation of specific-heat measurements. Methanol has been studied extensively by various methods, and the results are in very good agreement with one another.[4]

## 6.9. ENTROPY OF HYDROGEN

The entropy of hydrogen depends upon its composition. Johnston and coworkers[21] calculated the entropy of parahydrogen by using the measured specific heats up to 12°K and then making a Debye-type extrapolation of the heat capacity of the solid down to absolute zero. At the boiling point (20.76°K), the entropy comes out to be
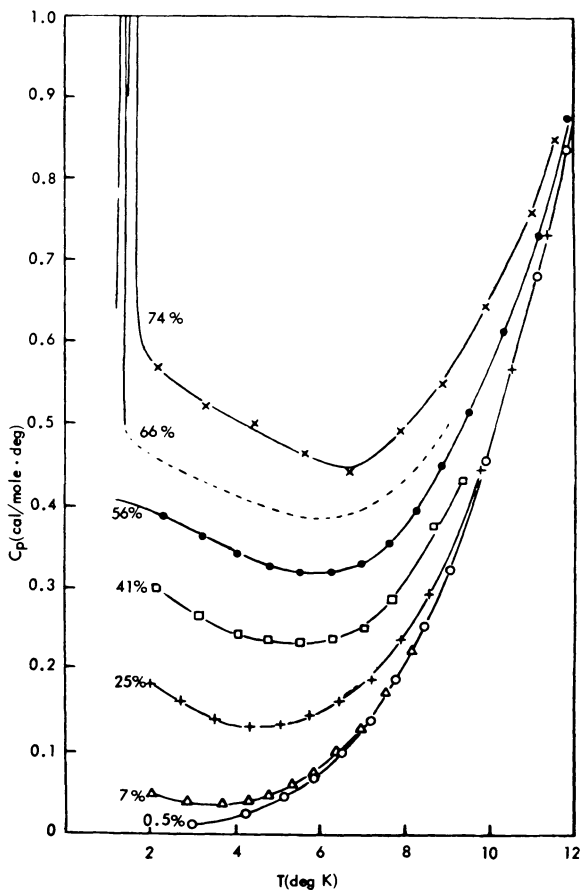


Fig. 6.5a. Heat capacities of mixtures of orthohydrogen and parahydrogen in the solid state.
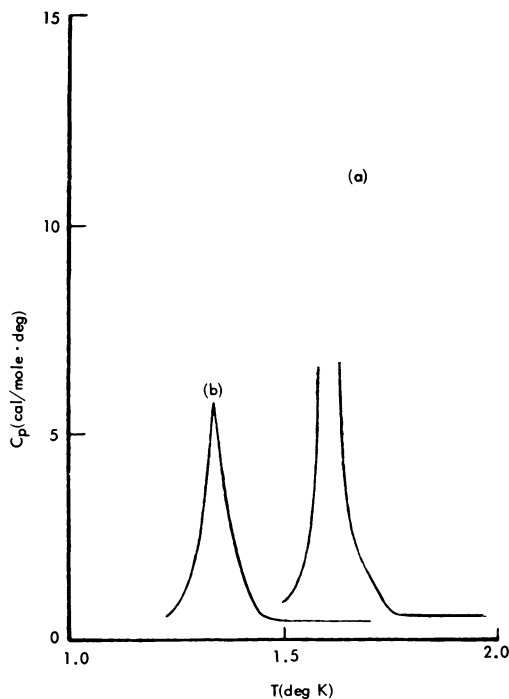
Fig. 6.5b. $\lambda$-peaks with ortho concentrations exceeding about $60\%$.[23] Curve (a) $= 74\%$ and curve (b) $= 66\%$ orthohydrogen.

$14.8 \pm 0.1$ cal/mole·deg. The statistical entropy is easily calculated from the translational and rotational functions and a small vibrational partition function. The value 14.76 agrees very well with the calorimetric evaluation.

A similar statistical calculation of the entropy of normal hydrogen shows that it exceeds that of parahydrogen by 4.29 cal/mole·deg. This excess arises from three sources. Normal hydrogen is a mixture of orthohydrogen and parahydrogen in the ratio $o:p = 3:1$, and the entropy of mixing is equal to $-R(\frac{1}{4}\ln\frac{1}{4} + \frac{3}{4}\ln\frac{3}{4}) \sim 1.14$ units. A second source is the nuclear-spin entropy of orthohydrogen. The ortho molecules, with a resultant nuclear spin $I = 1$, have three possible orientations, and the degeneracy will not be revealed until the specific heats are measured down to about $10^{-6}$°K. The excess entropy is $R\ln 3$ per mole of orthohydrogen, and so it contributes $\frac{3}{4}R\ln 3 \sim 1.64$ to the ordinary $3:1$ mixture.

A third contribution comes from the ordering of the rotational axes of the molecules at low temperatures. As mentioned earlier, ortho–para transitions take place only slowly in liquid and solid states, which makes it possible to measure the thermal properties of the condensed phases with various ortho–para concentrations.

Such measurements were first performed by Simon, Mendelssohn, and Ruheman[22] and more recently by Hill and Ricketson[23] and by Ahlers and Orttung.[24] Measurements above helium temperatures (Fig. 6.5a) show that the specific heats of solid solutions of ortho-hydrogen considerably exceed those of pure parahydrogen. With ortho concentrations in excess of about 60%, the specific heat exhibits a pronounced $\lambda$-peak at about 2°K (Fig. 6.5b). The additional specific heat increases with increasing ortho concentration, and the entropy associated with the anomaly is only a little lower than $R \ln 3$ per mole of orthohydrogen.

The excess entropy is in fact what is expected. The ground state of the ortho-molecule is the $j = 1$ rotational state, which, because of the low moment of inertia, has considerable energy. Solid hydrogen has a very open structure, largely on account of the high zero-point energy; therefore, the potential barriers opposing rotation of the molecules are small. The ortho molecules may be rotating right down to 0°K. The rotational level $j = 1$ is threefold degenerate, but since the molecular field in the solid is cubic and not spherical, different relative orientations have slightly differing energies of interaction. The lowest energy of the system occurs for an ordered arrangement of the axis of rotation; indeed, NMR experiments[25] show that the ortho molecules become ordered in this way. The specific-heat anomaly is due to this cooperative ordering process, though recent investigations[24] show that the details of the ordering process are more complicated than was originally supposed. It is evident that the removal of the threefold degeneracy gives an extra entropy $R \ln 3$ per mole of orthohydrogen, or $\frac{3}{4} R \ln 3 \sim 1.64$ per mole of normal hydrogen. The sum of the three contributions $(1.14 + 1.64 + 1.64 \sim 4.4 \text{ cal/mole·deg})$ is in satisfactory agreement with the calculated difference of 4.3 units.

A similar entropy contribution due to the removal of the three-fold degeneracy of para molecules is present in deuterium. Following the earlier experiments,[26] which revealed anomalous specific heats similar to those shown in 6.5a, Grenier and White[27] detected $\lambda$-peaks (as in Fig. 6.5b) at about 3°K in the specific heat of solid deuterium, with para concentrations of more than approximately 65%. They used a special enrichment procedure[10] to get para concentrations greater than the normal $33\frac{1}{3}$%. Taking into account the various contributions, there is satisfactory agreement between calorimetric and statistical entropies.

## REFERENCES

1. J. R. Partington and W. G. Shilling. *The Specific Heats of Gases*, Benn, London, 1924. A. Eucken, *Handbuch der Experimental Physik, VIII(I)* (1929), chapter 10.

2. E. Justi, *Spezifische Warme, Entropie, und Dissoziation technischer Gase*, Springer, Berlin, 1938.

3. J. E. Mayer and M. G. Mayer, *Statistical Mechanics,* Wiley, New York, 1940, chapters 6, 7, and 8. J. G. Aston and J. J. Fritz, *Thermodynamics and Statistical Thermodynamics*, Wiley, New York, 1959, chapters 18, 19, and 20.

4. J. S. Rowlinson, *The Perfect Gas*, Pergamon, Oxford, 1963, chapter 3.

5. G. Herzberg, *Infrared and Raman Spectra of Polyatomic Molecules*, Van Nostrand, New York, 1945, p. 501; *Spectra of Diatomic Molecules*, Van Nostrand, New York, 1950, p. 466. K. S. Pitzer, *Quantum Chemistry*, Prentice-Hall, Englewood Cliffs, N.J., 1953, chapter 9.

6. L. S. Kassel, *Chem. Rev.* **18**, 277 (1936). E. B. Wilson, *Chem. Rev.* **27**, 17 (1940).

7. H. W. Woolley, R. B. Scott, and F. G. Brickwedde, *J. Res. Nat. Bur. Std.* **41**, 379 (1948).

8. F. Hund, *Z. Physik* **42**, 93 (1927).

9. D. M. Dennison, *Proc. Roy. Soc. (London)*, *Ser. A* **115**, 483 (1927).

10. C. M. Cunningham, D. S. Chapin, and H. L. Johnston, *J. Am. Chem. Soc.* **80**, 2382 (1958).

11. W. M. Jones, *J. Chem. Phys.* **16**, 1077 (1948); **17**, 1062 (1949).

12. J. Wilks, *Third Law of Thermodynamics*, Oxford University Press, Oxford, 1961, chapter 5.

13. J. O. Clayton and W. F. Giauque, *J. Am. Chem. Soc.* **54**, 2610 (1932). (Carbon monoxide.) K. Clusius, *Z. Elektrochem.* **40**, 99 (1934); R. W. Blue and W. F. Giauque, *J. Am. Chem. Soc.* **57**, 991 (1935). (Nitrous oxide.) K. Clusius, L. Popp, and A. Frank, *Physica* **4**, 1105 (1937). (Monodeutro methane.) J. K. Koehler and W. F. Giauque, *J. Am. Chem. Soc.* **80**, 2659 (1958). (Perchloryl fluoride.) F. J. Bockoff, R. V. Petrella, and E. L. Pace, *J. Chem. Phys.* **32**, 799 (1960); **36**, 3502 (1962). (Sulfuryl fluoride.) H. L. Johnston and W. F. Giauque, *J. Am. Chem. Soc.* **51**, 3194 (1929). (Nitric oxide.) W. F. Giauque and J. W. Stout, *J. Am. Chem. Soc.* **58**, 1144 (1936). (Water.) E. A. Long and J. D. Kemp, *J. Am. Chem. Soc.* **58**, 1829 (1936). (Heavy water.)

14. J. P. McCullough, H. L. Finke, M. E. Gross, J. F. Messerly, and G. Waddington, *J. Phys. Chem.* **61**, 289 (1957).

15. W. J. Dulmage, E. A. Meyers, and W. N. Lipscomb, *Acta cryst.* **6**, 760 (1953).

16. L. Pauling, *J. Am. Chem. Soc.* **57**, 2680 (1935); *Nature of the Chemical Bond*, Cornell University Press, Ithaca, N.Y., 1960, p. 464.

17. R. Chidambaram, *Acta cryst.* **14**, 467 (1961).

18. K. S. Pitzer and L. V. Coulter, *J. Am. Chem. Soc.* **60**, 1310 (1938); G. Brodale and W. F. Giauque, *J. Am. Chem. Soc.* **80**, 2042 (1958). H. W. Ruben, D. H. Templeton, R. D. Rosenstein, and I. Olovsson, *J. Am. Chem. Soc.* **83**, 820 (1961).

19. A. Eucken and E. Karwat, *Z. phys. Chem.* **112**, 467 (1924). W. F. Giauque and R. Wiebe, *J. Am. Chem. Soc.* **51**, 1441 (1929). K. Clusius and D. Wolf, *Z. Naturforsch.* **2a**, 495 (1947).

20. E. B. Wilson, *Advan. Chem. Phys.* **2**, 367 (1959).

21. H. L. Johnston, J. T. Clarke, E. B. Rifkin, and E. C. Kerr, *J. Am. Chem. Soc.* **72**, 3933 (1950).

22. K. Mendelssohn, M. Ruheman, and F. Simon, *Z. phys. Chem.* **B15**, 121 (1931).

23. R. W. Hill and B. W. A. Ricketson, *Phil. Mag.* **45**, 277 (1954).

24. G. Ahlers and W. H. Orttung, *Phys. Rev.* **133**, A1642 (1964).

25. J. Hatton and B. V. Rollin, *Proc. Roy. Soc. (London)*, *Ser. A* **199**, 222 (1949). F. Reif and E. M. Purcell, *Phys. Rev.* **91**, 631 (1953). T. Sugawara, Y. Masuda, T. Kanda, and E. Kanda, *Sci. Rept. Res. Inst. Tohoku, Univ.* **A7**, 67 (1955). G. W. Smith and R. N. Housley, *Phys. Rev.* **117**, 732 (1960).

26. O. D. Gonzalez, D. White, and H. L. Johnston, *J. Chem. Phys.* **61**, 773 (1957).

27. G. Grenier and D. White, *J. Chem. Phys.* **40**, 3015 (1964).

*Chapter 7*

# Specific-Heat Anomalies

## 7.1. SPURIOUS AND GENUINE ANOMALIES

The idea that the specific heats of some materials show abnormal variations at certain temperatures was introduced as early as Chapter 1, and several examples of such uncommon behavior were mentioned in Chapters 3 to 6. Before embarking upon a systematic classification of such unusual specific-heat variations, it is worthwhile to digress a little upon what constitutes anomalous behavior. Any definition of an anomaly is to some extent negative in that it invokes the standards for normal behavior, which obviously depend upon the progress of our knowledge concerning the thermal properties of physical systems. Thus, deviations from Einstein and Debye models of specific heats, at one time considered to be anomalous variations of specific heats, are now taken as normal in the light of detailed lattice calculations. Similarly, the unexpected behavior of the specific heat of a superconductor is now viewed as a simple consequence of the onset of superconductivity in the electronic system. The possibility always exists that the puzzles of one era may become clarified in the succeeding years. Consequently, it is best to adopt as a pragmatic simplification that, in most substances and in many simple theoretical models of solids, the specific heat decreases continuously as the temperature is lowered. If there is an increase associated with reduction of temperatures, giving in effect a maximum in the heat capacity, the behavior is generally called a *specific-heat anomaly*. Although at one time such events were rarely observed, they are now known to occur in numerous substances. In general, if the origin of the effect is known, we shall call a finite small maximum a *peak* in the heat capacity and a large, nearly infinite, maximum a *singularity*. It appears best to reserve the term *anomaly* for the cases where the explanation is unknown.

It is useful to illustrate the above statements with some examples. For the majority of common solids, the typical low-temperature specific heat is that shown by the thick line in Fig. 7.1a, decreasing continuously to zero as 0°K is approached. A few substances exhibit a definite maximum as shown in Fig. 7.1b, a specific-heat peak. A practical case, that of nickel sulfate at low temperatures, was shown in Fig. 4.11. Here, on the basis of theoretical and experimental studies of thermal and other properties, it was possible to resolve the observations into a lattice contribution and a Schottky term, as shown schematically in Fig. 7.1b. Much effort has gone into the resolution of experimentally determined total specific heats into simple
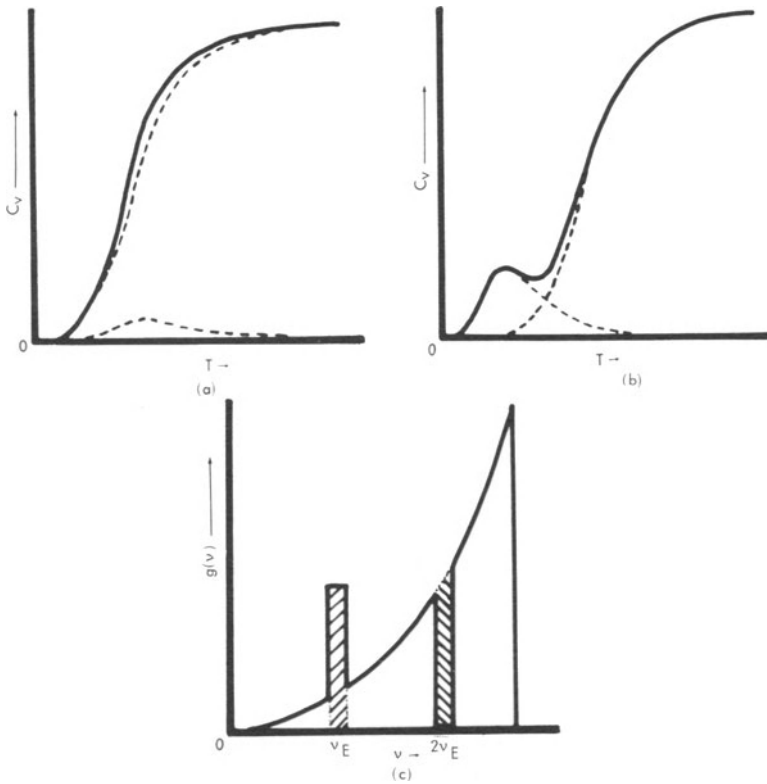
Fig. 7.1. (a) Typical specific-heat variation of many common solids (thick lines). Broken lines show a possible resolution into Debye and Schottky contributions. (b) Schematic picture of a specific heat peak. Broken lines show decomposition into lattice and Schottky contributions. (c) Frequency distribution for a combination of Debye and Schottky terms. The Schottky term is equivalent to removing frequencies at $2\nu_E$ and adding them at $\nu_E$ shown as shaded portions.

lattice, electronic, and other contributions so that the anomalous part can be discussed independently. Unfortunately, this sort of decomposition game, played with numerical data, can be carried to extremes. It was noticed by Simon in 1930 that the specific heats of many solids could be fitted very well by a combination of a Debye and a Schottky term, somewhat as shown by the broken lines in Fig. 7.1a. It was then postulated that the lattice follows the Debye variation, while the electronic system follows the Schottky relation as a result of excitation between the ground state and a higher energy state. With several adjustable constants, the agreement in such cases is, as expected, very good.

The underlying physical reason for this kind of agreement is as follows.[1] A comparison of the Schottky equation (4.25) for the case $g_0 = g_1$ with the Einstein equation (2.9) reveals that the Schottky term is the same as the difference $C_v(T_E/T) - C_v(2T_E/T)$ between two Einstein models with frequencies $v_E$ and $2v_E$. Thus, the above decomposition is equivalent to adding a number of frequencies at $v_E$ and removing the same number at $2v_E$ in the Debye spectrum. The resulting $g(v)$ (thick line in Fig. 7.1c) has a slightly better resemblance to the actual frequency spectra of solids—compare Figs. 2.5 to 2.8— than a single Debye spectrum, and the better representation of the specific heats by such a frequency spectrum is not surprising. With other approximate representations of $g(v)$, such as those attempted by Raman and coworkers, the situation is similar.

It is now natural to ask whether a Schottky term obtained by such a decomposition justifies considering the specific-heat variation to be anomalous. At present, such specific-heat contributions are not called anomalous. The Debye spectrum is now known beyond all doubts to be nothing more than a good approximation to the $g(v)$ of solids; a judicious combination of Debye and other terms is at best a better approximation. Hence, any peak separated out from the observations is artificial and without proper theoretical justification; the actual specific heat can be represented equally well by an appropriate $g(v)$, which can be studied and confirmed by other independent methods such as neutron-diffraction studies. It is only when there is an actual maximum in the observed total specific heat that the lattice and electronic modes are insufficient for an explanation. Therefore, a practical criterion for a specific-heat anomaly is the presence of a maximum in the temperature variation of specific heat.

It is thus clear that what could have been considered a specific-heat anomaly in, say, 1930 is now taken to be normal behavior of the lattice. Another way in which later studies establish the presence of normal behavior is in bringing to light insidious experimental errors.

In particular, three sources of error in many early observations have been revealed. Where hydrogen or helium exchange gas is used to cool the specimen to low temperatures, the desorption of the gas at low temperatures vitiates calorimetric studies by preventing the easy attainment of good vacuum insulation and by causing liberation of the heat of desorption. Secondly, small amounts of impurities, especially of materials which have pronounced specific-heat peaks, often result in apparent anomalies. Magnetic materials showing transitions at low temperatures should be scrupulously avoided. Thirdly, uncertainties in temperature scales may cause errors in the evaluation of heat capacities. Several anomalies reported earlier in many common materials[1] have now proved to be results of these experimental shortcomings.

## 7.2. COOPERATIVE AND NONCOOPERATIVE ANOMALIES

In discussing the model systems which show specific-heat peaks it is convenient to start with a system of independent particles or modes. Indeed, the simple models of solids and gases in Chapters 2, 3, and 6 invoked only such independent modes of excitation, namely, independent phonons, electrons, and molecules. The simplicity of such a system is that the total energy is just the sum of the energies of the various independent modes. Since there is no mutual inter-dependence among the modes, the system is called a *noncooperative* one. Under these conditions, a rather complete theoretical analysis of the system is possible. The examples of Schottky effect (Section 4.9), rotational specific heat of gases (Section 4.5), and the heat capacity of some liquids and solutions[2] show that even in these non-cooperative processes specific-heat maxima can occur. The practical examples of such peaks and their theoretical interpretation have been fully discussed elsewhere, and there is no need for further analysis in this chapter. As a matter of fact, the rotational specific heat of gases is so well understood that many authors do not classify its maximum as a specific-heat anomaly.

In some physical systems, the interactions among the constituents are so strong that the energy state of one constituent depends upon the energy states of its neighbors. For example, in a ferromagnet the probability of a given spin pointing along $+Z$ is large if the nearby spins also point along $+Z$ and small if they are aligned along $-Z$. Thus, the spin states are not mutually independent. The probability of transferring a particle to an excited state depends upon the degree to which the excited state is occupied. Under such conditions, the excited states are often too few until some critical mean energy, that is, some critical temperature, is approached. Then the process of

excitation by mutual *cooperative* action takes over and the particles of the system are very rapidly transfered to the excited states in the vicinity of the transition temperature. Thus, the energy of the system is changed in a small interval of temperature. In consequence, the cooperative transition is revealed in the specific heat as a pronounced singularity at the transition temperature $T_c$.

Several categories of cooperative phenomena are now known. The alignment of magnetic dipoles (spins), superconductivity of electronic systems, superfluidity in liquid helium, order–disorder transitions, and the onset of molecular rotation are some topics mentioned earlier. The phenomenon of ferroelectricity is analogous to ferromagnetism. There are other specific-heat singularities in rare-earth metals and at liquid-gas critical points. The present chapter will be concerned with these cooperative effects.

Specific-heat singularities due to magnetic interactions are by far the most frequent peaks observed at low temperatures. There are many ions which are paramagnetic; the presence of any one of them in a substance gives rise to either noncooperative Schottky peaks or cooperative ordering singularities. In the latter case, the ordered state at low temperatures may be ferro-, ferri-, or antiferromagnetic. Even in diamagnetic solids, the nuclear moments, if any, become ordered at sufficiently low temperatures. The experimental and theoretical aspects of these phenomena were discussed at some length in Chapter 4. Here it suffices to remark that if the spins become noncooperatively ordered, there is a smooth Schottky maximum, whereas in cooperative ordering the specific heat is probably infinite at the transition temperature $T_c$. Where sufficiently careful measurements have been made, the specific heat shows a logarithmic infinity on the low-temperature side of $T_c$. On the high-temperature side, it is not settled whether the singularity is logarithmic or of the power-law type.

Cooperative transitions in superconductors and superfluids were also fully discussed in earlier chapters. The two processes differ from the other cooperative phenomena in that the ordering takes place in the momentum space rather than in the coordinate space. For instance, a ferromagnet becomes ordered with all spins along one direction in the ordinary coordinate space. On the other hand, the superfluid properties of liquid $^4$He are basically the result of Bose condensation of the particles into zero-momentum states. The Cooper pairs, which are responsible for superconductivity, behave very much like condensed bosons. There are, however, differences between the specific-heat behavior of superfluids and superconductors. Liquid $^4$He exhibits the famous $\lambda$-transition at 2.17°K, with the heat capacity showing logarithmic infinities both below and above $T_\lambda$ (Section 5.5).

Superconductors show only a finite jump at the transition (Section 3.9). Further, liquid $^4$He has a specific-heat tail on the high-temperature side of the transition, whereas at temperatures higher than $T_c$, superconductors give no clue about their dramatic properties below the transition. There have been suggestions that superconductors should also exhibit $\lambda$-type singularities, but careful experiments have up to now failed to reveal any such behavior.[3] The transition in liquid $^3$He, if confirmed, should prove very interesting. Several authors have predicted a peculiar anisotropic state of the liquid below $T_c$.

With a variety of known cooperative effects, obviously no general theory of such processes can be given, and each effect is best treated on its own merits. Thereafter, it will be appropriate to show how cooperative phenomena can be interpreted in terms of simple models.

## 7.3. ORDER–DISORDER TRANSITIONS

In an ordinary alloy, the atoms are distributed at random over the available lattice sites. As the temperature is lowered, the third law of thermodynamics predicts that an ordered state having less entropy should result. However, in many cases the random arrangement is forcibly preserved by the interatomic potential barriers preventing the free movement of atoms. An illustration would be a typical tin–lead solder. This freezing-in of disorder has been mentioned earlier (Sections 5.9 and 6.7). In other cases, the material lowers its entropy by precipitating individual grains of the component pure metals. In a few cases, the alloy (say $A_mB_n$ of metals A and B) lowers its entropy by taking up a structure appropriate to a crystalline chemical compound $A_mB_n$. This last transformation is the one under consideration here.

A classic example is the alloy $\beta$-brass, CuZn. At or below room temperature, the substance has perfect cubic symmetry. The Zn atoms occupy the corners of a cubic unit cell, and the Cu atoms occupy the cube center. Thus, in this state $\beta$-brass may be visualized as two interpenetrating simple cubic lattices of Cu and Zn. At a temperature of about 1000°K, the structure is disordered in the sense that the Cu and Zn atoms occupy sites at random. As the temperature is raised from 0°K, the ordered state (schematically shown in Fig. 7.2a) is gradually transformed into the disordered state (shown in Fig. 7.2b), although the process occurs very rapidly in the vicinity of the transition temperature $T_c \approx 469$°C. The change in lattice structure is most easily followed by X-ray or neutron scattering. Many alloys, among them AuCu, AuCu$_3$, CuPt, and AgZn, show order–disorder transformations.[4]

O⟶A      ●⟶B                          ⊙⟶ A or B atom

(a)                              (b)                              (c)
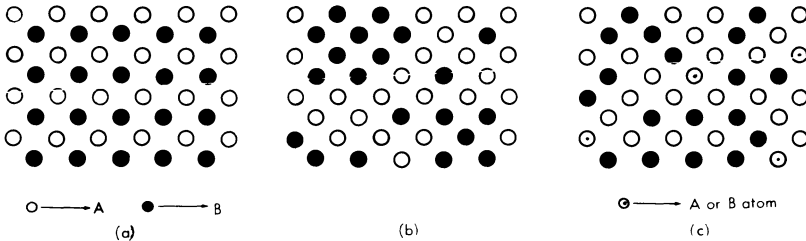
Fig. 7.2. Schematic view of order–disorder changes in an alloy AB: (a) ordered arrange-
ment, (b) random arrangement, (c) illustration of the difference between long-range
and short-range order.

The transformation is accompanied by changes in electrical,
mechanical, and thermal properties. The specific heat of CuZn near
its $T_c(\approx 469°C)$ is shown in Fig. 7.3a.[5] The $\lambda$-shaped peak charac-
teristic of cooperative transitions is evident. The specific heat has a
sharp rise below $T_c$ and retains a small tail above $T_c$. Although we
are not yet in a position to discuss the details of such specific-heat
curves, a simple rule for the excess entropy is easily formulated. If
the atoms have the possibility of choosing between $r$ configurations,
the associated entropy is

$$\Delta S = R \ln r \qquad (7.1)$$

per mole. Thus in $\beta$-brass $r = 2$; indeed, the excess entropy in Fig.
7.3a is found to be very close to $R \ln 2$. Since the excess arises from
the possibility of different configurations, $\Delta S$ is sometimes called the
*configurational entropy*.

So far, the idea of order has been used in a qualitative manner.
At this stage, we can introduce a quantitative description, used by
Bragg and Williams in 1934, of what is strictly long-range order.
Consider the alloy AB with an interpenetrating lattice of A and B.
We may refer to the sites corresponding to one interpenetrating lattice
as $\alpha$-sites and the sites of the other lattice as $\beta$-sites. In a completely
ordered state, let A atoms occupy $\alpha$-sites and B atoms $\beta$-sites. Then,
in a slightly disordered state, some atoms will be in right positions
(A on $\alpha$, B on $\beta$), while some will be in wrong positions (A on $\beta$,
B on $\alpha$). If there are $R$ right atoms and $W$ wrong atoms, the long-
range order parameter $\sigma_l$ may be defined as

$$\sigma_l = \frac{R - W}{R + W} \qquad (7.2)$$

When $W = 0$, there is complete order and $\sigma_l = 1$. The case $R = 0$,
$\sigma_l = -1$ also corresponds to a state of complete order, since by
interchanging the names of $\alpha$- and $\beta$-sites it becomes physically
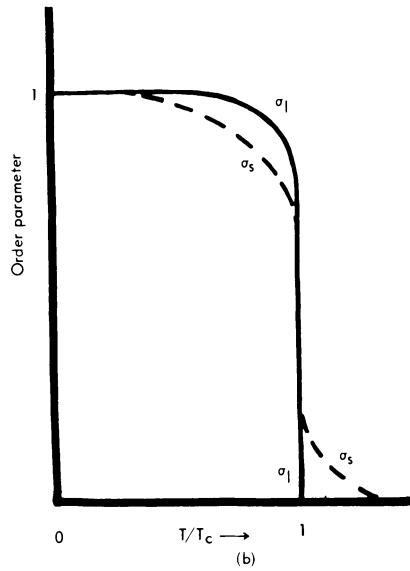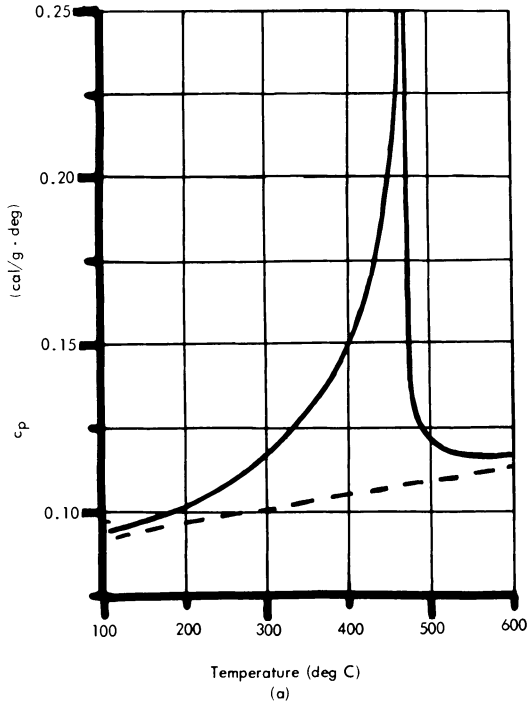
Fig. 7.3. (a) Specific heat of CuZn.[5] (b) Temperature variation of order parameters.

identical to the case $W = 0$. Complete disorder exists when there are as many right atoms as wrong ones, that is, when $R = W$ and $\sigma_l = 0$. Therefore, only the range between $\sigma_l = 1$ (complete order) and $\sigma_l = 0$ (complete disorder) is of physical interest. At very low temperatures, $\sigma_l$ is unity, and it drops rapidly to zero when $T_c$ is reached, as represented in Fig. 7.3b.

The short-range order parameter $\sigma_s$ may also be easily introduced, following the work of Bethe in 1935. In many systems, the interaction among the atoms is significant only for the nearest neighbors. For instance, the spin exchange integrals of Section 4.6 are nearest-neighbor interactions. Therefore, as a criterion of order we may compare the number of right pairs (AB type) and the number of wrong (AA or BB) pairs of near neighbors. An illustration will clarify this concept. From the point of view of long-range order defined by equation (7.2), the lattice of Fig. 7.2c is highly disordered. Yet nearly all atoms have unlike atoms as nearest neighbors. So if the relative number of right and wrong neighbors is taken as a measure of the ordering in the vicinity of any atom, the lattice is only slightly disordered. Consider an A atom. Let the probability that a given neighbor is a B atom be $(1 + \sigma_s)/2$ and the probability that it is an A atom be $(1 - \sigma_s)/2$. For complete order $\sigma_s = 1$ and for complete disorder $\sigma_s = 0$. Therefore, $\sigma_s$ is called the *short-range order parameter*. The temperature variation of $\sigma_s$ is shown schematically in Fig. 7.3b. As $T_c$ is approached, $\sigma_s$ decreases rapidly from unity, but even above $T_c$ short-range order persists for some temperatures.

## 7.4. ONSET OF MOLECULAR ROTATION

The nature of atomic motions in solids is obviously controlled by the interatomic forces. In rocksalt, the $Na^+$ ions are equally strongly bound to the six surrounding $Cl^-$ atoms, and it is hard to identify a single NaCl molecule or the molecular frequencies. If the intramolecular forces are comparable to the intermolecular forces, it is sometimes possible to identify distorted motions of parts of the molecules, for example, the $CO_3$ vibrations in solid $CaCO_3$. In the extreme case of loosely bonded molecules, the molecular motions are practically unaffected at high temperatures; it was mentioned in Section 6.7 that under such circumstances the molecules or radicals may be freely rotating. Consider as an example solid methane, in which the spherical $CH_4$ molecules are loosely held together by Van der Waals forces. The methane molecules are freely rotating at "high" temperatures. On reducing the energy content of the solid by cooling it to "low" temperatures, the rotational motion is found to die down in a cooperative way. The specific heat of methane,[6]
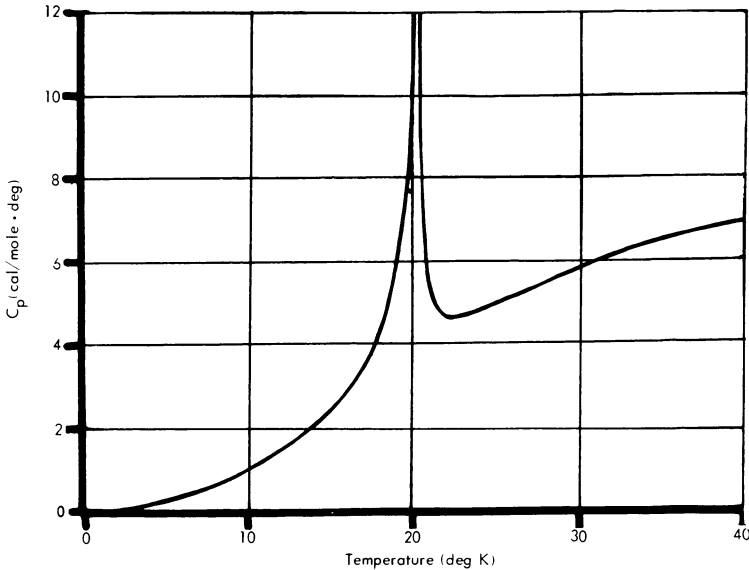
Fig. 7.4. Heat capacity of methane.[6]

given in Fig. 7.4, shows the familiar $\lambda$-peak. Structural studies,[7] in particular those in which magnetic resonance and neutron diffraction were used, reveal that the $CH_4$ molecules are freely rotating above $T_c = 20°K$. At lower temperatures, they perform hindered rotations or torsional oscillations backward and forward about a mean position.

The transition in solid hydrogen, treated in Section 6.9, is another well-known example of a cooperative onset of molecular rotation. In orthohydrogen, the axis of rotation, which is not unique above $T_c$, becomes ordered below the transition. Similar specific-heat singularities in hydrogen halides and in various ammonium salts were mentioned in Section 6.7. As a matter of fact, the specific-heat singularity in solid $NH_4Cl$, observed by Simon in 1922, was the first true $\lambda$-anomaly to be discovered. In many cases, the precise nature of molecular rotations is not yet clear, and the available evidence suggests that they differ from substance to substance. However, a discussion of the various individual cases[7] is not appropriate here.

## 7.5. FERROELECTRICITY

Solids belonging to ten of the thirty-two crystallographic classes lack inversion symmetry. They can exhibit electric polarization in the absence of an electric field, owing to the spontaneous alignment

of electric dipoles. In contrast to the magnetic case, this electric polarization cannot be observed under ordinary static conditions, because it is compensated by free charges on the surfaces. However, the polarization is temperature-dependent, and so changes in it can be deduced from the current flowing in a closed circuit when the temperature of the crystal is changed. For this reason, substances belonging to the ten noncentrosymmetric classes are called *pyroelectric*.

Some pyroelectrics have the additional property that the spontaneous polarization can be reversed in sense by an applied electric field. The material is then said to be *ferroelectric*. Thus, in ferroelectrics the polarization can be measured simply by reversing the applied electric field. In nonferroelectric pyroelectrics, dielectric breakdown occurs well before a field large enough to reverse the polarization can be applied. The dielectric behavior of a ferroelectric is complex. Not only is the relation between the polarization $P$ and the applied field $E$ nonlinear, but there is also a hysteresis loop, analogous to the ferromagnetic case. The alignment of the dipoles is opposed by thermal agitation. On increasing the temperature, the ordering is disturbed, and at a critical temperature, the ferroelectric Curie point, it breaks up. The crystal loses its ferroelectricity and becomes an ordinary dielectric (paraelectric state). Rochelle salt, ammonium dihydrogen phosphate, barium titanate, and triglycine sulfate are among the well-known ferroelectrics. There are several excellent reviews of this field.[8]

The onset of ferroelectric ordering gives rise to $\lambda$-type peaks in the heat capacity. The behavior of potassium dihydrogen phosphate (KDP), which is ferroelectric below 123°K, is typical of the specific-heat studies.[9] Superimposed on the usual lattice contribution is the configurational specific heat associated with ferroelectric ordering at 123°K (Fig. 7.5). The detailed behavior near the Curie point is slightly uncertain in most ferroelectrics because of the existence of thermal hysteresis; that is, the specific heat on cooling is slightly different from that on warming. The entropy associated with the excess specific heat is about 0.7 cal/mole·deg, which is close to the value $\frac{1}{2}R \ln 2$. The spontaneous polarization $P_s$ decreases slowly as the temperature is raised from 0°K, but drops rapidly as $T_c$ is approached. Just as in the magnetic case [equation (4.17)], the excess specific heat should be proportional to $dP_s^2/dT$. This relationship is approximately obeyed in KDP.[10] Further, there is evidence[10a] that the specific heat near $T_c$ may be fitted to logarithmic singularities, of the type discussed in Sections 4.6 and 4.7.

The similarity between ferroelectricity and ferromagnetism extends to other forms of ordering as well. Ferroelectricity and
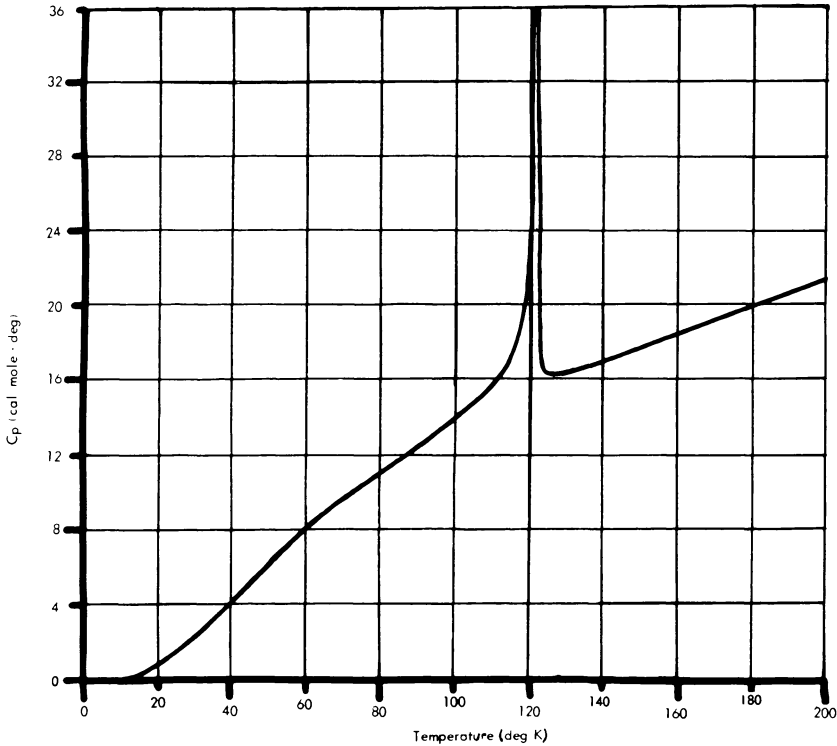
Fig. 7.5. Heat capacity of $KH_2PO_4$.[9]

antiferroelectricity are also known; these topics are discussed in the many reviews on the subject.[8] In spite of these similarities, the molecular basis of the electric phenomenon is apparently very different. Taking the example of $KH_2PO_4$, the deuterated $KD_2PO_4$ has a transition temperature ($\sim 213°K$) nearly double that of KDP. Yet the entropy associated with the transition is nearly the same in the two salts. The entropy excess suggests some form of order–disorder process, while the dependence on the mass of hydrogen shows that the hydrogen atoms are involved in the ordering. Indeed, the theoretical explanations of ferroelectricity, originally advanced by Mueller, Slater, and others, invoke an ordering of the hydrogen bonds. For a large number of compounds, order–disorder structures of the hydrogen bonds are possible.[8] In ionic ferroelectrics such as $BaTiO_3$, another mechanism has been suggested by Anderson, Cochran, and others.[11] This is based on the idea that in an optical mode (Section 2.8) the

adjacent charges vibrate out of phase. If the restoring forces and hence the frequency tend to zero, a spontaneous separation of charges, which is nothing but the spontaneous polarization under consideration here, is possible. Thus, it is suggested that as the temperature is lowered the frequency of some optical mode decreases rapidly and becomes zero at $T_c$. Such a mechanism, which is supported by neutron-diffraction studies on $SrTiO_3$, explains many observations on $BaTiO_3$-type ferroelectrics. These questions are treated at length in the reviews already cited.

## 7.6. TRANSITIONS IN RARE-EARTH METALS

The rare-earth metals, lanthanum (atomic number $Z = 57$) to lutetium ($Z = 71$), can be isolated and purified only with some special techniques developed in the last twenty years. Much of the work done before 1950 was on impure metals; as seen earlier, the impurities often have very disturbing effects on specific heats. Recent studies[12] on relatively pure metals have shown very complicated thermal and magnetic properties. The rare-earth metals show unusual types of ferro- and antiferromagnetic orderings[13] which give rise to these complicated phenomena. Thus, a discussion of the heat capacity of rare-earth metals should belong to Chapter 4. However, on account of the variety of abnormal effects observed and the very large gaps in our knowledge, these matters are considered here.

The electronic structure of the rare-earth metals may be written as Xe core—$4f^n$; $5s^2$, $5p^6$; $6s^2$, $5d^1$—although some exchange between the $4f$; and $5d$-shells takes place. As the atomic number $Z$ increases from 57 to 71, $n$ increases from 0 to 14. The $4f$-shells are largely screened by the closed $5s$- and $5p$-shells, so that magnetic and Stark interactions are weak. As a result of the subtle balance between these interactions and the normal thermal energy, the metals show very complicated thermal, magnetic, and other properties. A brief account of the specific-heat behavior will highlight the challenging problems in the study of these metals.

Lanthanum ($Z = 57$, $n = 0$) has no $4f$-electron, is a superconductor, and behaves in a normal way.

Cerium has one $4f$-electron and exhibits the complex specific-heat behavior shown in Fig. 7.6. As the specimen is cooled from room temperature, the specific heat follows the curve A in the region $200 > T > 120°K$. On warming from a low temperature, the specific heat follows the curve B, exhibiting a pronounced thermal hysteresis. Some latent heat is also evolved in the region $L$ around $100°K$. At $13°K$, there is a large peak in the specific heat, which is due to the onset of antiferromagnetism at lower temperatures. At about $200°K$,
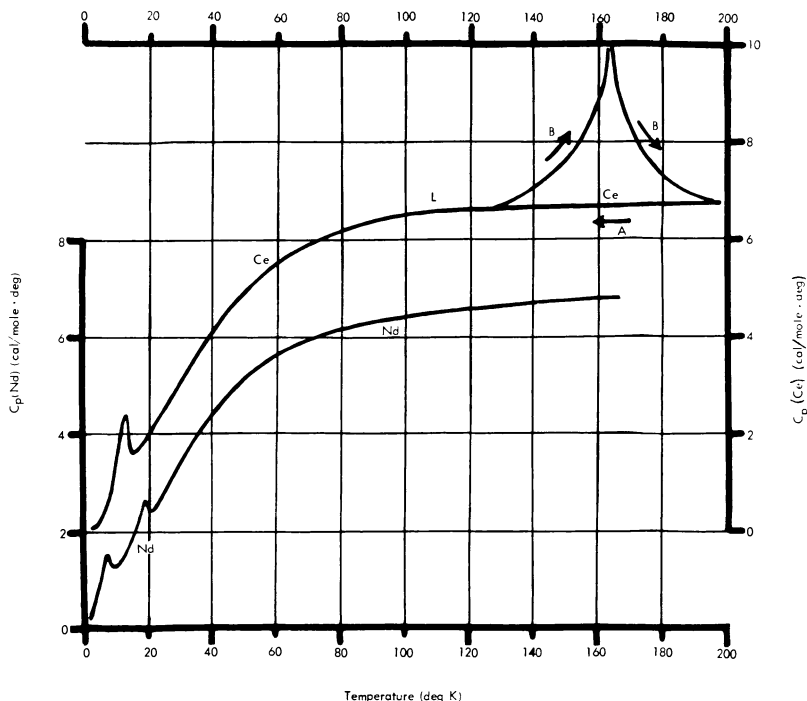
Fig. 7.6. Heat capacities of cerium and neodymium.[14]

the fcc lattice of cerium starts to undergo a transition into a com-
pressed fcc' lattice of about 15 % less volume. Besides the fcc' phase,
there is another hcp phase at low temperatures.[15] Apparently the
fcc ⇌ fcc' transition is an electronic one in which the magnetic
4 f-electron goes over into the 5d conduction band. These phase
changes involve very little rearrangement of atoms and show a pro-
nounced dependence upon the stresses and strains in the crystal, past
thermal history, and the state of crystalline imperfections. Thus, on
repeated cooling to 20°K and warming to 300°K, the hysteresis loop
at 160°K collapses and the peak at 13°K is enhanced. Such a sluggish
dependence upon thermal history is characteristic of martensitic
transformations,[16] of which another example, namely, that of sodium,
was mentioned in Section 2.10. At the present time, however, there is
no quantitative explanation of the hysteresis effects.

Praseodymium has a large specific-heat bump distributed around
40°K. Neodymium ($Z = 60$) has two peaks, one at 8°K and another
at 19°K (Fig. 7.6). Below 8°K, there is an ordering into the ordinary

antiferromagnetic state discussed in Section 4.2. The peak at 19°K is due to the onset of a special type of antiferromagnetism, which will be mentioned later (Fig. 7.8e). The peak in praseodymium also arises from a similar special type of antiferromagnetic ordering.[17]

The heat capacity of promethium, an element which has to be produced artificially, has not been studied so far. Samarium ($Z = 62$) has a sharp singularity at 15°K due to antiferromagnetic ordering. There is a second peak at 106°K, but as yet no corresponding anomaly in the magnetic behavior has been found. Europium is antiferro-magnetic below about 90°K.

The ferromagnetism of gadolinium below 289°K is very well known. The specific heat has a large $\lambda$-singularity at that temperature (Fig. 7.7). The next five metals, in which $n$ runs from 8 to 12, show complex ferro- and antiferromagnetic states. Terbium is paramagnetic down to 230°K, where it becomes ferromagnetic. Dysprosium (Fig. 7.7) is paramagnetic down to 175°K, when it becomes antiferro-magnetic, and then at 85°K it becomes ferromagnetic. There is a large $\lambda$-peak at 175°K and a symmetrical peak at 85°K. Holmium behaves in a similar manner, with a $\lambda$-peak at the Néel point (132°K) and a symmetrical peak at the ferromagnetic Curie point of 20°K. In between the two temperatures, the specific heat rises rather non-uniformly, a feature which is aggravated in erbium (Fig. 7.7). Between its Néel point of 80°K and its Curie point of 19°K, there is a rounded maximum at 54°K, just discernible in the scale of Fig. 7.7. This arises from complications in magnetic ordering, which are discussed below. Thulium becomes antiferromagnetic on cooling to 15°K. With these metals, the specific heat at the ferromagnetic transition shows con-siderable hysteresis.

In yttrium ($Z = 70$), the $5d$-electron goes into the $4f$-shell, which otherwise should have $n = 13$, and completes it. Therefore, the metal does not exhibit any striking magnetic or thermal phenomena. Like-wise, lutetium, which has a closed shell ($n = 14$) of $4f$-electrons, behaves normally.

Even this sketchy summary is enough to show that nearly every type of specific-heat abnormality is present in these metals. This complex behavior corresponds to the complicated magnetic structure, which is being slowly unravelled as a result of careful neutron-diffraction and magnetic measurements. Although the details of such studies[13] go beyond the scope of the present discussion, an indication of the complexity of the problem is appropriate here.

Simple cases of magnetic ordering were outlined in Section 4.2. Ferromagnetism corresponds to parallel alignment of adjacent spins and antiferromagnetism to antiparallel alignment. This simple arrangement holds good, for example, in ferromagnetic dysprosium,
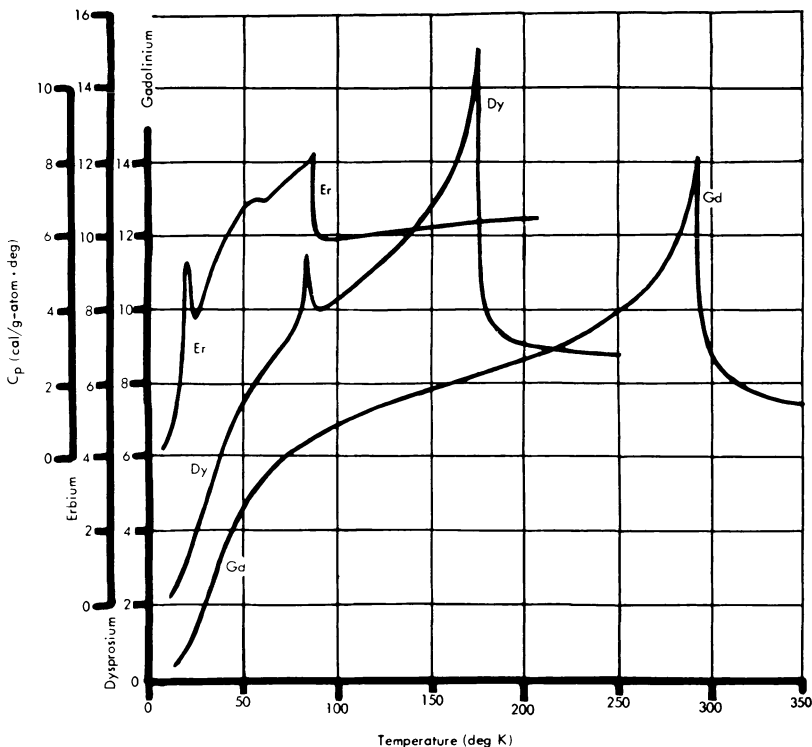
Fig. 7.7. Heat capacities of gadolinium, dysprosium, and erbium.[18] Note off-set scales for the ordinates.

$T < 85°K$, when the magnetic moments lie parallel in the basal plane (Fig. 7.8a). In the antiferromagnetic phase $(85° < T < 175°K)$, the resultant moment in each plane is rotated by an angle $\alpha$ with respect to the moment in the next plane (Fig. 7.8b), the angle $\alpha$ changing with $T$. It is evident that the magnetic moments in the hexagonal lattice lie on a spiral, the characteristic helicoidal structure, and that this ordering has no net moment on a bulk scale. The same helicoidal arrangement is found in terbium, also.

Holmium is more complex. In the ferromagnetic state, the magnetic moment has a common component normal to the hexagonal planes and a helicoidally ordered component in the basal plane (Fig. 7.8c). Thus, the ferromagnetic moment of holmium below $20°K$
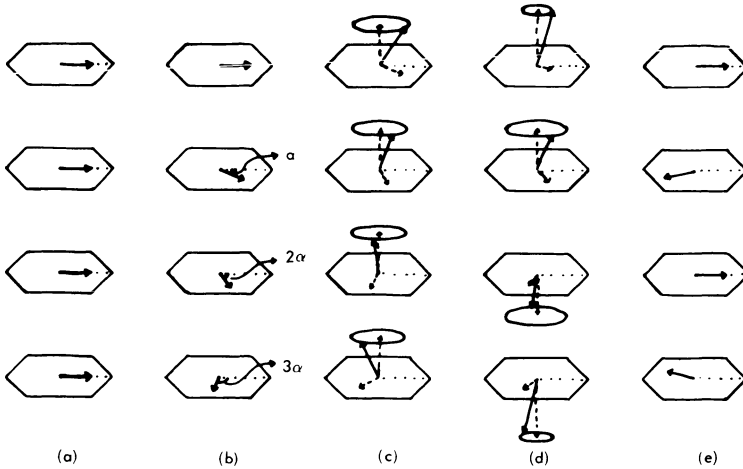
Fig. 7.8. Complex magnetic ordering in rare-earth metals: (a) collinear ferro-
magnetism—dysprosium, (b) helicoidal antiferromagnetism—dysprosium, (c)
helicoidal ferromagnetism—holmium and erbium, (d) cycloidal antiferro-
magnetism—erbium, (e) transverse oscillatory antiparallel ordering—praseo-
dymium and neodymium. The drawings are based on projections of regular
hexagons. In (a), the vector (arrow) always points toward the horizontal vertex.
In (b), the arrow moves uniformly in the plane, the rotation angles α, 2α, and 3α
being shown. In (c), the arrow rotates uniformly in the ellipse so that its pro-
jection in the plane (broken line) rotates uniformly in the plane while the
projection perpendicular to the plane is constant. In (d), the projection in the
plane rotates uniformly while the ellipses move up and down. In (e), the vector
is always in the plane and lies on either side of the main diagonal in the second
and fourth rows.

is due only to the component parallel to the hexagonal $c$-axis. This
component decreases with the increase of $T$, and in the antiferro-
magnetic state $(20 < T < 132°K)$, only the helical structure remains.

Ferromagnetic erbium has a structure similar to that shown in
Fig. 7.8c, a constant component along the $c$-axis and helicoidally
arranged components in the basal plane. In the antiferromagnetic
region $(19 < T < 80°K)$, the magnitude and sign of the moment along
$c$ vary periodically from layer to layer in accordance with a sine law
(Fig. 7.8d). Below about 52°K, the moments in the basal plane are
helicoidally ordered, but at higher temperatures they become dis-
ordered. This change of the basal components makes itself felt in
specific heats as a small bump at approximately 54°K, which was
mentioned earlier.

There remains one more type of magnetic ordering, which in the
absence of any better name may be called *transverse oscillatory anti-*

*parallel ordering.* Neodymium below 7°K has the usual type of collinear antiparallel ordering of the moments, which lie on the basal plane. Between 7 and 19°K, there is a superimposed sinusoidal modulation of the basal moments in a direction perpendicular to the usual ordering direction (Fig. 7.8e). This ordering disappears above 19°K and gives rise to a specific-heat bump at 19°K. A similar situation exists in praseodymium, also.

Any theoretical discussion of such types of magnetic ordering is bound to be complicated,[13] though considerable progress has been made recently. With a very delicate balance between thermal and magnetic forces, the situation offers a challenge to theoreticians and experimenters alike to improve the existing knowledge of the phenomenon.

## 7.7. LIQUID–GAS CRITICAL POINTS

A perusal of the specific-heat singularities mentioned earlier brings out the fact that they are associated with some change in the ordered state or a phase change. The close relation of the thermal properties to molecular ordering has been the aim of the discussions, while the relation of phase changes to phenomenological considerations has been left to Section 8.1. The liquid–gas phase equilibrium is historically important for having been the source of the idea of the equation of state. At the liquid–gas critical point (for convenience simply called *critical point* in this section), the isothermal bulk modulus vanishes, differences between liquid and gaseous states disappear, and the region is dominated by molecular fluctuations. Obviously, unusual effects in thermal properties should be expected. Early experiments showed a large peak as the critical point was approached. In the related case of critical liquid–liquid mixtures, the existence of singular behavior in specific heat[19] and other properties has also been known for some time. Nevertheless, it is only recently that specific heats have been measured near enough to the critical point to reveal the unusual behavior. Since the compressibility of the system is high in the critical region, a direct measurement of the specific heat at constant volume $C_v$ is possible using containers strong enough to withstand the critical pressure.

The first experiments of this kind were completed by Bagatskii, Voronel', and Gusak[20] on argon near its critical point; they showed that $C_v$ had a tendency to become infinite at $T_c$. Subsequent work[20] by Voronel' and coworkers on oxygen and by Little and Muldover on $^4$He has abundantly verified that $C_v$ tends to an infinite value at $T_c$. In the helium case, experiments to within $10^{-4}$°K of $T_c$ show that the approach to infinity is logarithmic in $|T - T_c|$ both below

and above $T_c$. The situation is very similar to the $\lambda$-transition at 2.17°K in liquid $^4$He (Section 5.5), and the coefficient of the logarithmic term is of the same order in both cases. The behavior of argon and oxygen appears to be more complicated. The original discussion indicated a logarithmic approach both below and above $T_c$ with the same slope (Fig. 7.9). Fisher[21] has analyzed the data again to show that although below $T_c$ the approach is certainly logarithmic, above $T_c$ it may be a power law of the form $c \propto (T - T_c)^{-1/5}$. Figure 7.9 shows the situation in the case of argon. Obviously, only further work can settle the exact nature of the approach to infinity on the high-temperature side.

The singularity in the specific heat at constant volume is of special interest. The experiments quoted earlier to show the possibility of infinite specific heats at some transitions all refer to the heat capacity at constant pressure or at constant saturation. Other parameters such as the coefficient of thermal expansion also show
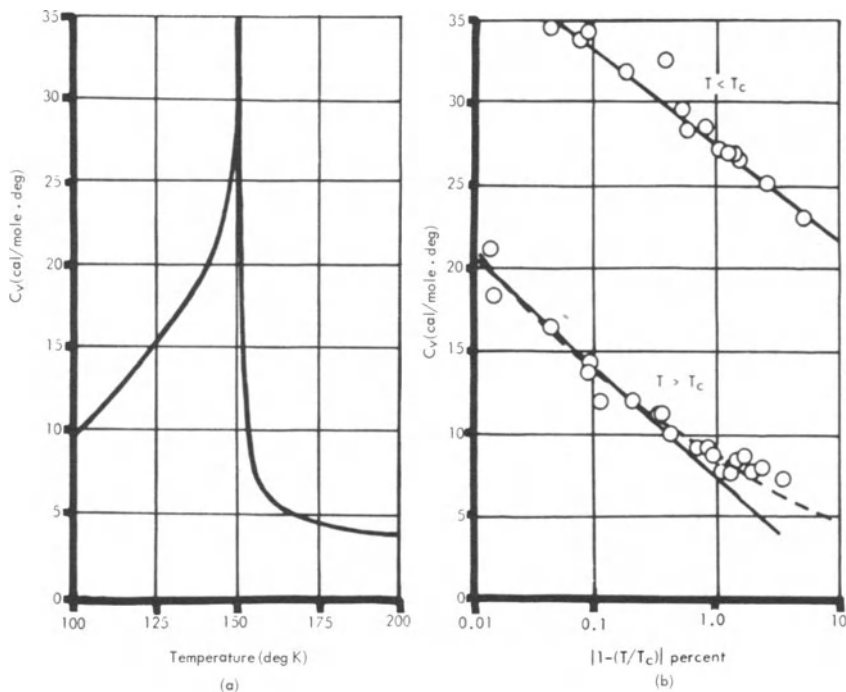


Fig. 7.9. (a) Heat capacity $C_v$ of argon. (b) Behavior near its liquid–gas critical temperature $T_c = 150.5°K$. Full lines refer to logarithmic singularity both above and below $T_c$. Broken line is a power-law fit above $T_c$ with an exponent $-\frac{1}{5}$.

singularities, and it was believed that though $C_p$ is infinite, $C_v$ remains finite. The phenomenological theories of phase transitions based on an expansion of some order parameters in powers of $|T - T_c|$, as originally done by Landau and Lifshitz, are based on such ideas. The experiments at the critical point show that, in some cases at least, such assumptions are not valid. The thermodynamic consequences of infinite singularities in $C_v$ have been considered by several authors.[22] It is found, for instance, that the adiabatic compressibility should tend to zero at $T_c$; experiments on sound propagation in $^4$He near the critical region verify this prediction.[23] It is somewhat amusing that while the theoretical two-dimensional Ising model gives a logarithmic infinity in $C_v$, it is only for an ideal incompressible lattice. The introduction of lattice compressibility results in a finite specific heat together with a latent heat at the transition.[24]

One might at first expect that the properties of gases are so well known that a satisfactory theory of the condensation into a liquid could easily be formulated. Unfortunately, it is not so. The interatomic forces in a gas normally play only a secondary role and may therefore be treated as small corrections to ideal gases. On the other hand, the phenomenon of condensation arises solely from the cohesive forces; in this limiting case, the usual methods of calculation do not work well. The principal theoretical contribution of sufficient generality is Mayer's demonstration of the existence of a condensation in the theory of nonideal gases.[7] Calculations based on simple models have been rather more successful. Mention should be made of Lee and Yang's analysis showing that the properties of a weakly interacting gas have some similarity to those of an Ising lattice (Section 4.6). The ferromagnetic ordering and the random paramagnetic arrangement are the respective formal analogs of the condensed and gaseous phases.[25] Near the transition temperature, the specific heats of ferromagnets and liquids show similar singularities, which lends some credence to this view, although it is not possible here to go into the details of the calculations.

## 7.8. MODELS OF COOPERATIVE TRANSITIONS

Having seen the variety of possible cooperative effects, it is obvious that no general theory of such phenomena is possible. The main difficulty in developing a theory of strongly interacting systems is that the total energy of the system can no longer be calculated from the simple sum of the energies of the individual particles, as was done earlier with systems of noninteracting particles. A natural way under such circumstances is to ask how the system is altered when a new particle is added to the existing $N$ particles—in other words,

to determine the response of the system to small perturbations. This approach is usually called the method of *Green's functions*; it is along these lines that much recent progress has been made. The mathematical techniques involved in such computations are quite esoteric. Even so, except for the case of superconductivity of electronic systems, no complete theory, applicable right up to the transition temperature, has been worked out for the phenomena of interest. Therefore, in an elementary text it is instructive to mention how the cooperative effect may be incorporated in simple models.

It turns out that the Ising lattice, introduced in connection with magnetic ordering (Section 4.6), is a reasonable model of many types of cooperative phenomena. In this model, spins are placed at lattice sites, and each spin can point along $+ Z$ or $- Z$. The interactions, which extend to nearest neighbors only, have two possible values, corresponding to parallel or antiparallel alignment of a pair of adjacent spins. It is not hard to see that the same model can be applied to order–disorder transformations, also. In such case, the atoms are at lattice sites and the atomic interactions have two possible values, corresponding to right or wrong pairing of nearest neighbors. Further, it was mentioned in the preceding section that the liquid–gas transformation can also be brought into the general scheme of Ising models. Other association problems, such as the ordering of hydrogen bonds, lead to similar mathematical calculations. Indeed, cooperative phenomena in quite different fields, such as traffic flow or melting of polymers, can be viewed against the same framework. Because of such varied applications, the Ising model has received considerable attention from theoreticians.[26]

It was mentioned in Section 4.6 that the exact solution of the three-dimensional Ising lattice has not been obtained so far. For two dimensions, Onsager showed in 1944 that the specific heat exhibits a logarithmic approach to infinity both above and below $T_c$. In three dimensions, approximate calculations show that the specific heat has the form

$$c \sim A \ln (T_c - T) + \ldots \qquad T < T_c$$
$$\sim B (T - T_c)^{-\alpha} + \ldots \qquad T > T_c, \alpha \sim \tfrac{1}{5}$$

although the behavior on the high-temperature side is not quite settled. The mathematical details of even these calculations are too specialized to be proper here.

The experimental evidence for a variety of transitions is consistent with the predicted variation in the lower temperature $(T < T_c)$ region. For $T > T_c$, the data can be fitted well by a power law in some cases and by a logarithmic term in some others. This remains a challenging unsolved problem.

Although the Ising lattice gives a workable model of configurational ordering, the complexity of the mathematical calculations has led to several further approximate models. The Weiss model of ferromagnetism and the Bragg–Williams model of order–disorder transitions and its extensions are some of the well-known simplifications of the Ising problem. All these calculations are still not quantitatively applicable to real physical systems, because of the restriction to nearest-neighbor interactions. Any consideration of more realistic interatomic forces appears to be too formidable a problem to be attempted at present.

So far, most $\lambda$-type specific-heat singularities have been ascribed to configurational ordering. The possibility exists, however, that the singularities may arise from the vibrational modes of the lattice. If some optical branch of the vibration spectrum approaches zero frequency, a $\lambda$-type of specific-heat singularity can result.[27] As mentioned in Section 7.5, if the frequency of an optical mode vanishes in an ionic crystal, it can give rise to ferroelectric polarization.

# REFERENCES

1. D. H. Parkinson, *Rept. Progr. Phys.* **21**, 226 (1958).
2. L. A. K. Staveley, K. R. Hart, and W. I. Tupman, *Dis. Faraday Soc.* **15**, 130 (1953). G. N. Lewis, M. Randall, K. S. Pitzer, and L. Brewer, *Thermodynamics*, McGraw Hill, New York, 1961, chapter 25.
3. J. F. Cochran, *Ann. Phys. (N.Y.)* **19**, 186 (1962).
4. H. Lipson, *Progr. Metal Phys.* **2**, 1 (1950). T. Muto and Y. Takagi, *Solid State Phys.* **1**, 193 (1955). L. Guttman, *Solid State Phys.* **3**, 145 (1956). E. W. Elcock, *Order–Disorder Phenomena*, Methuen, London, 1956.
5. H. Moser, *Phys. Z.* **37**, 737 (1936). C. Sykes and H. Wilkinson, *J. Inst. Metals* **61**, 223 (1937). C. W. Garland, *Phys. Rev.* **135**, A1696 (1964).
6. K. Clusius, *Z. phys. Chem.* **B3**, 41 (1929). K. Clusius and A. Perlick, *Z. phys. Chem.* **B24**, 313 (1934). J. H. Colwell, E. K. Gill, and J. A. Morrison, *J. Chem. Phys.* **36**, 2223 (1962).
7. H. N. V. Temperley, *Changes of State*, Cleaver-Hume, London, 1956.
8. E. T. Jaynes, *Ferroelectricity*, Princeton University Press, Princeton, 1953. A. F. Devonshire, *Advan. Phys.* **3**, 85 (1954). P. W. Forsberg, *Handbuch der Physik*, *XVII*, 264 (1956). W. Kanzig, *Solid State Phys.* **4**, 1 (1957). H. D. Megaw, *Ferroelectricity in Crystals*, Methuen, London, 1957. F. Jona and G. Shirane, *Ferroelectric Crystals*, Pergamon, Oxford, 1962. W. J. Merz, *Progr. Dielectrics* **4**, 101 (1962). A. F. Devonshire, *Rept. Progr. Phys.* **27**, 1 (1964).
9. J. Mendelssohn and K. Mendelssohn, *Nature* **144**, 595 (1939). C. C. Stephenson and J. G. Hooley, *J. Am. Chem. Soc.* **66**, 1397 (1944).
10. A. von Arx and W. Bantle, *Helv. phys. acta* **16**, 211 (1943).
10a. B. A. Strukov, *Soviet Phys. Solid State* **6**, 2278 (1965). J. Grindlay, *Phys. Letters* **18**, 239 (1965).
11. W. Cochran, *Advan. Phys.* **9**, 387 (1960); **10**, 401 (1961).
12. F. H. Spedding, S. Levigold, A. H. Daane, and L. D. Jennings, *Progr. Low Temp. Phys.* **2**, 368 (1957).
13. K. P. Belov, R. Z. Levitin, and S. A. Nikitin, *Soviet Phys. Uspekhi* **7**, 179 (1964). K. Yosida, *Progr. Low Temp. Phys.* **4**, 265 (1964). W. C. Koehler, *J. Appl. Phys.* **36**, 1078 (1965).

14. D. H. Parkinson, F. E. Simon, and F. H. Spedding, *Proc. Roy. Soc. (London)*, *Ser. A* **207**, 137 (1951). D. H. Parkinson and L. M. Roberts, *Proc. Phys. Soc. (London)*, *Ser. B* **70**, 471 (1957). O. V. Lounasmaa, *Phys. Rev.* **133**, A502 (1964).

15. C. J. McHargue and H. L. Yakel, *Acta Met.* **8**, 637 (1960). M. K. Wilkinson, H. R. Child, C. J. McHargue, W. C. Koehler, and E. O. Wollan, *Phys. Rev.* **122**, 1409 (1961). K. A. Gschneidner, R. O. Elliot, and R. R. McDonald, *J. Phys. Chem. Solids* **23**, 555 (1962).

16. C. S. Barrett and M. Cohen, in: *Phase Transformations in Solids* (R. Smoluchowski, J. E. Mayer, and W. A. Weyl, editors), Wiley, New York, 1951, chapters 13 and 17. M. A. Jaswon, *Research* **11**, 315 (1958).

17. R. M. Moon, J. W. Cable, and W. C. Koehler, *J. Appl. Phys.* **35**, 1041 (1964). J. W. Cable, R. M. Moon, W. C. Koehler, and E. O. Wollan, *Phys. Rev. Letters* **12**, 553 (1964).

18. M. Griffel, R. E. Skochdopole, and F. H. Spedding, *Phys. Rev.* **93**, 657 (1954); *J. Chem. Phys.* **23**, 2258 (1955); **25**, 75 (1956).

19. M. Fixman, *J. Chem. Phys.* **36**, 1957 (1962).

20. M. I. Bagatskii, A. V. Voronel', and V. G. Gusak, *Soviet Phys. JETP* **16**, 517 (1963). A. V. Voronel', Ya. R. Chashkin, V. A. Popov, and V. G. Simkin, *Soviet Phys. JETP* **18**, 568 (1964). W. A. Little and M. Moldover, *Proceedings of the Ninth International Conference on Low Temperature Physics* (Columbus, Ohio, 1964), Plenum Press, New York, 1965, p. 653.

21. M. E. Fisher, *Phys. Rev.* **136**, A1599 (1964).

22. M. Ya. Azbel', A. V. Voronel', and M. Sh. Giterman, *Soviet Phys. JETP* **19**, 457 (1964). C. N. Yang and C. P. Yang, *Phys. Rev. Letters* **13**, 303 (1964). R. B. Griffiths, *Phys. Rev. Letters* **14**, 623 (1965).

23. C. E. Chase, R. C. Williamson, and L. Tisza, *Phys. Rev. Letters* **13**, 467 (1964).

24. O. K. Rice, *J. Chem. Phys.* **22**, 1535 (1954). C. Domb, *J. Chem. Phys.* **25**, 783 (1956).

25. T. L. Hill, *Statistical Mechanics*, McGraw-Hill, New York, 1956, chapters 5 and 7.

26. G. F. Newell and E. W. Montroll, *Rev. Mod. Phys.* **25**, 353 (1953). H. S. Green and C. A. Hurst, *Order–Disorder Phenomena*, Interscience, New York, 1964.

27. H. B. Rosenstock, *J. Chem. Phys.* **35**, 420 (1961).

*Chapter 8*

# Miscellaneous Problems in Specific Heats

### 8.1. SPECIFIC HEAT NEAR PHASE TRANSITIONS

In the previous chapters, various aspects of specific heats of solids, liquids, and gases have been discussed. It is a common experience to find that two phases can coexist over a range of pressure and temperature. Consider, for instance, water and its vapor contained in a vessel of volume $V$. If the temperature is raised slightly, a small quantity of water is converted into steam, absorbing latent heat in the process, and a new equilibrium pressure is established. In a $P$–$T$ plane (Fig. 8.1), this will be represented as an equilibrium curve. Quantities such as the density, specific heat, and compressibility remain finite but different in the two phases. An interesting relation among the thermodynamic quantities at such an equilibrium curve is furnished by the Clausius–Clapeyron equation. To derive this, apply Maxwell's relation $(\partial P/\partial T)_v = (\partial S/\partial V)_T$ [equation (1.11)] to the
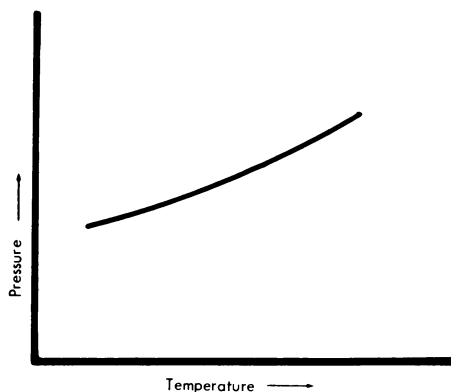


Fig. 8.1. Coexistence of two phases.

181

system. The latent heat $L_{12}$ is equal to $T\,dS$ at the phase boundary, and so

$$\frac{DP}{DT} = \frac{S_2 - S_1}{V_2 - V_1} = \frac{L_{12}}{T(V_2 - V_1)} \tag{8.1}$$

where $D/DT$ stands for the derivative along the equilibrium curve. This simple equation, in which all the quantities can be determined experimentally, forms a rigorous practical test of the first and second laws of thermodynamics. Nowadays, it is often used to calculate or check the latent heat when the vapor pressure of the liquid is known.

It turns out that this type of equilibrium among the phases is only one of the many possible types of phase changes.[1] The super-conducting phase transition at zero field (Section 3.9) shows no latent heat or volume change. Then the right-hand side of equation (8.1), being of the form 0/0, is indeterminate, whereas the left-hand side is found to have a definite value in practice. The Weiss model of ferro-magnetism (Section 4.5) and the Bragg–Williams model of order–disorder transition (Section 7.3) show a similar behavior. There are other phase changes where the specific heats become infinite. Magnetic transitions (Section 4.7) and the $\lambda$-transition in liquid $^4$He (Section 5.5) show logarithmic infinities in specific heats. It is obvious that the above simple considerations of phase equilibria must be generalized to include these possibilities.

It is convenient to start from the general thermodynamic condition for phase equilibrium, namely, the equality of the Gibbs' function of the two phases:

$$G_1 = G_2 \tag{8.2}$$

Further, $(\partial G/\partial T)_p = -S$ and $(\partial G/\partial P)_T = V$ [equation (1.10)]. In the ordinary phase change considered above, there are changes in $V$ and $S$, that is, in the first derivatives of $G$. Ehrenfest suggested that such changes should be called *transitions of the first order*. The condition for equilibrium along the equilibrium line (Fig. 8.1) is

$$\left(\frac{\partial G_1}{\partial P}\right)_T \delta P + \left(\frac{\partial G_1}{\partial T}\right)_P \delta T = \left(\frac{\partial G_2}{\partial P}\right)_T \delta P + \left(\frac{\partial G_2}{\partial T}\right)_P \delta T$$

or, rearranging,

$$\frac{DP}{DT} = \frac{S_2 - S_1}{V_2 - V_1}$$

which is the Clausius–Clapeyron equation. In the superconducting transition, there is no volume or entropy change, but the specific heat and compressibility are different; that is to say, the first derivatives

of $G$ are continuous but the second derivatives are not. Therefore, they are called *phase changes of the second order*. For such changes, consider the equilibrium along segments of $S$ and $V$ curves:

$$\left(\frac{\partial S_1}{\partial P}\right)_T \delta P + \left(\frac{\partial S_1}{\partial T}\right)_P \delta T = \left(\frac{\partial S_2}{\partial P}\right)_T \delta P + \left(\frac{\partial S_2}{\partial T}\right)_P \delta T$$

$$\left(\frac{\partial V_1}{\partial P}\right)_T \delta P + \left(\frac{\partial V_1}{\partial T}\right)_P \delta T = \left(\frac{\partial V_2}{\partial P}\right)_T \delta P + \left(\frac{\partial V_2}{\partial T}\right)_P \delta T$$

so

$$\frac{DP}{DT} = \frac{1}{TV}\frac{C_{p2} - C_{p1}}{\beta_2 - \beta_1} = \frac{\beta_2 - \beta_1}{k_{T2} - k_{T1}} \tag{8.3}$$

where $\beta$ is the volume expansion coefficient and $k_T$ is the isothermal compressibility. Equations (8.3) are called *Ehrenfest relations* for second-order phase changes and can also be obtained by applying L'Hospital's rule to equation (8.1) under these conditions. The superconducting phase change at zero field is a practical example of a second-order phase change. The available evidence (Section 3.9) is in reasonable agreement with the Ehrenfest relations. Theoretically, still higher order phase changes can exist, but so far no such cases have been experimentally observed.

In some situations, quantities such as the specific heat and volume expansion become infinite, when equation (8.3) reduces to an indeterminancy of the form $\infty/\infty$. A simple way of handling these $\lambda$-transitions was suggested by Pippard in 1956. Since $C_p$ becomes very large near $T_\lambda$, the entropy–temperature curve must have an almost vertical tangent at $T_\lambda$. On the other hand, $S_\lambda$ will be a smooth function of $P$, so that we may take $S$ as a function of $T$ and $P$ to be cylindrical in shape near $T_\lambda$. Thus,

$$S(P,T) = S_\lambda + f(P - \alpha T)$$

where $\alpha$ is the pressure coefficient of the $\lambda$-point $(DP/DT)_\lambda$ and $f$ is some function describing how the curve approaches the $\lambda$-point. Then

$$\left(\frac{\partial^2 S}{\partial P^2}\right)_T = f'' \qquad \left(\frac{\partial^2 S}{\partial T \partial P}\right) = -\alpha f'' \qquad \left(\frac{\partial^2 S}{\partial T^2}\right)_p = \alpha^2 f''$$

so that

$$\alpha = \frac{DP}{DT} = -\frac{(\partial^2 S/\partial T^2)_p}{\partial^2 S/\partial T \partial P} = -\frac{\partial^2 S/\partial T \partial P}{(\partial^2 S/\partial P^2)_T}$$

Making use of the Maxwell's relation [equation (1.11)],

$$\frac{\partial}{\partial T}\left(\frac{\partial S}{\partial T}\right)_p = \alpha\frac{\partial}{\partial T}\left(\frac{\partial V}{\partial T}\right)_p$$

and

$$\frac{\partial}{\partial P}\left(\frac{\partial S}{\partial T}\right)_p = \alpha\,\frac{\partial}{\partial P}\left(\frac{\partial V}{\partial T}\right)_p$$

Physically, these equations mean that in the vicinity of the $\lambda$-line $(\partial S/\partial T)_p$ is a linear function of $(\partial V/\partial T)_p$, and so

$$C_p = \left(\frac{DP}{DT}\right)_\lambda TV\beta + \text{constant} \tag{8.4a}$$

If $V(P,T)$ is treated in the same manner as $S(P,T)$, $(\partial V/\partial T)_p$ is seen to be a linear function of $(\partial V/\partial p)_T$ near the $\lambda$-point, and so

$$\beta = \left(\frac{DP}{DT}\right)_\lambda k_T + \text{constant} \tag{8.4b}$$

The relations (8.4) are called *Pippard's relations* for the $\lambda$-transition, and the cylindrical approximation should hold good very near the transition temperature. For several $\lambda$-type phase changes, the relations are found to be obeyed reasonably well. Figure 8.2 shows
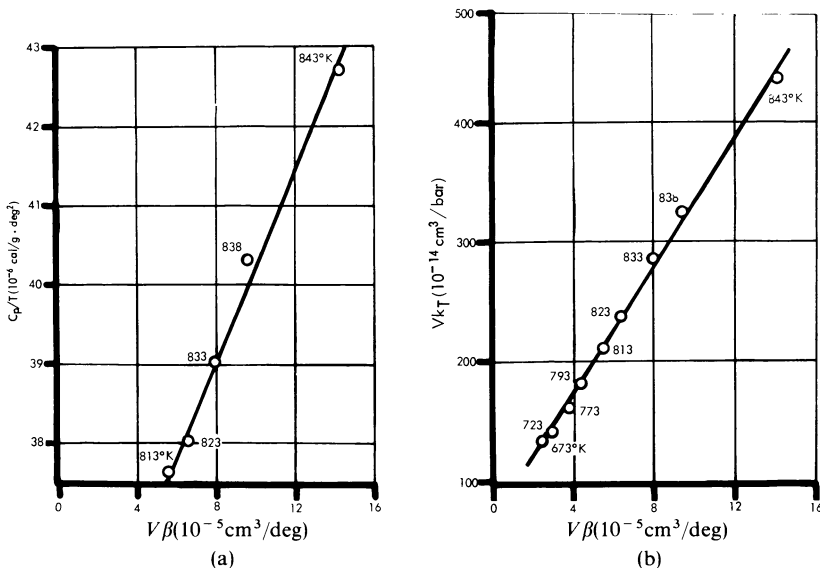


Fig. 8.2. Pippard's relations near $\alpha \rightleftharpoons \beta$ transition of quartz[2] at 574°C: (a) $c_p/T$ versus $V\beta$ [equation (8.4a)], (b) $V\beta$ versus $Vk_T$ [equation (8.4b)].

how closely ordinary $\alpha$-quartz follows equations (8.4) slightly below its transition temperature ($\sim$ 574°C) to the $\beta$-form.[2] More detailed studies on liquid $^4$He (Section 5.5) and ammonium chloride[3] show that equations (8.4) are obeyed quite well, but that its range of validity is much smaller above the transition than at lower temperatures.

In solids, other general relations are possible,[4] but so far they have found little use. Simple discussions of the various models of phase transitions and their application to physical systems are available elsewhere,[1,5] rendering a further analysis unnecessary here.

## 8.2. SPECIFIC HEAT AT SATURATED VAPOR PRESSURE

The discussion of the specific-heat behavior at coexistent phases leads naturally to an important mode of calorimetry, namely, the measurement of specific heat at constant saturation. Consider again the example of a liquid in contact with its saturated vapor in a closed vessel. $C_p$ and $C_v$ may easily be defined for the pure phases, but not for the total system. The heat applied at constant pressure is utilized as latent heat for evaporating the liquid without any rise of temperature, and an indeterminate infinite value of $C_p$ will be calculated. Under such conditions, it is best to consider what happens if the heating is done with the assumption that the pressure on the liquid is not constant but equal to the saturated vapor pressure corresponding to the temperature of the liquid. Using once again the notation $D/DT$ for heating along the liquid–vapor equilibrium curve, as in Fig. 8.1,

$$C_{\text{sat}} = T\frac{DS}{DT} \qquad (8.5)$$

The relation between $C_{\text{sat}}$ and $C_p$ of a liquid or vapor is easily found. For any quantity $x$, the variations at constant $P$ and along the $P$–$T$ equilibrium curve are connected by

$$\frac{Dx}{DT} = \left(\frac{\partial x}{\partial T}\right)_p + \left(\frac{\partial x}{\partial P}\right)_T \frac{DP}{DT}$$

Using Maxwell's relation $(\partial S/\partial P)_T = -(\partial V/\partial T)_p$ [equation (1.11)], it follows that

$$\frac{DS}{DT} = \left(\frac{\partial S}{\partial T}\right)_p - \left(\frac{\partial V}{\partial T}\right)_p \frac{DP}{DT}$$

Hence

$$C_{\text{sat}} = C_p - TV\beta\frac{DP}{DT} \qquad (8.6)$$

which was the relation mentioned in Section 5.2. For a solid in contact with its vapor, $C_{sat}$, defined as for a liquid, may be taken equal to $C_p$ for most practical purposes because the expansion coefficient and vapor pressure are both very small. In a liquid, $(C_p - C_{sat})/C_p$ is nearly zero at low temperatures and becomes about 10 to 20% near the boiling point. For a vapor, the situation is very different, because the volume expansion $\beta$ is 10 to 100 times larger than that of the liquid. In fact, $C_{sat}$ becomes negative at temperatures near the boiling point. Thus, superheated steam gets hotter if expanded adiabatically, a fact which is of importance in practical engineering applications.

If $C_{s1}$ denotes the specific heat of the liquid at constant saturation and $C_{s2}$ that of the vapor,

$$\frac{DL_{12}}{DT} = \frac{D}{DT}[T(S_2 - S_1)] = S_2 - S_1 + T\left(\frac{DS_2}{DT} - \frac{DS_1}{DT}\right)$$

$$= \frac{L_{12}}{T} + C_{s2} - C_{s1}$$

or

$$C_{s2} - C_{s1} = \frac{DL_{12}}{DT} - \frac{L_{12}}{T} \tag{8.7}$$

Equations (8.6) and (8.7) are of use in evaluating the specific heats if the liquid and its vapor are placed in a closed vessel to which heat is applied. Under these conditions, which are quite common in the calorimetry of liquids, the heat is used not only in heating the liquid and vapor but also in supplying latent heat. A full discussion of the procedures to be adopted under such conditions is given by Rowlinson.[6]

## 8.3. RELAXATION OF ROTATIONAL AND VIBRATIONAL SPECIFIC HEATS

It was mentioned in Section 4.8 that in paramagnetic salts the magnetic susceptibility shows dispersion as a function of the frequency of measurements. This paramagnetic relaxation arises basically because the magnetic dipoles require a finite time, of the order of $10^{-6}$ to $10^{-3}$ sec at room temperature, to attain thermal equilibrium with the lattice. So the susceptibility changes gradually from its isothermal low-frequency value to the adiabatic high-frequency value when the period of the applied AC signal scans the region of the relaxation time. A very similar phenomenon occurs if the ratio of the specific heats $\gamma = C_p/C_v$ is determined from the velocity of sound,

$c = (\gamma P/\rho)^{1/2}$. From its normal value at low frequencies, it increases to a limiting high-frequency value as the frequency of the sound wave becomes greater than the reciprocal of some relaxation time. For example, in hydrogen at STP, the velocity of sound increases by about 9% as the frequency becomes approximately 100 Mcps, which is just what is expected if $C_p/C_v$ increases from 1.40 to 1.67. The obvious interpretation of this acoustic relaxation would be that the rotational degrees of freedom require a finite time, of the order of $10^{-7}$ sec at STP, to come to equilibrium with the translatory motion.

Since the original observations on carbon dioxide in 1925 by Pierce, acoustical relaxation has been observed in numerous gases, liquids, solutions, and gas mixtures at frequencies from 10 to $10^9$ cps. However, the velocity does not always increase with the relaxation of all the rotational degrees of freedom as in the simple case considered above. Rotations about different axes may have different relaxation times $\tau$. Further, each vibrational mode has its characteristic $\tau$, and it is found that structural relaxation is possible in liquids, because the disturbances of the atomic structure caused by a sound wave take a finite time to attain the new values. Therefore, the interest in the field has been not so much concerned with the study of specific heats as with the molecular processes in liquids and gases. The rather extensive literature on the subject is adequately summarized in several places.[7]

## 8.4. DEFECTS IN SOLIDS

The solidified inert gases are often regarded as particularly simple solids. The interatomic forces are known reasonably well; therefore, a calculation of the heat capacity of the lattice, as in Chapter 2, should completely explain their specific heats. It turns out that this is not quite the case. The specific heat of solid argon,[8] shown in Fig. 8.3a, reveals a peculiar feature. As the melting point is approached, the specific heat rises very much above the Dulong–Petit value of about 6.5 cal/mole·deg. Solid krypton,[8] solid $^3$He,[9] and in fact a variety of solids[10] show a similar marked upward trend in specific heat below the melting point.

Such an increase above the classical value may arise from three causes: anharmonicity, the phenomenon of premelting, or generation of defects in the solid state. Detailed calculations show that in most cases anharmonic effects give an increase of $C_p$ no more than about a tenth of the observed excess. Premelting of solids[11] is a term applied to the phenomenon of abnormally large values of heat capacity and other properties sometimes observed very close to the melting point $T_M$. In these cases, the liquids also exhibit abnormally large values of
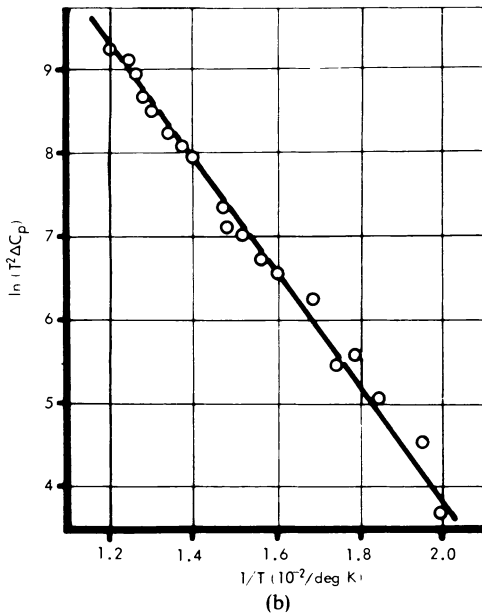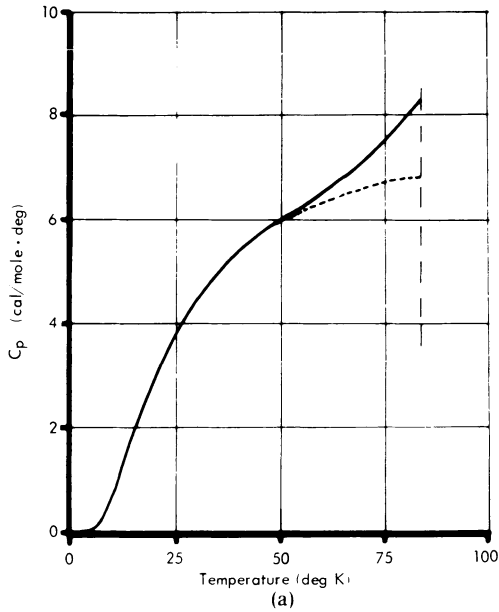
Fig. 8.3. (a) Heat capacity of solid argon (full line). Broken line is the value expected from the behavior below 40°K. (b) Plot of $\ln(T^2 \Delta C_p)$ against $1/T$.[8]

the various parameters as the freezing point is approached, the phenomenon of aftermelting in liquids.[10] They may arise from actual melting, at temperatures slightly different from the nominal $T_M$, in the regions of singularities such as dislocations and grain boundaries, where impurities have segregated. Then the latent heat associated with such regions may be measured as a pseudo specific heat. The subject appears to be somewhat controversial, because some authors[12] have carefully looked for these anomalies but did not find any. All the same, the magnitude and range of the excess specific heat in Fig. 8.3a rule out premelting as the cause of the observed behavior; there is now growing evidence that the explanation is to be sought in the thermal excitation of defects in the solid state.

Studies of diffusion, optical properties, and other phenomena in solids indicate that at temperatures above $T \approx \theta$, the perfect lattice arrangement is disturbed by various kinds of defects.[13] For example, an atom may have moved away from its lattice position, leaving a hole at its site, a vacancy defect, and an atom may occupy a nonlattice vacant space amid other atoms which are at their lattice positions, an interstitial atom. In a simple way, if $\varepsilon_d$ is the energy needed to form a defect, the number of defects $n_d$ at any temperature $T$ will be given by a Boltzmann factor

$$n_d = n_0 \exp\left(-\frac{\varepsilon_d}{kT}\right)$$

and the specific-heat contribution from such defects will be

$$\Delta C_v = \frac{d}{dT}(n_d \varepsilon_d) = \frac{n_0 \varepsilon_d^2}{kT^2} \exp\left(-\frac{\varepsilon_d}{kT}\right) \tag{8.8}$$

Thus, a plot of $\ln(T^2 \Delta C_v)$ against $1/T$ should be a straight line with a slope $-\varepsilon_d/k$. Similarly, a plot of $\ln(T^2 \Delta C_p)$ against $1/T$ will be a straight line with a slope $-h_d/k$, where $h_d$ is the enthalpy of formation of a defect. Figure 8.3b shows such a plot; the observations do fit the theoretical linear relationship with $h_d \sim 1250\,\text{cal/mole}$ in solid argon. The value is uncertain to about $\pm 5\%$, because $\Delta C_p$ depends slightly upon the method used to extrapolate the specific heat from below about 40°K in Fig. 8.3a. Similar $\Delta C_p = AT^{-2}\exp(-B/T)$ variations have been observed in solid $^3\text{He}$ and other substances.

Since the atomic forces and crystal structure of solidified inert gases are well known, several attempts have been made to calculate the values of $h_d$ from theoretical models; the values come out to be about 30% higher than the experimental results. The discrepancy arises from the fact that in the earlier models no relaxation of the stress field was assumed. On the other hand, it is more plausible that the atoms surrounding a vacancy defect move in slightly to

reduce the void, so that the volume of the vacancy is less than that of the atom which left that site. When this is taken into account,[14] there is better agreement with the experiments.

Similar specific-heat effects resulting from the presence of defects in the lattice structure are produced by heavy mechanical deformation,[15] neutron irradiation,[16] and self-irradiation in radioactive materials. In some cases, the specific heat is reduced, for example, by defects acting as traps for charge carriers in semiconductors and thereby reducing the number of "free" electrons or holes.

## 8.5. SURFACE EFFECTS

In the simple discussion of specific heats so far, it has been generally assumed that the internal energy, and hence the specific heat, is proportional to the mass of the substance; that is, they are extensive quantities (Section 1.2). As a matter of fact, statistical mechanics shows that this is a very good approximation (Section 2.5). Nevertheless, in special circumstances, as with finely divided powders, a contribution proportional to the surface area must be considered. It is qualitatively easy to visualize the nature of the effects, taking for simplicity the Debye model for an enumeration of the frequency distribution. In a finite solid, besides the longitudinal and transverse waves which propagate through the solid as if in an infinite medium, there are surface waves of the type considered by Rayleigh, Love, and others. The enumeration of the number of frequencies in a three-dimensional volume $V$, as in Section 2.5, gives the number of frequencies below $v$ as being proportional to $Vv^3$, while it is evident that a similar calculation for a two-dimensional surface of area $S$ will give a term proportional to $Sv^2$. Thus, the addition of surface contributions to the Debye term will result in

$$g(v)\, dv = \alpha_1 V v^2\, dv + \alpha_2 S v\, dv$$

The corresponding low-temperature specific heat will be

$$C_v = \beta_1 V T^3 + \beta_2 S T^2 \tag{8.9}$$

This behavior is indeed found in the specific heat of powdered materials. Figure 8.4 shows the specific heat, in the liquid-helium range, of MgO powder with an area of about $160\,M^2/g$, which corresponds to an edge length of about $100\,\text{Å}$ if all the particles are in the form of cubes.[17] The specific heat is represented well by an equation $C = 0.00459T^3 + 0.163T^2$ mJ/mole·deg, in which the $T^3$-term is the usual Debye term.
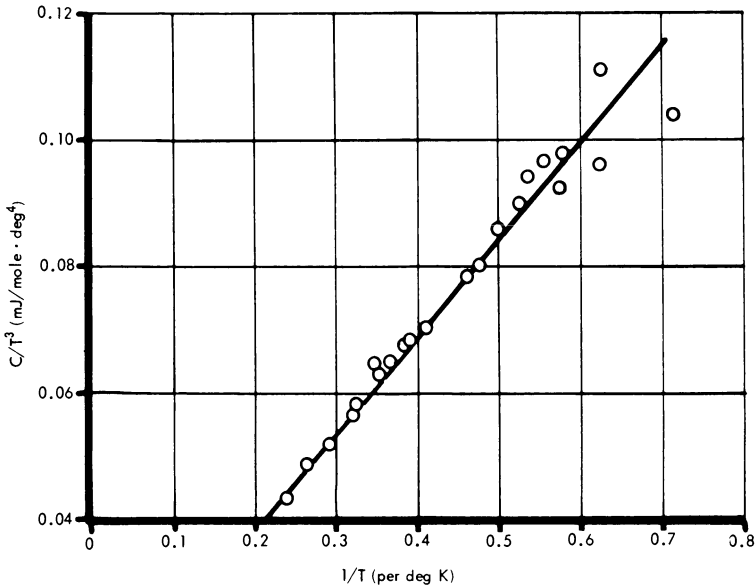
Fig. 8.4. Heat capacity of powdered magnesium oxide with grains of about 100 Å size.[17]

The full calculation of the surface contribution is a complex problem which as yet has not been solved satisfactorily. In the continuum model, it is possible to calculate with some difficulty the surface and volume modes of plates and rectangular parallelopipeds.[18] Apart from the usual shortcomings of a continuum model, there is a further assumption that the elastic behavior is not affected by the size of the specimen. On the other hand, it is obvious that the atoms near the surfaces are acted upon by forces very different from those exerted upon the atoms in the interior. Therefore, there is a spatial inhomogeneity of the lattice. The calculations with models of finite lattices are so involved that only beginnings have been made.[19] They show that, apart from the low-temperature effect given by equation (8.9), there should be very small differences at higher temperatures, because of the change in optical frequencies resulting from the presence of surface boundaries. The experimental observations are scanty, but it appears that the $ST^2$-term in equation (8.9) is two to three times larger than the theoretical estimates.[18] A full comparison between theory and experiment is not easy, because under the experimental conditions, in addition to the total surface area, the shape of the individual particles may also have some influence. Further, the possibility of thermal motions of whole grains of the

substance, behaving as though they were giant macromolecules, cannot be eliminated. The experiments also suffer from the fact that attaining thermal equilibrium in a fine powder is difficult. There is a real need for further experimental and theoretical studies.

## 8.6. COMPILATIONS OF SPECIFIC-HEAT DATA

A knowledge of specific heat is useful in so many fields of study that the literature on heat capacities is very extensive and is reported in diverse publications. Without the abstracting services of *Chemical Abstracts* and *Physics Abstracts*, the task of searching for the data on any particular material would be inordinately laborious. Apart from these sources, perhaps the best single reference, if the heat capacity of any substance is needed, is the sixth edition of *Landolt–Börnstein Zahlenwerte and Funktionen*, *Vol.* 2, *Part* 4 (Springer-Verlag, Berlin, 1961, 863 pages). This gives an exhaustive listing of the heat capacities of almost all materials investigated before 1958-1959. Special data of cryogenic interest are collected in the various publications of the National Bureau of Standards Cryogenic Engineering Laboratory, Boulder, Colorado. For example, *A Compendium of the Properties of Materials at Low Temperatures* (V. J. Johnson, editor, 1957) and *Specific Heats and Enthalpies of Technical Solids at Low Temperatures* (by R. J. Corruccini and J. J. Gniewek, 1960) contain useful information about the specific heat and other properties below 300°K. There are, of course, other reports by several groups of workers on various aspects of specific-heat studies, such as Debye temperatures or the properties of metals and gases; the references to them may be found without difficulty from the recent reviews cited at the end of the earlier chapters.

In the construction of calorimeters and other pieces of cryogenic equipment, various low-melting solders, glues, varnishes, and technical solids are often used. Their specific heats are needed for the design of such apparatus, especially because weight-for-weight they may contribute more thermal capacity than the standard construction materials such as copper, brass, and stainless steel. Unfortunately, the heat capacity depends upon the purity, method of preparation, and composition of these substances, so that for accurate work each sample must be individually investigated. For many other purposes, it is convenient to have some approximate values. Even so, no handy tabulation of the many measurements is available, and hence Table 8.I is given here as a summary of the properties of several such auxiliary materials used in cryogenic equipment.

The specific heats of several materials are quite high compared to those of, say, copper. In particular, if the heat capacity of some

## Table 8.I. Specific Heats $c_p$ (in mJ/g·deg K)

| T (deg K) | Cu | W.M. | So.So. | Aral. | Gly. | Bak. | G.E. | Pyr. |
|---|---|---|---|---|---|---|---|---|
| 2 | 0.03 | 0.06 | 0.06 | 0.24 | 0.4 | — | 0.31 | 0.025 |
| 5 | 0.16 | 1.39 | 1.17 | 4.6 | 4.8 | 5.3 | 6.1 | 0.38 |
| 10 | 0.86 | 13.4 | 11.7 | 27.2 | 22 | 19.2 | — | 4.2 |
| 20 | 7.7 | 46.0 | 47.5 | 81.1 | 110 | 66.7 | — | 27.4 |
| 50 | 99 | — | — | — | 380 | 237 | — | — |
| 100 | 254 | — | — | — | 1150 | — | — | — |
| 300 | 386 | — | — | — | — | — | — | — |

| T (deg K) | Sil. | Cons. | Man. | Mon. | St.St. | Tef. | Poly. | GR-S |
|---|---|---|---|---|---|---|---|---|
| 2 | 0.02 | 0.23 | 0.15 | 0.22 | 0.03 | 0.3 | — | — |
| 5 | 0.35 | 0.56 | 0.5 | 0.55 | 0.2 | 2.4 | 1.2 | 4.2 |
| 10 | 4.0 | 1.69 | — | 1.7 | 0.8 | 18 | 9.6 | 28 |
| 20 | 24.4 | 6.8 | — | 7.1 | 6 | 76 | 67.2 | 113 |
| 50 | 111 | 83 | — | — | 74 | 202 | 330 | 338 |
| 100 | 268 | 238 | — | 240 | 251 | 386 | 657 | 612 |
| 300 | 738 | — | — | 430 | 490 | 1010 | 2370 | 1900 |

W.M.  Wood's Metal (12.5 wt-% Sn, 12.5% Cd, 25% Pb, 50% Bi; m.p. 68°C). D. H. Parkinson and J. E. Quarrington, *Brit. J. Appl. Phys.* **5**, 219 (1954). Superconducting below ∼ 5°K.

So.So.  Soft solder (40 wt-% Pb, 60% Sn; m.p. ∼ 185°C). J. de Nobel and F. J. du Chatenier, *Physica* **29**, 1231 (1963). Superconducting below ∼7°K. Other compositions also investigated.

Aral.  Araldite Type I (baked according to instructions from manufacturers). D. H. Parkinson and J. E. Quarrington, *Brit. J. Appl. Phys.* **5**, 219 (1954).

Gly.  Glyptal varnish (air-dried at room temperature). N. Pearlman and P. H. Keesom, *Phys. Rev.* **88** 398 (1952). P. H. Keesom and G. Seidel, *Phys. Rev.* **113**, 33 (1959).

Bak.  Formite bakelite varnish V11105. R. W. Hill and P. L. Smith, *Phil. Mag.* **44**, 636 (1953).

G.E.  G.E. varnish 7031. N. E. Phillips, *Phys. Rev.* **114**, 676 (1959).

Pyr.  Pyrex glass. P. L. Smith and N. M. Wolcott, *Phil. Mag.* **1**, 854 (1956). Between 1.5 and 4.2°K, $c \approx 3.1 \times 10^{-3} T^3$ mJ/g·deg.

Sil.  Silica glass (vitreous silica or fused quartz). F. E. Simon and F. Lange, *Z. Physik* **38**, 227 (1926). E. F. Westrum, quoted in R. C. Lord and J. C. Morrow, *J. Chem. Phys.* **26**, 230 (1957). P. Flubacher, A. J. Leadbetter, J. A. Morrison, and B. Stoicheff, *J. Phys. Chem. Solids* **12**, 53 (1959).

Cons.  Constantan (60 wt-% Cu, 40% Ni). A. Eucken and H. Werth, *Z. anorg. allgem. Chem.* **188**, 152 (1930). W. H. Keesom and B. Kurrelmeyer, *Physica* **7**, 1003 (1940). J. C. Ho, H. R. O'Neal, and N. E. Phillips, *Rev. Sci. Instr.* **34**, 782 (1963), find a $T^{-2}$ increase of specific heat below 0.3°K.

Man.  Manganin (87% Cu, 13% Mn). J. C. Ho, H. R. O'Neal, and N. E. Phillips, *Rev. Sci. Instr.* **34**, 782 (1963). Between 0.25 and 1.5°K, $c \sim 0.0580T + 0.0112T^{-2}$ mJ/g·deg K.

Mon.   Monel (67 wt-% Ni, 30% Cu, 1.5% Fe, 1% Mn). W. F. Hampton and J. H.
       Mennie, *Can. J. Res.* 7, 677 (1932). W. H. Keesom and B. Kurrelmeyer,
       *Physica* 7, 1003 (1940).

St.St. Stainless steel. R. Kohlhass and M. Braun, *Arch. Eisenhüttenw.* 34, 391 (1963).
       F. J. du Chatenier, B. M. Boerstoel, and J. de Nobel, *Physica* 31, 1061 (1965).
       Below $\sim$ 300°K, values are nearly the same for $\gamma$-iron, manganese steel, and
       chrome–nickel steel.

Tef.   Teflon (polytetrafluoroethylene). Material has a transition around 160°K.
       G. T. Furukawa, R. E. McCoskey, and G. J. King, *J. Res. Nat. Bur. Std.* 49, 273
       (1952). Between 1.4 and 4.2°K, R. J. Noer, C. W. Dempsey, and J. E. Gordon,
       *Bull. Am. Phys. Soc.* 4, 108 (1959), give $c \sim 40 \times 10^{-3} T^3$ mJ/g·deg for teflon,
       $c \sim 63 \times 10^{-3} T^3$ for polystyrene, and $c \sim 35 \times 10^{-3} T^3$ for lucite. W. Reese
       and J. E. Tucker, *J. Chem. Phys.* 43, 105 (1965), give values for teflon, nylon, and
       Kel-F (1 to 4°K) also.

Poly.  Amorphous polyethylene. Glassy transition 200°K. B. Wunderlich, *J. Chem.
       Phys.* 37, 1203 (1962). (Material with various degrees of crystallinity also
       investigated.) I. V. Sochava and O. N. Trepeznikova, *Soviet Phys. Doklady* 2,
       164 (1957). (Data for polyvinyl alcohol also given.)

GR-S.  GR-S (Buna S) rubber (1,3-butadiene with 25 wt-% styrene). Second-order
       transition with hysteresis around 210°K. R. D. Rands, W. F. Ferguson, and
       J. L. Prather, *J. Res. Nat. Bur. Std.* 33, 63 (1944). Natural rubber studied by
       N. Bekkedahl and H. Matheson, *J. Res. Nat. Bur. Std.* 15, 505 (1934).

substance with low specific heat is to be measured, the thermal
capacity of a small amount of glue or solder used for attaching the
heater or thermometer may be comparable to that of the specimen
under study. Further, constantan and manganin, widely used for
winding heaters, are quite unsuitable below about 0.5°K because
of the $T^{-2}$ increase. At 0.1°K, for example, the specific heat of
manganin is nearly $10^3$ times that of copper.

## 8.7. TABULATIONS OF SPECIFIC-HEAT FUNCTIONS

The Einstein and Debye functions are widely used in calculating
the thermodynamic properties of gases and solids, as discussed in
detail elsewhere in this monograph. The Debye function for the
internal energy is also useful in cryogenic practice for calculating the
amount of refrigeration needed to cool an apparatus. For example,
let us calculate the amount of liquid $^4$He spent if its latent heat, equal
to 0.62 cal/cc, is used to cool 1 gram-atom of copper (1 gram-atom =
63.6 g of copper, Debye temperature of copper $\approx$ 310°K) from 300,
90, or 20°K to 4.2°K. Strictly, it is the change in enthalpy $\Delta H = \int C_p dT$
of copper which must be used for this purpose rather than an estimate
of the change in the internal energy $\Delta E = \int C_v dT$. However, $C_p - C_v$,
which depends upon the expansion coefficient and compressibility
and hence is not easily tabulated as a function of $T/\theta$, is usually small
enough to permit the calculation to be done using $\Delta E$ without any
serious error. Further, copper has no specific-heat anomaly in this

## Table 8.II

| $T$ | $\dfrac{\theta}{T}$ | $\dfrac{E(\text{Debye})}{3RT}$ | $E(\text{Debye})$ cal/mole |
|---|---|---|---|
| 300 | 1.03 | 0.666 | 1200 |
| 90 | 3.44 | 0.233 | 126 |
| 20 | 15.5 | 0.005 | 0.6 |
| 4.2 | 74 | 0.00004 | 0.001 |

region. So for various values of $\theta/T$, we look up the values of the Debye energy function $E(\text{Debye})/3RT$ in the *Appendix* and write out a table (Table 8.II), taking for simplicity $R \approx 2$ cal/mole·deg.

The change in internal energy between room temperature and liquid-helium temperature is about 1200 cal/mole. If the latent heat of liquid helium is used to bring about this reduction of temperature, about 2000 cc will be spent. A similar calculation shows that 200 cc is needed to cool 63.6 g of copper from 90 to 4.2°K, and only 1 cc from 20 to 4.2°K. The tremendous advantage of precooling any apparatus with liquid air and liquid hydrogen in order to conserve the supply of liquid helium was mentioned even in the *Introduction*.

Many tabulations of the Einstein and Debye functions were mentioned in Chapter 2. Some of these tables, especially the older ones, should be used with caution since the value of $R$ different from the present accepted 8.314 J/mole·deg = 1.987 cal/mole·deg has been used in them. The error caused by this is serious only at high temperatures, where the Debye specific heat approaches its limiting value of $3R$. A 1 % error in the specific heat at $T \sim \theta$ gives an error of nearly 10 % in the calculated value of $\theta$. One way to make the tables permanently useful is to give the values in a dimensionless form, that is, give $C_v/3R$ rather than $C_v$. Then, to find the specific heat at any given $T/\theta$, the entries must be multiplied by $3R$, but the tables themselves need not be changed every time an improvement in our knowledge of the value of $R$ takes place. This is the procedure followed in the tabulations of Overton and Hancock for the Einstein functions and those of Beattie for the Debye functions, which are at present the most accurate ones available. For rough calculations, a table to three figures is often sufficient, but for a variety of refined calculations it is necessary to have more accurate tables. Unfortunately, six-figure tables are not easily accessible. Beattie's six-figure tables were published in 1926, though they have been recently checked for accuracy, while the eight-figure tables of Overton and Hancock and the detailed tables of Hilsenrath and Ziegler are contained in laboratory reports rather than professional journals.

Therefore, six-figure tables of Einstein and Debye functions are given in a suitable form as an *Appendix* (with the permission of Professors Beattie and Overton).

# REFERENCES

1. H. N. V. Temperley, *Changes of States*, Cleaver-Hume, London, 1956. A. B. Pippard, *Elements of Classical Thermodynamics*, Cambridge University Press, Cambridge, 1957, chapters 8 and 9.
2. A. J. Hughes and A. W. Lawson, *J. Chem. Phys.* **36**, 2098 (1962).
3. C. W. Garland and J. S. Jones, *J. Chem. Phys.* **39**, 2874 (1963).
4. R. Viswanathan and E. S. R. Gopal, *Physica* **27**, 765, 981 (1961); **29**, 18 (1963). C. W. Garland, *J. Chem. Phys.* **41**, 1005 (1964). M. P. Mokhnatkin, *Soviet Phys.-Solid State* **5**, 1495 (1964).
5. D. Turnbull, *Solid State Phys.* **3**, 225 (1956).
6. J. S. Rowlinson, *Liquids and Liquid Mixtures*, Butterworth, London, 1959, p.40.
7. J. J. Markham, R. T. Beyer, and R. B. Lindsay, *Rev. Mod. Phys.* **23**, 353 (1951). R. O. Davies and J. Lamb, *Quart. Rev. Chem. Soc. (London)* **11**, 134 (1957). G. S. Verma, *Rev. Mod. Phys.* **31**, 1052 (1959). K. F. Herzfeld and T. A. Litovitz, *Absorption and Dispersion of Ultrasonic Waves*, Academic, New York, 1959.
8. P. Flubacher, A. J. Leadbetter, and J. A. Morrison, *Proc. Phys. Soc. (London)* **78**, 1449 (1961). R. H. Beaumont, H. Chihara, and J. A. Morrison, *Proc. Phys. Soc. (London)* **78**, 1462 (1961).
9. E. C. Heltemes and C. A. Swenson, *Phys. Rev. Letters*, **7**, 363 (1961); *Phys. Rev.* **128**, 1512 (62). D. O. Edwards, A. S. McWilliams, and J. G. Daunt, *Phys. Letters* **1**, 218 (1962). F. W. de Wette, *Phys. Rev.* **129**, 1160 (1963).
10. G. Borelius, *Solid State Phys.* **15**, 1 (1963).
11. A. R. Ubbelohde, *Quart. Rev. Chem. Soc.* (London) **4**, 356 (1950).
12. J. D. Hoffman and B. F. Decker, *J. Phys. Chem.* **57**, 520 (1953). R. E. Meyer and N. H. Nachtrieb, *J. Chem. Phys.* **23**, 405 (1955).
13. A. B. Lidiard, *Handbuch der Physik, XX (II)*, 246 (1957).
14. A. J. E. Foreman and A. B. Lidiard, *Phil. Mag.* **8**, 97 (1963). G. F. Nardelli and N. Terzi, *J. Phys. Chem. Solids* **25**, 815 (1964).
15. A. Eucken and H. Werth, *Z. anorg. allgem. Chem.* **188**, 152 (1930). C. G. Maier and C. T. Anderson, *J. Chem. Phys.* **2**, 513 (1934). D. L. Martin, *Can. J. Phys.* **38**, 17 (1960). F. A. Otter and D. E. Mapother, *Phys. Rev.* **125**, 1171 (1962).
16. P. H. Keesom, K. Lark-Horovitz, and N. Pearlman, *Science* **116**, 630 (1952). W. DeSorbo and W. W. Tyler, *J. Chem. Phys.* **26**, 244 (1957). B. B. Goodman, L. Montpetit, and L. Weil, *Compt. rend. acad, sci (Paris)* **248**, 956 (1959).
17. W. H. Lien and N. E. Phillips, *J. Chem. Phys.* **29**, 1415 (1958).
18. M. Dupuis, R. Mazo, and L. Onsager, *J. Chem. Phys.* **33**, 1452, (1960). R. Stratton, *J. Chem. Phys.* **37**, 2972 (1962).
19. A. A. Maradudin, E. W. Montroll, and G. H. Weiss, *Theory of Lattice Dynamics in the Harmonic Approximation*, Academic, New York, 1963, chapter 6.

# Appendix

The six-figure tables give the values of the internal energy $E$ and heat capacity at constant volume $C_v$ of solids in the Einstein and Debye models. The functions are tabulated in a dimensionless form as follows to make them permanently useful:

A. Einstein internal energy function [equation (2.9a)]:

$$\frac{E\,(\text{Einstein})}{3RT} = \frac{x}{e^x - 1} \qquad x = \frac{h\nu_E}{kT} = \frac{T_E}{T}$$

B. Einstein specific-heat function [equation 2.7)]:

$$\frac{C_v\,(\text{Einstein})}{3R} = \frac{x^2 e^x}{(e^x - 1)^2} \qquad x = \frac{T_E}{T}$$

C. Debye internal energy function [equation (2.16a)]:

$$\frac{E\,(\text{Debye})}{3RT} = \frac{3}{x^3}\int_0^x \frac{x^3\,dx}{e^x - 1} \qquad x = \frac{h\nu_D}{kT} = \frac{\theta}{T}$$

D. Debye specific-heat function [equation (2.17)]:

$$\frac{C_v\,(\text{Debye})}{3R} = \frac{3}{x^3}\int_0^x \frac{x^4 e^x\,dx}{(e^x - 1)^2} \qquad x = \frac{\theta}{T}$$

The presently accepted value of $R$ is 1.987 cal/mole · deg, or 8.314 J/mole·degK.

The functions A to D are tabulated at intervals of 0.01 over the useful range, namely, $T_E/T < 16$ in the Einstein functions and $\theta/T < 24$ in the Debye functions. Over most of the range, a linear interpolation gives an accuracy of nearly three to four units in the sixth significant figure. However, interpolation with second differences is recommended for accurate work. Following the usual procedure, a reduction by one unit of the fixed "characteristic" part is indicated by an underscoring

of the varying "mantissa" part. For example,

$$x = 1.61 \qquad \frac{E\,(\text{Einstein})}{3RT} = 0.4\,02217$$

$$= 1.62 \qquad\qquad = 0.3\,99695$$

$$= 3.48 \qquad\qquad = 0.11\,0618$$

$$= 3.49 \qquad\qquad = 0.10\,9797$$

Over wider ranges of $x$, the following approximations can be used with an error of about one unit in the sixth significant figure. At high temperatures,

$$\frac{E\,(\text{Einstein})}{3RT} \approx 1 - \frac{x}{2} + \frac{x^2}{12} - \frac{x^4}{720} \qquad x = \frac{T_E}{T} \gtrsim 0.1$$

$$\frac{C_v\,(\text{Einstein})}{3R} \approx 1 - \frac{x^2}{12} + \frac{x^4}{240}$$

$$\frac{E\,(\text{Debye})}{3RT} \approx 1 - \frac{3x}{8} + \frac{x^2}{20} - \frac{x^4}{1680} \qquad x = \theta/T \gtrsim 0.1$$

$$\frac{C_v\,(\text{Debye})}{3R} \approx 1 - \frac{x^2}{20} + \frac{x^4}{560}$$

while at low temperatures

$$\frac{E\,(\text{Einstein})}{3RT} \approx xe^{-x} \qquad x = \frac{T_E}{T} > 16$$

$$\frac{C_v\,(\text{Einstein})}{3R} \approx x^2 e^{-x}$$

$$\frac{E\,(\text{Debye})}{3RT} \approx \frac{19.481818}{x^3} \qquad x = \theta/T > 24$$

$$\frac{C_v\,(\text{Debye})}{3R} \approx \frac{77.92727}{x^3}$$

*A. Einstein Internal Energy Function*
      *E* (*Einstein*)/3*RT*

| x | 0 | 1 | 2 | 3 | 4 | 5 | 6 | 7 | 8 | 9 |
|---|---|---|---|---|---|---|---|---|---|---|
| 0.0 | 1.0 00000 | 95008 | 90033 | 85075 | 80133 | 75208 | 70300 | 65408 | 60533 | 55675 |
| 0.1 | .9 50833 | 46008 | 41200 | 36408 | 31633 | 26874 | 22132 | 17407 | 12699 | 08007 |
| 0.2 | 9 03331 | 98672 | 94030 | 89404 | 84795 | 80203 | 75627 | 71068 | 66525 | 61999 |
| 0.3 | 8 57489 | 52996 | 48519 | 44059 | 39615 | 35188 | 30777 | 26382 | 22004 | 17643 |
| 0.4 | .8 13298 | 08969 | 04657 | 00361 | 96082 | 91818 | 87571 | 83341 | 79127 | 74929 |
| 0.5 | 7 70747 | 66582 | 62432 | 58299 | 54183 | 50082 | 45998 | 41930 | 37877 | 33841 |
| 0.6 | 7 29822 | 25818 | 21830 | 17858 | 13903 | 09963 | 06039 | 02131 | 98240 | 94364 |
| 0.7 | .6 90504 | 86660 | 82831 | 79019 | 75222 | 71441 | 67676 | 63927 | 60193 | 56475 |
| 0.8 | 6 52773 | 49086 | 45415 | 41760 | 38120 | 34496 | 30887 | 27293 | 23715 | 20153 |
| 0.9 | 6 16606 | 13074 | 09558 | 06057 | 02571 | 99101 | 95646 | 92206 | 88781 | 85371 |
| 1.0 | 0.5 81977 | 78597 | 75233 | 71884 | 68549 | 65230 | 61926 | 58636 | 55361 | 52102 |
| 1.1 | 5 48857 | 45627 | 42411 | 39211 | 36025 | 32853 | 29697 | 26554 | 23427 | 20314 |
| 1.2 | 5 17215 | 14131 | 11062 | 08006 | 04965 | 01939 | 98927 | 95929 | 92945 | 89975 |
| 1.3 | 4 87020 | 84078 | 81151 | 78238 | 75339 | 72453 | 69582 | 66724 | 63881 | 61051 |
| 1.4 | .4 58235 | 55433 | 52644 | 49870 | 47108 | 44361 | 41627 | 38906 | 36199 | 33506 |
| 1.5 | 4 30825 | 28159 | 25505 | 22865 | 20238 | 17624 | 15024 | 12436 | 09862 | 07301 |
| 1.6 | 4 04753 | 02217 | 99695 | 97186 | 94689 | 92205 | 89734 | 87276 | 84831 | 82398 |
| 1.7 | .3 79978 | 77570 | 75175 | 72792 | 70422 | 68064 | 65719 | 63386 | 61065 | 58757 |
| 1.8 | 3 56461 | 54176 | 51904 | 49645 | 47397 | 45161 | 42937 | 40725 | 38525 | 36337 |
| 1.9 | 3 34160 | 31996 | 29843 | 27701 | 25572 | 23453 | 21347 | 19252 | 17168 | 15096 |
| 2.0 | 0.3 13035 | 10986 | 08948 | 06921 | 04905 | 02900 | 00907 | 98925 | 96953 | 94993 |
| 2.1 | .2 93044 | 91105 | 89178 | 87261 | 85355 | 83459 | 81575 | 79701 | 77838 | 75985 |
| 2.2 | 2 74143 | 72311 | 70490 | 68679 | 66879 | 65088 | 63308 | 61539 | 59779 | 58030 |
| 2.3 | 2 56291 | 54562 | 52842 | 51133 | 49434 | 47745 | 46065 | 44396 | 42736 | 41086 |
| 2.4 | .2 39445 | 37814 | 36193 | 34581 | 32979 | 31386 | 29803 | 28229 | 26665 | 25110 |
| 2.5 | 2 23564 | 22027 | 20500 | 18981 | 17472 | 15972 | 14480 | 12998 | 11525 | 10061 |
| 2.6 | 2 08605 | 07158 | 05721 | 04291 | 02871 | 01459 | 00056 | 98661 | 97275 | 95897 |
| 2.7 | .1 94528 | 93167 | 91815 | 90471 | 89135 | 87808 | 86488 | 85177 | 83874 | 82579 |
| 2.8 | 1 81293 | 80014 | 78743 | 77480 | 76225 | 74978 | 73738 | 72507 | 71283 | 70067 |
| 2.9 | 1 68858 | 67658 | 66464 | 65279 | 64101 | 62930 | 61767 | 60611 | 59462 | 58321 |
| 3.0 | 0.15 7187 | 6060 | 4941 | 3829 | 2724 | 1626 | 0535 | 9451 | 8374 | 7304 |
| 3.1 | .14 6241 | 5184 | 4135 | 3092 | 2057 | 1028 | 0005 | 8989 | 7980 | 6978 |
| 3.2 | 13 5982 | 4993 | 4010 | 3033 | 2063 | 1099 | 0142 | 9191 | 8246 | 7308 |
| 3.3 | 12 6376 | 5449 | 4530 | 3616 | 2708 | 1806 | 0910 | 0021 | 9137 | 8259 |
| 3.4 | .11 7387 | 6520 | 5660 | 4805 | 3957 | 3113 | 2276 | 1444 | 0618 | 9797 |
| 3.5 | 10 8982 | 8172 | 7368 | 6569 | 5776 | 4988 | 4206 | 3429 | 2657 | 1890 |
| 3.6 | 10 1129 | 0372 | 96214 | 88756 | 81348 | 73991 | 66685 | 59429 | 52223 | 45067 |
| 3.7 | .09 37960 | 30902 | 23893 | 16933 | 10020 | 03156 | 96339 | 89569 | 82847 | 76171 |
| 3.8 | 08 69542 | 62959 | 56421 | 49930 | 43484 | 37083 | 30727 | 24415 | 18147 | 11924 |
| 3.9 | 08 05744 | 99608 | 93515 | 87465 | 81458 | 75493 | 69570 | 63689 | 57849 | 52051 |

| x | 0 | 1 | 2 | 3 | 4 | 5 | 6 | 7 | 8 | 9 |
|---|---|---|---|---|---|---|---|---|---|---|
| 4.0 | 0.07 46294 | 40578 | 34903 | 29268 | 23673 | 18117 | 12602 | 07126 | 01688 | 96290 |
| 4.1 | .06 90930 | 85609 | 80326 | 75080 | 69872 | 64702 | 59569 | 54472 | 49413 | 44389 |
| 4.2 | 06 39402 | 34451 | 29536 | 24656 | 19812 | 15002 | 10228 | 05488 | 00782 | 96111 |
| 4.3 | 05 91473 | 86870 | 82299 | 77763 | 73259 | 68788 | 64349 | 59943 | 55569 | 51228 |
| 4.4 | .05 46918 | 42639 | 38392 | 34176 | 29991 | 25837 | 21714 | 17620 | 13557 | 09524 |
| 4.5 | 05 05521 | 01547 | 97602 | 93687 | 89801 | 85943 | 82114 | 78313 | 74541 | 70796 |
| 4.6 | 04 67079 | 63390 | 59729 | 56094 | 52487 | 48907 | 45353 | 41826 | 38325 | 34850 |
| 4.7 | .04 31402 | 27979 | 24582 | 21210 | 17863 | 14542 | 11246 | 07974 | 04727 | 01504 |
| 4.8 | 03 98306 | 95132 | 91981 | 88855 | 85752 | 82672 | 79616 | 76583 | 73572 | 70585 |
| 4.9 | 03 67620 | 64678 | 61758 | 58860 | 55984 | 53130 | 50298 | 47487 | 44698 | 41930 |
| 5.0 | 0.03 39183 | 36457 | 33752 | 31067 | 28403 | 25759 | 23136 | 20532 | 17949 | 15385 |
| 5.1 | .03 12841 | 10317 | 07812 | 05326 | 02859 | 00412 | 97983 | 95572 | 93181 | 90808 |
| 5.2 | 02 88453 | 86116 | 83797 | 81496 | 79213 | 76948 | 74700 | 72470 | 70257 | 68061 |
| 5.3 | 02 65882 | 63720 | 61574 | 59446 | 57334 | 55238 | 53159 | 51095 | 49048 | 47017 |
| 5.4 | .02 45002 | 43002 | 41018 | 39050 | 37097 | 35159 | 33236 | 31329 | 29436 | 27558 |
| 5.5 | 02 25695 | 23846 | 22012 | 20192 | 18387 | 16596 | 14819 | 13056 | 11306 | 09571 |
| 5.6 | 02 07849 | 06141 | 04446 | 02764 | 01096 | 99441 | 97799 | 96170 | 94554 | 92951 |
| 5.7 | .01 91360 | 89782 | 88217 | 86664 | 85123 | 83594 | 82078 | 80573 | 79081 | 77600 |
| 5.8 | 01 76131 | 74674 | 73229 | 71795 | 70372 | 68961 | 67561 | 66172 | 64794 | 63427 |
| 5.9 | 01 62071 | 60726 | 59392 | 58068 | 56755 | 55453 | 54160 | 52879 | 51607 | 50346 |
| 6.0 | 0.014 9095 | 7854 | 6622 | 5401 | 4190 | 2988 | 1796 | 0613 | 9440 | 8277 |
| 6.1 | .013 7122 | 5977 | 4842 | 3715 | 2598 | 1490 | 0390 | 9300 | 8218 | 7145 |
| 6.2 | 012 6081 | 5025 | 3978 | 2939 | 1909 | 0887 | 9873 | 8868 | 7870 | 6881 |
| 6.3 | 011 5900 | 4927 | 3962 | 3004 | 2054 | 1113 | 0178 | 9252 | 8332 | 7421 |
| 6.4 | .010 6517 | 5620 | 4730 | 3848 | 2973 | 2105 | 1244 | 0390 | 95436 | 87037 |
| 6.5 | 009 78707 | 70445 | 62250 | 54123 | 46062 | 38067 | 30138 | 22274 | 14474 | 06738 |
| 6.6 | 008 99066 | 91457 | 83910 | 76425 | 69002 | 61640 | 54338 | 47096 | 39914 | 32792 |
| 6.7 | .008 25727 | 18721 | 11773 | 04882 | 98048 | 91270 | 84548 | 77882 | 71271 | 64714 |
| 6.8 | 007 58212 | 51763 | 45367 | 39025 | 32735 | 26497 | 20311 | 14175 | 08091 | 02057 |
| 6.9 | 006 96073 | 90139 | 84254 | 78418 | 72630 | 66891 | 61199 | 55554 | 49956 | 44405 |
| 7.0 | 0.006 38900 | 33441 | 28027 | 22658 | 17334 | 12054 | 06818 | 01626 | 96477 | 91372 |
| 7.1 | .005 86308 | 81287 | 76308 | 71370 | 66474 | 61619 | 56804 | 52029 | 47294 | 42599 |
| 7.2 | 005 37943 | 33327 | 28748 | 24208 | 19707 | 15242 | 10816 | 06426 | 02073 | 97757 |
| 7.3 | 004 93477 | 89232 | 85024 | 80851 | 76712 | 72609 | 68540 | 64505 | 60505 | 56537 |
| 7.4 | .004 52604 | 48703 | 44835 | 41000 | 37197 | 33426 | 29687 | 25979 | 22303 | 18657 |
| 7.5 | 004 15043 | 11459 | 07905 | 04381 | 00887 | 97422 | 93987 | 90581 | 87203 | 83854 |
| 7.6 | 003 80534 | 77241 | 73976 | 70739 | 67530 | 64347 | 61192 | 58063 | 54961 | 51885 |
| 7.7 | .003 48835 | 45811 | 42813 | 39840 | 36892 | 33969 | 31071 | 28198 | 25349 | 22525 |
| 7.8 | 003 19724 | 16948 | 14194 | 11465 | 08758 | 06075 | 03414 | 00776 | 98160 | 95567 |
| 7.9 | 002 92996 | 90447 | 87919 | 85413 | 82929 | 80465 | 78023 | 75601 | 73201 | 70820 |

| x | 0 | 1 | 2 | 3 | 4 | 5 | 6 | 7 | 8 | 9 |
|---|---|---|---|---|---|---|---|---|---|---|
| 8.0 | 0.002 68460 | 66120 | 63800 | 61500 | 59220 | 56959 | 54717 | 52495 | 50292 | 48107 |
| 8.1 | .002 45941 | 43794 | 41665 | 39555 | 37462 | 35387 | 33330 | 31291 | 29269 | 27265 |
| 8.2 | 002 25278 | 23308 | 21354 | 19418 | 17498 | 15595 | 13708 | 11837 | 09982 | 08143 |
| 8.3 | 002 06320 | 04513 | 02721 | 00945 | 99184 | 97438 | 95707 | 93991 | 92290 | 90603 |
| 8.4 | .001 88931 | 87273 | 85630 | 84001 | 82386 | 80785 | 79197 | 77623 | 76063 | 74517 |
| 8.5 | 001 72983 | 71463 | 69956 | 68462 | 66981 | 65513 | 64058 | 62615 | 61184 | 59766 |
| 8.6 | 001 58360 | 56966 | 55585 | 54215 | 52857 | 51511 | 50177 | 48854 | 47543 | 46243 |
| 8.7 | .001 44954 | 43676 | 42410 | 41154 | 39909 | 38676 | 37452 | 36240 | 35038 | 33846 |
| 8.8 | 001 32665 | 31494 | 30333 | 29183 | 28042 | 26911 | 25790 | 24688 | 23577 | 22485 |
| 8.9 | 001 21403 | 20330 | 19266 | 18211 | 17166 | 16130 | 15103 | 14084 | 13075 | 12074 |
| 9.0 | 0.0011 1083 | 0099 | 9125 | 8158 | 7201 | 6251 | 5310 | 4377 | 3453 | 2536 |
| 9.1 | .0010 1627 | 0726 | 98336 | 89485 | 80711 | 72014 | 63393 | 54848 | 46377 | 37980 |
| 9.2 | 0009 29656 | 21406 | 13227 | 05120 | 97084 | 89118 | 81222 | 73395 | 65637 | 57946 |
| 9.3 | 0008 50323 | 42767 | 35277 | 27852 | 20492 | 13197 | 05966 | 98799 | 91694 | 84651 |
| 9.4 | .0007 77671 | 70751 | 63892 | 57094 | 50355 | 43675 | 37054 | 30491 | 23985 | 17537 |
| 9.5 | 0007 11146 | 04810 | 98530 | 92306 | 86136 | 80020 | 73959 | 67950 | 61995 | 56091 |
| 9.6 | 0006 50240 | 44440 | 38691 | 32993 | 27345 | 21747 | 16198 | 10698 | 05246 | 99842 |
| 9.7 | .0005 94486 | 89178 | 83915 | 78700 | 73530 | 68406 | 63327 | 58293 | 53303 | 48358 |
| 9.8 | 0005 43456 | 38597 | 33781 | 29008 | 24277 | 19587 | 14939 | 10332 | 05766 | 01240 |
| 9.9 | 0004 96754 | 92308 | 87901 | 83533 | 79204 | 74913 | 70659 | 66444 | 62266 | 58125 |
| 10.0 | 0.0004 54020 | 49952 | 45919 | 41923 | 37962 | 34036 | 30144 | 26287 | 22465 | 18676 |
| 10.1 | .0004 14921 | 11199 | 07510 | 03853 | 00229 | 96638 | 93078 | 89550 | 86053 | 82587 |
| 10.2 | 0003 79151 | 75747 | 72372 | 69028 | 65713 | 62427 | 59171 | 55944 | 52745 | 49575 |
| 10.3 | 0003 46433 | 43318 | 40232 | 37173 | 34141 | 31136 | 28158 | 25206 | 22281 | 19381 |
| 10.4 | .0003 16507 | 13659 | 10837 | 08039 | 05266 | 02518 | 99795 | 97095 | 94420 | 91769 |
| 10.5 | 0002 89141 | 86536 | 83955 | 81397 | 78861 | 76348 | 73858 | 71390 | 68944 | 66519 |
| 10.6 | 0002 64116 | 61735 | 59375 | 57036 | 54717 | 52420 | 50143 | 47886 | 45650 | 43433 |
| 10.7 | .0002 41236 | 39059 | 36901 | 34763 | 32644 | 30543 | 28461 | 26398 | 24354 | 22327 |
| 10.8 | 0002 20319 | 18329 | 16356 | 14402 | 12464 | 10544 | 08641 | 06755 | 04886 | 03034 |
| 10.9 | 0002 01198 | 99379 | 97576 | 95789 | 94019 | 92264 | 90524 | 88801 | 87092 | 85400 |
| 11.0 | 0.0001 83722 | 82059 | 80411 | 78778 | 77160 | 75556 | 73966 | 72391 | 70830 | 69283 |
| 11.1 | .00016 7749 | 6230 | 4724 | 3231 | 1752 | 0287 | 8834 | 7395 | 5968 | 4554 |
| 11.2 | 00015 3153 | 1765 | 0388 | 9025 | 7673 | 6334 | 5007 | 3691 | 2388 | 1096 |
| 11.3 | 00013 9816 | 8547 | 7290 | 6044 | 4809 | 3585 | 2373 | 1171 | 9980 | 8800 |
| 11.4 | .00012 7630 | 6471 | 5322 | 4184 | 3056 | 1938 | 0830 | 9732 | 8644 | 7566 |
| 11.5 | 00011 6497 | 5438 | 4389 | 3349 | 2319 | 1297 | 0285 | 9282 | 8289 | 7304 |
| 11.6 | 00010 6328 | 5360 | 4402 | 3452 | 2511 | 1578 | 0653 | 97374 | 88296 | 79300 |
| 11.7 | .00009 70385 | 61550 | 52796 | 44120 | 35523 | 27003 | 18560 | 10194 | 01903 | 93686 |
| 11.8 | 00008 85544 | 77476 | 69481 | 61557 | 53706 | 45925 | 38215 | 30574 | 23002 | 15499 |
| 11.9 | 00008 08064 | 00696 | 93394 | 86159 | 78989 | 71883 | 64842 | 57865 | 50951 | 44100 |

| x | | 0 | 1 | 2 | 3 | 4 | 5 | 6 | 7 | 8 | 9 |
|---|---|---|---|---|---|---|---|---|---|---|---|
| 12.0 | 0.00007 | 37310 | 30582 | 23915 | 17308 | 10761 | 04273 | 97844 | 91473 | 85160 | 78904 |
| 12.1 | .00006 | 72705 | 66562 | 60474 | 54442 | 48464 | 42541 | 36671 | 30854 | 25090 | 19379 |
| 12.2 | 00006 | 13719 | 08110 | 02552 | 97045 | 91588 | 86180 | 80821 | 75511 | 70248 | 65034 |
| 12.3 | 00005 | 59867 | 54747 | 49673 | 44646 | 39664 | 34727 | 29835 | 24987 | 20184 | 15424 |
| 12.4 | .00005 | 10707 | 06033 | 01402 | 96812 | 92265 | 87758 | 83293 | 78868 | 74483 | 70139 |
| 12.5 | 00004 | 65833 | 61567 | 57340 | 53151 | 49000 | 44887 | 40811 | 36772 | 32770 | 28805 |
| 12.6 | 00004 | 24875 | 20982 | 17123 | 13300 | 09512 | 05758 | 02038 | 98352 | 94700 | 91080 |
| 12.7 | .00003 | 87494 | 83941 | 80419 | 76930 | 73473 | 70047 | 66652 | 63288 | 59955 | 56653 |
| 12.8 | 00003 | 53380 | 50137 | 46924 | 43740 | 40585 | 37458 | 34361 | 31291 | 28249 | 25236 |
| 12.9 | 00003 | 22249 | 19290 | 16358 | 13453 | 10574 | 07721 | 04894 | 02094 | 99318 | 96568 |
| 13.0 | 0.00002 | 93843 | 91143 | 88468 | 85817 | 83190 | 80588 | 78009 | 75453 | 72921 | 70412 |
| 13.1 | .00002 | 67926 | 65462 | 63021 | 60603 | 58206 | 55832 | 53479 | 51147 | 48837 | 46548 |
| 13.2 | 00002 | 44280 | 42032 | 39806 | 37599 | 35413 | 33246 | 31100 | 28973 | 26865 | 24777 |
| 13.3 | 00002 | 22708 | 20658 | 18626 | 16613 | 14619 | 12643 | 10685 | 08744 | 06822 | 04917 |
| 13.4 | .00002 | 03030 | 01159 | 99306 | 97470 | 95651 | 93848 | 92062 | 90292 | 88539 | 86801 |
| 13.5 | 00001 | 85080 | 83374 | 81684 | 80009 | 78350 | 76705 | 75076 | 73462 | 71863 | 70278 |
| 13.6 | 00001 | 68708 | 67152 | 65610 | 64083 | 62569 | 61070 | 59584 | 58112 | 56653 | 55207 |
| 13.7 | .00001 | 53775 | 52356 | 50950 | 49557 | 48177 | 46809 | 45454 | 44112 | 42781 | 41463 |
| 13.8 | 00001 | 40157 | 38863 | 37581 | 36311 | 35052 | 33805 | 32569 | 31345 | 30132 | 28930 |
| 13.9 | 00001 | 27739 | 26558 | 25389 | 24231 | 23083 | 21946 | 20819 | 19702 | 18596 | 17500 |
| 14.0 | 0.000011 | 6414 | 5338 | 4272 | 3216 | 2169 | 1132 | 0105 | 9087 | 8078 | 7078 |
| 14.1 | .000010 | 6088 | 5107 | 4135 | 3172 | 2218 | 1272 | 0335 | 94071 | 84874 | 75762 |
| 14.2 | 000009 | 66734 | 57789 | 48926 | 40145 | 31444 | 22824 | 14283 | 05820 | 97436 | 89128 |
| 14.3 | 000008 | 80897 | 72742 | 64662 | 56656 | 48724 | 40865 | 33079 | 25364 | 17720 | 10146 |
| 14.4 | .000008 | 02643 | 95208 | 87842 | 80544 | 73313 | 66148 | 59050 | 52017 | 45049 | 38145 |
| 14.5 | 000007 | 31304 | 24527 | 17812 | 11159 | 04568 | 98037 | 91566 | 85156 | 78804 | 72510 |
| 14.6 | 000006 | 66275 | 60097 | 53977 | 47912 | 41904 | 35951 | 30053 | 24209 | 18420 | 12683 |
| 14.7 | .000006 | 07000 | 01369 | 95790 | 90263 | 84786 | 79360 | 73984 | 68658 | 63381 | 58153 |
| 14.8 | 000005 | 52973 | 47840 | 42755 | 37717 | 32726 | 27781 | 22881 | 18027 | 13217 | 08452 |
| 14.9 | 000005 | 03731 | 99053 | 94419 | 89828 | 85279 | 80772 | 76306 | 71882 | 67499 | 63156 |
| 15.0 | 0.000004 | 58854 | 54591 | 50367 | 46183 | 42037 | 37930 | 33861 | 29829 | 25834 | 21877 |
| 15.1 | .000004 | 17956 | 14071 | 10222 | 06409 | 02631 | 98888 | 95180 | 91506 | 87866 | 84260 |
| 15.2 | 000003 | 80687 | 77147 | 73639 | 70165 | 66722 | 63311 | 59932 | 56584 | 53268 | 49981 |
| 15.3 | 000003 | 46726 | 43500 | 40304 | 37138 | 34001 | 30893 | 27814 | 24764 | 21742 | 18747 |
| 15.4 | .000003 | 15781 | 12842 | 09930 | 07045 | 04187 | 01355 | 98550 | 95770 | 93017 | 90289 |
| 15.5 | 000002 | 87586 | 84908 | 82255 | 79626 | 77022 | 74442 | 71886 | 69354 | 66845 | 64360 |
| 15.6 | 000002 | 61897 | 59457 | 57040 | 54646 | 52273 | 49923 | 47594 | 45287 | 43001 | 40737 |
| 15.7 | .000002 | 38493 | 36271 | 34069 | 31887 | 29726 | 27584 | 25463 | 23361 | 21279 | 19216 |
| 15.8 | 000002 | 17172 | 15147 | 13141 | 11154 | 09185 | 07234 | 05302 | 03387 | 01490 | 99611 |
| 15.9 | 000001 | 97749 | 95905 | 94077 | 92267 | 90473 | 88696 | 86936 | 85192 | 83464 | 81752 |
| 16.0 | 0.000001 | 80056 | | | | | | | | | |

$$E / 3RT = x\,e^{-x} \quad \text{when} \quad x > 16 .$$

*B. Einstein Specific Heat Function*
$C_v$ *(Einstein)/3R*

| x | 0 | 1 | 2 | 3 | 4 | 5 | 6 | 7 | 8 | 9 |
|---|---|---|---|---|---|---|---|---|---|---|
| 0.0 | 1.0 00000 | 99992 | 99967 | 99925 | 99867 | 99792 | 99700 | 99592 | 99467 | 99325 |
| 0.1 | .9 99167 | 98992 | 98801 | 98593 | 98368 | 98127 | 97869 | 97595 | 97304 | 96997 |
| 0.2 | 9 96673 | 96333 | 95976 | 95603 | 95214 | 94808 | 94386 | 93947 | 93492 | 93021 |
| 0.3 | 9 92534 | 92030 | 91510 | 90974 | 90422 | 89854 | 89270 | 88669 | 88053 | 87421 |
| 0.4 | .9 86773 | 86109 | 85429 | 84733 | 84022 | 83295 | 82552 | 81793 | 81019 | 80230 |
| 0.5 | 9 79425 | 78604 | 77768 | 76917 | 76050 | 75168 | 74271 | 73359 | 72432 | 71490 |
| 0.6 | 9 70532 | 69560 | 68573 | 67571 | 66555 | 65523 | 64477 | 63417 | 62341 | 61252 |
| 0.7 | .9 60148 | 59030 | 57897 | 56750 | 55589 | 54415 | 53226 | 52023 | 50806 | 49575 |
| 0.8 | 9 48331 | 47073 | 45801 | 44516 | 43218 | 41906 | 40581 | 39242 | 37891 | 36526 |
| 0.9 | 9 35148 | 33758 | 32354 | 30938 | 29509 | 28068 | 26614 | 25147 | 23668 | 22177 |
| 1.0 | 0.9 20674 | 19158 | 17630 | 16091 | 14540 | 12976 | 11401 | 09815 | 08217 | 06607 |
| 1.1 | .9 04986 | 03354 | 01710 | 00056 | 98390 | 96714 | 95026 | 93328 | 91619 | 89900 |
| 1.2 | 8 88170 | 86430 | 84679 | 82918 | 81147 | 79366 | 77575 | 75774 | 73964 | 72144 |
| 1.3 | 8 70314 | 68474 | 66626 | 64768 | 62900 | 61024 | 59139 | 57244 | 55341 | 53429 |
| 1.4 | .8 51509 | 49580 | 47642 | 45696 | 43742 | 41780 | 39809 | 37831 | 35844 | 33850 |
| 1.5 | 8 31849 | 29839 | 27822 | 25798 | 23766 | 21728 | 19682 | 17629 | 15569 | 13502 |
| 1.6 | 8 11429 | 09349 | 07262 | 05169 | 03070 | 00964 | 98852 | 96734 | 94610 | 92481 |
| 1.7 | .7 90345 | 88204 | 86057 | 83905 | 81747 | 79584 | 77416 | 75243 | 73064 | 70881 |
| 1.8 | 7 68693 | 66500 | 64303 | 62101 | 59894 | 57684 | 55469 | 53249 | 51026 | 48799 |
| 1.9 | 7 46568 | 44333 | 42094 | 39852 | 37606 | 35356 | 33104 | 30848 | 28589 | 26327 |
| 2.0 | 0.7 24062 | 21794 | 19523 | 17249 | 14973 | 12694 | 10413 | 08130 | 05844 | 03556 |
| 2.1 | .7 01266 | 98974 | 96680 | 94384 | 92086 | 89787 | 87486 | 85184 | 82880 | 80575 |
| 2.2 | 6 78269 | 75961 | 73652 | 71343 | 69032 | 66721 | 64408 | 62096 | 59782 | 57468 |
| 2.3 | 6 55154 | 52839 | 50524 | 48209 | 45893 | 43578 | 41262 | 38947 | 36632 | 34317 |
| 2.4 | .6 32002 | 29688 | 27374 | 25061 | 22748 | 20437 | 18125 | 15815 | 13506 | 11197 |
| 2.5 | 6 08890 | 06584 | 04279 | 01975 | 99673 | 97372 | 95072 | 92774 | 90477 | 88183 |
| 2.6 | 5 85890 | 83598 | 81309 | 79021 | 76736 | 74452 | 72171 | 69892 | 67615 | 65340 |
| 2.7 | .5 63068 | 60798 | 58530 | 56265 | 54003 | 51743 | 49486 | 47232 | 44980 | 42732 |
| 2.8 | 5 40486 | 38244 | 36004 | 33767 | 31534 | 29304 | 27077 | 24853 | 22633 | 20416 |
| 2.9 | 5 18203 | 15993 | 13786 | 11584 | 09385 | 07189 | 04997 | 02810 | 00625 | 98445 |
| 3.0 | 0.4 96269 | 94097 | 91929 | 89764 | 87604 | 85448 | 83296 | 81149 | 79006 | 76867 |
| 3.1 | .4 74732 | 72602 | 70476 | 68355 | 66238 | 64125 | 62018 | 59915 | 57816 | 55722 |
| 3.2 | 4 53633 | 51549 | 49470 | 47395 | 45325 | 43260 | 41200 | 39145 | 37095 | 35050 |
| 3.3 | 4 33010 | 30975 | 28946 | 26921 | 24901 | 22887 | 20878 | 18874 | 16876 | 14882 |
| 3.4 | .4 12894 | 10912 | 08935 | 06963 | 04996 | 03036 | 01080 | 99130 | 97186 | 95247 |
| 3.5 | 3 93313 | 91386 | 89463 | 87547 | 85636 | 83731 | 81831 | 79937 | 78049 | 76167 |
| 3.6 | 3 74290 | 72419 | 70554 | 68695 | 66841 | 64993 | 63152 | 61316 | 59486 | 57661 |
| 3.7 | .3 55843 | 54031 | 52224 | 50424 | 48629 | 46840 | 45058 | 43281 | 41510 | 39746 |
| 3.8 | 3 37987 | 36234 | 34488 | 32747 | 31012 | 29284 | 27562 | 25845 | 24135 | 22431 |
| 3.9 | 3 20733 | 19041 | 17355 | 15675 | 14001 | 12333 | 10672 | 09017 | 07367 | 05724 |

| x | 0 | 1 | 2 | 3 | 4 | 5 | 6 | 7 | 8 | 9 |
|---|---|---|---|---|---|---|---|---|---|---|
| 4.0 | 0.3 04087 | 02456 | 00832 | 99213 | 97601 | 95995 | 94394 | 92800 | 91213 | 89631 |
| 4.1 | .2 88055 | 86486 | 84923 | 83365 | 81814 | 80270 | 78731 | 77198 | 75672 | 74152 |
| 4.2 | 2 72637 | 71129 | 69627 | 68132 | 66642 | 65158 | 63681 | 62210 | 60744 | 59285 |
| 4.3 | 2 57832 | 56385 | 54944 | 53509 | 52081 | 50658 | 49241 | 47831 | 46426 | 45027 |
| 4.4 | .2 43635 | 42248 | 40868 | 39494 | 38125 | 36763 | 35406 | 34056 | 32711 | 31372 |
| 4.5 | 2 30040 | 28713 | 27392 | 26077 | 24768 | 23465 | 22168 | 20877 | 19591 | 18312 |
| 4.6 | 2 17038 | 15770 | 14508 | 13252 | 12001 | 10757 | 09518 | 08285 | 07057 | 05836 |
| 4.7 | .2 04620 | 03410 | 02205 | 01006 | 99813 | 98626 | 97444 | 96268 | 95097 | 93933 |
| 4.8 | 1 92773 | 91620 | 90471 | 89329 | 88192 | 87060 | 85934 | 84814 | 83699 | 82589 |
| 4.9 | 1 81485 | 80387 | 79294 | 78206 | 77123 | 76046 | 74975 | 73909 | 72848 | 71792 |
| 5.0 | 0.17 0742 | 9697 | 8657 | 7623 | 6594 | 5570 | 4551 | 3537 | 2529 | 1526 |
| 5.1 | .16 0528 | 9535 | 8547 | 7564 | 6587 | 5614 | 4647 | 3685 | 2727 | 1775 |
| 5.2 | 15 0827 | 9885 | 8948 | 8015 | 7087 | 6165 | 5247 | 4334 | 3426 | 2523 |
| 5.3 | 14 1624 | 0731 | 9842 | 8958 | 8078 | 7204 | 6334 | 5469 | 4608 | 3752 |
| 5.4 | .13 2901 | 2055 | 1213 | 0376 | 9543 | 8715 | 7891 | 7072 | 6257 | 5447 |
| 5.5 | 12 4642 | 3840 | 3044 | 2251 | 1463 | 0680 | 9901 | 9126 | 8355 | 7589 |
| 5.6 | 11 6827 | 6070 | 5317 | 4568 | 3823 | 3082 | 2346 | 1613 | 0885 | 0161 |
| 5.7 | .10 9442 | 8726 | 8014 | 7307 | 6603 | 5904 | 5208 | 4517 | 3829 | 3146 |
| 5.8 | 10 2466 | 1791 | 1119 | 0451 | 97875 | 91275 | 84713 | 78189 | 71704 | 65257 |
| 5.9 | 09 58847 | 52475 | 46140 | 39843 | 33583 | 27359 | 21173 | 15023 | 08910 | 02832 |
| 6.0 | 0.08 96791 | 90786 | 84816 | 78882 | 72984 | 67121 | 61293 | 55499 | 49741 | 44017 |
| 6.1 | .08 38327 | 32672 | 27051 | 21464 | 15910 | 10390 | 04904 | 99451 | 94031 | 88644 |
| 6.2 | 07 83289 | 77967 | 72678 | 67421 | 62196 | 57004 | 51843 | 46713 | 41615 | 36549 |
| 6.3 | 07 31513 | 26509 | 21536 | 16593 | 11681 | 06799 | 01948 | 97126 | 92335 | 87573 |
| 6.4 | .06 82841 | 78139 | 73465 | 68821 | 64206 | 59620 | 55063 | 50534 | 46034 | 41561 |
| 6.5 | 06 37117 | 32701 | 28313 | 23953 | 19620 | 15314 | 11036 | 06784 | 02560 | 98363 |
| 6.6 | 05 94192 | 90048 | 85930 | 81838 | 77772 | 73733 | 69719 | 65731 | 61768 | 57831 |
| 6.7 | .05 53919 | 50032 | 46171 | 42334 | 38521 | 34734 | 30970 | 27231 | 23516 | 19826 |
| 6.8 | 05 16159 | 12516 | 08896 | 05300 | 01728 | 98178 | 94652 | 91149 | 87668 | 84210 |
| 6.9 | 04 80775 | 77363 | 73972 | 70604 | 67258 | 63934 | 60632 | 57351 | 54092 | 50854 |
| 7.0 | 0.04 47638 | 44443 | 41269 | 38116 | 34984 | 31873 | 28782 | 25712 | 22662 | 19632 |
| 7.1 | .04 16623 | 13633 | 10663 | 07714 | 04783 | 01873 | 98982 | 96110 | 93257 | 90423 |
| 7.2 | 03 87609 | 84813 | 82036 | 79277 | 76538 | 73816 | 71113 | 68428 | 65761 | 63112 |
| 7.3 | 03 60481 | 57868 | 55273 | 52695 | 50134 | 47591 | 45065 | 42556 | 40064 | 37590 |
| 7.4 | .03 35132 | 32690 | 30266 | 27857 | 25466 | 23090 | 20731 | 18388 | 16061 | 13750 |
| 7.5 | 03 11454 | 09175 | 06911 | 04662 | 02429 | 00212 | 98009 | 95822 | 93650 | 91493 |
| 7.6 | 02 89350 | 87223 | 85110 | 83012 | 80928 | 78858 | 76803 | 74762 | 72736 | 70723 |
| 7.7 | .02 68725 | 66740 | 64769 | 62812 | 60868 | 58938 | 57021 | 55118 | 53228 | 51351 |
| 7.8 | 02 49487 | 47636 | 45799 | 43974 | 42162 | 40362 | 38575 | 36801 | 35039 | 33290 |
| 7.9 | 02 31553 | 29828 | 28115 | 26414 | 24725 | 23049 | 21384 | 19730 | 18089 | 16459 |

| x | 0 | 1 | 2 | 3 | 4 | 5 | 6 | 7 | 8 | 9 |
|------|------|------|------|------|------|------|------|------|------|------|
| 8.0 | 0.02 14840 | 13233 | 11638 | 10053 | 08480 | 06918 | 05367 | 03827 | 02298 | 00780 |
| 8.1 | .01 99273 | 97776 | 96291 | 94815 | 93350 | 91896 | 90452 | 89018 | 87595 | 86182 |
| 8.2 | 01 84779 | 83385 | 82002 | 80629 | 79266 | 77912 | 76568 | 75234 | 73909 | 72594 |
| 8.3 | 01 71288 | 69992 | 68705 | 67427 | 66159 | 64900 | 63649 | 62408 | 61176 | 59952 |
| 8.4 | .01 58738 | 57532 | 56335 | 55147 | 53967 | 52796 | 51633 | 50479 | 49333 | 48195 |
| 8.5 | 01 47066 | 45945 | 44832 | 43727 | 42630 | 41541 | 40460 | 39387 | 38322 | 37265 |
| 8.6 | 01 36215 | 35173 | 34138 | 33111 | 32092 | 31080 | 30076 | 29079 | 28089 | 27106 |
| 8.7 | .01 26131 | 25163 | 24202 | 23247 | 22300 | 21360 | 20427 | 19501 | 18582 | 17669 |
| 8.8 | 01 16763 | 15864 | 14971 | 14085 | 13205 | 12332 | 11466 | 10606 | 09752 | 08904 |
| 8.9 | 01 08063 | 07228 | 06399 | 05577 | 04760 | 03950 | 03145 | 02347 | 01554 | 00767 |
| 9.0 | 0.009 99866 | 92116 | 84423 | 76788 | 69210 | 61688 | 54222 | 46812 | 39457 | 32157 |
| 9.1 | .009 24911 | 17720 | 10582 | 03498 | 96466 | 89488 | 82561 | 75687 | 68864 | 62092 |
| 9.2 | 008 55370 | 48700 | 42079 | 35508 | 28986 | 22513 | 16089 | 09714 | 03386 | 97106 |
| 9.3 | 007 90873 | 84687 | 78547 | 72454 | 66407 | 60406 | 54449 | 48538 | 42671 | 36849 |
| 9.4 | .007 31071 | 25336 | 19645 | 13997 | 08391 | 02828 | 97307 | 91828 | 86391 | 80994 |
| 9.5 | 006 75639 | 70324 | 65050 | 59815 | 54621 | 49466 | 44350 | 39273 | 34235 | 29235 |
| 9.6 | 006 24273 | 19348 | 14462 | 09612 | 04800 | 00024 | 95285 | 90582 | 85915 | 81283 |
| 9.7 | .005 76687 | 72126 | 67600 | 63108 | 58651 | 54228 | 49839 | 45484 | 41161 | 36872 |
| 9.8 | 005 32616 | 28393 | 24202 | 20043 | 15916 | 11820 | 07757 | 03724 | 99722 | 95752 |
| 9.9 | 004 91811 | 87901 | 84022 | 80172 | 76351 | 72561 | 68799 | 65066 | 61363 | 57687 |
| 10.0 | 0.004 54041 | 50422 | 46831 | 43268 | 39733 | 36225 | 32744 | 29290 | 25862 | 22461 |
| 10.1 | .004 19087 | 15739 | 12416 | 09120 | 05849 | 02603 | 99383 | 96187 | 93016 | 89870 |
| 10.2 | 003 86749 | 83651 | 80578 | 77529 | 74503 | 71501 | 68522 | 65567 | 62634 | 59725 |
| 10.3 | 003 56838 | 53973 | 51131 | 48311 | 45513 | 42737 | 39982 | 37249 | 34538 | 31847 |
| 10.4 | .003 29178 | 26529 | 23901 | 21294 | 18707 | 16141 | 13594 | 11068 | 08561 | 06074 |
| 10.5 | 003 03606 | 01158 | 98729 | 96319 | 93928 | 91555 | 89202 | 86866 | 84549 | 82251 |
| 10.6 | 002 79970 | 77708 | 75463 | 73236 | 71026 | 68834 | 66659 | 64501 | 62360 | 60236 |
| 10.7 | .002 58129 | 56038 | 53964 | 51906 | 49865 | 47839 | 45830 | 43836 | 41858 | 39896 |
| 10.8 | 002 37950 | 36018 | 34102 | 32201 | 30316 | 28445 | 26589 | 24747 | 22921 | 21108 |
| 10.9 | 002 19310 | 17527 | 15757 | 14002 | 12260 | 10532 | 08818 | 07118 | 05431 | 03758 |
| 11.0 | 0.002 02097 | 00450 | 98816 | 97195 | 95587 | 93992 | 92410 | 90840 | 89282 | 87737 |
| 11.1 | .001 86205 | 84684 | 83176 | 81679 | 80195 | 78722 | 77261 | 75812 | 74375 | 72949 |
| 11.2 | 001 71534 | 70130 | 68738 | 67357 | 65987 | 64628 | 63280 | 61942 | 60615 | 59299 |
| 11.3 | 001 57994 | 56699 | 55414 | 54139 | 52875 | 51621 | 50377 | 49143 | 47919 | 46704 |
| 11.4 | .0014 5500 | 4305 | 3119 | 1944 | 0777 | 9620 | 8473 | 7334 | 6205 | 5084 |
| 11.5 | 0013 3973 | 2871 | 1777 | 0693 | 9617 | 8550 | 7491 | 6441 | 5399 | 4366 |
| 11.6 | 0012 3341 | 2324 | 1316 | 0316 | 9323 | 8339 | 7363 | 6395 | 5434 | 4481 |
| 11.7 | .0011 3536 | 2598 | 1669 | 0746 | 9831 | 8924 | 8024 | 7131 | 6245 | 5366 |
| 11.8 | 0010 4495 | 3631 | 2773 | 1923 | 1079 | 0243 | 94130 | 85898 | 77733 | 69635 |
| 11.9 | 0009 61602 | 53635 | 45732 | 37893 | 30118 | 22407 | 14757 | 07170 | 99645 | 92181 |

| x | 0 | 1 | 2 | 3 | 4 | 5 | 6 | 7 | 8 | 9 |
|---|---|---|---|---|---|---|---|---|---|---|
| 12.0 | 0.0008 84777 | 77434 | 70151 | 62927 | 55761 | 48654 | 41605 | 34613 | 27678 | 20800 |
| 12.1 | .0008 13977 | 07211 | 00499 | 93842 | 87240 | 80691 | 74196 | 67754 | 61364 | 55026 |
| 12.2 | 0007 48741 | 42506 | 36323 | 30190 | 24107 | 18074 | 12090 | 06155 | 00268 | 94430 |
| 12.3 | 0006 88640 | 82897 | 77201 | 71551 | 65948 | 60391 | 54879 | 49412 | 43990 | 38613 |
| 12.4 | .0006 33279 | 27990 | 22744 | 17540 | 12380 | 07262 | 02185 | 97151 | 92158 | 87205 |
| 14.5 | 0005 82294 | 77423 | 72592 | 67800 | 63048 | 58335 | 53661 | 49025 | 44427 | 39867 |
| 12.6 | 0005 35345 | 30860 | 26411 | 22000 | 17624 | 13285 | 08982 | 04713 | 00481 | 96282 |
| 12.7 | .0004 92119 | 87990 | 83895 | 79834 | 75806 | 71811 | 67850 | 63921 | 60024 | 56160 |
| 12.8 | 0004 52327 | 48527 | 44757 | 41019 | 37312 | 33635 | 29989 | 26373 | 22786 | 19230 |
| 12.9 | 0004 15703 | 12205 | 08736 | 05295 | 01883 | 98500 | 95144 | 91816 | 88516 | 85243 |
| 13.0 | 0.0003 81997 | 78779 | 75586 | 72421 | 69281 | 66168 | 63080 | 60018 | 56981 | 53970 |
| 13.1 | .0003 50983 | 48022 | 45085 | 42172 | 39284 | 36419 | 33579 | 30761 | 27968 | 25197 |
| 13.2 | 0003 22450 | 19725 | 17023 | 14344 | 11687 | 09052 | 06439 | 03847 | 01278 | 98729 |
| 13.3 | 0002 96202 | 93696 | 91211 | 88746 | 86302 | 83879 | 81475 | 79092 | 76728 | 74384 |
| 13.4 | .0002 72060 | 69755 | 67470 | 65203 | 62955 | 60726 | 58516 | 56324 | 54151 | 51995 |
| 13.5 | 0002 49858 | 47738 | 45637 | 43552 | 41486 | 39436 | 37404 | 35388 | 33390 | 31408 |
| 13.6 | 0002 29443 | 27494 | 25561 | 23645 | 21745 | 19860 | 17992 | 16139 | 14301 | 12479 |
| 13.7 | .0002 10672 | 08881 | 07104 | 05342 | 03596 | 01863 | 00145 | 98442 | 96753 | 95078 |
| 13.8 | 0001 93417 | 91770 | 90137 | 88518 | 86912 | 85320 | 83741 | 82175 | 80623 | 79083 |
| 13.9 | 0001 77557 | 76043 | 74542 | 73054 | 71578 | 70114 | 68663 | 67224 | 65798 | 64383 |
| 14.0 | 0.00016 2980 | 1589 | 0209 | 8842 | 7485 | 6141 | 4807 | 3485 | 2174 | 0874 |
| 14.1 | .00014 9585 | 8306 | 7039 | 5782 | 4536 | 3300 | 2075 | 0860 | 9655 | 8461 |
| 14.2 | 00013 7276 | 6102 | 4937 | 3783 | 2638 | 1502 | 0377 | 9261 | 8154 | 7056 |
| 14.3 | 00012 5968 | 4889 | 3820 | 2759 | 1707 | 0664 | 9630 | 8605 | 7588 | 6580 |
| 14.4 | .00011 5581 | 4590 | 3607 | 2633 | 1666 | 0708 | 9759 | 8817 | 7883 | 6957 |
| 14.5 | 00010 6039 | 5129 | 4226 | 3332 | 2444 | 1564 | 0692 | 98272 | 89696 | 81193 |
| 14.6 | 00009 72762 | 64403 | 56114 | 47896 | 39748 | 31669 | 23658 | 15715 | 07840 | 00032 |
| 14.7 | .00008 92290 | 84614 | 77003 | 69457 | 61975 | 54556 | 47201 | 39908 | 32677 | 25508 |
| 14.8 | 00008 18400 | 11352 | 04364 | 97435 | 90566 | 83755 | 77002 | 70306 | 63667 | 57085 |
| 14.9 | 00007 50559 | 44089 | 37674 | 31313 | 25007 | 18754 | 12554 | 06408 | 00314 | 94271 |
| 15.0 | 0.00006 88281 | 82341 | 76452 | 70613 | 64824 | 59085 | 53394 | 47752 | 42158 | 36612 |
| 15.1 | .00006 31113 | 25662 | 20256 | 14897 | 09584 | 04316 | 99093 | 93915 | 88781 | 83690 |
| 15.2 | 00005 78648 | 73640 | 68679 | 63761 | 58885 | 54050 | 49257 | 44505 | 39793 | 35122 |
| 15.3 | 00005 30490 | 25899 | 21346 | 16833 | 12358 | 07922 | 03523 | 99162 | 94839 | 90552 |
| 15.4 | .00004 86303 | 82089 | 77912 | 73771 | 69665 | 65594 | 61558 | 57557 | 53590 | 49657 |
| 15.5 | 00004 45758 | 41892 | 38060 | 34260 | 30493 | 26758 | 23055 | 19384 | 15745 | 12137 |
| 15.6 | 00004 08560 | 05013 | 01497 | 98011 | 94555 | 91129 | 87732 | 84365 | 81026 | 77716 |
| 15.7 | .00003 74435 | 71181 | 67956 | 64758 | 61588 | 58446 | 55330 | 52241 | 49178 | 46142 |
| 15.8 | 00003 43132 | 40148 | 37190 | 34257 | 31349 | 28467 | 25609 | 22775 | 19967 | 17182 |
| 15.9 | 00003 14421 | 11685 | 08971 | 06281 | 03615 | 00971 | 98350 | 95752 | 93176 | 90622 |
| 16.0 | 0.00002 88090 | | | | | | | | | |

$$C_v / 3R = x^2 e^{-x} \quad \text{when } x > 16.$$

*C. Debye Internal Energy Function*
*E (Debye)/3RT*

| x | 0 | 1 | 2 | 3 | 4 | 5 | 6 | 7 | 8 | 9 |
|---|---|---|---|---|---|---|---|---|---|---|
| 0.0 | 1.0 00000 | 96255 | 92520 | 88795 | 85080 | 81375 | 77680 | 73995 | 70320 | 66655 |
| 0.1 | .9 63000 | 59355 | 55720 | 52095 | 48480 | 44875 | 41280 | 37695 | 34119 | 30554 |
| 0.2 | 9 26999 | 23454 | 19919 | 16393 | 12878 | 09373 | 05877 | 02392 | 98916 | 95451 |
| 0.3 | 8 91995 | 88550 | 85114 | 81688 | 78272 | 74866 | 71470 | 68084 | 64708 | 61341 |
| 0.4 | .8 57985 | 54638 | 51302 | 47975 | 44658 | 41351 | 38053 | 34766 | 31489 | 28221 |
| 0.5 | 8 24963 | 21715 | 18477 | 15248 | 12030 | 08821 | 05622 | 02433 | 99253 | 96083 |
| 0.6 | 7 92923 | 89773 | 86633 | 83502 | 80381 | 77270 | 74168 | 71076 | 67994 | 64921 |
| 0.7 | .7 61858 | 58805 | 55762 | 52728 | 49703 | 46689 | 43684 | 40688 | 37702 | 34726 |
| 0.8 | 7 31759 | 28802 | 25854 | 22916 | 19987 | 17068 | 14159 | 11259 | 08368 | 05487 |
| 0.9 | 7 02615 | 99753 | 96900 | 94057 | 91223 | 88398 | 85583 | 82777 | 79981 | 77193 |
| 1.0 | 0.6 74415 | 71647 | 68888 | 66138 | 63397 | 60666 | 57944 | 55231 | 52527 | 49833 |
| 1.1 | .6 47148 | 44472 | 41805 | 39147 | 36498 | 33859 | 31228 | 28607 | 25995 | 23392 |
| 1.2 | 6 20798 | 18213 | 15637 | 13070 | 10512 | 07963 | 05422 | 02891 | 00369 | 97856 |
| 1.3 | 5 95351 | 92856 | 90369 | 87891 | 85422 | 82962 | 80511 | 78068 | 75634 | 73209 |
| 1.4 | .5 70793 | 68386 | 65987 | 63596 | 61215 | 58842 | 56478 | 54122 | 51775 | 49437 |
| 1.5 | 5 47107 | 44785 | 42472 | 40168 | 37872 | 35585 | 33306 | 31036 | 28774 | 26520 |
| 1.6 | 5 24275 | 22038 | 19809 | 17589 | 15377 | 13174 | 10979 | 08792 | 06613 | 04442 |
| 1.7 | .5 02280 | 00126 | 97980 | 95842 | 93712 | 91590 | 89477 | 87371 | 85274 | 83184 |
| 1.8 | 4 81103 | 79030 | 76964 | 74907 | 72857 | 70816 | 68782 | 66756 | 64738 | 62728 |
| 1.9 | 4 60726 | 58731 | 56745 | 54766 | 52794 | 50831 | 48875 | 46927 | 44987 | 43054 |
| 2.0 | 0.4 41128 | 39211 | 37301 | 35398 | 33503 | 31616 | 29736 | 27864 | 25999 | 24141 |
| 2.1 | .4 22291 | 20448 | 18613 | 16785 | 14965 | 13151 | 11345 | 09547 | 07755 | 05971 |
| 2.2 | 4 04194 | 02424 | 00661 | 98906 | 97157 | 95416 | 93682 | 91955 | 90235 | 88522 |
| 2.3 | 3 86816 | 85117 | 83425 | 81740 | 80062 | 78390 | 76726 | 75068 | 73418 | 71774 |
| 2.4 | .3 70137 | 68507 | 66883 | 65266 | 63656 | 62053 | 60456 | 58866 | 57283 | 55706 |
| 2.5 | 3 54136 | 52572 | 51015 | 49465 | 47921 | 46383 | 44852 | 43328 | 41810 | 40298 |
| 2.6 | 3 38793 | 37294 | 35801 | 34315 | 32835 | 31361 | 29893 | 28432 | 26977 | 25528 |
| 2.7 | .3 24086 | 22649 | 21219 | 19795 | 18377 | 16965 | 15559 | 14159 | 12765 | 11377 |
| 2.8 | 3 09995 | 08619 | 07249 | 05885 | 04527 | 03174 | 01828 | 00487 | 99152 | 97823 |
| 2.9 | 2 96500 | 95182 | 93870 | 92564 | 91264 | 89969 | 88680 | 87397 | 86119 | 84847 |
| 3.0 | 0.28 3580 | 2319 | 1063 | 9813 | 8568 | 7329 | 6095 | 4867 | 3644 | 2427 |
| 3.1 | .27 1215 | 0008 | 8807 | 7610 | 6419 | 5234 | 4054 | 2879 | 1709 | 0544 |
| 3.2 | 25 9385 | 8230 | 7081 | 5937 | 4798 | 3664 | 2535 | 1412 | 0293 | 9179 |
| 3.3 | 24 8070 | 6966 | 5868 | 4774 | 3684 | 2600 | 1521 | 0447 | 9377 | 8312 |
| 3.4 | .23 7252 | 6197 | 5146 | 4101 | 3060 | 2023 | 0991 | 9964 | 8942 | 7924 |
| 3.5 | 22 6911 | 5903 | 4899 | 3899 | 2904 | 1914 | 0928 | 9947 | 8970 | 7998 |
| 3.6 | 21 7030 | 6066 | 5107 | 4152 | 3201 | 2255 | 1313 | 0376 | 9442 | 8513 |
| 3.7 | .20 7589 | 6668 | 5752 | 4840 | 3932 | 3028 | 2128 | 1233 | 0341 | 9454 |
| 3.8 | 19 8571 | 7692 | 6817 | 5945 | 5078 | 4215 | 3356 | 2501 | 1650 | 0803 |
| 3.9 | 18 9959 | 9120 | 8284 | 7452 | 6624 | 5800 | 4980 | 4164 | 3351 | 2542 |

| x | 0 | 1 | 2 | 3 | 4 | 5 | 6 | 7 | 8 | 9 |
|---|---|---|---|---|---|---|---|---|---|---|
| 4.0 | 0.18 1737 | 0935 | 0138 | 9344 | 8553 | 7767 | 6984 | 6204 | 5428 | 4656 |
| 4.1 | .17 3888 | 3123 | 2361 | 1603 | 0849 | 0098 | 9351 | 8607 | 7866 | 7129 |
| 4.2 | 16 6396 | 5666 | 4939 | 4216 | 3496 | 2779 | 2066 | 1356 | 0649 | 9946 |
| 4.3 | 15 9246 | 8549 | 7856 | 7166 | 6479 | 5795 | 5114 | 4437 | 3763 | 3092 |
| 4.4 | .15 2424 | 1759 | 1097 | 0439 | 9783 | 9131 | 8482 | 7835 | 7192 | 6552 |
| 4.5 | 14 5914 | 5280 | 4649 | 4021 | 3395 | 2773 | 2153 | 1537 | 0923 | 0312 |
| 4.6 | 13 9704 | 9099 | 8497 | 7898 | 7301 | 6707 | 6116 | 5528 | 4943 | 4360 |
| 4.7 | .13 3780 | 3203 | 2628 | 2057 | 1488 | 0921 | 0357 | 9796 | 9238 | 8682 |
| 4.8 | 12 8129 | 7579 | 7031 | 6485 | 5942 | 5402 | 4864 | 4329 | 3797 | 3267 |
| 4.9 | 12 2739 | 2214 | 1691 | 1171 | 0653 | 0138 | 9625 | 9114 | 8606 | 8101 |
| 5.0 | 0.11 7598 | 7097 | 6598 | 6102 | 5608 | 5116 | 4627 | 4140 | 3656 | 3174 |
| 5.1 | .11 2694 | 2216 | 1740 | 1267 | 0796 | 0327 | 9861 | 9396 | 8934 | 8474 |
| 5.2 | 10 8016 | 7561 | 7107 | 6656 | 6206 | 5759 | 5314 | 4871 | 4430 | 3992 |
| 5.3 | 10 3555 | 3120 | 2688 | 2257 | 1829 | 1402 | 0978 | 0555 | 0135 | 97163 |
| 5.4 | .09 92997 | 88852 | 84726 | 80619 | 76531 | 72463 | 68414 | 64384 | 60373 | 56381 |
| 5.5 | 09 52408 | 48453 | 44517 | 40600 | 36701 | 32821 | 28958 | 25114 | 21288 | 17480 |
| 5.6 | 09 13690 | 09917 | 06162 | 02425 | 98706 | 95004 | 91319 | 87652 | 84002 | 80369 |
| 5.7 | .08 76753 | 73155 | 69573 | 66007 | 62459 | 58927 | 55412 | 51913 | 48431 | 44965 |
| 5.8 | 08 41515 | 38082 | 34664 | 31263 | 27877 | 24508 | 21154 | 17815 | 14493 | 11186 |
| 5.9 | 08 07894 | 04618 | 01357 | 98112 | 94881 | 91666 | 88466 | 85280 | 82110 | 78954 |
| 6.0 | 0.07 75813 | 72687 | 69575 | 66478 | 63395 | 60327 | 57273 | 54233 | 51208 | 48196 |
| 6.1 | .07 45198 | 42215 | 39245 | 36289 | 33347 | 30419 | 27504 | 24603 | 21715 | 18841 |
| 6.2 | 07 15980 | 13132 | 10297 | 07476 | 04668 | 01873 | 99090 | 96321 | 93564 | 90821 |
| 6.3 | 06 88090 | 85371 | 82665 | 79972 | 77291 | 74623 | 71967 | 69323 | 66691 | 64072 |
| 6.4 | .06 61465 | 58869 | 56286 | 53715 | 51155 | 48607 | 46071 | 43547 | 41034 | 38533 |
| 6.5 | 06 36043 | 33565 | 31098 | 28643 | 26199 | 23766 | 21344 | 18934 | 16534 | 14146 |
| 6.6 | 06 11768 | 09402 | 07046 | 04701 | 02366 | 00043 | 97730 | 95428 | 93136 | 90854 |
| 6.7 | .05 88583 | 86323 | 84073 | 81833 | 79603 | 77384 | 75174 | 72975 | 70785 | 68606 |
| 6.8 | 05 66437 | 64277 | 62127 | 59987 | 57857 | 55737 | 53626 | 51525 | 49433 | 47351 |
| 6.9 | 05 45278 | 43214 | 41160 | 39115 | 37080 | 35053 | 33036 | 31028 | 29029 | 27039 |
| 7.0 | 0.05 25059 | 23087 | 21123 | 19169 | 17224 | 15287 | 13359 | 11440 | 09530 | 07628 |
| 7.1 | .05 05734 | 03849 | 01973 | 00105 | 98245 | 96394 | 94551 | 92716 | 90890 | 89071 |
| 7.2 | 04 87261 | 85459 | 83665 | 81879 | 80101 | 78331 | 76569 | 74815 | 73068 | 71329 |
| 7.3 | 04 69598 | 67875 | 66160 | 64452 | 62752 | 61059 | 59374 | 57696 | 56026 | 54363 |
| 7.4 | .04 52707 | 51059 | 49418 | 47785 | 46158 | 44539 | 42927 | 41322 | 39725 | 38134 |
| 7.5 | 04 36550 | 34974 | 33404 | 31841 | 30285 | 28736 | 27194 | 25658 | 24129 | 22607 |
| 7.6 | 04 21092 | 19583 | 18081 | 16586 | 15097 | 13615 | 12139 | 10669 | 09206 | 07750 |
| 7.7 | .04 06299 | 04855 | 03418 | 01987 | 00562 | 99143 | 97730 | 96323 | 94923 | 93529 |
| 7.8 | 03 92140 | 90758 | 89382 | 88011 | 86647 | 85289 | 83936 | 82590 | 81249 | 79914 |
| 7.9 | 03 78584 | 77261 | 75943 | 74631 | 73324 | 72023 | 70728 | 69439 | 68155 | 66876 |

| x | 0 | 1 | 2 | 3 | 4 | 5 | 6 | 7 | 8 | 9 |
|---|---|---|---|---|---|---|---|---|---|---|
| 8.0 | 0.036 5603 | 4335 | 3073 | 1816 | 0565 | 9319 | 8078 | 6843 | 5613 | 4388 |
| 8.1 | .035 3169 | 1954 | 0745 | 9541 | 8342 | 7149 | 5960 | 4776 | 3598 | 2424 |
| 8.2 | 034 1256 | 0092 | 8933 | 7780 | 6631 | 5487 | 4348 | 3213 | 2084 | 0959 |
| 8.3 | 032 9839 | 8724 | 7613 | 6507 | 5406 | 4310 | 3218 | 2130 | 1048 | 9970 |
| 8.4 | .031 8896 | 7827 | 6762 | 5702 | 4646 | 3594 | 2547 | 1505 | 0467 | 9433 |
| 8.5 | 030 8403 | 7378 | 6357 | 5340 | 4328 | 3319 | 2315 | 1315 | 0319 | 9328 |
| 8.6 | 029 8340 | 7357 | 6378 | 5402 | 4431 | 3464 | 2500 | 1541 | 0586 | 9634 |
| 8.7 | .028 8687 | 7744 | 6804 | 5868 | 4936 | 4008 | 3084 | 2163 | 1247 | 0334 |
| 8.8 | 027 9424 | 8519 | 7617 | 6719 | 5825 | 4934 | 4047 | 3163 | 2283 | 1407 |
| 8.9 | 027 0534 | 9665 | 8799 | 7937 | 7078 | 6223 | 5371 | 4523 | 3678 | 2837 |
| 9.0 | 0.026 1999 | 1164 | 0333 | 9505 | 8681 | 7859 | 7041 | 6227 | 5416 | 4608 |
| 9.1 | .025 3803 | 3001 | 2203 | 1408 | 0616 | 9827 | 9041 | 8259 | 7479 | 6703 |
| 9.2 | 024 5930 | 5160 | 4393 | 3629 | 2868 | 2110 | 1355 | 0603 | 9854 | 9108 |
| 9.3 | 023 8365 | 7625 | 6888 | 6154 | 5423 | 4694 | 3969 | 3246 | 2526 | 1809 |
| 9.4 | .023 1095 | 0384 | 9676 | 8970 | 8267 | 7567 | 6869 | 6174 | 5482 | 4793 |
| 9.5 | 022 4107 | 3423 | 2741 | 2063 | 1387 | 0714 | 0043 | 9375 | 8709 | 8046 |
| 9.6 | 021 7386 | 6728 | 6073 | 5421 | 4771 | 4123 | 3478 | 2835 | 2195 | 1558 |
| 9.7 | .021 0923 | 0290 | 9659 | 9031 | 8406 | 7783 | 7162 | 6544 | 5928 | 5315 |
| 9.8 | 020 4704 | 4095 | 3488 | 2884 | 2282 | 1683 | 1085 | 0490 | 9897 | 9307 |
| 9.9 | 019 8719 | 8133 | 7549 | 6967 | 6388 | 5811 | 5236 | 4663 | 4092 | 3524 |
| 10.0 | 0.019 2958 | 2393 | 1831 | 1271 | 0714 | 0158 | 9604 | 9053 | 8503 | 7956 |
| 10.1 | .018 7410 | 6867 | 6326 | 5787 | 5249 | 4714 | 4181 | 3650 | 3120 | 2593 |
| 10.2 | 018 2068 | 1544 | 1023 | 0504 | 9986 | 9470 | 8957 | 8445 | 7935 | 7427 |
| 10.3 | 017 6921 | 6416 | 5914 | 5413 | 4915 | 4418 | 3923 | 3430 | 2938 | 2449 |
| 10.4 | .017 1961 | 1475 | 0991 | 0508 | 0027 | 9548 | 9071 | 8596 | 8122 | 7650 |
| 10.5 | 016 7180 | 6711 | 6244 | 5779 | 5316 | 4854 | 4394 | 3936 | 3479 | 3024 |
| 10.6 | 016 2570 | 2118 | 1668 | 1220 | 0773 | 0328 | 9884 | 9442 | 9001 | 8562 |
| 10.7 | .015 8125 | 7689 | 7255 | 6822 | 6391 | 5962 | 5534 | 5107 | 4682 | 4259 |
| 10.8 | 015 3837 | 3416 | 2997 | 2580 | 2164 | 1749 | 1336 | 0925 | 0515 | 0106 |
| 10.9 | 014 9699 | 9293 | 8889 | 8486 | 8084 | 7684 | 7286 | 6888 | 6492 | 6098 |
| 11.0 | 0.014 5705 | 5313 | 4923 | 4534 | 4146 | 3760 | 3375 | 2992 | 2610 | 2229 |
| 11.1 | .014 1849 | 1471 | 1094 | 0719 | 0345 | 9972 | 9600 | 9230 | 8861 | 8493 |
| 11.2 | 013 8126 | 7761 | 7397 | 7034 | 6673 | 6313 | 5954 | 5596 | 5239 | 4884 |
| 11.3 | 013 4530 | 4177 | 3826 | 3475 | 3126 | 2778 | 2431 | 2085 | 1741 | 1398 |
| 11.4 | .013 1056 | 0715 | 0375 | 0036 | 9699 | 9362 | 9027 | 8693 | 8360 | 8029 |
| 11.5 | 012 7698 | 7368 | 7040 | 6713 | 6387 | 6061 | 5737 | 5415 | 5093 | 4772 |
| 11.6 | 012 4452 | 4134 | 3816 | 3500 | 3184 | 2870 | 2557 | 2245 | 1934 | 1623 |
| 11.7 | .012 1314 | 1006 | 0699 | 0393 | 0088 | 9784 | 9481 | 9179 | 8878 | 8578 |
| 11.8 | 011 8279 | 7982 | 7685 | 7389 | 7094 | 6799 | 6506 | 6214 | 5923 | 5633 |
| 11.9 | 011 5344 | 5055 | 4768 | 4482 | 4196 | 3912 | 3628 | 3346 | 3064 | 2783 |

$E(\text{Debye})/3\,RT$

| x | 0 | 1 | 2 | 3 | 4 | 5 | 6 | 7 | 8 | 9 |
|---|---|---|---|---|---|---|---|---|---|---|
| 12.0 | 0.011 2503 | 2224 | 1946 | 1669 | 1393 | 1118 | 0843 | 0570 | 0297 | 0025 |
| 12.1 | .010 9754 | 9484 | 9215 | 8947 | 8679 | 8413 | 8147 | 7882 | 7618 | 7355 |
| 12.2 | 010 7093 | 6832 | 6571 | 6311 | 6052 | 5794 | 5537 | 5281 | 5025 | 4770 |
| 12.3 | 010 4516 | 4263 | 4011 | 3759 | 3509 | 3259 | 3010 | 2761 | 2514 | 2267 |
| 12.4 | .010 2021 | 1776 | 1531 | 1288 | 1045 | 0803 | 0561 | 0321 | 0081 | 98419 |
| 12.5 | 009 96036 | 93661 | 91293 | 88932 | 86579 | 84233 | 81895 | 79564 | 77240 | 74923 |
| 12.6 | 009 72614 | 70312 | 68017 | 65730 | 63449 | 61176 | 58909 | 56650 | 54398 | 52153 |
| 12.7 | .009 49915 | 47683 | 45459 | 43241 | 41031 | 38827 | 36630 | 34440 | 32257 | 30080 |
| 12.8 | 009 27910 | 25747 | 23591 | 21441 | 19298 | 17161 | 15031 | 12907 | 10790 | 08680 |
| 12.9 | 009 06576 | 04478 | 02387 | 00302 | 98224 | 96152 | 94086 | 92027 | 89974 | 87927 |
| 13.0 | 0.008 85886 | 83851 | 81823 | 79801 | 77785 | 75775 | 73771 | 71774 | 69782 | 67796 |
| 13.1 | .008 65817 | 63843 | 61875 | 59914 | 57958 | 56008 | 54064 | 52125 | 50193 | 48266 |
| 13.2 | 008 46345 | 44430 | 42521 | 40617 | 38719 | 36827 | 34941 | 33060 | 31184 | 29314 |
| 13.3 | 008 27450 | 25592 | 23739 | 21891 | 20049 | 18212 | 16381 | 14555 | 12735 | 10920 |
| 13.4 | .008 09111 | 07306 | 05507 | 03714 | 01926 | 00143 | 98365 | 96592 | 94825 | 93063 |
| 13.5 | 007 91306 | 89554 | 87807 | 86066 | 84330 | 82598 | 80872 | 79151 | 77435 | 75724 |
| 13.6 | 007 74017 | 72316 | 70620 | 68929 | 67242 | 65561 | 63884 | 62213 | 60546 | 58884 |
| 13.7 | .007 57226 | 55574 | 53927 | 52284 | 50646 | 49012 | 47384 | 45760 | 44140 | 42526 |
| 13.8 | 007 40916 | 39310 | 37710 | 36114 | 34522 | 32935 | 31353 | 29775 | 28201 | 26632 |
| 13.9 | 007 25068 | 23508 | 21953 | 20402 | 18855 | 17313 | 15775 | 14242 | 12713 | 11188 |
| 14.0 | 0.007 09668 | 08152 | 06640 | 05132 | 03629 | 02130 | 00636 | 99145 | 97659 | 96177 |
| 14.1 | .006 94699 | 93225 | 91755 | 90290 | 88829 | 87371 | 85918 | 84469 | 83024 | 81583 |
| 14.2 | 006 80146 | 78713 | 77285 | 75860 | 74439 | 73022 | 71609 | 70200 | 68795 | 67394 |
| 14.3 | 006 65996 | 64603 | 63213 | 61828 | 60446 | 59068 | 57694 | 56323 | 54957 | 53594 |
| 14.4 | .006 52235 | 50880 | 49528 | 48180 | 46836 | 45496 | 44159 | 42826 | 41497 | 40171 |
| 14.5 | 006 38849 | 37531 | 36216 | 34905 | 33597 | 32293 | 30992 | 29695 | 28402 | 27112 |
| 14.6 | 006 25826 | 24543 | 23264 | 21988 | 20716 | 19447 | 18181 | 16919 | 15661 | 14405 |
| 14.7 | .006 13153 | 11905 | 10660 | 09418 | 08180 | 06945 | 05714 | 04485 | 03260 | 02039 |
| 14.8 | 006 00820 | 99605 | 98393 | 97185 | 95979 | 94777 | 93578 | 92383 | 91190 | 90001 |
| 14.9 | 005 88815 | 87632 | 86452 | 85275 | 84102 | 82932 | 81764 | 80600 | 79439 | 78281 |
| 15.0 | 0.0057 7126 | 5975 | 4826 | 3680 | 2537 | 1398 | 0261 | 9128 | 7997 | 6869 |
| 15.1 | .0056 5745 | 4623 | 3504 | 2388 | 1276 | 0166 | 9059 | 7955 | 6853 | 5755 |
| 15.2 | 0055 4660 | 3567 | 2478 | 1391 | 0307 | 9226 | 8147 | 7072 | 5999 | 4929 |
| 15.3 | 0054 3862 | 2798 | 1736 | 0677 | 9621 | 8568 | 7518 | 6470 | 5425 | 4382 |
| 15.4 | .0053 3342 | 2305 | 1271 | 0239 | 9210 | 8184 | 7160 | 6139 | 5121 | 4105 |
| 15.5 | 0052 3092 | 2081 | 1073 | 0068 | 9065 | 8065 | 7067 | 6072 | 5080 | 4090 |
| 15.6 | 0051 3102 | 2117 | 1135 | 0155 | 9177 | 8202 | 7230 | 6260 | 5292 | 4327 |
| 15.7 | .0050 3365 | 2405 | 1447 | 0492 | 9539 | 8588 | 7640 | 6694 | 5751 | 4810 |
| 15.8 | 0049 3872 | 2936 | 2002 | 1070 | 0141 | 9215 | 8290 | 7368 | 6448 | 5531 |
| 15.9 | 0048 4616 | 3703 | 2792 | 1884 | 0978 | 0074 | 9173 | 8274 | 7377 | 6482 |

| x | 0 | 1 | 2 | 3 | 4 | 5 | 6 | 7 | 8 | 9 |
|---|---|---|---|---|---|---|---|---|---|---|
| 16.0 | 0.0047 5589 | 4699 | 3811 | 2925 | 2042 | 1160 | 0281 | 9404 | 8529 | 7656 |
| 16.1 | .0046 6786 | 5917 | 5051 | 4187 | 3325 | 2465 | 1607 | 0752 | 9898 | 9047 |
| 16.2 | 0045 8198 | 7350 | 6505 | 5662 | 4821 | 3982 | 3146 | 2311 | 1478 | 0647 |
| 16.3 | 0044 9819 | 8992 | 8167 | 7345 | 6524 | 5706 | 4889 | 4075 | 3262 | 2451 |
| 16.4 | .0044 1643 | 0836 | 0031 | 9229 | 8428 | 7629 | 6832 | 6037 | 5244 | 4453 |
| 16.5 | 0043 3664 | 2876 | 2091 | 1307 | 0526 | 9746 | 8968 | 8192 | 7418 | 6646 |
| 16.6 | 0042 5875 | 5107 | 4340 | 3575 | 2812 | 2051 | 1292 | 0534 | 9778 | 9024 |
| 16.7 | .0041 8272 | 7522 | 6774 | 6027 | 5282 | 4539 | 3797 | 3058 | 2320 | 1584 |
| 16.8 | 0041 0849 | 0117 | 9386 | 8656 | 7929 | 7203 | 6479 | 5757 | 5037 | 4318 |
| 16.9 | 0040 3601 | 2885 | 2171 | 1459 | 0749 | 0040 | 9333 | 8628 | 7924 | 7222 |
| 17.0 | 0.0039 6521 | 5822 | 5125 | 4430 | 3736 | 3044 | 2353 | 1664 | 0977 | 0291 |
| 17.1 | .0038 9606 | 8924 | 8243 | 7563 | 6885 | 6209 | 5535 | 4862 | 4190 | 3520 |
| 17.2 | 0038 2852 | 2185 | 1519 | 0855 | 0193 | 9532 | 8873 | 8216 | 7560 | 6905 |
| 17.3 | 0037 6252 | 5600 | 4950 | 4301 | 3654 | 3009 | 2365 | 1722 | 1081 | 0441 |
| 17.4 | .0036 9803 | 9166 | 8531 | 7897 | 7264 | 6633 | 6004 | 5376 | 4749 | 4124 |
| 17.5 | 0036 3500 | 2878 | 2257 | 1637 | 1019 | 0403 | 9787 | 9173 | 8561 | 7950 |
| 17.6 | 0035 7340 | 6732 | 6125 | 5519 | 4915 | 4312 | 3711 | 3110 | 2512 | 1914 |
| 17.7 | .0035 1318 | 0723 | 0130 | 9538 | 8947 | 8358 | 7770 | 7183 | 6598 | 6014 |
| 17.8 | 0034 5431 | 4849 | 4269 | 3690 | 3113 | 2536 | 1961 | 1388 | 0815 | 0244 |
| 17.9 | 0033 9674 | 9106 | 8538 | 7972 | 7408 | 6844 | 6282 | 5721 | 5161 | 4602 |
| 18.0 | 0.0033 4045 | 3489 | 2934 | 2380 | 1828 | 1277 | 0727 | 0178 | 9631 | 9084 |
| 18.1 | .0032 8539 | 7995 | 7453 | 6911 | 6371 | 5832 | 5294 | 4757 | 4221 | 3687 |
| 18.2 | 0032 3154 | 2622 | 2091 | 1561 | 1033 | 0505 | 9979 | 9454 | 8930 | 8407 |
| 18.3 | 0031 7886 | 7365 | 6846 | 6327 | 5810 | 5294 | 4779 | 4266 | 3753 | 3241 |
| 18.4 | .0031 2731 | 2222 | 1714 | 1206 | 0700 | 0196 | 9692 | 9189 | 8687 | 8187 |
| 18.5 | 0030 7687 | 7189 | 6692 | 6195 | 5700 | 5206 | 4713 | 4221 | 3730 | 3240 |
| 18.6 | 0030 2752 | 2264 | 1777 | 1291 | 0807 | 0323 | 9841 | 9359 | 8879 | 8399 |
| 18.7 | .0029 7921 | 7443 | 6967 | 6492 | 6017 | 5544 | 5072 | 4600 | 4130 | 3661 |
| 18.8 | 0029 3192 | 2725 | 2258 | 1793 | 1329 | 0865 | 0403 | 9942 | 9481 | 9022 |
| 18.9 | 0028 8563 | 8106 | 7649 | 7193 | 6739 | 6285 | 5832 | 5381 | 4930 | 4480 |
| 19.0 | 0.0028 4031 | 3583 | 3136 | 2690 | 2245 | 1800 | 1357 | 0915 | 0473 | 0033 |
| 19.1 | .0027 9593 | 9155 | 8717 | 8280 | 7844 | 7409 | 6975 | 6542 | 6109 | 5678 |
| 19.2 | 0027 5247 | 4818 | 4389 | 3961 | 3534 | 3108 | 2683 | 2259 | 1835 | 1413 |
| 19.3 | 0027 0991 | 0570 | 0151 | 9732 | 9313 | 8896 | 8480 | 8064 | 7649 | 7235 |
| 19.4 | .0026 6822 | 6410 | 5999 | 5588 | 5179 | 4770 | 4362 | 3955 | 3549 | 3143 |
| 19.5 | 0026 2738 | 2335 | 1932 | 1530 | 1128 | 0728 | 0328 | 9929 | 9531 | 9134 |
| 19.6 | 0025 8738 | 8342 | 7947 | 7553 | 7160 | 6768 | 6376 | 5985 | 5595 | 5206 |
| 19.7 | .0025 4817 | 4430 | 4043 | 3657 | 3272 | 2887 | 2503 | 2120 | 1738 | 1357 |
| 19.8 | 0025 0976 | 0596 | 0217 | 9839 | 9461 | 9084 | 8708 | 8333 | 7958 | 7585 |
| 19.9 | 0024 7212 | 6839 | 6468 | 6097 | 5727 | 5358 | 4989 | 4621 | 4254 | 3888 |

| x | 0 | 1 | 2 | 3 | 4 | 5 | 6 | 7 | 8 | 9 |
|---|---|---|---|---|---|---|---|---|---|---|
| 20.0 | 0.0024 3522 | 3157 | 2793 | 2429 | 2067 | 1705 | 1343 | 0983 | 0623 | 0264 |
| 20.1 | .0023 9905 | 9548 | 9191 | 8834 | 8479 | 8124 | 7770 | 7416 | 7064 | 6712 |
| 20.2 | 0023 6360 | 6010 | 5660 | 5310 | 4962 | 4614 | 4266 | 3920 | 3574 | 3229 |
| 20.3 | 0023 2884 | 2540 | 2197 | 1855 | 1513 | 1172 | 0832 | 0492 | 0153 | 9814 |
| 20.4 | .0022 9476 | 9139 | 8803 | 8467 | 8132 | 7797 | 7463 | 7130 | 6798 | 6466 |
| 20.5 | 0022 6135 | 5804 | 5474 | 5145 | 4816 | 4488 | 4161 | 3834 | 3508 | 3182 |
| 20.6 | 0022 2857 | 2533 | 2210 | 1887 | 1564 | 1242 | 0921 | 0601 | 0281 | 9962 |
| 20.7 | .0021 9643 | 9325 | 9008 | 8691 | 8375 | 8059 | 7744 | 7430 | 7116 | 6803 |
| 20.8 | 0021 6491 | 6179 | 5867 | 5556 | 5246 | 4937 | 4628 | 4319 | 4012 | 3705 |
| 20.9 | 0021 3398 | 3092 | 2786 | 2481 | 2177 | 1874 | 1571 | 1268 | 0966 | 0665 |
| 21.0 | 0.0021 0364 | 0064 | 9764 | 9465 | 9166 | 8868 | 8571 | 8274 | 7978 | 7682 |
| 21.1 | .0020 7387 | 7092 | 6798 | 6505 | 6212 | 5920 | 5628 | 5337 | 5046 | 4756 |
| 21.2 | 0020 4466 | 4177 | 3889 | 3601 | 3313 | 3026 | 2740 | 2454 | 2169 | 1884 |
| 21.3 | 0020 1600 | 1316 | 1033 | 0750 | 0468 | 0187 | 9906 | 9625 | 9345 | 9066 |
| 21.4 | .0019 8787 | 8509 | 8231 | 7953 | 7676 | 7400 | 7124 | 6849 | 6574 | 6300 |
| 21.5 | 0019 6026 | 5753 | 5480 | 5208 | 4936 | 4665 | 4394 | 4124 | 3854 | 3585 |
| 21.6 | 0019 3316 | 3048 | 2780 | 2513 | 2246 | 1980 | 1714 | 1449 | 1184 | 0920 |
| 21.7 | .0019 0656 | 0393 | 0130 | 9867 | 9605 | 9344 | 9083 | 8823 | 8563 | 8303 |
| 21.8 | 0018 8044 | 7786 | 7528 | 7270 | 7013 | 6756 | 6500 | 6244 | 5989 | 5734 |
| 21.9 | 0018 5480 | 5226 | 4973 | 4720 | 4467 | 4215 | 3964 | 3713 | 3462 | 3212 |
| 22.0 | 0.0018 2962 | 2713 | 2464 | 2216 | 1968 | 1720 | 1473 | 1227 | 0981 | 0735 |
| 22.1 | .0018 0490 | 0245 | 0001 | 9757 | 9513 | 9270 | 9028 | 8786 | 8544 | 8303 |
| 22.2 | 0017 8062 | 7821 | 7581 | 7342 | 7103 | 6864 | 6626 | 6388 | 6150 | 5913 |
| 22.3 | 0017 5677 | 5441 | 5205 | 4970 | 4735 | 4501 | 4267 | 4033 | 3800 | 3567 |
| 22.4 | .0017 3335 | 3103 | 2871 | 2640 | 2409 | 2179 | 1949 | 1720 | 1491 | 1262 |
| 22.5 | 0017 1034 | 0806 | 0578 | 0351 | 0125 | 9899 | 9673 | 9447 | 9222 | 8998 |
| 22.6 | 0016 8774 | 8550 | 8326 | 8103 | 7880 | 7658 | 7436 | 7215 | 6994 | 6773 |
| 22.7 | .0016 6553 | 6333 | 6113 | 5894 | 5675 | 5457 | 5239 | 5021 | 4804 | 4587 |
| 22.8 | 0016 4371 | 4155 | 3939 | 3724 | 3509 | 3294 | 3080 | 2866 | 2653 | 2440 |
| 22.9 | 0016 2227 | 2015 | 1803 | 1591 | 1380 | 1169 | 0958 | 0748 | 0539 | 0329 |
| 23.0 | 0.0016 0120 | 9911 | 9703 | 9495 | 9288 | 9080 | 8873 | 8667 | 8461 | 8255 |
| 23.1 | .0015 8050 | 7845 | 7640 | 7435 | 7231 | 7028 | 6824 | 6621 | 6419 | 6217 |
| 23.2 | 0015 6015 | 5813 | 5612 | 5411 | 5210 | 5010 | 4810 | 4611 | 4412 | 4213 |
| 23.3 | 0015 4014 | 3816 | 3619 | 3421 | 3224 | 3027 | 2831 | 2635 | 2439 | 2243 |
| 23.4 | .0015 2048 | 1854 | 1659 | 1465 | 1271 | 1078 | 0885 | 0692 | 0499 | 0307 |
| 23.5 | 0015 0116 | 9924 | 9733 | 9542 | 9352 | 9162 | 8972 | 8782 | 8593 | 8404 |
| 23.6 | 0014 8215 | 8027 | 7839 | 7652 | 7464 | 7277 | 7091 | 6904 | 6718 | 6533 |
| 23.7 | .0014 6347 | 6162 | 5977 | 5793 | 5609 | 5425 | 5241 | 5058 | 4875 | 4693 |
| 23.8 | 0014 4510 | 4328 | 4147 | 3965 | 3784 | 3603 | 3423 | 3243 | 3063 | 2883 |
| 23.9 | 0014 2704 | 2525 | 2346 | 2168 | 1990 | 1812 | 1634 | 1457 | 1280 | 1104 |
| 24.0 | 0.0014 0928 | | | | | | | | | |

$$E/3RT \; = \; 19.481818/x^3 \quad \text{when } x > 24.$$

### D. Debye Specific Heat Function
### $C_v(Debye)/3R$

| x | 0 | 1 | 2 | 3 | 4 | 5 | 6 | 7 | 8 | 9 |
|---|---|---|---|---|---|---|---|---|---|---|
| 0.0 | 1.0 00000 | 99995 | 99980 | 99955 | 99920 | 99875 | 99820 | 99755 | 99680 | 99595 |
| 0.1 | .9 99500 | 99395 | 99280 | 99156 | 99021 | 98878 | 98721 | 98556 | 98382 | 98197 |
| 0.2 | 9 98003 | 97798 | 97584 | 97360 | 97126 | 96882 | 96628 | 96364 | 96091 | 95808 |
| 0.3 | 9 95514 | 95211 | 94899 | 94576 | 94244 | 93902 | 93550 | 93188 | 92817 | 92436 |
| 0.4 | .9 92045 | 91645 | 91235 | 90816 | 90387 | 89948 | 89500 | 89042 | 88574 | 88097 |
| 0.5 | 9 87611 | 87115 | 86610 | 86095 | 85571 | 85037 | 84494 | 83942 | 83380 | 82809 |
| 0.6 | 9 82229 | 81639 | 81041 | 80433 | 79816 | 79190 | 78554 | 77910 | 77256 | 76594 |
| 0.7 | .9 75922 | 75242 | 74552 | 73854 | 73147 | 72430 | 71705 | 70971 | 70229 | 69477 |
| 0.8 | 9 68717 | 67948 | 67171 | 66385 | 65590 | 64787 | 63975 | 63155 | 62326 | 61489 |
| 0.9 | 9 60643 | 59789 | 58927 | 58056 | 57177 | 56290 | 55395 | 54491 | 53580 | 52660 |
| 1.0 | 0.9 51732 | 50796 | 49853 | 48901 | 47941 | 46974 | 45999 | 45016 | 44025 | 43026 |
| 1.1 | .9 42020 | 41006 | 39985 | 38956 | 37919 | 36875 | 35824 | 34765 | 33699 | 32626 |
| 1.2 | 9 31545 | 30457 | 29362 | 28259 | 27150 | 26033 | 24910 | 23779 | 22642 | 21498 |
| 1.3 | 9 20346 | 19188 | 18024 | 16852 | 15674 | 14489 | 13298 | 12100 | 10895 | 09684 |
| 1.4 | .9 08467 | 07243 | 06013 | 04777 | 03534 | 02286 | 01031 | 99770 | 98503 | 97230 |
| 1.5 | 8 95951 | 94666 | 93375 | 92078 | 90775 | 89467 | 88153 | 86834 | 85509 | 84178 |
| 1.6 | 8 82842 | 81500 | 80153 | 78800 | 77442 | 76079 | 74711 | 73337 | 71959 | 70575 |
| 1.7 | .8 69186 | 67792 | 66394 | 64990 | 63581 | 62168 | 60750 | 59327 | 57900 | 56468 |
| 1.8 | 8 55031 | 53590 | 52144 | 50694 | 49239 | 47780 | 46317 | 44850 | 43378 | 41902 |
| 1.9 | 8 40423 | 38939 | 37451 | 35959 | 34463 | 32963 | 31460 | 29952 | 28441 | 26926 |
| 2.0 | 0.8 25408 | 23886 | 22361 | 20832 | 19299 | 17763 | 16224 | 14681 | 13135 | 11586 |
| 2.1 | .8 10034 | 08479 | 06920 | 05359 | 03794 | 02227 | 00656 | 99083 | 97507 | 95928 |
| 2.2 | 7 94347 | 92763 | 91176 | 89586 | 87994 | 86400 | 84803 | 83203 | 81602 | 79998 |
| 2.3 | 7 78391 | 76783 | 75172 | 73559 | 71944 | 70327 | 68708 | 67087 | 65464 | 63839 |
| 2.4 | .7 62212 | 60584 | 58954 | 57322 | 55688 | 54053 | 52416 | 50777 | 49137 | 47496 |
| 2.5 | 7 45853 | 44209 | 42563 | 40916 | 39268 | 37619 | 35968 | 34316 | 32664 | 31010 |
| 2.6 | 7 29355 | 27699 | 26042 | 24385 | 22726 | 21067 | 19407 | 17746 | 16084 | 14422 |
| 2.7 | .7 12759 | 11095 | 09431 | 07766 | 06101 | 04436 | 02770 | 01104 | 99437 | 97770 |
| 2.8 | 6 96103 | 94435 | 92768 | 91100 | 89432 | 87764 | 86096 | 84428 | 82760 | 81092 |
| 2.9 | 6 79424 | 77757 | 76089 | 74422 | 72754 | 71087 | 69421 | 67755 | 66089 | 64423 |
| 3.0 | 0.6 62758 | 61093 | 59429 | 57766 | 56103 | 54440 | 52778 | 51117 | 49456 | 47796 |
| 3.1 | .6 46137 | 44479 | 42821 | 41165 | 39509 | 37854 | 36200 | 34546 | 32894 | 31243 |
| 3.2 | 6 29593 | 27944 | 26296 | 24649 | 23003 | 21359 | 19715 | 18073 | 16432 | 14792 |
| 3.3 | 6 13154 | 11517 | 09881 | 08247 | 06614 | 04983 | 03353 | 01724 | 00097 | 98472 |
| 3.4 | .5 96848 | 95226 | 93605 | 91986 | 90369 | 88753 | 87139 | 85526 | 83916 | 82307 |
| 3.5 | 5 80700 | 79095 | 77491 | 75889 | 74290 | 72692 | 71096 | 69502 | 67910 | 66320 |
| 3.6 | 5 64732 | 63146 | 61562 | 59980 | 58400 | 56823 | 55247 | 53674 | 52102 | 50533 |
| 3.7 | .5 48966 | 47401 | 45839 | 44279 | 42721 | 41165 | 39611 | 38060 | 36511 | 34965 |
| 3.8 | 5 33421 | 31879 | 30340 | 28803 | 27268 | 25736 | 24207 | 22680 | 21155 | 19633 |
| 3.9 | 5 18113 | 16596 | 15082 | 13570 | 12061 | 10554 | 09050 | 07548 | 06049 | 04553 |

$C_v(\text{Debye})/3\,R$

| x | 0 | 1 | 2 | 3 | 4 | 5 | 6 | 7 | 8 | 9 |
|---|---|---|---|---|---|---|---|---|---|---|
| 4.0 | 0.5 03059 | 01568 | 00080 | 98595 | 97112 | 95632 | 94154 | 92679 | 91207 | 89738 |
| 4.1 | .4 88272 | 86808 | 85347 | 83889 | 82434 | 80982 | 79532 | 78086 | 76642 | 75201 |
| 4.2 | 4 73763 | 72328 | 70896 | 69466 | 68040 | 66616 | 65196 | 63778 | 62363 | 60952 |
| 4.3 | 4 59543 | 58137 | 56734 | 55334 | 53938 | 52544 | 51153 | 49765 | 48380 | 46999 |
| 4.4 | .4 45620 | 44244 | 42872 | 41502 | 40136 | 38772 | 37412 | 36055 | 34701 | 33350 |
| 4.5 | 4 32002 | 30657 | 29315 | 27976 | 26641 | 25308 | 23979 | 22653 | 21330 | 20010 |
| 4.6 | 4 18693 | 17380 | 16069 | 14762 | 13458 | 12157 | 10859 | 09565 | 08273 | 06985 |
| 4.7 | .4 05700 | 04418 | 03139 | 01864 | 00591 | 99322 | 98056 | 96794 | 95534 | 94278 |
| 4.8 | 3 93025 | 91775 | 90528 | 89284 | 88044 | 86807 | 85573 | 84342 | 83114 | 81890 |
| 4.9 | 3 80669 | 79451 | 78237 | 77025 | 75817 | 74612 | 73410 | 72211 | 71016 | 69824 |
| 5.0 | 0.36 8635 | 7449 | 6267 | 5087 | 3911 | 2738 | 1568 | 0402 | 9239 | 8079 |
| 5.1 | .35 6922 | 5768 | 4618 | 3470 | 2326 | 1186 | 0048 | 8913 | 7782 | 6654 |
| 5.2 | 34 5529 | 4408 | 3289 | 2174 | 1062 | 9953 | 8847 | 7744 | 6645 | 5549 |
| 5.3 | 33 4456 | 3366 | 2279 | 1195 | 0115 | 9038 | 7963 | 6892 | 5825 | 4760 |
| 5.4 | .32 3698 | 2640 | 1585 | 0533 | 9484 | 8438 | 7395 | 6355 | 5319 | 4285 |
| 5.5 | 31 3255 | 2228 | 1203 | 0182 | 9164 | 8149 | 7138 | 6129 | 5123 | 4121 |
| 5.6 | 30 3121 | 2125 | 1131 | 0141 | 9154 | 8169 | 7188 | 6210 | 5235 | 4262 |
| 5.7 | .29 3293 | 2327 | 1364 | 0404 | 9447 | 8493 | 7541 | 6593 | 5648 | 4706 |
| 5.8 | 28 3767 | 2830 | 1897 | 0967 | 0039 | 9115 | 8193 | 7275 | 6359 | 5446 |
| 5.9 | 27 4536 | 3629 | 2725 | 1824 | 0926 | 0031 | 9138 | 8249 | 7362 | 6478 |
| 6.0 | 0.26 5597 | 4719 | 3843 | 2971 | 2101 | 1234 | 0370 | 9509 | 8651 | 7795 |
| 6.1 | .25 6943 | 6093 | 5246 | 4401 | 3559 | 2721 | 1885 | 1051 | 0221 | 9393 |
| 6.2 | 24 8568 | 7745 | 6926 | 6109 | 5295 | 4483 | 3674 | 2868 | 2065 | 1264 |
| 6.3 | 24 0466 | 9670 | 8878 | 8088 | 7300 | 6515 | 5733 | 4954 | 4177 | 3403 |
| 6.4 | .23 2631 | 1862 | 1095 | 0331 | 9570 | 8811 | 8055 | 7302 | 6551 | 5802 |
| 6.5 | 22 5056 | 4313 | 3572 | 2834 | 2098 | 1364 | 0633 | 9905 | 9179 | 8456 |
| 6.6 | 21 7735 | 7017 | 6301 | 5588 | 4877 | 4168 | 3462 | 2758 | 2057 | 1358 |
| 6.7 | .21 0662 | 9968 | 9276 | 8587 | 7900 | 7215 | 6533 | 5853 | 5176 | 4501 |
| 6.8 | 20 3828 | 3158 | 2490 | 1824 | 1161 | 0500 | 9841 | 9185 | 8530 | 7878 |
| 6.9 | 19 7229 | 6581 | 5936 | 5294 | 4653 | 4015 | 3379 | 2745 | 2113 | 1484 |
| 7.0 | 0.19 0856 | 0231 | 9609 | 8988 | 8370 | 7753 | 7139 | 6527 | 5917 | 5310 |
| 7.1 | .18 4704 | 4101 | 3500 | 2901 | 2304 | 1709 | 1116 | 0526 | 9937 | 9351 |
| 7.2 | 17 8766 | 8184 | 7604 | 7025 | 6449 | 5875 | 5303 | 4733 | 4165 | 3599 |
| 7.3 | 17 3035 | 2473 | 1913 | 1355 | 0799 | 0245 | 9693 | 9143 | 8595 | 8049 |
| 7.4 | .16 7505 | 6963 | 6422 | 5884 | 5347 | 4813 | 4280 | 3750 | 3221 | 2694 |
| 7.5 | 16 2169 | 1646 | 1124 | 0605 | 0087 | 9572 | 9058 | 8546 | 8036 | 7527 |
| 7.6 | 15 7021 | 6516 | 6013 | 5512 | 5013 | 4515 | 4020 | 3526 | 3034 | 2543 |
| 7.7 | .15 2055 | 1568 | 1083 | 0599 | 0118 | 9638 | 9160 | 8683 | 8209 | 7736 |
| 7.8 | 14 7264 | 6795 | 6327 | 5861 | 5396 | 4933 | 4472 | 4013 | 3555 | 3098 |
| 7.9 | 14 2644 | 2191 | 1740 | 1290 | 0842 | 0395 | 9951 | 9508 | 9066 | 8626 |

| x | 0 | 1 | 2 | 3 | 4 | 5 | 6 | 7 | 8 | 9 |
|---|---|---|---|---|---|---|---|---|---|---|
| 8.0 | 0.13 8187 | 7750 | 7315 | 6881 | 6449 | 6019 | 5590 | 5162 | 4736 | 4312 |
| 8.1 | .13 3889 | 3468 | 3048 | 2630 | 2213 | 1798 | 1384 | 0972 | 0561 | 0152 |
| 8.2 | 12 9744 | 9338 | 8933 | 8529 | 8127 | 7727 | 7328 | 6930 | 6534 | 6139 |
| 8.3 | 12 5746 | 5354 | 4964 | 4575 | 4187 | 3801 | 3416 | 3032 | 2650 | 2270 |
| 8.4 | .12 1890 | 1512 | 1136 | 0761 | 0387 | 0014 | 9643 | 9273 | 8905 | 8538 |
| 8.5 | 11 8172 | 7807 | 7444 | 7082 | 6722 | 6362 | 6004 | 5648 | 5292 | 4938 |
| 8.6 | 11 4585 | 4234 | 3883 | 3534 | 3187 | 2840 | 2495 | 2151 | 1808 | 1466 |
| 8.7 | .11 1126 | 0787 | 0449 | 0113 | 9777 | 9443 | 9110 | 8778 | 8447 | 8118 |
| 8.8 | 10 7790 | 7463 | 7137 | 6812 | 6489 | 6166 | 5845 | 5525 | 5206 | 4888 |
| 8.9 | 10 4572 | 4256 | 3942 | 3628 | 3316 | 3005 | 2695 | 2387 | 2079 | 1773 |
| 9.0 | 0.10 1467 | 1163 | 0859 | 0557 | 0256 | 99562 | 96573 | 93594 | 90626 | 87669 |
| 9.1 | ·09 84722 | 81786 | 78861 | 75946 | 73041 | 70146 | 67262 | 64389 | 61525 | 58672 |
| 9.2 | 09 55829 | 52996 | 50174 | 47361 | 44558 | 41766 | 38983 | 36210 | 33448 | 30695 |
| 9.3 | 09 27951 | 25218 | 22494 | 19780 | 17076 | 14381 | 11696 | 09021 | 06355 | 03698 |
| 9.4 | ·09 01051 | 98414 | 95785 | 93166 | 90557 | 87956 | 85365 | 82783 | 80210 | 77646 |
| 9.5 | 08 75092 | 72546 | 70010 | 67482 | 64964 | 62454 | 59953 | 57461 | 54978 | 52504 |
| 9.6 | 08 50038 | 47581 | 45133 | 42693 | 40262 | 37840 | 35426 | 33020 | 30623 | 28235 |
| 9.7 | ·08 25855 | 23483 | 21120 | 18765 | 16418 | 14080 | 11750 | 09428 | 07114 | 04808 |
| 9.8 | 08 02510 | 00221 | 97939 | 95666 | 93400 | 91142 | 88893 | 86651 | 84417 | 82191 |
| 9.9 | 07 79972 | 77762 | 75559 | 73364 | 71176 | 68996 | 66824 | 64659 | 62502 | 60352 |
| 10.0 | 0.07 58210 | 56075 | 53948 | 51828 | 49716 | 47611 | 45513 | 43422 | 41339 | 39263 |
| 10.1 | ·07 37194 | 35133 | 33078 | 31031 | 28991 | 26957 | 24931 | 22912 | 20900 | 18895 |
| 10.2 | 07 16897 | 14905 | 12921 | 10943 | 08973 | 07009 | 05051 | 03101 | 01157 | 99220 |
| 10.3 | 06 97290 | 95366 | 93449 | 91539 | 89635 | 87738 | 85847 | 83962 | 82084 | 80213 |
| 10.4 | ·06 78348 | 76489 | 74637 | 72791 | 70952 | 69118 | 67291 | 65470 | 63656 | 61848 |
| 10.5 | 06 60045 | 58249 | 56459 | 54676 | 52898 | 51126 | 49361 | 47601 | 45847 | 44100 |
| 10.6 | 06 42358 | 40622 | 38892 | 37168 | 35450 | 33738 | 32031 | 30330 | 28635 | 26946 |
| 10.7 | ·06 25263 | 23585 | 21913 | 20246 | 18585 | 16930 | 15280 | 13636 | 11997 | 10364 |
| 10.8 | 06 08737 | 07115 | 05498 | 03887 | 02281 | 00681 | 99086 | 97496 | 95912 | 94333 |
| 10.9 | 05 92759 | 91190 | 89627 | 88069 | 86516 | 84969 | 83426 | 81889 | 80357 | 78830 |
| 11.0 | 0.05 77308 | 75791 | 74280 | 72773 | 71271 | 69774 | 68283 | 66796 | 65314 | 63837 |
| 11.1 | ·05 62365 | 60898 | 59436 | 57978 | 56526 | 55078 | 53635 | 52197 | 50763 | 49334 |
| 11.2 | 05 47910 | 46491 | 45076 | 43666 | 42261 | 40860 | 39464 | 38073 | 36686 | 35304 |
| 11.3 | 05 33926 | 32552 | 31183 | 29819 | 28460 | 27104 | 25753 | 24407 | 23065 | 21727 |
| 11.4 | ·05 20394 | 19065 | 17740 | 16420 | 15104 | 13792 | 12484 | 11181 | 09882 | 08587 |
| 11.5 | 05 07297 | 06011 | 04728 | 03450 | 02177 | 00907 | 99641 | 98380 | 97122 | 95869 |
| 11.6 | 04 94620 | 93374 | 92133 | 90896 | 89663 | 88433 | 87208 | 85987 | 84769 | 83556 |
| 11.7 | ·04 82346 | 81140 | 79938 | 78740 | 77546 | 76356 | 75169 | 73987 | 72808 | 71633 |
| 11.8 | 04 70461 | 69294 | 68130 | 66969 | 65813 | 64660 | 63511 | 62366 | 61224 | 60085 |
| 11.9 | 04 58951 | 57820 | 56693 | 55569 | 54448 | 53332 | 52219 | 51109 | 50003 | 48900 |

| x | 0 | 1 | 2 | 3 | 4 | 5 | 6 | 7 | 8 | 9 |
|---|---|---|---|---|---|---|---|---|---|---|
| 12.0 | 0.044 7801 | 6705 | 5613 | 4525 | 3439 | 2357 | 1279 | 0204 | 9132 | 8064 |
| 12.1 | ·043 6999 | 5937 | 4879 | 3824 | 2772 | 1724 | 0679 | 9637 | 8599 | 7563 |
| 12.2 | 042 6531 | 5502 | 4477 | 3454 | 2435 | 1419 | 0406 | 9397 | 8390 | 7386 |
| 12.3 | 041 6386 | 5389 | 4395 | 3404 | 2416 | 1431 | 0449 | 9470 | 8494 | 7522 |
| 12.4 | ·040 6552 | 5585 | 4621 | 3660 | 2703 | 1748 | 0796 | 9847 | 8901 | 7957 |
| 12.5 | 039 7017 | 6080 | 5145 | 4213 | 3285 | 2359 | 1435 | 0515 | 9598 | 8683 |
| 12.6 | 038 7771 | 6862 | 5956 | 5052 | 4151 | 3253 | 2358 | 1465 | 0575 | 9688 |
| 12.7 | ·037 8803 | 7921 | 7042 | 6166 | 5292 | 4421 | 3552 | 2686 | 1823 | 0962 |
| 12.8 | 037 0104 | 9249 | 8396 | 7545 | 6697 | 5852 | 5009 | 4169 | 3331 | 2496 |
| 12.9 | 036 1664 | 0834 | 0006 | 9181 | 8358 | 7538 | 6720 | 5904 | 5091 | 4281 |
| 13.0 | 0.035 3473 | 2667 | 1864 | 1063 | 0264 | 9468 | 8674 | 7883 | 7094 | 6307 |
| 13.1 | ·034 5523 | 4741 | 3961 | 3184 | 2409 | 1639 | 0865 | 0097 | 9331 | 8567 |
| 13.2 | 033 7805 | 7046 | 6289 | 5534 | 4782 | 4031 | 3283 | 2537 | 1793 | 1051 |
| 13.3 | 033 0312 | 9575 | 8840 | 8107 | 7376 | 6647 | 5920 | 5196 | 4474 | 3753 |
| 13.4 | .032 3035 | 2319 | 1605 | 0893 | 0183 | 9475 | 8770 | 8066 | 7364 | 6665 |
| 13.5 | 031 5967 | 5272 | 4578 | 3886 | 3197 | 2509 | 1824 | 1140 | 0458 | 9779 |
| 13.6 | 030 9101 | 8425 | 7751 | 7079 | 6409 | 5741 | 5075 | 4411 | 3748 | 3088 |
| 13.7 | .030 2429 | 1773 | 1118 | 0465 | 9814 | 9164 | 8517 | 7872 | 7228 | 6586 |
| 13.8 | 029 5946 | 5308 | 4671 | 4037 | 3404 | 2773 | 2144 | 1516 | 0890 | 0266 |
| 13.9 | 028 9644 | 9024 | 8405 | 7788 | 7173 | 6559 | 5948 | 5338 | 4729 | 4123 |
| 14.0 | 0.028 3518 | 2915 | 2313 | 1713 | 1115 | 0519 | 9924 | 9331 | 8739 | 8149 |
| 14.1 | .027 7561 | 6975 | 6390 | 5806 | 5225 | 4645 | 4066 | 3489 | 2914 | 2341 |
| 14.2 | 027 1769 | 1198 | 0629 | 0062 | 9496 | 8932 | 8369 | 7808 | 7249 | 6691 |
| 14.3 | 026 6134 | 5579 | 5026 | 4474 | 3924 | 3375 | 2828 | 2282 | 1737 | 1194 |
| 14.4 | .026 0653 | 0113 | 9575 | 9038 | 8502 | 7968 | 7436 | 6905 | 6375 | 5847 |
| 14.5 | 025 5320 | 4795 | 4271 | 3748 | 3227 | 2708 | 2190 | 1673 | 1157 | 0643 |
| 14.6 | 025 0130 | 9619 | 9109 | 8601 | 8094 | 7588 | 7083 | 6580 | 6079 | 5578 |
| 14.7 | .024 5079 | 4582 | 4085 | 3590 | 3097 | 2604 | 2113 | 1624 | 1135 | 0648 |
| 14.8 | 024 0162 | 9678 | 9195 | 8713 | 8232 | 7753 | 7275 | 6798 | 6322 | 5848 |
| 14.9 | 023 5375 | 4903 | 4432 | 3963 | 3495 | 3028 | 2563 | 2098 | 1635 | 1174 |
| 15.0 | 0.023 0713 | 0253 | 9795 | 9338 | 8882 | 8428 | 7974 | 7522 | 7071 | 6621 |
| 15.1 | .022 6172 | 5725 | 5279 | 4833 | 4389 | 3947 | 3505 | 3064 | 2625 | 2187 |
| 15.2 | 022 1750 | 1314 | 0879 | 0445 | 0013 | 9581 | 9151 | 8722 | 8294 | 7867 |
| 15.3 | 021 7441 | 7016 | 6592 | 6170 | 5748 | 5328 | 4909 | 4490 | 4073 | 3657 |
| 15.4 | .021 3242 | 2828 | 2415 | 2004 | 1593 | 1183 | 0775 | 0367 | 9960 | 9555 |
| 15.5 | 020 9150 | 8747 | 8345 | 7943 | 7543 | 7144 | 6745 | 6348 | 5952 | 5557 |
| 15.6 | 020 5162 | 4769 | 4377 | 3985 | 3595 | 3206 | 2818 | 2430 | 2044 | 1659 |
| 15.7 | .020 1274 | 0891 | 0508 | 0127 | 9747 | 9367 | 8988 | 8611 | 8234 | 7858 |
| 15.8 | 019 7484 | 7110 | 6737 | 6365 | 5994 | 5624 | 5254 | 4886 | 4519 | 4152 |
| 15.9 | 019 3787 | 3422 | 3059 | 2696 | 2334 | 1973 | 1613 | 1254 | 0896 | 0538 |

| x | 0 | 1 | 2 | 3 | 4 | 5 | 6 | 7 | 8 | 9 |
|---|---|---|---|---|---|---|---|---|---|---|
| 16.0 | 0.019 0182 | 9826 | 9471 | 9118 | 8765 | 8413 | 8061 | 7711 | 7361 | 7013 |
| 16.1 | .018 6665 | 6318 | 5972 | 5627 | 5283 | 4939 | 4596 | 4255 | 3914 | 3574 |
| 16.2 | 018 3234 | 2896 | 2558 | 2221 | 1885 | 1550 | 1216 | 0882 | 0550 | 0218 |
| 16.3 | 017 9887 | 9556 | 9227 | 8898 | 8570 | 8243 | 7917 | 7592 | 7267 | 6943 |
| 16.4 | .017 6620 | 6298 | 5976 | 5655 | 5335 | 5016 | 4698 | 4380 | 4063 | 3747 |
| 16.5 | 017 3432 | 3117 | 2803 | 2490 | 2178 | 1866 | 1555 | 1245 | 0936 | 0627 |
| 16.6 | 017 0319 | 0012 | 9706 | 9400 | 9095 | 8791 | 8488 | 8185 | 7883 | 7582 |
| 16.7 | .016 7281 | 6981 | 6682 | 6383 | 6086 | 5789 | 5492 | 5197 | 4902 | 4608 |
| 16.8 | 016 4314 | 4021 | 3729 | 3438 | 3147 | 2857 | 2568 | 2279 | 1991 | 1704 |
| 16.9 | 016 1417 | 1131 | 0846 | 0561 | 0277 | 9994 | 9711 | 9429 | 9148 | 8867 |
| 17.0 | 0.015 8587 | 8308 | 8029 | 7751 | 7474 | 7197 | 6921 | 6646 | 6371 | 6097 |
| 17.1 | .015 5823 | 5550 | 5278 | 5007 | 4736 | 4465 | 4196 | 3927 | 3658 | 3390 |
| 17.2 | 015 3123 | 2857 | 2591 | 2325 | 2060 | 1796 | 1533 | 1270 | 1008 | 0746 |
| 17.3 | 015 0485 | 0224 | 9964 | 9705 | 9446 | 9188 | 8931 | 8674 | 8418 | 8162 |
| 17.4 | .014 7907 | 7652 | 7398 | 7145 | 6892 | 6640 | 6388 | 6137 | 5886 | 5636 |
| 17.5 | 014 5387 | 5138 | 4890 | 4642 | 4395 | 4148 | 3902 | 3657 | 3412 | 3168 |
| 17.6 | 014 2924 | 2681 | 2438 | 2196 | 1954 | 1713 | 1473 | 1233 | 0994 | 0755 |
| 17.7 | .014 0516 | 0278 | 0041 | 9804 | 9568 | 9333 | 9098 | 8863 | 8629 | 8395 |
| 17.8 | 013 8162 | 7930 | 7698 | 7467 | 7236 | 7005 | 6775 | 6546 | 6317 | 6089 |
| 17.9 | 013 5861 | 5633 | 5406 | 5180 | 4954 | 4729 | 4504 | 4280 | 4056 | 3833 |
| 18.0 | 0.013 3610 | 3387 | 3165 | 2944 | 2723 | 2503 | 2283 | 2064 | 1845 | 1626 |
| 18.1 | .013 1408 | 1191 | 0974 | 0757 | 0541 | 0326 | 0110 | 9896 | 9682 | 9468 |
| 18.2 | 012 9255 | 9042 | 8830 | 8618 | 8407 | 8196 | 7985 | 7775 | 7566 | 7357 |
| 18.3 | 012 7148 | 6940 | 6732 | 6525 | 6318 | 6112 | 5906 | 5700 | 5495 | 5291 |
| 18.4 | .012 5087 | 4883 | 4680 | 4477 | 4275 | 4073 | 3871 | 3670 | 3470 | 3270 |
| 18.5 | 012 3070 | 2871 | 2672 | 2473 | 2275 | 2078 | 1881 | 1684 | 1487 | 1291 |
| 18.6 | 012 1096 | 0901 | 0706 | 0512 | 0318 | 0125 | 9932 | 9739 | 9547 | 9355 |
| 18.7 | .011 9164 | 8973 | 8783 | 8593 | 8403 | 8214 | 8025 | 7836 | 7648 | 7460 |
| 18.8 | 011 7273 | 7086 | 6900 | 6714 | 6528 | 6342 | 6157 | 5973 | 5789 | 5605 |
| 18.9 | 011 5422 | 5239 | 5056 | 4874 | 4692 | 4511 | 4330 | 4149 | 3969 | 3789 |
| 19.0 | 0.011 3609 | 3430 | 3251 | 3073 | 2895 | 2717 | 2540 | 2363 | 2186 | 2010 |
| 19.1 | .011 1834 | 1659 | 1484 | 1309 | 1135 | 0961 | 0787 | 0614 | 0441 | 0268 |
| 19.2 | 011 0096 | 9924 | 9753 | 9582 | 9411 | 9241 | 9071 | 8901 | 8732 | 8563 |
| 19.3 | 010 8394 | 8226 | 8058 | 7890 | 7723 | 7556 | 7390 | 7223 | 7057 | 6892 |
| 19.4 | .010 6727 | 6562 | 6397 | 6233 | 6069 | 5906 | 5743 | 5580 | 5417 | 5255 |
| 19.5 | 010 5093 | 4932 | 4771 | 4610 | 4449 | 4289 | 4129 | 3970 | 3811 | 3652 |
| 19.6 | 010 3493 | 3335 | 3177 | 3019 | 2862 | 2705 | 2549 | 2392 | 2236 | 2081 |
| 19.7 | .010 1925 | 1770 | 1616 | 1461 | 1307 | 1153 | 1000 | 0845 | 0694 | 0541 |
| 19.8 | 010 0389 | 0237 | 0085 | 99341 | 97830 | 96323 | 94819 | 93318 | 91820 | 90325 |
| 19.9 | 009 88833 | 87344 | 85858 | 84375 | 82894 | 81417 | 79943 | 78472 | 77003 | 75538 |

| x | 0 | 1 | 2 | 3 | 4 | 5 | 6 | 7 | 8 | 9 |
|---|---|---|---|---|---|---|---|---|---|---|
| 20.0 | 0.009 74076 | 72616 | 71160 | 69706 | 68255 | 66807 | 65362 | 63920 | 62481 | 61044 |
| 20.1 | .009 59611 | 58180 | 56752 | 55327 | 53905 | 52485 | 51069 | 49655 | 48244 | 46836 |
| 20.2 | 009 45430 | 44028 | 42628 | 41231 | 39837 | 38445 | 37056 | 35670 | 34287 | 32906 |
| 20.3 | 009 31528 | 30153 | 28781 | 27411 | 26044 | 24679 | 23317 | 21958 | 20602 | 19248 |
| 20.4 | .009 17897 | 16549 | 15203 | 13860 | 12519 | 11181 | 09846 | 08513 | 07183 | 05856 |
| 20.5 | 009 04531 | 03208 | 01889 | 00572 | 99257 | 97945 | 96635 | 95328 | 94024 | 92722 |
| 20.6 | 008 91423 | 90126 | 88831 | 87539 | 86250 | 84963 | 83679 | 82397 | 81118 | 79841 |
| 20.7 | .008 78566 | 77294 | 76025 | 74758 | 73493 | 72231 | 70971 | 69714 | 68459 | 67206 |
| 20.8 | 008 65956 | 64708 | 63463 | 62220 | 60980 | 59742 | 58506 | 57272 | 56041 | 54812 |
| 20.9 | 008 53586 | 52362 | 51140 | 49921 | 48704 | 47489 | 46277 | 45067 | 43859 | 42654 |
| 21.0 | 0.0084 1451 | 0250 | 9051 | 7855 | 6661 | 5469 | 4279 | 3092 | 1907 | 0724 |
| 21.1 | .0082 9544 | 8366 | 7190 | 6016 | 4844 | 3675 | 2507 | 1342 | 0180 | 9019 |
| 21.2 | 0081 7861 | 6704 | 5550 | 4399 | 3249 | 2101 | 0956 | 9813 | 8672 | 7533 |
| 21.3 | 0080 6396 | 5261 | 4129 | 2998 | 1870 | 0744 | 9620 | 8498 | 7378 | 6260 |
| 21.4 | .0079 5144 | 4031 | 2919 | 1810 | 0702 | 9597 | 8494 | 7393 | 6293 | 5196 |
| 21.5 | 0078 4101 | 3008 | 1917 | 0828 | 9741 | 8656 | 7573 | 6492 | 5413 | 4336 |
| 21.6 | 0077 3262 | 2189 | 1118 | 0049 | 8982 | 7917 | 6853 | 5792 | 4733 | 3676 |
| 21.7 | 0076 2621 | 1567 | 0516 | 9467 | 8419 | 7373 | 6330 | 5288 | 4248 | 3210 |
| 21.8 | 0075 2174 | 1140 | 0108 | 9078 | 8049 | 7022 | 5998 | 4975 | 3954 | 2935 |
| 21.9 | 0074 1918 | 0902 | 9889 | 8877 | 7867 | 6859 | 5853 | 4849 | 3846 | 2846 |
| 22.0 | 0.0073 1847 | 0850 | 9854 | 8861 | 7869 | 6879 | 5891 | 4905 | 3921 | 2938 |
| 22.1 | .0072 1957 | 0978 | 0001 | 9025 | 8051 | 7079 | 6109 | 5140 | 4173 | 3208 |
| 22.2 | 0071 2245 | 1283 | 0323 | 9365 | 8409 | 7454 | 6501 | 5550 | 4600 | 3652 |
| 22.3 | 0070 2706 | 1762 | 0819 | 9878 | 8939 | 8001 | 7065 | 6130 | 5198 | 4267 |
| 22.4 | .0069 3337 | 2409 | 1483 | 0559 | 9636 | 8715 | 7795 | 6878 | 5961 | 5047 |
| 22.5 | 0068 4134 | 3222 | 2313 | 1405 | 0498 | 9593 | 8690 | 7788 | 6888 | 5990 |
| 22.6 | 0067 5093 | 4197 | 3303 | 2411 | 1521 | 0632 | 9744 | 8858 | 7974 | 7091 |
| 22.7 | .0066 6210 | 5330 | 4452 | 3576 | 2701 | 1827 | 0955 | 0085 | 9216 | 8348 |
| 22.8 | 0065 7483 | 6618 | 5755 | 4894 | 4034 | 3176 | 2319 | 1464 | 0610 | 9758 |
| 22.9 | 0064 8907 | 8058 | 7210 | 6363 | 5518 | 4675 | 3833 | 2992 | 2153 | 1316 |
| 23.0 | 0.0064 0480 | 9645 | 8812 | 7980 | 7150 | 6321 | 5493 | 4667 | 3843 | 3020 |
| 23.1 | .0063 2198 | 1378 | 0559 | 9741 | 8925 | 8110 | 7297 | 6485 | 5675 | 4866 |
| 23.2 | 0062 4058 | 3252 | 2447 | 1643 | 0841 | 0041 | 9241 | 8443 | 7647 | 6852 |
| 23.3 | 0061 6058 | 5265 | 4474 | 3684 | 2896 | 2109 | 1323 | 0538 | 9755 | 8973 |
| 23.4 | .0060 8193 | 7414 | 6636 | 5860 | 5085 | 4311 | 3539 | 2768 | 1998 | 1229 |
| 23.5 | 0060 0462 | 9696 | 8931 | 8168 | 7406 | 6645 | 5886 | 5128 | 4371 | 3616 |
| 23.6 | 0059 2861 | 2108 | 1357 | 0606 | 9857 | 9109 | 8362 | 7617 | 6873 | 6130 |
| 23.7 | .0058 5388 | 4648 | 3909 | 3171 | 2434 | 1699 | 0965 | 0232 | 9500 | 8770 |
| 23.8 | 0057 8041 | 7313 | 6586 | 5860 | 5136 | 4413 | 3691 | 2970 | 2251 | 1532 |
| 23.9 | 0057 0815 | 0099 | 9385 | 8671 | 7959 | 7248 | 6538 | 5829 | 5121 | 4415 |
| 24.0 | 0.0056 3710 | | | | | | | | | |

$$C_v/3R = 77.92727/x^3 \quad \text{when} \quad x > 24.$$

# Author Index

# Subject Index

234